Disordered systems

Cargèse

Leticia F. Cugliandolo
leticia@lpthe.jussieu.fr
Laboratoire de Physique Théorique et Hautes Energies de Jussieu

May 30, 2011

Contents

1 Introduction

1.1 Falling out of equilibrium

This introduction is not really adapted to this set of lectures but it gives an idea of the out of equilibrium glassy problems. See the slides for a more adequate introduction to the lectures.

In standard condensed matter or statistical physics focus is set on **equilibrium** systems. Microcanonical, canonical or grand canonical ensembles are used depending on the conditions one is interested in. The relaxation of a tiny perturbation away from equilibrium is also sometimes described in textbooks and undergraduate courses.

More recently, attention has turned to the study of the evolution of similar macroscopic systems in **far from equilibrium** conditions. These can be achieved by changing the properties of the environment (e.g. the temperature) in a canonical setting or by changing a parameter in the system's Hamiltonian in a microcanonical one. The procedure of rapidly (ideally instantaneously) changing a parameter is called a **quench**. Right after both types of quenches the initial configuration is not one of equilibrium at the new conditions and the systems subsequently evolve in an out of equilibrium fashion. The relaxation towards the new equilibrium (if possible) could be fast (and not interesting for our purposes) or it could be very slow (and thus the object of our study). There are plenty of examples of the latter. Dissipative ones include systems quenched through a phase transition and later undergoing domain growth, and problems with competing interactions that behave as glasses. Energy conserving ones are of great interest at presence due to the rapid growth of activity in cold-atom systems.

Out of equilibrium situations can also be established by **driving** a system, that otherwise would reach equilibrium in observable time-scales, with an external pertubation. In the context of macroscopic systems an interesting example is the one of sheared complex liquids. Yet another interesting case is the one of powders that stay in static metastable states unless externally perturbed by tapping, vibration or shear that drives them out of equilibrium and makes them slowly evolve towards more compact config-

urations. Such situations are usually called non-equilibrium steady states (NESS). But also small systems can be driven out of equilibrium with external perturbations. Transport in nano-structures is the quantum (small) counterpart phenomenon of these cases, also of special interest at present.

In the study of *macroscopic out of equilibrium systems* a number of questions one would like to give an answer to naturally arise. Among these are:

1. Is the (instantaneous) **structure** out of equilibrium similar to the one in equilibrium?
2. What **microscopic/mesoscopic relaxation mechanism** takes place after the quench?
3. Does the system quickly settle into a stationary state? In more technical terms, is there a finite relaxation time to reach a steady state?
4. Can one describe the states of the system sometime after the quench with some kind of **effective equilibrium-like measure**?
5. Are there **thermodynamic concepts**, such as temperature, entropy, free-energy, playing a role in the non-equilibrium relaxation?

In the last 20 years or so a rather complete theory of the dynamics of **classical macroscopic systems evolving slowly out of equilibrium, in a small entropy production limit** (asymptotic regime after a quench, small drives), that encompasses the situations described above has been developed. This is a **mean-field theory** type in the sense that it applies strictly to models with long-range interactions or in the infinite dimensional limit. It is, however, proposed that many aspects of it also apply to systems with short-range interactions although with some caveats. A number of finite dimensional problems have been solved demonstrating this fact.

In several cases of practical interest, **quantum effects** play an important rôle. For instance, glassy phases at very low temperatures have been identified in a large variety of materials (spin-glass like systems, interacting electrons with disorder, materials undergoing super-conductor transitions, metallic glasses, etc.). Clearly, the driven case is also very important in systems with quantum fluctuations. Take for instance a molecule or an interacting electronic system driven by an external current applied via the coupling to leads at different chemical potential. It is then necessary to settle whether the approach developed and the results obtained for the classical dynamics in a limit of small entropy production carries through when quantum fluctuations are included.

In these notes we start by exposing some examples of the **phenomenology** of out of equilibrium dynamics we are interested in. We focus on classical problems and their precise setting. Next we go into the **formalism** used to deal with these problems. The basic techniques used to study classical glassy models with or without disorder are relatively well documented in the literature (the replica trick, scaling arguments and droplet theories, the dynamic functional method used to derive macroscopic equations from the microscopic Langevin dynamics, functional renormalization, Montecarlo and molecular dynamic numerical methods). On the contrary, the techniques needed to deal with the statics and dynamics of quantum macroscopic systems are much less known in general. I shall briefly discuss the role played by the environment in a quantum system and introduce and compare the equilibrium and dynamic approaches.

Concretely, we recall some features of the Langevin formalism and its generating function. We dwell initially with some emblematic aspects of classical macroscopic systems slowly evolving out of equilibrium. Concerning models, we focus on two, that are intimately related: the $O(N)$ **model in the large N limit** that is used to describe **coarsening phenomena**, and the **random manifold**, that finds applications to many physical problems like charge density waves, high-Tc superconductors, etc. Both problems are of **field-theoretical** type and can be treated both **classically and quantum mechanically**. These two models are ideal for the purpose of introducing and discussing formalism and some basic ideas we would wish to convey in these lectures. Before entering the technical part we explain the two-fold meaning of the word **disorder** by introducing the glass problem and some of the numerous questions it raises.

1.2 Structural and quenched disorder: glassy physics

While the understanding of equilibrium phases, the existence of phase transitions as well as the characterization of critical phenomena are well understood in clean systems, as soon as **competing interactions** or geometric frustration are included one faces the possibility of destroying this simple picture by giving way to novel phenomena like **glassy** behaviour.

Competing interactions can be dynamic, also called **annealed** or **quenched**. A simple example illustrates the former: the Lennard-Jones potential (see

Fig. 1-left) that gives an effective interaction between *soft*[1] particles in a liquid has a repulsive and an attractive part, depending on the distance between the particles, a set of dynamic variables. In this example, the interactions depend on the positions of the particles and evolve with them. Quenched competing interactions are fixed in the observational time-scale and they transmit 'contradictory' messages. Typical examples are systems with ferromagnetic and/or antiferromagnetic exchanges that are not organised in a simple way with respect to the geometry and connectivity of the lattice such as spin-glasses [2] (see Fig. 1-right).

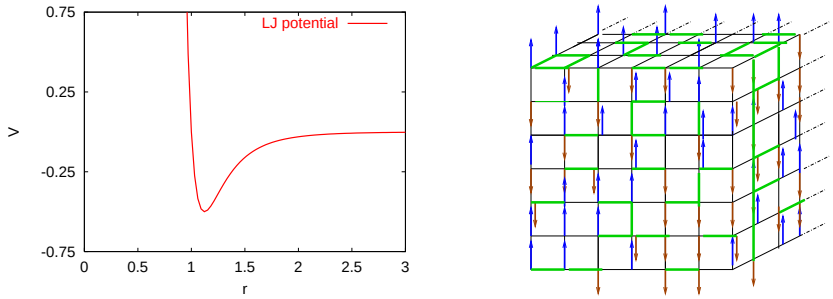

Figure 1: Left: The Lennard-Jones potential. Right: the Edwards-Anderson $3d$ spin-glass.

When competing interactions are present the low-temperature configurations may look disordered but still have macroscopic properties of a kind of crystalline state. Again, cooling down a liquid to obtain a glass is helpful to exemplify what we mean here: the liquid cannot support stress and flows while the glass has solid-like properties as crystals, it can support stress and does not easily flow in reasonable time-scales (this is why glasses can be made of glass!) However, when looked at a microscopic scale, one does not identify any important structural difference between the liquid and the glass: no simple long-range structural order has been identified for glasses. Moreover, there is no clear evidence for a phase transition between the liquid and the glass. At present one can only talk about a dynamic crossover. The glassy regime is however usually called a *glassy phase* and it is sometimes said to be a *disordered phase* due to the lack of a clear structural order – this does not mean that there is no order whatsoever (see Fig. 3 for an example of a

[1]Soft means that the particles can overlap at the price of an energy cost. In the case this is forbidden one works with *hard* particles.

system with a liquid, a crystal and glassy phase). Lennard-Jones binary mixtures are prototypical examples of systems that undergo a glass transition (or crossover) when cooled across the glass temperature T_g or when compressed across a density n_g [1].

In the paragraphs above we characterized the low temperature regime of certain particle models and claimed that their structure is disordered (at list at first sight). Another sense in which the word **disorder** is used is to characterize the **interactions**. Quenched interactions are initially drawn from a probability distribution. Annealed interactions may have a slow time-dependence. Both lead to *disorder*. These can be realized by coupling strengths as in the magnetic example in Fig. 1, but also by magnetic fields, pinning centers, potential energies, *etc.* Disordered interactions usually lead to low-temperature behaviour that is similar to the one observed in systems with dynamic competing interactions.

There are many types of glasses and they occur over an astounding range of scales from macroscopic to microscopic. Macroscopic examples include **granular media** like sand and powders. Unless fluidized by shaking or during flow these quickly settle into jammed, amorphous configurations. Jamming can also be caused by applying stress, in response to which the material may effectively convert from a fluid to a solid, refusing further flow. Temperature (and of course quantum fluctuations as well) is totally irrelevant for these systems since the grains are typically big, say, of $1mm$ radius. **Colloidal suspensions** contain smaller (typically micrometre-sized) particles suspended in a liquid and form the basis of many paints and coatings. Again, at high density such materials tend to become glassy unless crystallization is specifically encouraged (and can even form arrested gels at low densities if attractive forces are also present). On smaller scales still, there are atomic and **molecular glasses**: window glass is formed by quick cooling of a silica melt, and of obvious everyday importance. The plastics in drink bottles and the like are also glasses produced by cooling, the constituent particles being long polymer molecules. Critical temperatures are of the order of 80C for, say, PVC and these systems are glassy at room temperature. Finally, on the nanoscale, glasses are also formed by vortex lines in type-II superconductors. **Atomic glasses** with very low critical temperature, of the order of $10mK$, have also been studied in great detail.

In these lectures we shall only deal with a canonical setting, the microcanonical one being more relevant to quantum systems that we shall not discuss here. Disordered systems (in both senses) are usually in contact

with external reservoirs at fixed temperature; their description is done in the canonical (or grand-canonical in particle systems with the possibility of particle exchange with the environment) ensemble.

Many questions arise for the **static properties** of systems with competing interactions. Some of them, that we shall discuss in the rest of the course are:

1. Are there equilibrium phase transitions between low-temperature and high temperature phases?
2. Is there any kind of order at low temperatures?
3. At the phase transition, if there is one, does all the machinery developed for clean systems apply?
4. Are these phases, and critical phenomena or dynamic crossovers, the same or very different when disorder is quenched or annealed?
5. What is the mechanism leading to glassiness?

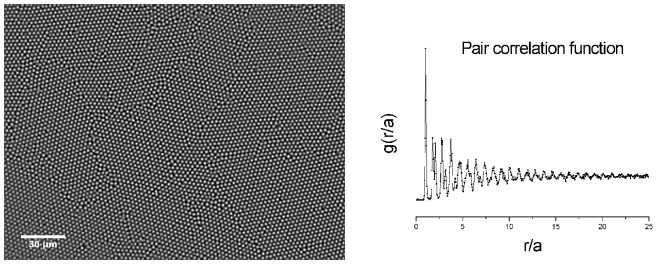

Figure 2: A crystal in a $2d$ colloidal suspension of hard spheres

In practice a further complication appears. Usually, disordered phases are prepared with a relatively rapid quench from the high temperature phase. When approaching a characteristic temperature the systems cannot follow the pace of evolution dictated by the environment and **fall out of equilibrium** [3]. Indeed, without entering into the rich details of the glass phenomenology we just mention here that their key feature is that below some characteristic temperature T_g, or above a critical density ρ_g, the relaxation time goes beyond the experimentally accessible time-scales and the system is next bound to evolve out of equilibrium. Although the mechanism leading to such a slow relaxation is unknown – and might be different in different cases – the out of equilibrium relaxation presents very similar properties. The left

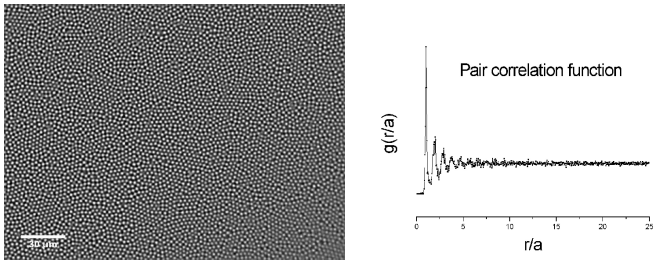

Figure 3: A liquid or a glass in a $2d$ colloidal suspension of hard spheres.

panel in Fig. 4 shows one aspect of glassy dynamics, aging, as shown by the two-time relaxation of the self-correlation of a colloidal suspension, that is remarkably similar to the decay of the magnetic correlation in the Ising model shown in the right panel and in Fig. 26.

A purely static description, based on the use of the canonical (or grand-canonical) partition function is then not sufficient. One is forced to include the time evolution of the individual agents (spins, particles, molecules) and from it derive the macroscopic *time-dependent* properties of the full system. The microscopic time-evolution is given by a stochastic process. The macroscopic evolution is usually very slow and, in probability terms, it is not a small perturbation around the Gibbs-Boltzmann distribution function but rather something quite different. This gives rise to new interesting phenomena.

The questions that arise in the *non-equilibrium* context are

1. How to characterize the non-equilibrium dynamics of glassy systems phenomenologically.
2. Which are the minimal models that reproduce the phenomenology.
3. Which is the relation between the behavior of these and other non-equilibrium systems, in particular, those kept away from equilibrium by external forces, currents, *etc.*
4. Which features are generic to all systems with slow dynamics.
5. Whether one could extend the equilibrium statistical mechanics ideas; *e.g.* can one use temperature, entropy and other thermodynamic concepts out of equilibrium?
6. Related to the previous item, whether one can construct a non-equilibrium measure that would substitute the Gibbs-Boltzmann one in certain cases.

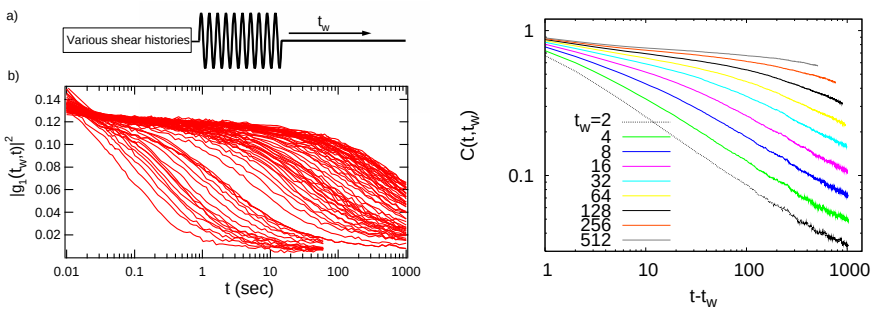

Figure 4: Left: two-time evolution of the self-correlation in a colloidal suspension initialized by applying a shearing rate (data from Viasnoff and Lequeux) The longer the waiting time the slower the decay. Right: two-time evolution in the bi-dimensional Ising model quenched below its phase transition at T_c. A two-scale relaxation with a clear plateau at a special value of the correlation is seen in the double logarithmic scale. We shall discuss this feature at length in the lectures.

An out of equilibrium situation can be externally maintained by applying forces and thus injecting energy into the system and driving it. There are several ways to do this and we explain below two quite typical ones that serve also as theoretical traditional examples.

Rheological measurements are common in soft condensed matter; they consist in driving the systems out of equilibrium by applying an external force that does not derive from a potential (e.g. shear, shaking, etc.). The dynamics of the system under the effect of such a strong perturbation is then monitored.

The effect of shear on domain growth is one of great technological and theoretical importance. The growth of domains is anisotropic and there might be different growing lengths in different directions. Moreover, it is not clear whether shear might interrupt growth altogether giving rise to a non-equilibrium stationary state or whether coarsening might continue for ever. Shear is also commonly used to study the mechanical properties of diverse glasses.

Another setting is to couple the system to **different external reservoirs** all in equilibrium but at different temperature or chemical potential thus inducing a heat or a particle current through the system. This set-up is

relevant to quantum situations in which one can couple a system to, say, a number of leads at different chemical potential. The heat transport problem in classical physics also belongs to this class.

1.3 Interdisciplinary aspects

The theory of disordered systems has become quite interdisciplinary in the sense that problems in computer science, biology or even sociology and finance have disorder aspects and can be mimicked with similar models and solved with similar methods to the ones we shall discuss here.

1.3.1 Optimization problems

The most convenient area of application is, most probably, the one of *combinatorial optimisation* in computer science [4]. These problems can usually be stated in a form that corresponds to minimizing a cost (energy) function over a large set of variables. Typically these cost functions have a very large number of local minima – an exponential function of the number of variables – separated by barriers that scale with N and finding the truly absolute minimum is hardly non-trivial. Many interesting optimisation problems have the great advantage of being defined on random graphs and are then mean-field in nature. The mean-field machinery that we shall discuss at length is then applicable to these problems with minor (or not so minor) modifications due to the finite connectivity of the networks. Let us illustrate this with one example. In *graph partitioning* the problem is how to partition, in the optimal way, a graph with N vertices and K links between them in two groups of equal size $N/2$ and the minimal the number of edges between them. This problem is encountered, for example, in computer design where one wishes to partition the circuits of a computer between two chips.

Complexity theory in computer science, and the classification of optimisation problems in classes of complexity – P for problems solved with algorithms that use a number of operations that grows as a polynomial of the number of variables, *e.g.* as N^2 or even N^{100}, NP for problems for which no polynomial algorithm is known and one needs a number of operations that grow exponentially with N, *etc.* – applies to the worst instance of a problem. Worst instance, in the graph-partitioning example, means the worst possible

realization of the connections between the nodes. Knowing which one this is is already a very hard problem!

But one can try to study optimisation problems on average, meaning that the question is to characterize the *typical* – and not the *worst* – realization of a problem. The use of techniques developed in the field of disordered physical systems, notably spin-glasses, have proven extremely useful to tackle typical single randomly generated instances of hard optimization problems.

Note that in statistical mechanics information about averaged macroscopic quantities is most often sufficiently satisfactory to consider a problem solved. In the optimisation context one seeks for exact microscopic configurations that correspond to the exact ground state and averaged information is not enough. Nevertheless, knowledge about the averaged behaviour can give us qualitative information about the problem that might be helpful to design powerful algorithms to attack single instances.

1.3.2 Biological applications

In the biological context disordered models have been used to describe neural networks, *i.e.* an ensemble of many neurons (typically $N \sim 10^9$ in the human brain) with a very elevated connectivity. Indeed, each neuron is connected to $\sim 10^4$ other neurons and receiving and sending messages *via* their axons. Moreover, there is no clear-cut notion of distance in the sense that axons can be very long and connections between neurons that are far away have been detected. Hebb proposed that the memory lies in the connections and the peculiarity of neural networks is that the connectivity must then change in time to incorporate the process of learning.

The simplest neural network models [5] represent neurons with Boolean variables or spins, that either fire or are quiescent. The interactions link pairs of neurons and they are assumed to be symmetric (which is definitely not true). Memory of an object, action, *etc.* is associated to a certain pattern of neuronal activity. It is then represented by an N-component vector in which each component corresponds to the activity of each neuron. Finally, sums over products of these patterns constitute the interactions. As in optimization problems, one can study the particular case associated to a number of chosen specific patterns to be stored and later recalled by the network, or one can try to answer questions on average, as how many typical patterns can a network of N neurons store. The models then become fully-connected or dilute models of spins with quenched disorder.

Another field of application of disordered system techniques is the description of hetero-polymers and, most importantly, protein folding. The question is how to describe the folding of a linear primary structure (just the sequence of different amino-acids along the main backbone chain) into an (almost) unique compact native structure whose shape is intimately related to the biological function of the protein. In modeling these very complex systems one proposes that the non-random, selected through evolution, macromolecules may be mimicked by random polymers. This assumption is based on the fact that amino-acids along the chain are indeed very different. One then uses monomer-monomer and/or monomer-solvent interactions that are drawn from some probability distribution and are fixed in time (quenched disorder). Still, a long bridge between the theoretical physicists' and the biologists' approaches remain to be crossed. Some of the important missing links are: proteins are mesoscopic objects with of the order of 100 monomers thus far from the thermodynamic limit; interest is in the particular, and not averaged, case in biology, in other words, one would really like to know what is the secondary structure of a particular primary sequence; *etc.*

1.3.3 Dynamics

In all these interdisciplinary problems dynamical questions are very important. In the combinatorial optimisation context, the complexity of a problem is given by the time needed to solve it. In this context, the microscopic dynamics is not dictated by physical rules but it can be chosen at will to render the resolution of the problem as fast as possible. However, glassy aspects, as the proliferation of metastable states separated by barriers that grow very fast with the number of variables can hinder the resolutions of these problems in polynomial time for *any* algorithm.

In the neural network context the microscopic dynamics cannot be chosen at will but, in general, will not be as simple as the single spin flip ones used in more conventional physical problems. Still, if the disordered modelling is correct, glassy aspects can render recall very slow due to the presence of metastable states for certain values of the parameters.

In the protein folding problem it is clear that the time needed to reach the secondary structure from an initially stretched configuration depends strongly on the existence of metastable states that could trap the (hetero)

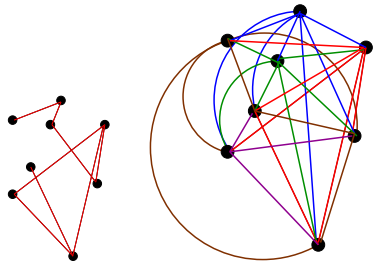

Figure 5: Left: random graph with finite connectivity; right: the fully-connected case.

polymer. Glassy aspects have been conjectured to appear in this context too.

1.4 Summary

The main steps in the development and application of Statistical Mechanics ideas to macroscopic cooperative systems have been (1) the development of the basic ideas (Boltzmann-Gibbs); (2) the recognition of collective phenomena and the identification and mean-field description of phase transitions (Curie-Weiss); (3) the correct description of critical phenomena with scaling theories and the renormalization group (Kadanoff, Widom, M. Fisher, Wilson) and more recently the development of conformal field theories for two-dimensional systems; (4) the study of stochastic processes and time-dependent properties (Langevin, Fokker-Planck, Glauber, *etc.*).

To describe disordered systems the same route has been followed. There is no doubt that, in principle, Equilibrium Statistical Mechanics yields the static properties of these systems. Although this might be a little irrelevant from the practical point of view since, most disordered systems are out of equilibrium in laboratory time-scales, it is certainly a necessary step on which one can try to build a truly dynamic theory. The mean-field study – step (2) – of the equilibrium properties of disordered systems, in particular those with quenched disorder, has revealed an incredibly rich theoretical structure. We still do not know whether it carries through to finite dimensional cases. Even though, it is definitely interesting *per se* and it finds a very promising field of application in combinatorial optimisation problems that are defined on random networks with mean-field character. Scaling arguments have been applied to describe finite dimensional disordered systems but they remain – as

their parent ones for clean systems – quite phenomenological and difficult to put to sufficiently restrictive numerical or experimental test. The extension of renormalisation group methods to systems with quenched disorder is also under development and still needs quite a lot of work – step (3). As for the out of equilibrium dynamics of these systems, again, it has been solved at the mean-field level but little is known in finite dimensions – apart from numerical simulations or the solution to toy models. As in its static counterpart, the results from the study of dynamic mean-field models have been very rich and they have suggested a number of new phenomena later searched for in numerical simulations and experiments of finite dimensional systems. In this sense, these solutions have been a very important source of inspiration.

2 Phase transitions

2.1 Order and disorder

Take a piece of material in contact with an external reservoir. The material will be characterized by certain observables, energy, magnetization, *etc.*. To characterize macroscopic systems it is convenient to consider densities of energy, magnetization, *etc*, by diving the macroscopic value by the number of particles (or the volume) of the system. The external environment will be characterized by some parameters, like the temperature, magnetic field, pressure, *etc.* In principle, one is able to tune the latter and the former will be a function of them.

Sharp changes in the behavior of macroscopic systems at critical point (lines) in parameter space have been observed experimentally. These correspond to phase transitions, a non-trivial collective phenomenon appearing in the thermodynamic limit. In this Section we shall review the main features of, and analytic approaches used to study, phase transitions.

When one cools down a magnetic sample it undergoes a sharp change in structure, as shown by a sharp change in its macroscopic properties, at a well-defined value of the temperature which is called the *critical temperature* or the Curie temperature. Assuming that this *annealing* process is done in equilibrium, that is to say, that at each temperature step the system manages to equilibrate with its environment after a relatively short transient – an assumption that is far from being true in *glassy* systems but that can be safely assumed in this context – the two states above and below T_c are equilibrium states that can be studied with the standard Statistical Mechanics tools.

More precisely, at T_c the equilibrium magnetization density changes from 0 above T_c to a finite value below T_c. The high temperature state is a *disordered* paramagnet while the low temperature state is an *ordered* ferromagnet.

One identifies the magnetization density as the *order parameter* of the phase transition. It is a macroscopic observable that vanishes above the transition and takes a continuously varying value below T_c. The transition is said to be continuous since the order parameter grows continuously from zero at T_c.

If one looks in more detail into the behavior of the variation of the mag-

netization density close T_c one would realize that the magnetic *susceptibility*,

$$\left.\frac{\partial m_h}{\partial h}\right|_{h=0} = \left.\frac{\partial}{\partial h}\left(-\frac{\partial}{\partial h} f_h\right)\right|_{h=0} \tag{2.1}$$

i.e. the linear variation of the magnetization density with respect to its conjugate magnetic field h diverges when approaching the transition from both sides. As the second identity shows, the susceptibility is just a second derivative of the free-energy density. Thus, a divergence of the susceptibility indicates a *non-analyticity* of the free-energy density. This can occur only in the infinite volume or *thermodynamic limit*, $N \to \infty$. Otherwise the free-energy density is just the logarithm of the partition function, a finite number of terms that are exponentials of analytic functions of the parameters, and thus an analytic function of the external parameters itself.

What is observed near such a critical temperature are called *critical phenomena*. Since the pioneering work of Curie, Langevin and others, the two phases, paramagnetic and ferromagnetic are well-understood. Qualitative arguments as well as the mean-field approach capture the two phases and their main characteristics. However, what happens close to the critical point has remained difficult to describe quantitatively until the development of scaling and the renormalization group.

2.2 Discussion

Let us discuss some important concepts, pinning fields, broken ergodicity and broken symmetry, with the help of a concrete example, the Ising model. The dicussion is however much more general and introduces the concepts mentioned above.

2.2.1 Order parameters

An order parameter is generically defined as a quantity – the average of an observable – that vanishes in one phase and is different from zero in another one (or other ones). One must notice though that the order parameter is not unique (any power of an order parameter is itself an order parameter) and that there can exist transition without an order parameter as the Kosterlitz-Thouless one in the $2d$ xy model. In the rest of this course we focus on problem that do have an order parameter defined as the thermal average of some observable.

2.2.2 Thermodynamic limit

The abrupt change in the order parameter at a particular value of the external parameters (T, h) is associated to the divergence of some derivative of the free-energy with respect to one of these parameters. The free-energy is a sum of positive terms. In a system with a finite number of degrees of freedom (as, for instance, in an Ising spin model where the sum has 2^N terms with N the number of spins) such a sum is an analytic function of the parameters. Thus, no derivative can diverge. One can then have a phase transition only in the *thermodynamic limit* in which the number of degrees of freedom diverges.

2.2.3 Pinning field

In the absence of a magnetic field for pair interactions the energy is an even function of the spins, $E(\vec{s}) = E(-\vec{s})$ and, consequently, the equilibrium magnetization density computed as an average over *all* spin configurations with their canonical weight, $e^{-\beta H}$, vanishes at *all* temperatures.

At high temperatures, $m = 0$ characterizes completely the equilibrium properties of the system since there is a unique paramagnetic state with vanishing magnetization density. At low temperatures instead if we perform an experiment we *do observe* a net magnetization density. In practice, what happens is that when the experimenter takes the system through the transition one cannot avoid the application of tiny external fields – the experimental set-up, the Earth... – and there is always a small *pinning field* that actually selects one of the two possible equilibrium states, with positive of negative magnetization density, allowed by symmetry. In the course of time, the experimentalist should see the full magnetization density reverse, however, this is not seen in practice since astronomical time-scales would be needed. We shall see this phenomenon at work when solving mean-field models exactly below.

2.2.4 Broken ergodicity

Introducing dynamics into the problem[2], ergodicity breaking can be stated as the fact that the temporal average over a long (but finite) time window is different from the statical one, with the sum running over all configurations

[2]Note that Ising model does not have a natural dynamics associated to it. We shall see in Section **??** how a dynamic rule is attributed to the evolution of the spins.

with their associated Gibbs-Boltzmann weight:

$$\overline{A} \neq \langle A \rangle \, . \tag{2.2}$$

In practice the temporal average is done in a long but finite interval $\tau_0 \ll \tau < \infty$. During this time, the system is positively or negatively magnetized depending on whether it is in one or the other degenerate equilibrium states. Thus, the temporal average of the orientation of the spins, for instance, yields a non-vanishing result $\overline{A} = m \neq 0$. If, instead, one computes the statistical average summing over *all* configurations of the spins, the result is zero, as one can see using just symmetry arguments. The reason for the discrepancy is that with the time average we are actually summing over half of the available configurations of the system. If time τ is not as large as a function of N, the trajectory does not have enough time to visit all configurations in phase space. One can reconcile the two results by, in the statistical average, summing only over the configurations with positive (or negative) magnetization density. We shall see this at work in a concrete calculation below.

2.2.5 Spontaneous broken symmetry

In the absence of an external field the Hamiltonian is symmetric with respect to the simultaneous reversal of all spins, $s_i \to -s_i$ for all i. The phase transition corresponds to a *spontaneous symmetry breaking* between the states of positive and negative magnetization. One can determine the one that is chosen when going through T_c either by applying a small *pinning field* that is taken to zero only after the thermodynamic limit ($h \to 0$ $N \to \infty$), or by imposing adequate boundary conditions like, for instance, all spins pointing up on the borders of the sample. Once a system sets into one of the equilibrium states this is completely stable in the $N \to \infty$ limit.

Ergodicity breaking necessarily accompanies spontaneous symmetry breaking but the reverse is not true. Indeed, spontaneous symmetry breaking generates disjoint ergodic regions in phase space, related by the broken symmetry, but one cannot prove that these are the only ergodic components in total generality. Mean-field spin-glass models provide a counterexample of this implication with a number of equilibrium states not related by symmetry.

2.3 Mean-field theory

In spite of their apparent simplicity, the statics of ferromagnetic Ising models has been solved analytically only in one and two dimensions. The mean-field approximation allows one to solve the Ising model in *any* spatial dimensionality. Even if the qualitative results obtained are correct, the quantitative comparison to experimental and numerical data shows that the approximation fails below an *upper critical dimension* d_u in the sense that it does not capture correctly the behaviour of the systems close to the critical point. It is however very instructive to see the mean-field approximation at work.

2.3.1 The naive mean-field approximation

The naive mean-field approximation consists in assuming that the probability density of the system's spin configuration is factorizable in independent factors

$$P(\{s_i\}) = \prod_{i=1}^{N} P_i(s_i) \qquad \text{with} \qquad P_i(s_i) = \frac{1+m_i}{2}\delta_{s_i,1} + \frac{1-m_i}{2}\delta_{s_i,-1} \quad (2.3)$$

and $m_i = \langle\, s_i \,\rangle$, where the thermal average has to be interpreted in the restricted sense described in the previous sections, *i.e.* taken over one ergodic component, in such a way that $m_i \neq 0$. Note that one introduces an order-parameter dependence in the probabilities. Using this assumption one can compute the total free-energy

$$F = U - TS \quad (2.4)$$

where the energy average is taken with the factorized probability distribution (2.3) and the entropy S is given by ($k_B = 1$)

$$S = -\sum_{\{s_i\}} P(\{s_i\}) \ln P(\{s_i\}) \; . \quad (2.5)$$

One can use this approximation to treat finite dimensional models. [3] Applied to the d-dimensional pure ferromagnetic Ising model with nearest-neighbor interactions on a cubic lattice $J_{ij} = J/2$ for nearest-neighbors and

[3] Note that this approximation amounts to replace the exact equation $m_i = \langle \tanh \beta(h + \sum_j J_{ij} s_j) \rangle$ by $m_i = \tanh \beta(h + \sum_j J_{ij} m_j)$.

zero otherwise. One finds the internal energy

$$U = -\frac{J}{2}\sum_{\langle ij\rangle}\langle s_i s_j\rangle - h\sum_i \langle s_i\rangle = -\frac{J}{2}\sum_{\langle ij\rangle} m_i m_j - h\sum_i m_i \ , \qquad (2.6)$$

and the entropy

$$\begin{aligned} S &= -\sum_{s_i=\pm 1}\prod_{k=1}^{N} P_k(s_k)\ln\prod_{l=1}^{N} P_l(s_l) = -\sum_{l=1}^{N}\sum_{s_n=\pm 1}\left[P_l(s_l)\ln P_l(s_l)\prod_{k(\neq l)} P_k(s_k)\right] \\ &= -\sum_{l=1}^{N}\sum_{s_l=\pm 1} P_l(s_l)\ln P_l(s_l) \\ &= -\sum_i \left[\frac{1+m_i}{2}\ln\frac{1+m_i}{2} + \frac{1-m_i}{2}\ln\frac{1-m_i}{2}\right] \ . \end{aligned} \qquad (2.7)$$

For a uniformly applied magnetic field, all local magnetization equal the total density one, $m_i = m$, and one has the 'order-parameter dependent' free-energy density:

$$f(m) = -dJm^2 - hm + T\left[\frac{1+m}{2}\ln\frac{1+m}{2} + \frac{1-m}{2}\ln\frac{1-m}{2}\right] \ . \qquad (2.8)$$

The extrema, $df(m)/dm = 0$, are given by

$$m = \tanh\left(\beta 2dJm + \beta h\right) \ , \qquad (2.9)$$

with the factor $2d$ coming from the connectivity of the cubic lattice. The stable states are those that also satisfy $d^2f/dm^2 > 0$. This *equation of state* predicts a second order phase transition at $T_c = 2dJ$ when $h = 0$.

Taking the derivative of m with respect to h and the limit $h \to 0^{\pm}$ one easily finds that

$$\chi \equiv \partial m/\partial h|_{h\to 0^{\pm}} = \frac{\beta}{\cosh^2(2dJ\beta m) - 2dJ\beta} \qquad (2.10)$$

that, when $T \to T_c$ approaches

$$\chi \to \frac{T/T_c}{|T - T_c|} \sim \frac{1}{|T - T_c|} \ , \qquad (2.11)$$

and diverges as $|T - T_c|$.

This result is qualitatively correct in the sense that T_c increases with increasing d but the actual value is incorrect in all finite dimensions. In particular, this treatment predicts a finite T_c in $d = 1$ which is clearly wrong. The critical behavior is also incorrect in all finite d, with exponents that do not depend on dimensionality and take the mean-field values. Still, the nature of the *qualitative* paramagnetic-ferromagnetic transition in $d > 1$ is correctly captured. We postpone the study of the solutions to eq. (2.9) to the next Subsection where we shall treat a similar, and in some respects, more general case.

Having an expression for the free-energy density as a function of the order parameter, that is determined by eq. (2.9), one can compute all observables and, in particular, their critical behavior. The Taylor expansion of the free-energy in powers of m, close to the critical point where $m \sim 0$, yields the familiar crossover from a function with a single minima at m to the double well form:

$$-\beta f(m) \sim \frac{1}{2}(T - 2dJ)m^2 + \frac{T}{12}m^4 - hm \; . \tag{2.12}$$

Indeed, below $T = 2dJ = T_c$ the sign of the quadratic term becomes negative and the function develops two minima away from $m = 0$.

Another way of deriving the mean-field approximation is to first single out a spin s_i and then write

$$s_j = m + \delta s_j \tag{2.13}$$

for the surrounding spins, with $\delta s_j \ll m$. One then replaces s_j by this expression in the quadratic term in the energy, where m is the global magnetization density. Keeping only the leading term, one finds a model with N non-interacting Ising spins coupled to a field, h_{eff}, that depends on m, $H(m) = -h_{eff} \sum_i s_i = -(Jzm + h) \sum_i s_i$, where h is a uniform external field and z is the connectivity of the lattice, $z = 2d$ for the cubic case. One has to determine m self-consistently by requiring $\langle s_i \rangle = m$. This way of presenting the approximation makes the "mean field" character of it more transparent. This approach is what is usually called Weiss mean-field theory.

One can see that the more spins interact with the chosen one the closer the spin sees an average field, *i.e.* the mean-field. The number of interacting spins increases with the range of interaction and the dimension in a problem with nearest neighbour interactions on a lattice.

2.3.2 The fully-connected Ising ferromagnet

Let us now solve exactly the fully-connected Ising ferromagnet with interactions between all p uplets of spins in an external field:

$$H = -\sum_{i_1 \neq \ldots \neq i_p} J_{i_1 \ldots i_p} s_{i_1} \ldots s_{i_p} - \sum_i h_i s_i \ , \tag{2.14}$$

$s_i = \pm 1$, $i = 1, \ldots, N$. For the sake of generality we use a generic interaction strength $J_{i_1 \ldots i_p}$. The ferromagnetic model corresponds to

$$J_{i_1 \ldots i_p} = \frac{J}{p! N^{p-1}} \tag{2.15}$$

with $0 < J = O(1)$, *i.e.* finite, and p is a fixed integer parameter, $p = 2$ or $p = 3$ or ..., that defines the model. The normalization with N^{p-1} of the first term ensures an extensive energy in the ferromagnetic state at low temperatures, and thus a sensible thermodynamic limit. The factor $p!$ is chosen for later convenience. This model is a source of inspiration for more elaborate ones with dilution and/or disorder.

Naive mean-field approximation

Using the factorization of the joint probability density that defines the mean-field approximation, one finds

$$\begin{aligned} F(\{m_i\}) &= -\sum_{i_1 \neq \ldots \neq i_p} J_{i_1 \ldots i_p} m_{i_1} \ldots m_{i_p} - \sum_i h_i m_i \\ &\quad + T \sum_{i=1}^{N} \left[\frac{1+m_i}{2} \ln \frac{1+m_i}{2} + \frac{1-m_i}{2} \ln \frac{1-m_i}{2} \right] \ . \end{aligned} \tag{2.16}$$

Note that a Taylor expansion of the entropic contribution around $m_i = 0$ leads to a polynomial expression that is the starting point in the Landau theory of second order phase transitions.

The local magnetizations, m_i, are then determined by requiring that they minimize the free-energy density, $\partial f(\{m_j\})/\partial m_i = 0$ and a positive definite Hessian, $\partial^2 f(\{m_j\})/\partial m_i \partial m_j$ (*i.e.* with all eigenvalues being positive at the extremal value). This yields

$$m_i = \tanh \left(p\beta \sum_{i_2 \neq \ldots \neq i_p} J_{i i_2 \ldots i_p} m_{i_2} \ldots m_{i_p} + \beta h_i \right) \tag{2.17}$$

If $J_{i_1 \ldots i_p} = J/(p! N^{p-1})$ for all p uplets and the applied field is uniform, $h_i = h$, one can take $m_i = m$ for all i and these expressions become (2.19) and (2.22) below, respectively. The mean-field approximation is exact for the fully-connected pure Ising ferromagnet, as we shall show below. [Note that the fully-connected limit of the model with pair interactions ($p = 2$) is correctly attained by taking $J \to J/N$ and $2d \to N$ in (2.9) leading to $T_c = J$.]

Exact solution

Let us solve the ferromagnetic model exactly. The sum over spin configurations in the partition function can be traded for a sum over the variable, $x = N^{-1} \sum_{i=1}^{N} s_i$, that takes values $x = -1, -1 + 2/N, -1 + 4/N, \ldots, 1 - 4/N, 1 - 2/N, 1$. Neglecting subdominant terms in N, one then writes

$$Z = \sum_x e^{-N\beta f(x)} \tag{2.18}$$

with the x-parameter dependent 'free-energy density'

$$f(x) = -\frac{J}{p!} x^p - hx + T \left[\frac{1+x}{2} \ln \frac{1+x}{2} + \frac{1-x}{2} \ln \frac{1-x}{2} \right] . \tag{2.19}$$

The first two terms are the energetic contribution while the third one is of entropic origin since $N!/(N(1+x)/2)!(N(1-x)/2)!$ spin configurations have the same magnetization density. The average of the parameter x is simply the averaged magnetization density:

$$\langle\, x \,\rangle = \frac{1}{N} \sum_{i=1}^{N} \langle\, s_i \,\rangle = m \tag{2.20}$$

In the large N limit, the partition function – and all averages of x – can be evaluated in the saddle-point approximation

$$Z \approx \sum_\alpha e^{-N\beta f(x_{sp}^\alpha)} \qquad , \tag{2.21}$$

where x_{sp}^α are the absolute minima of $f(x)$ given by the solutions to $\partial f(x)/\partial x|_{x_{sp}} = 0$,

$$x_{sp} = \tanh \left(\frac{\beta J}{(p-1)!} x_{sp}^{p-1} + \beta h \right) , \tag{2.22}$$

together with the conditions $d^2 f(x)/dx^2|_{x_{sp}^\alpha} > 0$. Note that the contributing saddle-points should be degenerate, *i.e.* have the same $f(x_{sp}^\alpha)$ for all α,

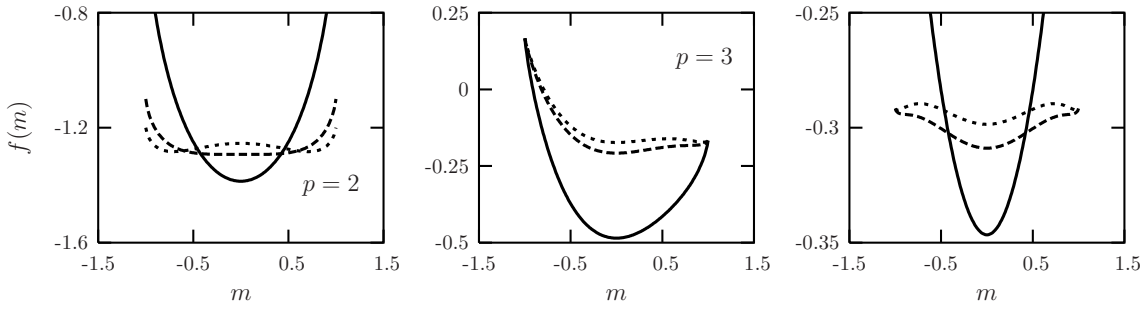

Figure 6: The free-energy density $f(m)$ of the $p = 2$ (left), $p = 3$ (center) and $p = 4$ (right) models at three values of the temperature $T < T_c$ (light dashed line), $T = T_c$ (dark dashed line) and $T > T_c$ (solid line) and with no applied field. (The curves have been translated vertically.)

otherwise their contribution is exponentially suppressed. The sum over α then just provides a numerical factor of two in the case $h = 0$. Now, since

$$x_{sp} = -\partial f(x)/\partial h|_{x_{sp}} = \langle\, x \,\rangle = m \;, \tag{2.23}$$

as we shall show in Eq. (2.24), the solutions to the saddle-point equations determine the order parameter. We shall next describe the phases and phase transition qualitatively and we shall later justify this description analytically.

Model in a finite field

In a finite magnetic field, eq. (2.22) has a unique positive – negative – solution for positive – negative – h at all temperatures. The model is ferromagnetic at all temperatures and there is no phase transition in this parameter.

2nd order transition for $p = 2$

In the absence of a magnetic field this model has a paramagnetic-ferromagnetic phase transition at a finite T_c. The order of the phase transition depends on the value of p. This can be seen from the temperature dependence of the free-energy density (2.19). Figure 6 displays $f(x)$ in the absence of a magnetic field at three values of T for the $p = 2$ (left), $p = 3$ (center) and $p = 4$ (right) models (we call the independent variable m since the stationary points of $f(x)$

are located at the magnetization density of the equilibrium and metastable states, as we shall show below). At high temperature the unique minimum is $m = 0$ in all cases. For $p = 2$, when one reaches T_c, the $m = 0$ minimum splits in two that slowly separate and move towards higher values of $|m|$ when T decreases until reaching $|m| = 1$ at $T = 0$ (see Fig. 6-left). The transition occurs at $T_c = J$ as can be easily seen from a graphical solution to eq. (2.22), see Fig. 7-left. Close but below T_c, the magnetization increases as $m \sim (T_c - T)^{\frac{1}{2}}$. The linear magnetic susceptibility has the usual Curie behavior at very high temperature, $\chi \approx \beta$, and it diverges as $\chi \sim |T - T_c|^{-1}$ on both sides of the critical point. The order parameter is continuous at T_c and the transition is of second-order thermodynamically.

1st order transition for $p > 2$

For $p > 2$ the situation changes. For even values of p, at T^* two minima (and two maxima) at $|m| \neq 0$ appear. These coexist as metastable states with the stable minimum at $m = 0$ until a temperature T_c at which the three free-energy densities coincide, see Fig. 6-right. Below T_c the $m = 0$ minimum continues to exist but the $|m| \neq 0$ ones are favored since they have a lower free-energy density. For odd values of p the free-energy density is not symmetric with respect to $m = 0$. A single minimum at $m^* > 0$ appears at T^* and at T_c it reaches the free-energy density of the paramagnetic one, $f(m^*) = f(0)$, see Fig. 6-center. Below T_c the equilibrium state is the ferromagnetic minimum. For all $p > 2$ the order parameter is discontinuous at T_c, it jumps from zero at T_c^+ to a finite value at T_c^-. The linear magnetic susceptibility also jumps at T_c. While it equals β on the paramagnetic side, it takes a finite value given by eqn. (2.25) evaluated at m^* on the ferromagnetic one. In consequence, the transition is of first-order.

Pinning field, broken ergodicity and spontaneous broken symmetry

The saddle-point equation (2.22) for $p = 2$ [or the mean-field equation (2.9)] admits two equivalent solutions in no field. What do they correspond to? They are the magnetization density of the equilibrium ferromagnetic states with positive and negative value. At $T < T_c$ if one computes $m = N^{-1} \sum_{i=1}^{N} \langle s_i \rangle = \sum_x e^{-\beta N f(x)} x$ summing over the two minima of the free-energy density one finds $m = 0$ as expected by symmetry. Instead, if one computes the averaged magnetization density with the partition sum restricted to the configurations with positive (or negative) x one finds

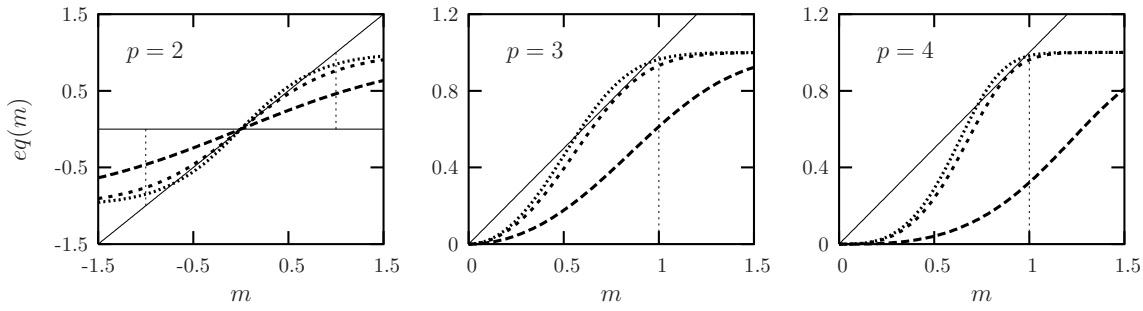

Figure 7: Graphical solution to the equation fixing the order parameter x for $p = 2$ (left), $p = 3$ (center) and $p = 4$ (right) ferromagnetic models at three values of the temperature $T < T^*$, $T = T^*$ and $T > T^*$ and with no applied field. Note that the rhs of this equation is antisymmetric with respect to $m \to -m$ for odd values of p while it is symmetric under the same transformation for even values of p. We show the positive quadrant only to enlarge the figure. T^* is the temperature at which a second minimum appears in the cases $p = 3$ and $p = 4$.

$m = |m_{sp}|$ (or $m = -|m_{sp}|$).

In practice, the restricted sum is performed by applying a small magnetic field, computing the statistical properties in the $N \to \infty$ limit, and then setting the field to zero. In other words,

$$m_{\pm} \equiv \frac{1}{N} \sum_{i=1}^{N} \langle\, s_i \,\rangle_{\pm} = \left(\frac{1}{\beta N} \, \frac{\partial \ln Z}{\partial h} \right) \Bigg|_{h \to 0^{\pm}} = - \left. \frac{\partial f(x_{sp})}{\partial h} \right|_{h \to 0^{\pm}} = \pm |x_{sp}| \quad (2.24)$$

By taking the $N \to \infty$ limit in a field one selects the positive (or negatively) magnetized states.

For all odd values of p the phase transition is not associated to symmetry breaking, since there is only one non-degenerate minimum of the free-energy density that corresponds to the equilibrium state at low temperature. The application of a pinning field is then superfluous.

For any even value of p and at all temperatures the free-energy density in the absence of the field is symmetric with respect to $m \to -m$, see the left and right panels in Fig. 6. The phase transition corresponds to a *spontaneous symmetry breaking* between the states of positive and negative magnetization. One can determine the one that is chosen when going through T_c either by applying a small *pinning field* that is taken to zero only after the thermodynamic limit, or by imposing adequate boundary conditions. Once a system sets into one of the equilibrium states this is completely stable in the $N \to \infty$ limit. In pure static terms this means that one can separate the sum over all spin configurations into independent sums over different sectors of phase space that correspond to each equilibrium state. In dynamic terms it means that temporal and statistical averages (taken over all configurations) in an infinite system do not coincide.

The magnetic linear susceptibility for generic p is a simple generalization of the expression in (2.10) and it is given by

$$\chi \equiv \left. \frac{\partial m}{\partial h} \right|_{h \to 0^{\pm}} = \left. \frac{\partial x_{sp}}{\partial h} \right|_{h \to 0^{\pm}} = \frac{\beta}{\cosh^2\!\left(\frac{\beta J}{(p-1)!}\, x_{sp}^{p-1}\right) - \frac{\beta J}{(p-2)!} x_{sp}^{p-2}} \,. \quad (2.25)$$

For $p = 2$, at $T > T_c$, $x_{sp} = 0$ the susceptibility is given by $(T - J)^{-1}$ predicting the second order phase transition with a divergent susceptibility at $T_c = J$. Approaching T_c from below the two magnetized states have the same divergent susceptibility, $\chi \sim (T_c - T)^{-1}$.

For $p > 2$, at $T > T_c$, $x_{sp} = 0$ and the susceptibility takes the Curie form $\chi = \beta$. The Curie law, $\chi = \beta$, jumps to a different value at the critical temperature due to the fact that x_{sp} jumps.

3 Disordered systems

No material is perfectly homogeneous: impurities of different kinds are distributed randomly throughout the samples.

A natural effect of disorder should be to lower the critical temperature. Much attention has been payed to the effect of weak disorder on phase transitions, that is to say, situations in which the nature of the ordered and disordered phases is not modified by the impurities but the critical phenomenon is. On the one hand, the critical exponents of second order phase transitions might be modified by disorder, on the other hand, disorder may smooth out the discontinuities of first order phase transitions rendering them of second order. Strong disorder instead changes the nature of the low-temperature phase and before discussing the critical phenomenon one needs to understand how to characterize the new ordered 'glassy' phase.

In this Section we shall discuss several types of *quenched* disorder and models that account for it. We shall also overview some of the theoretical methods used to deal with the static properties of models with quenched disorder, namely, scaling arguments and the droplet theory, mean-field equations, and the replica method.

3.1 Quenched and annealed disorder

First, one has to distinguish between quenched and annealed disorder. Imagine that one mixes some random impurities in a melt and then very slowly cools it down in such a way that the impurities and the host remain in thermal equilibrium. If one wants to study the statistical properties of the full system one has to compute the full partition function, summing over all configurations of original components and impurities. This is called annealed disorder. In the opposite case in which upon cooling the host and impurities do not equilibrate but the impurities remain blocked in random fixed positions, one talks about quenched disorder. Basically, the relaxation time associated with the diffusion of the impurities in the sample is so long that these remain trapped:

$$\tau_o \sim 10^{-12} - 10^{-15}\text{sec} \ll t_{obs} \sim 10^{4}\text{sec} \ll t_{diff} \ , \tag{3.1}$$

where τ_o is the microscopic time associated to the typical scale needed to reverse a spin.

The former case is easier to treat analytically but is less physically relevant. The latter is the one that leads to new phenomena and ideas that we shall discuss next.

3.2 Bond disorder: the case of spin-glasses

Spin-glasses are alloys in which magnetic impurities substitute the original atoms in positions randomly selected during the chemical preparation of the sample. The interactions between the impurities are of RKKY type:

$$V_{rkky} = -J \, \frac{\cos(2k_F r_{ij})}{r_{ij}^3} \, s_i s_j \tag{3.2}$$

with $r_{ij} = |\vec{r}_i - \vec{r}_j|$ the distance between them and s_i a spin variable that represents their magnetic moment. Clearly, the location of the impurities varies from sample to sample. The time-scale for diffusion of the magnetic impurities is much longer than the time-scale for spin flips. Thus, for all practical purposes the positions $\vec{r}_i$ can be associated to quenched random variables distributed according to a uniform probability distribution that in turn implies a probability distribution of the exchanges. This is quenched disorder.

3.2.1 Lack of homogeneity

It is clear that the presence of quench disorder, in the form of random interactions, fields, dilution, *etc.* breaks spatial homogeneity and renders single samples heterogenous. Homogeneity is recovered though, if one performs an average over all possible realizations of disorder, each weighted with its own probability.

3.2.2 Frustration

Depending on the value of the distance r_{ij} the numerator in eq. (3.2) can be positive or negative implying that both ferromagnetic and antiferromagnetic interactions exist. This leads to frustration, which means that some two-body interactions cannot be satisfied by any spin configuration. An example with four sites and four links is shown in Fig. 8-left, where

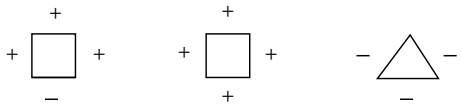

Figure 8: A frustrated (left) and an unfrustrated (center) square plaquette. A frustrated triangular plaquette (right).

we took three positive exchanges and one negative one all, for simplicity, with the same absolute value, J. Four configurations minimize the energy, $E_f = -2J$, but none of them satisfies the lower link. One can easily check that any closed loop such that the product of the interactions takes a negative sign is frustrated. Frustration naturally leads to a higher energy and a larger degeneracy of the number of ground states. This is again easy to grasp by comparing the number of ground states of the frustrated plaquette in Fig. 8-left to its unfrustrated counterpart shown on the central panel. Indeed, the energy and degeneracy of the ground state of the unfrustrated plaquette are $E_u = -4J$ and $n_u = 2$, respectively.

Frustration may also be due to pure geometrical constraints. The canonical example is an anti-ferromagnet on a triangular lattice in which each plaquette is frustrated, see Fig. 8-right. This is generically called geometric frustration.

In short, frustration arises when the geometry of the lattice and/or the nature of the interactions make impossible to simultaneously minimize the energy of all pair couplings between the spins. Any loop of connected spins is said to be frustrated if the product of the signs of connecting bonds is negative. In general, energy and entropy of the ground states increase due to frustration.

3.2.3 Gauge invariance

The gauge transformation

$$s'_i = \tau_i s_i \ , \qquad J'_{ij} = \tau_i J_{ij} \tau_j \ , \qquad \text{with} \qquad \tau_i = \pm 1 \tag{3.3}$$

leaves the energy and the partition function of an Ising spin model with two-body interactions invariant:

$$E_J[\{s\}] = E_{J'}[\{s'\}] \qquad Z_J = Z_{J'} \ . \tag{3.4}$$

This invariance means that all thermodynamic quantities are independent of the particular choice of the quenched disordered interactions.

Whenever it exists a set of τ_is such that frustration can be eliminated from all loops in the model, the effects of disorder are less strong than in trully frustrated cases, see the example of the Mattis model in Sect. 2.3.2.

3.2.4 Self-averageness

If each sample is characterized by its own realization of the exchanges, should one expect a totally different behavior from sample to sample? Fortunately, many generic static and dynamic properties of spin-glasses (and other systems with quenched disorder) do not depend on the specific realization of the random couplings and are self-averaging. This means that the typical value is equal to the average over the disorder:

$$A_J^{typ} = [\, A_J \,] \tag{3.5}$$

in the thermodynamic limit. More precisely, in self-averaging quantities sample-to-sample fluctuations with respect to the mean value are expected to be $\mathrm{O}(N^{-a})$ with $a > 0$. Roughly, observables that involve summing over the entire volume of the system are expected to be self-averaging. In particular, the free-energy density of models with short-ranged interactions is expected to be self-averaging in this limit.

An example: the disordered Ising chain

The meaning of this property can be grasped from the solution of the random bond Ising chain defined by the energy function $E = -\sum_i J_i s_i s_{i+1}$ with spin variables $s_i = \pm$, for $i = 1, \ldots, N$ and random bonds J_i independently taken from a probability distribution $P(J_i)$. For simplicity, we consider periodic boundary conditions. The disorder-dependent partition function reads

$$Z_J = \sum_{\{s_i = \pm 1\}} e^{\beta \sum_i J_i s_i s_{i+1}} \tag{3.6}$$

and this can be readily computed introducing the change of variables $\sigma_i \equiv s_i s_{i+1}$. One finds.

$$Z_J = \prod_i 2\cosh(\beta J_i) \qquad \Rightarrow \qquad -\beta F_J = \sum_i \ln\cosh(\beta J_i) + N \ln 2\,. \tag{3.7}$$

The partition function is a *product* of *i.i.d.* random variables and it is itself a random variable with a log-normal distribution. The free-energy density

instead is a *sum* of *i.i.d.* random variables and, using the central limit theorem, in the large N limit becomes a Gaussian random variable narrowly peaked at its maximum. The typical value, given by the maximum of the Gaussian distribution, coincides with the average, $\lim_{N\to\infty} f_J^{typ} - [\, f_J \,] = 0$.

General argument

A simple argument justifies the self-averageness of the free-energy density in generic finite dimensional systems with short-range interactions. Let us divide a, say, cubic system of volume $V = L^d$ in n subsystems, say also cubes, of volume $v = \ell^d$ with $V = nv$. If the interactions are short-ranged, the total free-energy is the sum of two terms, a contribution from the bulk of the subsystems and a contribution from the interfaces between the subsystems: $-\beta F_J = \ln Z_J = \ln \sum_{conf} e^{-\beta E_J(conf)} = \ln \sum_{conf} e^{-\beta E_J(bulk) - \beta E_J(surf)} \approx \ln \sum_{bulk} e^{-\beta E_J(bulk)} + \ln \sum_{surf} e^{-\beta E_J(surf)} = -\beta F_J^{bulk} - \beta F_J^{surf}$ (we neglected the contributions from the interaction between surface and bulk). If the interaction extends over a short distance σ and the linear size of the boxes is $\ell \gg \sigma$, the surface energy is negligible with respect to the bulk one and $-\beta F_J \approx \ln \sum_{bulk} e^{-\beta E_J(bulk)}$. In the thermodynamic limit, the disorder dependent free-energy is then a sum of $n = (L/\ell)^d$ random numbers, each one being the disorder dependent free-energy of the bulk of each subsystem: $-\beta F_J \approx \sum_{k=1}^{n} \ln \sum_{bulk_k} e^{-\beta E_J(bulk_k)}$. In the limit of a very large number of subsystems ($L \gg \ell$ or $n \gg 1$) the central limit theorem implies that the total free-energy is Gaussian distributed with the maximum reached at a value F_J^{typ} that coincides with the average over all realizations of the randomness $[\, F_J \,]$. Morever, the dispersion about the typical value vanishes in the large n limit, $\sigma_{F_J}/[\, F_J \,] \propto \sqrt{n}/n = n^{-1/2} \to 0$ in the large n limit. Similarly, $\sigma_{f_J}/[f_J] \sim O(n^{-1/2})$ where $f_J = F_J/N$ is the intensive free-energy. In a sufficiently large system the typical F_J is then very close to the averaged $[\, F_J \,]$ and one can compute the latter to understand the static properties of typical systems.

Lack of self-averageness in the correlation functions

Once one has $[F_J]$, one derives all disordered average thermal averages by taking derivatives of the disordered averaged free-energy with respect to sources introduced in the partition function. For example,

$$[\, \langle\, s_i \,\rangle\,] = - \left. \frac{\partial [\, F_J \,]}{\partial h_i} \right|_{h_i=0} , \tag{3.8}$$

$$[\langle s_i s_j \rangle - \langle s_i \rangle \langle s_j \rangle] = T \left. \frac{\partial [F_J]}{\partial h_i h_j} \right|_{h_i=0} , \tag{3.9}$$

with $E \to E - \sum_i h_i s_i$. Connected correlation functions, though, *are not* self-averaging quantities. This can be seen, again, studying the random bond Ising chain:

$$\langle s_i s_j \rangle_J - \langle s_i \rangle_J \langle s_j \rangle_J = Z_J^{-1} \frac{\partial}{\partial \beta J_i} \ldots \frac{\partial}{\partial \beta J_j} Z_J = \tanh(\beta J_i) \ldots \tanh(\beta J_j) \tag{3.10}$$

where we used $\langle s_i \rangle = 0$ (valid for a distribution of random bonds with zero mean) and the dots indicate all sites on the chain between the ending points i and j. The last expression is a product of random variables and it is not equal to its average (3.9) – not even in the large separation limit $|\vec{r}_i - \vec{r}_j| \to \infty$.

3.3 Models with quenched disorder

3.3.1 Spin-glass models

In the early 70s Edwards and Anderson proposed a rather simple model that should capture the main features of spin-glasses. The interactions (3.2) decay with a cubic power of the distance and hence they are relatively short-ranged. This suggests to put the spins on a regular cubic lattice model and to trade the randomness in the positions into random nearest neighbor exchanges taken from a Gaussian probability distribution:

$$E_{ea} = -\sum_{\langle ij \rangle} J_{ij} s_i s_j \qquad \text{with} \qquad P(J_{ij}) = (2\pi\sigma^2)^{-\frac{1}{2}} \, e^{-\frac{J_{ij}^2}{2\sigma^2}} . \tag{3.11}$$

The precise form of the probability distribution of the exchanges is suppose not to be important, though some authors claim that there might be non-universality with respect to it.

A natural extension of the EA model in which all spins interact has been proposed by Sherrington and Kirkpatrick

$$E = -\sum_{i \neq j} J_{ij} s_i s_j - \sum_i h_i s_i \tag{3.12}$$

and it is called the SK model. The interaction strengths J_{ij} are taken from a Gaussian pdf and they scale with N in such a way that the thermodynamic

is non-trivial:

$$P(J_{ij}) = (2\pi\sigma_N^2)^{-\frac{1}{2}}\, e^{-\frac{J_{ij}^2}{2\sigma_N^2}} \qquad\qquad \sigma_N^2 = \sigma^2 N\ . \tag{3.13}$$

The first two-moments of the exchange distribution are $[J_{ij}] = 0$ and $[J_{ij}^2] = J^2/(2N)$. This is a case for which a mean-field theory is expected to be exact.

A further extension of the EA model is called the *p spin model*

$$E = -\sum_{i_1<\ldots<i_p} J_{i_1\ldots i_p} s_{i_1}\ldots s_{i_p} - \sum_i h_i s_i \tag{3.14}$$

with $p \geq 3$. The sum can also be written as $\sum_{i_1<i_2<\ldots<i_p} = 1/p! \sum_{i_1\neq i_2\neq i_p}$. The exchanges are now taken from a Gaussian probability distribution

$$P(J_{ij}) = (2\pi\sigma_N^2)^{-\frac{1}{2}}\, e^{-\frac{J_{ij}^2}{2\sigma_N^2}} \qquad\qquad \sigma_N^2 = J^2 p!/(2N^{p-1})\ . \tag{3.15}$$

with $[J_{i_1\ldots i_p}] = 0$ and $[J_{i_1\ldots i_p}^2] = \frac{J^2 p!}{2N^{p-1}}$. Indeed, an extensive free-energy is achieved by scaling $J_{i_1\ldots i_p}$ with $N^{-(p-1)/2}$. This scaling can be justified as follows. The local field $h_i = 1/(p-1)! \sum_{ii_2\neq i_p} J_{ii_2\ldots i_p} m_{i_2}\ldots m_{i_p}$ should be of order one. At low temperatures the m_i's take plus and minus signs. In particular, we estimate the order of magnitude of this term by working at $T = 0$ and taking $m_i = \pm 1$ with probability $\frac{1}{2}$. In order to keep the discussion simple, let us take $p = 2$. In this case, if the strengths J_{ij}, are of order one, h_i is a sum of N *i.i.d.* random variables, with zero mean and unit variance[4], and h_i has zero mean and variance equal to N. Therefore, one can argue that h_i is of order $\sqrt{N}$. To make it finite we then chose J_{ij} to be of order $1/\sqrt{N}$ or, in other words, we impose $[\,J_{ij}^2\,] = J^2/(2N)$. The generalization to $p \geq 2$ is straightforward.

Cases that find an application in computer science are defined on random graphs with fixed or fluctuating finite connectivity. In the latter case one places the spins on the vertices of a graph with links between couples or groups of p spins chosen with a probability c. These are called dilute spin-glasses.

Exercise. Study the statics of the fully connected p-spin ferromagnet in which all coupling exchanges are equal to J. Distinguish the cases $p = 2$ from $p > 2$. What are the order of the phase transitions?

[4]The calculation goes as follow: $\langle\, F_i \,\rangle = \sum_j J_{ij} \langle\, m_j \,\rangle = 0$ and $\langle\, F_i^2 \,\rangle = \sum_{jk} J_{ij} J_{ik} \langle\, m_j m_k \,\rangle = \sum_j J_{ij}^2$

3.3.2 Random ferromagnets

Let us now discuss some, *a priori* simpler cases. An example is the Mattis random magnet in which the interaction strengths are given by

$$J_{i_1 \ldots i_p} = \xi_{i_1} \ldots \xi_{i_p} \qquad \text{with} \qquad \xi_j = \pm \quad \text{with} \quad p = 1/2 \; . \tag{3.16}$$

In this case a simple *gauge transformation*, $\eta_i \equiv \xi_i s_i$, allows one to transform the disordered model in a ferromagnet, showing that there was no true frustration in the system.

Random bond ferromagnets (RBFMs) are systems in which the strengths of the interactions are not all identical but their sign is always positive. One can imagine such a exchange as the sum of two terms:

$$J_{ij} = J + \delta J_{ij} \; , \qquad \text{with} \qquad \delta J_{ij} \qquad \text{small and random} \; . \tag{3.17}$$

There is no frustration in these systems either.

Models with site or link dilution are also interesting:

$$E_{site\ dil} = -J \textstyle\sum_{\langle ij \rangle} s_i s_j \epsilon_i \epsilon_j \; , \qquad E_{link\ dil} = -J \textstyle\sum_{\langle ij \rangle} s_i s_j \epsilon_{ij} \; , \qquad . \tag{3.18}$$

with $P(\epsilon_i = 0, 1) = p, 1 - p$ in the first case and $P(\epsilon_{ij} = 0, 1) = p, 1 - p$ in the second.

Link randomness is not the only type of disorder encountered experimentally. Random fields, that couple linearly to the magnetic moments, are also quite common; the classical model is the *ferromagnetic random field Ising model* (RFIM):

$$E_{rfim} = -J \sum_{\langle ij \rangle} s_i s_j - \sum_i s_i h_i \qquad \text{with} \qquad P(h_i) = (2\pi\sigma^2)^{-\frac{1}{2}} \; e^{-\frac{h_i^2}{2\sigma^2}} \; . \tag{3.19}$$

The *dilute antiferromagnet in a uniform magnetic field* is believed to behave similarly to the ferromagnetic random field Ising model. Experimental realizations of the former are common and measurements have been performed in samples like $Rb_2Co_{0.7}Mg_{0.3}F_4$.

Note that the up-down Ising symmetry is preserved in models in which the impurities (the J_{ij}'s) couple to the local energy (and there is no applied external field) while it is not in models in which they couple to the local order parameter (as the RFIM).

The random fields give rise to many metastable states that modify the equilibrium and non-equilibrium behaviour of the RFIM. In one dimension the RFIM does not order at all, in $d = 2$ there is strong evidence that the model is disordered even at zero temperature, in $d = 3$ it there is a finite temperature transition towards a ferromagnetic state. Whether there is a glassy phase near zero temperture and close to the critical point is still and open problem.

The RFIM at zero temperature has been proposed to yield a generic description of material cracking through a series of avalaches. In this problem one cracking domain triggers others, of which size, depends on the quenched disorder in the samples. In a random magnetic system this phenomenon corresponds to the variation of the magnetization in discrete steps as the external field is adiabatically increased (the time scale for an avalanche to take place is much shorter than the time-scale to modify the field) and it is accessed using Barkhausen noise experiments. Disorder is responsible for the jerky motion of the domain walls. The distribution of sizes and duration of the avalanches is found to decay with a power law tail cut-off at a given size. The value of the cut-off size depends on the strength of the random field and it moves to infinity at the critical point.

3.3.3 Random manifolds

Once again, disorder is not only present in magnetic systems. An example that has received much attention is the so-called random manifold. This is a d dimensional directed elastic manifold moving in an embedding $N + d$ dimensional space under the effect of a quenched random potential. The simplest case with $d = 0$ corresponds to a particle moving in an embedding space with N dimensions. If, for instance $N = 1$, the particle moves on a line, if $N = 2$ it moves on a plane and so on and so forth. If $d = 1$ one has a line that can represent a domain wall, a polymer, a vortex line, *etc.* The fact that the line is directed means it has a preferred direction, in particular, it does not have overhangs. If the line moves in a plane, the embedding space has $(N = 1) + (d = 1)$ dimensions. One usually describes the system with an N-dimensional coordinate, $\vec{\phi}$, that locates in the transverse space each point on the manifold, represented by the internal d-dimensional coordinate $\vec{x}$,

The elastic energy is $E_{elas} = \gamma \int d^d x \sqrt{1 + (\nabla \phi(\vec{x}))^2}$ with γ the deformation cost of a unit surface. Assuming the deformaiton is small one

can linearize this expression and get, upto an additive constant, $E_{elas} = \frac{\gamma}{2}\int d^dx\ (\nabla\phi(\vec{x}))^2$.

Disorder is introduced in the form of a random potential energy at each point in the $N+d$ dimensional space. The manifold feels, then a potential $V(\vec{\phi}(\vec{x}),\vec{x})$ characterized by its pdf. If the random potential is the result of a large number of impurities, the central limit theorem implies that its probability density is Gaussian. Just by shifting the energy scale one can set its average to zero, $[\,V\,]=0$. As for its correlations, one typically assumes, for simplicity, that they exist in the transverse direction only:

$$[\,V(\vec{\phi}(\vec{x}),\vec{x})V(\vec{\phi}'(\vec{x}'),\vec{x}')\,] = \delta^d(\vec{x}-\vec{x}')\mathcal{V}(\vec{\phi},\vec{\phi}')\ . \tag{3.20}$$

If one further assumes that there is a statistical isotropy and translational invariance of the correlations, $\mathcal{V}(\vec{\phi},\vec{\phi}') = W/\Delta^2\ \mathcal{V}(|\vec{\phi}-\vec{\phi}'|/\Delta)$ with Δ a correlation length and $(W\Delta^{d-2})^{1/2}$ the strength of the disorder. The disorder can now be of two types: short-ranged if $\mathcal{V}$ falls to zero at infinity sufficiently rapidly and long-range if it either grows with distance or has a slow decay to zero. An example involving both cases is given by the power law $\mathcal{V}(z) = (\theta+z)^{-\gamma}$ where θ is a short distance cut-off and γ controls the range of the correlations with $\gamma>1$ being short-ranged and $\gamma<1$ being long-ranged.

The random manifold model is then

$$H = \int d^dx \left[\frac{\gamma}{2}\left(\nabla\phi(\vec{x})\right)^2 + V(\vec{\phi}(\vec{x}),\vec{x})\right]\ . \tag{3.21}$$

This model also describes directed domain walls in random systems. One can derive it in the long length-scales limit by taking the continuum limit of the pure Ising part (that leads to the elastic term) and the random part (that leads to the second disordered potential). In the pure Ising model the second term is a constant that can be set to zero while the first one implies that the ground state is a perfectly flat wall, as expected. In cases with quenched disorder, the long-ranged and short-ranged random potentials mimic cases in which the interfaces are attracted by pinning centers ('random field' type) or the phases are attracted by disorder ('random bond' type), respectively. For instance, random bond disorder is typically described by a Gaussian pdf with zero mean and delta-correlated $[V(\vec{\phi}(\vec{x}),\vec{x}),V(\vec{\phi}'(\vec{x}'),\vec{x}')] = W\Delta^{d-2}\ \delta^d(\vec{x}-\vec{x}')\delta(\vec{\phi}-\vec{\phi}')$.

3.4 The spin-glass transition

Let us now discuss a problem in which disorder is so strong as to modify the nature of the low temperature phase. If this is so, one needs to define a new order parameter, capable of identifying order in this phase.

3.4.1 The simplest order parameter

The spin-glass equilibrium phase is one in which spins "freeze" in randomly-looking configurations. In finite dimensions these configurations are spatially irregular. A snapshot looks statistical identical to a high temperature paramagnetic configuration in which spins point in both directions. However, while at high temperatures the spins flip rapidly and another snapshot taken immediately after would look completely different from the previous one, at low temperatures two snapshots taken at close times are highly correlated.

In a spin-glass state the local magnetization is expected to take a non-zero value, $m_i = \langle\, s_i \,\rangle \neq 0$, where the average is interpreted in the restricted sense introduced in the discussion of ferromagnets, that we shall call here within a pure state (the notion of a pure state will be made more precise below). Instead, the total magnetization density, $m = N^{-1} \sum_{i=1}^{N} m_i$, vanishes since one expects to have as many averaged local magnetization pointing up ($m_i > 0$) as spins pointing down ($m_i < 0$) with each possible value of $|m_i|$. Thus, the *total magnetization*, m, of a spin-glass vanishes at all temperatures and it is not a good order parameter.

The spin-glass transition is characterized by a finite peak in the linear magnetic susceptibility and a diverging non-linear magnetic susceptibility. Let us discuss the former first and show how it yields evidence for the freezing of the local magnetic moments. For a generic magnetic model such that the magnetic field couples linearly to the Ising spin, $E \to E - \sum_i h_i s_i$, the linear susceptibility is related, via the static *fluctuation-dissipation theorem* to the correlations of the fluctuations of the magnetization:

$$\chi_{ij} \equiv \left. \frac{\partial \langle\, s_i \,\rangle_h}{\partial h_j} \right|_{h=0} = \beta \, \langle \, (s_i - \langle\, s_i \,\rangle)(s_j - \langle\, s_j \,\rangle) \, \rangle \; . \tag{3.22}$$

The averages in the rhs are taken without perturbing field. This relation is proven by using the definition of $\langle\, s_i \,\rangle_h$ and simply computing the derivative with respect to h_j. In particular,

$$\chi_{ii} = \beta \, \langle \, (s_i - \langle\, s_i \,\rangle)^2 \, \rangle = \beta \left(1 - m_i^2\right) \geq 0 \; , \tag{3.23}$$

with $m_i = \langle\, s_i \,\rangle$. The total susceptibility measured experimentally is $\chi \equiv N^{-1} \sum_{ij} \chi_{ij}$. On the experimental side we do not expect to see $O(1)$ sample-

to-sample fluctuations in this global quantity. On the analytical side one can use a similar argument to the one presented in Sect. 2.3.2 to argue that χ should be self-averaging (it is a sum over the entire volume of site-dependent terms). Thus, the experimentally observed susceptibility of sufficiently large samples should be given by

$$\chi = [\,\chi\,] = N^{-1} \sum_{ij} [\,\chi_{ij}\,] \approx N^{-1} \sum_{i} [\,\chi_{ii}\,] = N^{-1} \sum_{i} \beta \left(1 - [\,m_i^2\,]\right) \ , \quad (3.24)$$

since we can expect that cross-terms will be subleading in the large N limit under the disorder average (note that χ_{ij} can take negative values). The fall of χ at low temperatures with respect to its value at T_c, *i.e.* the *cusp* observed experimentally, signals the freezing of the *local magnetizations*, m_i, in the non-zero values that are more favourable thermodynamically. Note that this argument is based on the assumption that the measurement is done in equilibrium.

Thus, the natural and simpler global order parameter that characterizes the spin-glass transition is

$$q \equiv N^{-1} \sum_{i} [\,m_i^2\,] \quad (3.25)$$

as proposed in the seminal 1975 Edwards-Anderson paper. q vanishes in the high temperature phase since all m_i are zero but it does not in the low temperature phase since the square power takes care of the different signs. Averaging over disorder eliminates the site dependence. Thus, q is also given by

$$q = [\,m_i^2\,] \ . \quad (3.26)$$

These definitions, natural as they seem at a first glance, hide a subtle distinction that we discuss below.

3.4.2 Pure states and more subtle order parameters

Let us *keep disorder fixed* and imagine that there remain more than two pure or equilibrium states in the selected sample. A factor of two takes into account the spin reversal symmetry. in the following we shall consider half the phase space, getting rid of this 'trivial' symmetry. Consider the disorder-dependent quantity

$$q_J = N^{-1} \sum_{i} m_i^2 \quad (3.27)$$

where the m_i depend on the realization of the exchanges. Then, two possibilities for the statistical average in $m_i = \langle s_i \rangle$ have to be distinguished:

Restricted averages

If we interpret the statistical average in the same restricted sense as the one discussed in the paramagnetic - ferromagnetic transition of the usual Ising model, *i.e.* under a pinning field that selects *one* chosen pure state, in (3.27) we define a disorder and pure state dependent Edwards-Anderson parameter,

$$q^{\alpha}_{J\,ea} = N^{-1} \sum_{i}^{N} (m^{\alpha}_i)^2 \ , \tag{3.28}$$

where we label α the selected pure state. Although $q^{\alpha}_{J\,ea}$ could depend on α it turns out that in all known cases it does not and the α label is superfluos.

In addition, $q^{\alpha}_{J\,ea}$ could fluctuate from sample to sample since the individual m_i do. It turns out that in the thermodynamic limit $q_{J\,ea}$ does not fluctuate. With this in mind we shall later use

$$q_{ea} = q^{\alpha}_{ea} = q_{J}{}^{\alpha}_{ea} \tag{3.29}$$

for the intra-state average. This is the interpretation of the order parameter proposed by Edwards-Anderson who did not take into account the possibility that is discussed next.

In the clean Ising model, had we taken into account all the phase space, $\alpha = 1, 2$ and $m^{\alpha}_i = \langle s_i \rangle_{\alpha}$ with $m^{(1)}_i = -m^{(2)}_i > 0$. If we kept only half of it $\alpha = 1$ and $m_i = m > 0$, say. The dependence on J does not exist in this case from the very definition of the model.

Full statistical averages

If, instead, the statistical average in m_i runs over *all* possible equilibrium states (on half the phase space, that is to say, eliminating spin-reversal) the quantity (3.27) has non-trivial contributions from overlaps between different states. Imagine each state has a probability weigth w^J_{α} (in the ferromagnetic phase of the Ising model one has only two pure states with $w_1 = w_2 = 1/2$ and $m_i = 1/2\langle s_i \rangle_1 + 1/2 \langle s_i \rangle_2 = 0$) then

$$q_J = N^{-1} \sum_{i=1}^{N} \left(\sum_{\alpha} w^J_{\alpha} m^{\alpha}_i \right)^2 \ . \tag{3.30}$$

In the ferromagnetic transition $\alpha = 1$, $q = q_{ea} = m^2$, and q_{ea} and q are identical order parameters.

In the disorder case, $q_J^\alpha{}_{ea}$ takes the same value on all equilibrium states independently of there being only two (as in the usual ferromagnetic phase) or more (as we shall see appearing in fully-connected spin-glass models). Therefore it does not allow us to distinguish between the two-state and the many-state scenarii. Instead, q_J does.

Having defined a disorder-dependent order parameter, q_J, and its disorder average, q, that explains the decay of the susceptibility below T_c, we still have to study whether this order parameter characterises the low temperature phase completely. It will turn out that the the knowledge of q is not enough, at least in fully-connected and dilute spin-glass models. Indeed, one needs to consider the probability distribution of the fluctuating q_J quantity, $P(q_J)$. The more pertinent definition of an order parameter as being given by such a probability distribution allows one to distinguish between the simple, two-state, and the many-state scenarii.

In practice, a way to compute the probability distribution of the order parameter is by using an overlap – or correlation – between two spin configurations, say $\{s_i\}$ and $\{\sigma_i\}$, defined as

$$q_{s\sigma}^J = N^{-1} \sum_i \langle\ s_i \sigma_i\ \rangle \tag{3.31}$$

where $\langle\ \ldots\ \rangle$ is an unrestricted thermal average. $q_{s\sigma}^J$ takes values between -1 and 1. It equals one if $\{s_i\}$ and $\{\sigma_i\}$ differ in a number of spins that is smaller than $O(N)$, it equals -1 when the two configurations are totally anticorrelated – with the same proviso concerning a number of spins that is not $O(N)$ – and it equals zero when $\{s_i\}$ and $\{\sigma_i\}$ are completely uncorrelated. Note that the *self-overlap* of a configuration with itself is identically one for Ising spins. Other values are also possible. A related definition is the one of the Hamming distance:

$$d_{s\sigma}^J = N^{-1} \sum_{i=1}^{N} \langle\ (s_i - \sigma_i)^2\ \rangle = 2(1 - q_{s\sigma}^J)\ . \tag{3.32}$$

The overlap can be computed by running a Monte Carlo simulation, equilibrating a sample and recording many equilibrium configurations. With them one computes the overlap and should find a histogram with two peaks at q_{ea} and $-q_{ea}$ (the values of the overlap when the two configurations fall

in the same pure state or in the sign reversed ones) and, in cases with many different pure states, other peaks at other values of $q^J_{s\sigma}$. This is observed in the SK model as exemplified in Fig. **??**. Note that $q^J_{s\sigma}$ is related to the q definition above.

3.4.3 Pinning fields

In the discussion of the ferromagnetic phase transition one establishes that one of the two equilibrium states, related by spin reversal symmetry, is chosen by a small pinning field that is taken to zero after the thermodynamic limit, $\lim_{h\to 0}\lim_{N\to\infty}$.

In a problem with quenched disorder it is no longer feasible to choose and apply a magnetic field that is correlated to the statistical averaged local magnetization in a single pure state since this configuration is not known! Moreover, the remanent magnetic field that might be left in any experience will certainly not be correlated with any special pure state of the system at hand.

Which is then the statistical average relevant to describe experiments? We shall come back to this point below.

3.4.4 Divergent susceptibility

In a pure magnetic system with a second-order phase transition the susceptibility of the order parameter to a field that couples linearly to it diverges when approaching the transition from both sides. In a paramagnet, one induces a local magnetization with a local field

$$m_i = \langle\, s_i \,\rangle = \sum_{j=1}^{N} \chi_{ij} h_j \tag{3.33}$$

with χ_{ij} the linear susceptibilities, the magnetic energy given by $E = E_0 - \sum_i s_i h_i$, and the field set to zero at the end of the calculation. Using this expression, the order parameter in the high temperature phase becomes

$$q = q_{ea} = \frac{1}{N}\sum_{i=1}^{N} [\, m_i^2 \,] = \frac{1}{N}\sum_{i=1}^{N}\sum_{j=1}^{N}\sum_{k=1}^{N} [\, \chi_{ij}\chi_{ik} h_j h_k \,] \tag{3.34}$$

If the applied fields are random and taken from a probability distribution such that $\overline{h_j h_k} = \sigma^2 \delta_{jk}$ one can replace $h_j h_k$ by $\sigma^2\delta_{jk}$ and obtain

$$q = \frac{1}{N}\sum_{i=1}^{N} [\, m_i^2 \,] = \frac{1}{N}\sum_{i=1}^{N}\sum_{j=1}^{N} [\, \chi_{ij}^2 \,]\, \sigma^2 \equiv \chi_{SG}\, \sigma^2 \,. \tag{3.35}$$

σ^2 acts as a field conjugated to the order parameter. (One can also argue that a uniform field looks random to a spin-glass sample and therefore the same result holds. It is more natural though to use a trully random field since a uniform one induces a net magnetization in the sample.) The *spin-glass susceptibility* is then defined as

$$\chi_{SG} \equiv \frac{1}{N}\sum_{ij}\left[\,\chi_{ij}^2\,\right] = \frac{\beta^2}{N}\sum_{ij}\left[\,(\langle\, s_i s_j\,\rangle - \langle\, s_i\,\rangle\langle\, s_j\,\rangle)^2\,\right] = \frac{\beta^2}{N}\sum_{ij}\left[\,\langle\, s_i s_j\,\rangle^2\,\right] \tag{3.36}$$

in the high T phase and one finds that it diverges as $T \to T_c^+$ as expected in a second-order phase transition. (Note that there is no cancelation of crossed terms because of the square.) Indeed, the divergence of χ_{SG} is related to the divergence of the non-linear magnetic susceptibility that is measurable experimentally and numerically. An expansion of the total mangnetization in powers of a uniform field h acting as $E \to E - h\sum_i s_i$ is

$$M_h = \chi h - \frac{\chi^{(3)}}{6}h^3 + \dots\ , \tag{3.37}$$

and the first non-linear susceptibility is then given by

$$-\chi^{(3)} \equiv \left.\frac{\partial^3 M_h}{\partial h^3}\right|_{h=0} = -\beta^{-1}\left.\frac{\partial^4 \ln Z_h}{\partial h^4}\right|_{h=0} = -\frac{\beta^3 N}{3}\left\langle\left(\sum_i s_i\right)^4\right\rangle_c \tag{3.38}$$

with the subindex c indicating that the quartic correlation function is connected. Above T_c, $m_i = 0$ at zero field,

$$\chi^{(3)} = \beta^3\sum_{ijkl}\left(\langle\, s_i s_j s_k s_l\,\rangle - 3\langle\, s_i s_j\,\rangle\langle\, s_k s_l\,\rangle\right) = \frac{\beta^3}{N}3\left(4N - 6\sum_{ij}\langle\, s_i s_j\,\rangle^2\right)\ , \tag{3.39}$$

and one can identify χ_{SG} when $i = k$ and $j = l$ plus many other terms that we assume are finite. Then,

$$\chi^{(3)} = \beta(\chi_{SG} - \frac{2}{3}\beta^2)\ . \tag{3.40}$$

This quantity can be accessed experimentally. A careful experimental measurement of $\chi^{(3)}$, $\chi^{(5)}$ and $\chi^{(7)}$ done by L. Lévy demonstrated that all these susceptibilities diverge at T_c.

3.4.5 Calorimetry

No cusp in the specific heat of spin-glasses is seen experimentally. Since one expects a second order phase transition this means that the divergence of this quantity must be very weak.

3.4.6 Scaling

Having identified an order parameter, the linear and the non-linear susceptibility one can now check whether there is a static phase transition and, if it is of second order, whether the usual scaling laws apply. Many experiments have been devoted to this task. It is by now quite accepted that Ising spin-glasses in $3d$ have a conventional second order phase transition. Still, the exponents are difficult to obtain and there is no real consensus about their values. There are two main reasons for this: one is that as T_c is approached the dynamics becomes so slow that equilibrium measurements cannot really be done. Critical data are thus restricted to $T > T_c$. The other reason is that the actual value of T_c is difficult to determine and the value used has an important influence on the critical exponents. Possibly, the most used technique to determine the exponents is *via* the scaling relation for the non-linear susceptibility:

$$\chi_{nl} = t^{\beta} f\left(\frac{h^2}{t^{\gamma+\beta}}\right) \tag{3.41}$$

with $t = |T - T_c|/T_c$ and one finds, approximately, the values given in Table 1.

d	β	γ	δ	α	ν	η
∞	1	1	2	-1	$\frac{1}{2}$	0
3	0.5	4	9			

Table 1: Critical exponents in the Ising spin-glass transitions.

3.5 The TAP approach

Disordered models have quenched random interactions. Due to the fluctuating values of the exchanges, one expects that the equilibrium configurations be such that *in each equilibrium state* the spins freeze in different directions.

The local averaged magnetizations need not be identical, on the contrary one expects $\langle\, s_i \,\rangle = m_i$ and, if many states exist, each of them can be identified by the vector $(m_1, \ldots, m_N)$.

One may try to use the naive mean-field equations (2.17) to characterize the low temperature properties of these models at *fixed quenched disorder* and determine then the different $(m_1, \ldots, m_N)$ values. It has been shown by Thouless-Anderson-Palmer (TAP) [**?**, **?**] that these equations are not completely correct even in the fully-connected disordered case: a term which is called the Onsager reaction term is missing. This term represents the reaction of the spin i: the magnetization of the spin i produces a field $h'_j = J_{ji} m_i = J_{ij} m_i$ on spin j; this field induces a magnetization $m_j = \chi_{jj} h'_j = \chi_{jj} J_{ij} m_i$ on the spin j and this in turn produces a mean-field $h'_i = J_{ij} m_j = J_{ij} \chi_{jj} J_{ij} m_i = \chi_{jj} J_{ij}^2 m_i$ on the site i. The equilibrium fluctuatio-dissipation relation between susceptibilities and connected correlations implies $\chi_{jj} = \beta \,\langle\, (s_j - \langle\, s_j \,\rangle)^2 \,\rangle = \beta(1 - m_j^2)$ and one then has $h_i = \beta(1 - m_j^2) J_{ij}^2 m_i$. The idea of Onsager – or *cavity method* – is that one has to study the ordering of the spin i in the absence of its own effect on the rest of the system. Thus, the field h'_i has to be subtracted from the mean-field created by the other spins in the sample, *i.e.* $h_i^{corr} = \sum_j J_{ij} m_j + h_i - \beta m_i \sum_j J_{ij}^2 (1 - m_j^2)$ where h_i is the external field.

The generalization of this argument to p spin interactions is not so straighforward. An alternative derivation has been given by Biroli []. The TAP equations for p-spin fully connected models read

$$m_i = \tanh\left[\beta\left(\sum_{i_2 \neq \ldots \neq i_p} \frac{1}{(p-1)!} J_{i i_2 \ldots i_p} m_{i_2} \ldots m_{i_p} + \beta m_i J_{i i_2 \ldots i_p}^2 (1 - m_{i_2}^2) \ldots (1 - m_{i_p}^2) + h_i\right)\right] . \tag{3.42}$$

the first contribution to the internal field is proportional to $J_{i 1_2 \ldots i_p} \sim N^{-(p-1)/2}$ and once the $p-1$ sums performed it is of order one. The reaction term instead is proportional to $J_{i i_2 \ldots i_p}^2$ and, again, a simple power counting shows that it is $O(1)$. Thus, In disordered systems the reaction term is of the same order of the usual mean-field; a correct mean-field description has to include it. In the ferromagnetic case this term can be neglected since it is subleading in N. Using the fact that there is a sum over a very large number of elements, $J_{i_1 \ldots i_p}^2$ can be replaced by its site-independent variance $[J_{i_1 \ldots i_p}^2] = p! J^2 / (2N^{p-1})$ in the last term in (3.42). Introducing the Edwards-Anderson parameter $q_{ea} = N^{-1} \sum_{i=1} m_i^2$ (note that we study the system in

one pure state) the TAP equations follow:

$$m_i = \tanh\left[\beta\left(\frac{1}{(p-1)!}\sum_{i_2\neq\ldots\neq i_p} J_{ii_2\ldots i_p} m_{i_2}\ldots m_{i_p} + h_i - \frac{\beta J^2 p}{2} m_i (1-q_{ea})^{p-1}\right)\right] . \tag{3.43}$$

The argument leading to the Onsager reaction term can be generalized to include the combined effect of the magnetization of spin i on a sequence of spins in the sample, *i.e.* the effect on i on j and then on k that comes back to i. These higher order terms are indeed negligible only if the series of all higher order effects does not diverge. The ensuing condition is $1 > \beta^2\ (1 - 2q_{ea} + N^{-1}\sum_i m_i^4)$.

The importance of the reaction term becomes clear from the analysis of the linearized equations, expected to describe the second order critical behaviour for the SK model ($p = 2$) in the absence of an applied field. The TAP equations become $m_i \sim \beta(\sum_j J_{ij} m_j - \beta J^2 m_i + h_i)$. A change of basis to the one in which the J_{ij} matrix is diagonal leads to $m_\lambda \sim \beta(\lambda - \beta J^2) m_\lambda + \beta h_\lambda$. The staggered susceptibility then reads

$$\chi_\lambda \equiv \left.\frac{\partial m_\lambda}{\partial h_\lambda}\right|_{h=0} = \beta\ \left(1 - 2\beta J_\lambda + (\beta J)^2\right)^{-1} . \tag{3.44}$$

The staggered susceptibility for the largest eigenvalue of an interaction matrix in the Gaussian ensemble, $J_\lambda^{max} = 2J$, diverges at $\beta_c J = 1$. Note that without the reaction term the divergence appears at the inexact value $T^* = 2T_c$ (see Sect. 3.6 for the replica solution of the SK model).

The TAP equations are the extremization conditions on the TAP free-energy density:

$$\begin{aligned} f(\{m_i\}) \;=\; & -\frac{1}{p!}\sum_{i_1\neq\ldots\neq i_p} J_{i_1\ldots i_p} m_{i_1}\ldots m_{i_p} - \frac{\beta}{4p}\sum_{i_1\neq\ldots\neq i_p} J^2_{i_1\ldots i_p}(1-m_{i_1}^2)\ldots(1-m_{i_p}^2) \\ & - \sum_i h_i m_i + T\sum_{i=1}^N \left[\frac{1+m_i}{2}\ln\frac{1+m_i}{2} + \frac{1-m_i}{2}\ln\frac{1-m_i}{2}\right] . \end{aligned} \tag{3.45}$$

The free-energy density as a function of the local magnetizations m_i defines what is usually called *the free-energy landscape*. Note that this function depends on $N \gg 1$ variables, m_i, and these are not necessarily identical in the disordered case in which the interactions between different groups of

spins are different. The stability properties of each extreme $\{m_l^*\}$ are given by the eigenvalues of the Hessian matrix

$$\mathcal{H}_{ij} \equiv \left. \frac{\partial f(\{m_k\})}{\partial m_i \partial m_j} \right|_{\{m_l^*\}} . \tag{3.46}$$

The number of positive, negative and vanishing eigenvalues determine then the number of directions in which the extreme is a minimum, a maximum or marginal. The sets $\{m_l^*\}$ for which $f(\{m_l^*\})$ is the absolute minima yield a first definition of equilibrium or pure states.

The TAP equations apply to $\{m_i\}$ and not to the configurations $\{s_i\}$. The values of the $\{m_i\}$ are determined as minima of the TAP free-energy density, $f(\{m_i\})$, and they not need to be the same as those of the energy, $H(\{s_i\})$, a confusion sometimes encountered in the glassy literature. The coincidence of the two can only occur at $T \to 0$.

3.5.1 The complexity or configurational entropy

There are a number of interesting questions about the extreme of the TAP free-energy landscape, or even its simpler version in which the Onsager term is neglected, that help us understanding the static behaviour of disordered systems:

1. For a given temperature, T, how many solutions to the mean-field equations exist? The number of solutions can be calculated using

$$\mathcal{N}_J = \prod_i \int_{-1}^{1} dm_i \, \delta(m_i - m_i^*) = \prod_i \int_{-1}^{1} dm_i \, \delta(\mathrm{eq}_i) \left| \det \frac{\partial \mathrm{eq}_i}{\partial m_j} \right| . \tag{3.47}$$

   $\{m_i^*\}$ are the solutions to the TAP equations that we write as $\{\mathrm{eq}_i = 0\}$. The last factor is the normalization of the delta function after the change of variables, it ensures that we count one each time the integration variables touch a solution to the TAP equations independently of its stability properties.
   We define the *complexity* or the *configurational entropy* as the logarithm of the number of solutions at temperature T divided by N:

$$\Sigma_J(T) \equiv N^{-1} \ln \mathcal{N}_J(T) . \tag{3.48}$$

   The normalization with N suggests that the number of solutions is actually an exponential of N. We shall come back to this very important point below.

2. Does $\mathcal{N}_J(T)$ dependend on T and does it change abruptly at particular values of T that may or may not coincide with static and dynamic phase transitions?
3. One can define a free-energy level dependent complexity

$$\Sigma_J(f,T) \equiv N^{-1} \ln \mathcal{N}_J(f,T) \tag{3.49}$$

where $\mathcal{N}_J(f,T)$ is the number solutions in the interval $[f, f+df]$ at temperature T.
4. From these solutions, one can identify the minima as well as all saddles of different type, *i.e.* with different indeces K. These are different kinds to metastable states. Geometry constrains the number of metastable states to satisfy Morse theorem that states $\sum_{l=1}^{\mathcal{N}}(-1)^{\kappa_l} = 1$, where κ_l is the number of negative eigenvalues of the Hessian evaluated at the solution l, for any continuous and well-behaved function diverging at infinity in all directions.
One can then count the number of solutions to the TAP equations of each index, $\mathcal{N}_J(K,T)$, and define the corresponding complexity

$$\Sigma_J(K,T) \equiv N^{-1} \ln \mathcal{N}_J(K,T) \,, \tag{3.50}$$

or even work at fixed free-energy density

$$\Sigma_J(K,f,T) \equiv N^{-1} \ln \mathcal{N}_J(K,f,T) \,. \tag{3.51}$$

Even more interestingly, one can analyse how are the free-energy densities of different saddles are organized. For instance, one can check whether all maxima are much higher in free-energy density than minima, *etc.*
5. What is the barrier, $\Delta f = f_1 - f_0$, between ground states and first excited states? How does this barrier scale with the actual free-energy difference, Δf between these states? The answer to this question is necessary to estimate the nucleation radius for the reversal of a droplet under an applied field, for instance.

The definitions of complexity given above are disorder-dependent. One might then expect that the complexity will show sample-to-sample fluctuations and be characterized by a probability distribution. The *quenched complexity*, $\Sigma^{quenched}$, is then the most likely value of Σ_J, it is defined through

$\max P(\Sigma_J) = P(\Sigma^{quenched})$. In practice, this is very difficult to compute. Most analytic results concern the *annealed* complexity

$$\Sigma_{ann} \equiv N^{-1} \ln [\, \mathcal{N}_J \,] = N^{-1} \ln [\, e^{N\Sigma_J} \,] \; . \tag{3.52}$$

One can show that the annealed complexity is smaller or equal than the quenched one.

3.5.2 Weighted averages

Having identified many solutions to the TAP equations in the low-T phase one needs to determine now how to compute statistical averages. A natural proposal is to give a probability weight to each solution, w_α, and to use it to average the value the observable of interest:

$$\langle \, O \, \rangle = \sum_\alpha \; w_\alpha^J \; O_\alpha \tag{3.53}$$

where α labels the TAP solutions, $O_\alpha = O(\{m_i^\alpha\})$ is the value that the observable O takes in the TAP solution α, and w_α^J are their statistical weights, satisfying the normalization condition $\sum_\alpha w_\alpha^J = 1$. Two examples can illustrate the meaning of this average. In a spin-glass problem, if $O = s_i$, then $O_\alpha = m_i^\alpha$. In an Ising model in its ferromagnetic phase, if $O = s_i$, then $O_\alpha = m_i^\alpha = \pm m$ and $w_\alpha = 1/2$. Within the TAP approach one proposes

$$w_\alpha^J = \frac{e^{-\beta F_\alpha^J}}{\sum_\gamma e^{-\beta F_\gamma^J}} \tag{3.54}$$

with F_α^J the total free-energy of the α-solution to the TAP equations. The discrete sum can be transformed into an integral over free-energy densities, introducing the degeneracy of solutions quantified by the free-energy density dependent complexity:

$$\langle \, O \, \rangle = \frac{1}{Z} \int df \, e^{-N\beta f} \mathcal{N}_J(f,T) O(f) = \frac{1}{Z} \int df \, e^{-N(\beta f - \Sigma_J(f,T))} \; O(f) \; . \tag{3.55}$$

The normalization is the 'partition function'

$$Z = \int df e^{-N\beta f} \mathcal{N}_J(f,T) = \int df \, e^{-N(\beta f - \Sigma_J(f,T))} \; . \tag{3.56}$$

We assumed that the labelling by α can be traded by a labelling by f that implies that at the same free-energy density level f the observable O takes

the same value. In the $N \to \infty$ limit these integrals can be evaluated by saddle-point, provided the parenthesis is positive. The disorder-dependent complexity is generally approximated with the annealed value introduced in eq. (3.52).

The equilibrium free-energy

The total equilibrium free-energy density, using the saddle-point method to evaluate the partition function Z in eq. (3.56), reads

$$-\beta f_{eq} = N^{-1} \ln Z = \min_f \left[f - T\Sigma_J(f,T) \right] \equiv \min_f \Phi_J(f,T) \tag{3.57}$$

It is clear that $\Phi_J(f,T)$ is the Landau free-energy density of the problem with f playing the rôle of the energy and Σ_J of the entropy. If we use $f = (E - TS)/N = e - Ts$ with E the actual energy and S the microscopic entropy one has

$$\Phi_J(f,T) = e - T\left(s + \Sigma_J(f,T)\right) \ . \tag{3.58}$$

Thus, Σ_J is an extra contribution to the total entropy that is due to the exponentially large number of metastable states. Note that we do not distinguish here their stability.

Note that Σ_J is subtracted from the total free-energy. Thus, it is possible that in some cases states with a *higher* free-energy density but *very numerous* have a *lower* total free-energy density than lower lying states that are less numerous. Collectively, higher states dominate the equilibrium measure in these cases.

The order parameter

The Edwards-Anderson parameter is understood as a property of a single state. Within the TAP formalism on then has

$$q_{EA}^{\alpha} = N^{-1} \sum_i (m_i^{\alpha})^2 \ . \tag{3.59}$$

An average over pure states yields $\sum_\alpha w_\alpha^J (m_i^\alpha)^2$.

Instead, the statistical *equilibrium* magnetization, $m_i = \langle s_i \rangle = \sum_\alpha w_\alpha^J m_i^\alpha$, squared is

$$q_J \equiv \langle\, s_i \,\rangle^2 = m_i^2 = \left(\sum_\alpha w_\alpha^J m_i^\alpha \right)^2 = \sum_{\alpha\beta} w_\alpha^J w_\beta^J \ m_i^\alpha m_i^\beta \ . \tag{3.60}$$

If there are multiple phases, the latter sum has crossed contributions from terms with $\alpha \neq \beta$. These sums, as in a usual paramagnetic-ferromagnetic transition have to be taken over half space-space, otherwise global up-down reversal would imply the cancellation of all cross-terms.

3.5.3 Metastable states in two families of models

High temperatures

For all models, at high temperatures $f(m_i)$ is characterized by a single stable absolute minimum in which all local magnetizations vanish, as expected; this is the paramagnetic state. The $m_i = 0$ for all i minimum continues to exist at all temperatures. However, even if it is still the global absolute minimum of the TAP free-energy density, f_{TAP}, at low temperatures it becomes unstable thermodynamically, and it is substituted as the equilibrium state, by other non-trivial configurations with $m_i \neq 0$ that are the absolute minima of Φ. Note the difference with the ferromagnetic problem for which the paramagnetic solution is no longer a minimum below T_c.

3.5.4 Low temperatures

At low temperature many equilibrium states appear (and not just two as in an Ising ferromagnetic model) and they are not related by symmetry (as spin reversal in the Ising ferromagnet or a rotational symmetry in the Heisenberg ferromagnet). These are characterized by non-zero values of the local magnetizations m_i that are different in different states.

At low-temperatures both the naive mean-field equations and the TAP equations have an *exponential in N number of solutions* and still an exponential in N number of them correspond to absolute minima of the m_i-dependent free-energy density. This means that $\Sigma_J(T)$ and even $\Sigma_J(0, f_0, T)$ are quantities $O(1)$. These minima can be identified as *different* states that could be accessed by applying the corresponding site-dependent pinning fields.

The derivation and understanding of the structure of the TAP free-energy landscape is quite subtle and goes beyond the scope of these Lectures. Still, we shall briefly present their structure for the SK and p-spin models to give a flavor of their complexity.

<u>The SK model</u>

The first calculation of the complexity in the SK model appeared in 1980. After 25 years of research the structure of the free-energy landscape in this system is still a matter of discussion. At present, the picture that emerges is the following. The temperature-dependent annealed complexity is a decreasing function of temperature that vanishes only at T_c but takes a very small value already at $\sim 0.6T_c$. Surprisingly enough, at finite but large N the TAP solutions come in pairs of minima and saddles of type one, that is to say, extrema with only one unstable direction. These states are connected by a mode that is softer the larger the number of spins: they coalesce and become marginally stable in the limit $N \to \infty$. Numerical simulations show that starting from the saddle-point and following the 'left' direction along the soft mode one falls into the minimum; instead, following the 'right' direction along the same mode one falls into the paramagnetic solution. The free-energy difference between the minimum and saddle decreases for increasing N and one finds, numerically, an averaged $\Delta f \sim N^{-1.4}$. The extensive complexity of minima and type-one saddles is identical in the large N limit, $\Sigma(0,T) = \Sigma(1,T) + O(N^{-1})$ [Aspelmeier, Bray, Moore (06)] in such a way that the Morse theorem is respected. The free-energy dependent annealed complexity is a smooth function of f with support on a finite interval $[f_0, f_1]$ and maximum at f_{max}. The Bray and Moore annealed calculation (with supersymmetry breaking) yields $f_{max} = -0.654$, $\Sigma_{max} = 0.052$, $\Sigma''(f_{max}) = 8.9$. The probability of finding a solution with free-energy density f can be expressed as

$$p(f,T) = \frac{\mathcal{N}(f,T)}{\mathcal{N}(T)} = \frac{e^{N\Sigma(f,T)}}{\mathcal{N}(T)} \sim \sqrt{\frac{N\Sigma''(f_{max})}{2\pi}}\; e^{-\frac{N}{2}|\Sigma''(f_{max})|(f-f_{max})^2} \;, \tag{3.61}$$

where we evaluated the total number of solutions, $\mathcal{N}(T) = \int df e^{N\Sigma(f,T)}$, by steepest descent The complexity vanishes linearly close to f_0: $\Sigma(f,T) \sim \lambda(f - f_0)$ with $\lambda < \beta$.

Only the lowest lying TAP solutions contribute to the statistical weight. The complexity does not contribute to Φ in the large N limit:

$$\begin{aligned} \Phi &= \beta f - \Sigma_{ann}(f,T) \simeq \beta f - (f - f_0)\lambda \\ \frac{\partial \Phi}{\partial f} &\simeq \beta - \lambda > 0 \qquad \text{iff} \qquad \beta > \lambda \end{aligned} \tag{3.62}$$

and $\Phi_{min} \simeq \beta f_{min} = \beta f_0$. See Fig. **??**. The 'total' free-energy density in the exponential is just the free-energy density of each low-lying solution.

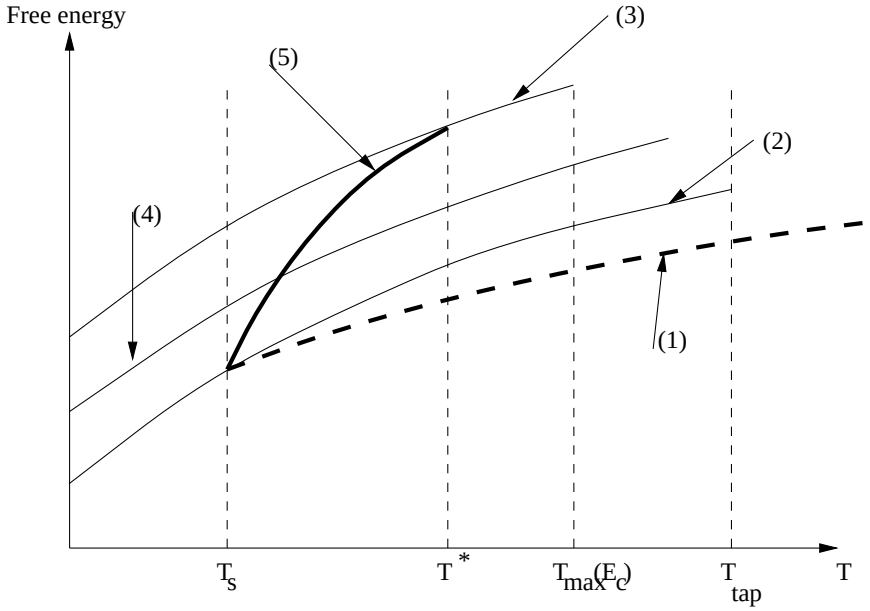

Figure 9: The TAP free-energy as a function of T in the spherical p-spin model. (1) : free energy of the paramagnetic solution for $T > T^*$, F_{tot} for $T < T^*$; (2) : free energy of the lowest TAP states, with zero temperature energy E_{min}; (3) : free energy of the highest TAP states, corresponding to E_c; (4) : an intermediate value of E_0 leads to an intermediate value of f at any temperature; (5) : $f_{eq}(T)$; the difference between curves (5) and (1) gives the complexity $TS_c(f_{eq}(T), T)$.

The (spherical) p-spin model

The number and structure of saddle-points is particularly interesting in the $p \geq 3$ cases and it is indeed the reason why these models, with a random first order transition, have been proposed to mimic the structural glass arrest. The $p \geq 3$ model has been studied in great detail in the spherical case, that is to say, when spins are not Ising variables but satisfy the global constraint, $\sum_{i=1}^{N} s_i^2 = N$.

Although in general the minima of the mean-field free energy do not coincide with the minima of the Hamiltonian, they do in the spherical p-spin model. Their positions in the phase space does not depend on temperature, while their self-overlap does. At $T = 0$ a state (stable or metastable) is just a

minimum (absolute or local) of the energy. For increasing T energy minima get dressed up by thermal fluctuations, and become states. Thus, the states can be labeled by their zero-temperature energy E^0.

The complexity is given by

$$\Sigma(E) = \frac{1}{2}\left[-\ln\frac{pz^2}{2} + \frac{p-1}{2}z^2 - \frac{2}{p^2z^2} + \frac{2-p}{p}\right] , \tag{3.63}$$

where z is

$$z = \left[-E^0 - \sqrt{E^{0\,2} - E_c^2}\right]/(p-1) . \tag{3.64}$$

The complexity vanishes at

$$E^0 = E_{min} = f(p) , \tag{3.65}$$

the ground state of the system, and it is real for zero-temperature energies $E < E_{th}$ with

$$E_{th} = -\sqrt{\frac{2(p-1)}{p}} . \tag{3.66}$$

E_{min} is the zero-T energy one finds with the replica calculation using a 1-step RSB *Ansatz* as we shall see below. The finite-T energy of a state α is

$$E_\alpha = q_\alpha^{\frac{p}{2}} E_\alpha^0 - \frac{1}{2T}\left[(p-1)q_\alpha^p - pq_\alpha^{p-1} + 1\right] . \tag{3.67}$$

This means that:

1. There can be only a finite number of states with $E < E_0$.
2. It can be shown that below E_{th} minima dominate on average.
3. Above E_{th} one can show that there are states but these are unstable.

Each zero-temperature state is characterized by unit N-vector s_i^α and it gives rise to a finite-T state characterized by $m_i^\alpha = \sqrt{q(E,T)}s_i^\alpha$ with $q(E,T)$ given by

$$q^{p-2}(1-q)^2 = T^2\,\frac{(E + \sqrt{E^2 - E_{th}^2})^2}{(p-1)^2} . \tag{3.68}$$

($q(E, T = 0) = 1$ and at finite T the solution with q closest to 1 has to be chosen.) The self-overlap at the threshold energy, $E - E_{th}$, is then

$$q_{th}^{p-2}(1-q_{th})^2 = T^2\,\frac{2}{p(p-1)} . \tag{3.69}$$

Another way for the q equation to stop having solution, is by increasing the temperature, $T > T_{max}(E^0)$, at fixed bare energy E^0. This means that, even though minima of the energy do not depend on the temperature, states, i.e. minima of the free energy do. When the temperature becomes too large, the paramagnetic states becomes the only pure ergodic states, even though the energy landscape is broken up in many basins of the energy minima. This is just one particularly evident demonstration of the fundamental different between pure states and energy minima. $T_{max}(E^0)$ is obtained as the limiting temperature for which eq. (3.68) admits a solution. It is given by

$$T_{max}(E^0) = \left(\frac{2}{p}\right)\left(\frac{p-1}{-E^0 - \sqrt{E^{0\,2} - E_{th}^2}}\right)\left(\frac{p-2}{p}\right)^{\frac{p-2}{2}} . \tag{3.70}$$

T_{max} is a decreasing function of E^0. The last states to disappear then are the ones with minimum energu E_{min}, ceasing to exist at $T_{TAP} \equiv= T_{max}(E_{min})$.

Below a temperature T_d, an exponential (in N) number of metastable states contribute to the thermodynamics in such a non-trivial way that their combined contribution to the observables makes them those of a paramagnet. Even if each of these states is non-trivial (the m_i's are different from zero) the statistical average over all of them yields results that are identical to those of a paramagnet, that is to say, the free-energy density is $-1/(4T)$ as in the $m_i = 0$ paramagnetic solution. One finds

$$T_d = \sqrt{\frac{p(p-2)^{p-2}}{2(p-1)^{p-1}}} . \tag{3.71}$$

At a lower temperature T_s ($T_s < T_d$) there is an entropy crisis, less than an exponential number of metastable states survive, and there is a *static phase transition* to a glassy state.

In the p-spin models there is a range of temperatures in which high lying states dominate this sum since they are sufficiently numerous so as to have a complexity that renders the cimbined term $\beta f - \Sigma_J(f, T)$ smaller (in actual calculations the disorder dependent complexity is approximated by its annealed value). In short:

1. Above T_d the (unique) paramagnetic solution dominates, $q = 0$ and $\Phi = f = -1/(4T)$.

2. In the interval $T \in [T_s, T_d]$ an exponentially large number of states (with $q \neq 0$ given by the solution to $pq^{p-2}(1-q) = 2T^2$) dominate the partition sum. $\Phi = -1/(4T)$ appearing as the continuation of the paramagnetic solution.
3. At $T < T_s$ the lowest TAP states with $E^0 = E_{min}$ control the partition sum. Their total free-energy Φ is different from $-1/(4T)$.

This picture is confirmed with other studies that include the use of pinning fields adapted to the disordered situation, the effective portential for two coupled real replicas, and the dynamic approach.

Low temperatures, entropy crisis

The interval of definition of $\Phi(E,T)$ is the same as $\Sigma(E)$, that is $E \in [E_{min} : E_{th}]$. Assuming that at a given temperature T the energy $E_{eq}(T)$ minimizing Φ lies in this interval, what happens if we lower the temperature? Remember that the complexity is an increasing function of E, as of course is $f(E,T)$. When T decreases we favor states with lower free energy and lower complexity, and therefore E_{eq} decreases. As a result, it must exist a temperature T_s, such that, $E_{eq}(T_s) = E_{min}$ and thus, $\Sigma(E_{eq}(T)) = \Sigma(E_{min}) = 0$. Below T_s the bare energy E_{eq} cannot decrease any further: there are no other states below the ground states E_{min}. Thus, $E_{eq}(T) = E_{min}$ for each temperature $T \leq T_s$. As a result, if we plot the complexity of equilibrium states $\Sigma(E_{eq}(T))$ as a function of the temperature, we find a discontinuity of the first derivative at T_s, where the complexity vanishes. A thermodynamic transition takes place at T_s: below this temperature equilibrium is no longer dominated by metastable states, but by the lowest lying states, which have zero complexity and lowest free energy density.

We shall show that T_s is the transition temperature found with a replica calculation. The temperature where equilibrium is given for the first time by the lowest energy states, is equal to the static transition temperature. Above T_s the partition function is dominated by an exponentially large number of states, each with high free energy and thus low statistical weight, such that they are not captured by the overlap distribution $P(q)$. At T_s the number of these states becomes sub-exponential and their weight nonzero, such that the $P(q)$ develops a secondary peak at $q_s \neq 0$.

The threshold

The stability analysis of the states on the threshold shows that these are

marginal, in the sense that they have many flat directions. This feature is very important for the relaxational dynamics of these systems.

Organization

The ordering of the TAP states in terms of their free-energy value and their stability has been very deeply analyzed in a number of papers. For a summary see the review articles by Cavagna and Zamponi.

Finite dimensions

In finite-dimensional systems, only equilibrium states can break the ergodicity, i.e. states with the lowest free energy density. In other words, the system cannot remain trapped for an infinite time in a metastable state, because in finite dimension free energy barriers surrounding metastable states are always finite.

The extra free energy of a droplet of size r of equilibrium phase in a background metastable phase has a positive interface contribution which grows as r^{d-1}, and a negative volume contribution which grows as r^d,

$$\Delta f = \sigma r^{d-1} - \delta f \; r^d \tag{3.72}$$

where here σ is the surface tension and δf is the bulk free energy difference between the two phases. This function has always a maximum, whose finite height gives the free energy barrier to nucleation of the equilibrium phase (note that at coexistence $\delta f = 0$ and the barrier is infinite). Therefore, if initially in a metastable states the system will, sooner or later, collapse in the stable state with lower free energy density. For this reason, in finite dimension we cannot decompose the Gibbs measure in metastable components. When this is done, it is always understood that the decomposition is only valid for finite times, i.e times much smaller than the time needed for the stable equilibrium state to take over. On the other hand, in mean-field systems (infinite dimension), barriers between metastable states may be infinite in the thermodynamic limit, and it is therefore possible to call pure states also metastable states, and to assign them a Gibbs weight w_α^J. We will analyze a mean-field spin-glass model, so that we will be allowed to perform the decomposition above even for metastable states.

Comments

There is a close relationship between the topological properties of the model and its dynamical behavior. In particular, the slowing down of the

dynamics above but close to T_d is connected to the presence of saddles, whose instability decreases with decreasing energy. In fact, we have seen that the threshold energy level E_{th} separating saddles from minima, can be associated to the temperature $T_{th} = T_d$, marking the passage from ergodicity to ergodicity breaking. In this context the dynamical transition can be seen as a topological transition. The plateau of the dynamical correlation function, which has an interpretation in terms of cage effect in liquids, may be reinterpreted as a pseudo-thermalization inside a saddle with a very small number of unstable modes.

3.6 The replica method

A picture that is consistent with the one arising from the naive mean-field approximation but contradicts the initial assumption of the droplet model arises from the *exact* solution of fully-connected spin-glass models. These results are obtained using a method which is called the *replica trick* and that we shall briefly present below.

In Sect. 2.3.2 we argued that the typical properties of a disordered system can be computed from the disorder averaged free-energy

$$[\, F_J \,] \equiv \int dJ P(J) F_J \; . \tag{3.73}$$

One then needs to average the logarithm of the partition funtion. In the annealed approximation one exchanges the ln with the average over disorder and, basically, considers the interactions equilibrated at the same temperature T as the spins:

$$[\, \ln Z_J \,] \sim \ln [\, Z_J \,] \; . \tag{3.74}$$

This approximation turns out to be correct at high temperatures but incorrect at low ones.

The replica method allows one to compute $[\, F_J \,]$ for fully-connected models. It is based on the smart use of the identity

$$\ln Z_J = \lim_{n \to 0} \frac{Z_J^n - 1}{n} \; . \tag{3.75}$$

The idea is to compute the right-hand-side for finite and integer $n = 1, 2, \ldots$ and then perform the analytic continuation to $n \to 0$. Care should be taken in this step: for some models the analytic continuation may be not unique.

It turns out that this is indeed the case for the emblematic Sherrington-Kirkpatrick model, as discussed by Palmer and van Hemmen in 1979 though it has also been recently shown that the free-energy $f(T)$ obtained by Parisi with the replica trick is exact!

The disorder averaged free-energy is given by

$$-\beta[\, F_J \,] = -\int dJ P(J) \ln Z_J = -\lim_{n\to 0} \frac{1}{n} \left(\int dJ P(J) Z_J^n - 1 \right) \,, \qquad (3.76)$$

where we have exchanged the limit $n \to 0$ with the integration over the exchanges. For *integer* n the *replicated* partition function, Z_J^n, reads

$$Z_J^n = \sum_{\{s_i^a\}} e^{-\beta[E_J(\{s_i^1\})+\ldots+E_J(\{s_i^n\}]} \,. \qquad (3.77)$$

Here $\sum_{\{s_i^a\}} \equiv \sum_{\{s_i^1=\pm 1\}} \cdots \sum_{\{s_i^n=\pm 1\}}$. Z_J^n corresponds to n identical copies of the original system, that is to say, all of them with the same realization of the disorder. Each copy is characterized by an ensemble of N spins, $\{s_i^a\}$. We label the copies with a replica index $a = 1, \ldots, n$. For p-spin disordered spin models Z_J^n takes the form

$$Z_J^n = \sum_{\{s_i^a\}} e^{\beta \sum_{a=1}^n \left[\sum_{i_1 \neq \ldots \neq i_p} J_{i_1 \ldots i_p} s_{i_1}^a \ldots s_{i_p}^a + \sum_i h_i s_i^a \right]} \,. \qquad (3.78)$$

The average over disorder amounts to computing a Gaussian integral for each set of spin indices $i_1, \ldots i_p$. One finds

$$[\, Z_J^n \,] = \sum_{\{s_i^a\}} e^{\frac{\beta^2 J^2}{2N^{p-1}} \sum_{i_1 \neq \ldots \neq i_p} (\sum_a s_{i_1}^a \ldots s_{i_p}^a)^2 + \beta \sum_a \sum_i h_i s_i^a} \equiv \sum_{\{s_i^a\}} e^{-\beta F(\{s_i^a\})} \,. \qquad (3.79)$$

The function $\beta F(\{s_i^a\})$ is not random. It depends on the spin variables only but it includes terms that couple different replica indices:

$$\beta F(\{s_i^a\}) \approx -\frac{N\beta^2 J^2}{2} \left[\sum_{a \neq b} \left(\frac{1}{N} \sum_i s_i^a s_i^b \right)^p + n \right] - \beta \sum_a \sum_i h_i s_i^a \,. \qquad (3.80)$$

In writing the last expression we have dropped terms that are subleading in N (in complete analogy with what we have done for the pure p spin ferromagnet). The constant term $-Nn\beta^2 J^2/2$ originates in the terms with $a = b$, for which $(s_i^a)^2 = 1$.

To summarize, we started with an interacting spin model. Next, we enlarged the number of variables from N spins to $N \times n$ replicated spins by introducing n non-interacting copies of the system. By integrating out the disorder we decoupled the sites but we payed the price of coupling the replicas. Hitherto the replica indices act as a formal tool introduced to compute the average over the bond distribution. Nothing distinguishes one replica from another and, in consequence, the "free-energy" $F(\{s_i^a\})$ is invariant under permutations of the replica indices.

The next step to follow is to identify the order parameters and transform the free-energy into an order-parameter dependent expression to be rendered extremal at their equilibrium values. In a spin-glass problem we already know that the order parameter is not the global magnetization as in a pure magnetic system but the parameter q – or more generally the overlap between states. Within the replica calculation an *overlap between replicas*

$$q_{ab} \equiv N^{-1} \sum_i s_i^a s_i^b \tag{3.81}$$

naturally appeared in eq. (3.80). The idea is to write the free-energy density as a function of the order parameter q_{ab} and look for their extreme in complete analogy with what has been done for the fully-connected ferromagnet. This is, of course, a tricky business, since the order parameter is here a matrix with number of elements n going to zero! A recipe for identifying the form of the order parameter (or the correct saddle-point solution) has been proposed by G. Parisi in the late 70s and early 80s. This solution has been recently proven to be exact for mean-field models by two mathematical physics, F. Guerra and M. Talagrand. Whether the very rich physical structure that derives from this rather formal solution survives in finite dimensional systems remains a subject of debate.

Introducing the Gaussian integral

$$\int dq_{ab}\; e^{\beta J q_{ab} \sum_i s_i^a s_i^b - \frac{N}{2} q_{ab}^2} = e^{\frac{N}{2}\left(\frac{1}{N}\beta J \sum_i s_i^a s_i^b\right)^2} \tag{3.82}$$

for each pair of replica indices $a \neq b$, one decouples the site indeces, i, and the averaged replicated partition function can be rewritten as

$$[Z_J^n] = \int \prod_{a \neq b} dq_{ab}\; e^{-\beta F(q_{ab})} \tag{3.83}$$

and

$$\beta F(q_{ab}) = -\frac{N\beta^2 J^2}{2}\left[-\sum_{a\neq b} q_{ab}^p + n\right] - N\ln\zeta(q_{ab})\ , \tag{3.84}$$

$$\zeta(q_{ab}) = \sum_{s_a} e^{-\beta H(q_{ab},s_a)}\ ,\quad H(q_{ab},s_a) = -J\sum_{ab} q_{ab}s_a s_b - h\sum_a s_a \tag{3.85}$$

where for simplicity we set $h_i = h$. The factor N in front of $\ln\zeta$ comes from the decoupling of the site indeces. Note that the transformation (3.82) serves to uncouple the sites and to obtain then the very useful factor N in front of the exponential. The partition function $Z(q_{ab})$ is the one of a fully-connected Ising model with interaction matrix q_{ab}.

Saddle-point evaluation

Having extracted a factor N in the exponential suggests to evaluate the integral over q_{ab} with the saddle-point method. This, of course, involves the *a priori* dangerous exchange of limits $N\to\infty$ and $n\to 0$. The replica theory relies on this assumption. One then writes

$$\lim_{N\to\infty} -[\,f_J\,] \to -\lim_{n\to 0}\frac{1}{n} f(q_{ab}^{sp}) \tag{3.86}$$

and searches for the solutions to the $n(n-1)/2$ extremization equations

$$\left.\frac{\delta f(q_{ab})}{\delta q_{cd}}\right|_{q_{ef}^{sp}} = 0\ . \tag{3.87}$$

In usual saddle-point evaluations the saddle-point one should use is (are) the one(s) that correspond to absolute minima of the free-energy density. In the replica calculation the number of variables is $n(n-1)/2$ that becomes negative! when $n<1$ and makes the saddle-point evaluation tricky. In order to avoid unphysical complex results one needs to focus on the saddle-points with positive (or at least semi-positive) definite Hessian

$$\mathcal{H} \equiv \left.\frac{\partial f(q_{ab})}{\partial q_{cd}\partial q_{ef}}\right|_{q_{ab}^{sp}}\ , \tag{3.88}$$

and these sometimes corresponds to *maxima* (instead of minima) of the free-energy density.

The saddle-point equations are also self-consistency equations

$$q_{ab}^{sp} = \langle s_a s_b \rangle_{H(q_{ab},\{s_a\})} = [\, \langle s_a s_b \rangle \,] \tag{3.89}$$

where the second member means that the average is performed with the *single site Hamiltonian* $H(q_{ab}, s_a)$ and the third member is just one of the averages we would like to compute.

The partition function in eq. (3.85) cannot be computed for generic q_{ab} since there is no large n limit to exploit on the contrary, $n \to 0$. Thus, one usually looks for solutions to eqs. (3.87) within a certain family of matrices q_{ab}. We discuss below the relevant parametrizations.

Replica symmetry (RS)

In principle, nothing distinguishes one replica from another one. This is the reason why Sherrington and Kirkpatrick looked for solutions that preserve replica symmetry:

$$q_{ab} = q \;, \qquad \text{for all } a \neq b \;. \tag{3.90}$$

Inserting this *Ansatz* in (3.84) and (3.85) and taking $n \to 0$ one finds

$$q = \int_{-\infty}^{\infty} \frac{dz}{\sqrt{2\pi}}\, e^{-z^2/2}\, \tanh^2\left(\beta\sqrt{\frac{pq^{p-1}}{2}}z + \beta h\right) \;. \tag{3.91}$$

This equation resembles strongly the one for the magnetization density of the p-spin ferromagnet, eq. (2.22).

Let us first discuss the case $p = 2$, *i.e.* the SK model. In the absence of a magnetic field, one finds a second order phase transition at $T_s = J$ from a paramagnetic ($q = 0$) to a spin-glass phase with $q \neq 0$. In the presence of a field there is no phase transition. SK soon realized though that there is something wrong with this solution: the entropy at zero temperature is negative, $S(0) = -1/(2\pi)$, and this is impossible for a model with discrete spins, for which S is strictly positive. de Almeida and Thouless later showed that the reason for this failure is that the replica symmetric saddle-point is not stable, since the Hessian (3.88) is not positive definite and has negative eigenvalues. The eigenvalue responsible for the instability of the replica symmetric solution is called the *replicon*.

Comparison with the TAP equations shows that the RS *Ansatz* corresponds to the assumption that the local fields $h_i = \sum_{i_{i_1}\ldots i_{i_p}} J_{i_1\ldots i_p} m_{i_1} \ldots m_{i_p} +$

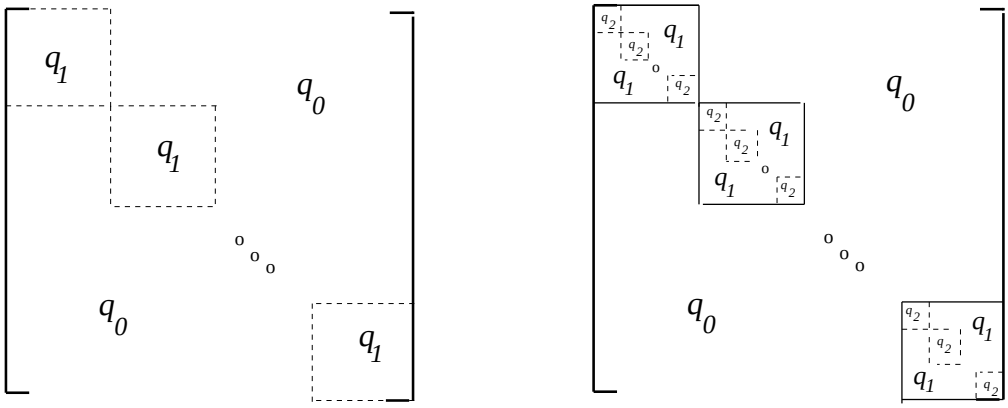

Figure 10: Left: a one-step replica symmetry breaking (1RSB) *Ansatz*. Right: a two-step replica symmetry breaking *Ansatz*. The elements on the main diagonal vanish identically. In the 1RSB case the diagonal blocks have size $m \times m$. In the 2RSB the proceudre is repeated and one has blocks of size $m_1 \times m_1$ with smaller diagonal blocks of size $m_2 \times m_2$.

h are independent and have a Gaussian distribution with average h and variance $\sigma^2 = J^2 q^{p-1}$. Numerical simulations clearly show that this assumption is invalid.

Interestingly enough, the numerical values for several physical quantities obtained with the replica symmetric solution do not disagree much with numerical results. For instance, the ground state zero-temperature energy density is $E^0 = -0.798$ while with numerical simulations one finds $E^0 \sim -0.76$.

For the $p > 2$ model one finds that the replica symmetric solution is stable at all temperatures. However, the problem of the negative entropy remains and should be solved by another solution. The transition must then have aspects of a first-order one, with another solution appearing at low temperatures and becoming the most convenient one at the transition.

One step replica symmetry breaking

The next challenge is to device a replica symmetry breaking *Ansatz*, in the form of a matrix q_{ab} that is not invariant under permutations of rows or columns. There is no first principles way of doing this, instead, the structure of the *Ansatz* is the result of trial and error. Indeed, a kind of minimal way

to break the replica symmetry is to propose a structure in blocks as the one shown in Fig. 10-left. The diagonal elements are set to zero as in the RS case. Square blocks of linear size m close to the main diagonal are filled with a paramater q_1. The elements in the rest of the matrix take a different value q_0 and one takes $0 \leq q_0 \leq q_1$. The matrix q_{ab} depends on three parameters $q_0,\ q_1,\ m$ and one has to find the values such that the free-energy density is *maximized*! The conditions for a extreme are

$$\frac{\partial f(q_0, q_1, m)}{\partial q_0} = \frac{\partial f(q_0, q_1, m)}{\partial q_1} = \frac{\partial f(q_0, q_1, m)}{\partial m} = 0 \ . \tag{3.92}$$

In the SK model ($p = 2$) the 1RSB *Ansatz* yields a second order phase transition ($q_0 = q_1 = 0$ and $m = 1$ at criticality) at a critical temperature $T_s = J$, that remains unchanged with respect to the one predicted by the RS *Ansatz*. The 1RSB solution is still unstable below T_s and in all the low temperature phase. One notices, however, that the zero temperature entropy, even if still negative and incorrect, takes a value that is closer to zero, $S(T = 0) \approx -0.01$, the ground state energy is closer to the value obtained numerically, and the replicon eigenvalue even if still negative has an absolute value that is closer to zero. All this suggest that the 1RSB *Ansatz* is closer to the exact solution.

Instead, in all cases with $p \geq 3$ the 1RSB *Ansatz* is stable below the static critical temperature T_s and all the way up to a new characteristic temperature $0 < T_f < T_s$. Moreover, one can prove that in this range of temperatures the model is solved exactly by this *Ansatz*. The critical behaviour is quite peculiar: while the order parameters q_0 and q_1 jump at the transition from a vanishing value in the paramagnetic phase to a non-zero value right below T_s, all thermodynamic quantities are continuous since $m = 1$ at T_s and all q_0 and q_1 dependent terms appear multiplied by $1 - m$. This is a mixed type of transition that has been baptized *random first-order*. Note that disorder weakens the critical behaviour in the $p \geq 3$-spin models. In the limit $p \to \infty$ the solutions become $m = T/T_c$, $q_0 = 0$ and $q = 1$.

<u>k-step replica symmetry breaking</u>

The natural way to generalize the 1RSB *Ansatz* is to propose a k-step one. In each step the off-diagonal blocks are left unchanged while the diagonal ones of size m_k are broken as in the first step thus generating smaller square blocks of size m_{k+1}, close to the diagonal. At a generic k-step RSB scheme one has

$$0 \leq q_0 \leq q_1 \leq \ldots \leq q_{k-1} \leq q_k \leq 1 \ , \tag{3.93}$$

$$n = m_0 \geq m_1 \geq \ldots \geq m_k \geq m_{k+1} \ , \tag{3.94}$$

parameters. In the $n \to 0$ limit the ordering of the parameters m is reversed

$$0 = m_0 \leq m_1 \leq \ldots \leq m_k \leq m_{k+1} \ . \tag{3.95}$$

In the SK model one finds that any finite k-step RSB *Ansatz* remains unstable. However, increasing the number of breaking levels the results continue to improve with, in particular, the zero temperature entropy getting closer to zero. In the $p \geq 3$ case instead one finds that the 2RSB *Ansatz* has, as unique solution to the saddle-point equations, one that boils down to the 1RSB case. This suggests that the 1RSB *Ansatz* is stable as can also be checked with the analysis of the Hessian eigenvalues: the replicon is stricly positive for all $p \geq 3$.

Full replica symmetry breaking

In order to construct the full RSB solution the breaking procedure is iterated an infinite number of times. The full RSB *Ansatz* thus obtained generalizes the block structure to an infinite sequence by introducing a function

$$q(x) = q_i \ , \qquad m_{i+1} < x < m_i \tag{3.96}$$

with $0 \leq x \leq 1$. Introducing $q(x)$ sums over replicas are traded by integrals over x; for instance

$$\frac{1}{n} \sum_{a \neq b} q_{ab}^l = \int_0^1 dx \ q^l(x) \ . \tag{3.97}$$

The free-energy density becomes a functional of the function $q(x)$. The extremization condition is then a hard functional equation. A Landau expansion – expected to be valid close to the assumed second order phase transition – simplifies the task of solving it. For the SK model one finds

$$q(x) = \begin{cases} \frac{x}{2} \ , & 0 \leq x \leq x_1 = 2q(1) \ , \\ q_{ea} \equiv q_{max} = q(1) \ , & x_1 = 2q(1) \leq x \leq 1 \ , \end{cases} \tag{3.98}$$

at first order in $|T - T_c|$, with $q(1) = |T - T_c|/T_c$ and $x_1 = 2q(1)$. The stability analysis yields a vanishing replicon eigenvalue signalling that the full RSB solution is *marginally stable*.

One can also recover the particular case of the 1RSB using a $q(x)$ with two plateaux, at q_0 and q_1 and the breaking point at $x = m$.

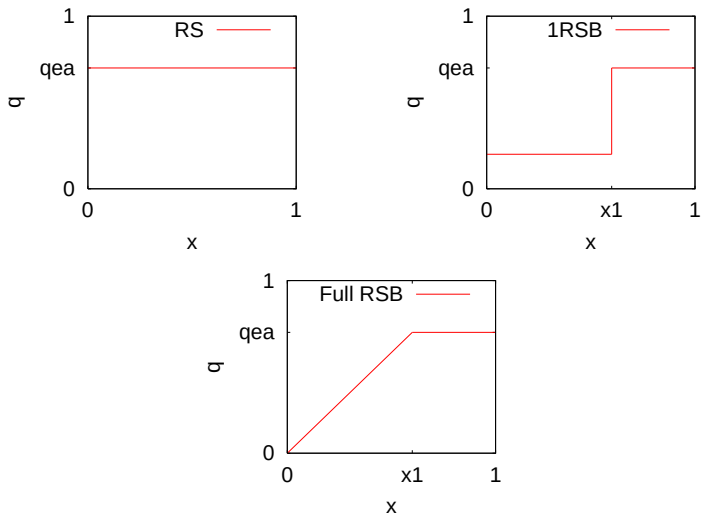

Figure 11: The function $q(x)$ for a replica symmetric (left), one step replica symmetry breaking (center) and full replica symmetry breaking *Ansätze*.

Marginality condition

In the discussion above we chose the extreme that *maximize* the free-energy density since we were interested in studying equilibrium properties. We could, instead, use a different prescription, though *a priori* not justified, and select other solutions. For example, we can impose that the solution is *marginally stable* by requiring that the replicon eigenvalue vanishes. In the $p = 2$ this leads to identical results to the ones obtained with the usual prescription since the full-RSB *Ansatz* is in any case marginally stable. In the p-spin models with $p \geq 3$ instead it turns out that the averaged properties obtained in this way correspond to the asymptotic values derived with the stochastic dynamics starting from random initial conditions. This is quite a remarkable result and we shall discuss it in more detail in Sect. **??**.

3.6.1 Interpretation of replica results

Let us now discuss the implications of the solution to fully-connected disordered models obtained with the, for the moment, rather abstract replica formalism.

The interpretation uses heavily the identification of *pure states*. Their

definition is a tricky matter that we shall not discuss in detail here. We shall just assume it can be done and use the analogy with the ferromagnetic system – and its two pure states – and the TAP results at fixed disorder. As we already know, which are the pure states, its properties, number, *etc.* can depend on the quenched disorder realization and fluctuate from sample to sample. We shall keep this in mind in the rest of our discussion.

Let us then distinguish the averages computed within a pure state and over all configuration space. In a ferromagnet with no applied magnetic field this is simple to grasp: at high temperatures there is just one state, the paramagnet, while at low temperatures there are two, the states with positive and negative magnetization. If one computes the averaged magnetization restricted to the state of positive (negative) magnetization one finds $m_{eq} > 0$ ($m_{eq} < 0$); instead, summing over all configurations $m_{eq} = 0$ even at low temperatures. Now, if one considers systems with more than just two pure states, and one labels them with Greeks indices, averages within such states are denoted $\langle O \rangle_\alpha$ while averages taken with the full Gibbs measure are expressed as

$$\langle\, O \,\rangle = \sum_\alpha w_\alpha^J \,\langle\, O \,\rangle_\alpha \,. \tag{3.99}$$

w_α^J is the probability of the α state given by

$$w_\alpha^J = \frac{e^{-\beta F_\alpha^J}}{Z_J} \,, \qquad \text{with} \qquad Z_J = \sum_\alpha e^{-\beta F_\alpha^J} \tag{3.100}$$

and thus satisfying the normalization condition $\sum_\alpha w_\alpha^J = 1$. F_α^J can be interpreted as the total free-energy of the state α. These probabilities, as well as the state dependent averages, will show sample-to-sample fluctuations.

One can then define an overlap between states:

$$q_{J\alpha\beta} \equiv N^{-1} \sum_i \langle s_i \rangle_\alpha \langle s_i \rangle_\beta = N^{-1} \sum_i m_i^\alpha m_i^\beta \tag{3.101}$$

and assume rename the self-overlap the 'Edwards-Anderson parameter'

$$q_{J\alpha\alpha} \equiv N^{-1} \sum_i \langle s_i \rangle_\alpha \langle s_i \rangle_\alpha \equiv q_{J ea} \,. \tag{3.102}$$

The statistics of possible overlaps is then characterized by a probability function

$$P_J(q) \equiv \sum_{\alpha\beta} w_\alpha^J w_\beta^J \,\delta(q - q_{\alpha\beta}) \,, \tag{3.103}$$

where we included a subindex J to stress the fact that this is a strongly sample-dependent quantity. Again, a ferromagnetic model serves to illustrate the meaning of $P_J(q)$. First, there is no disorder in this case so the J label is irrelevant. Second, the high-T equilibrium phase is paramagnetic, with $q = 0$. $P(q)$ is then a delta function with weight 1 (see the left panel in Fig. 12). In the low-T phase there are only two pure states with identical statistical properties and $q_{ea} = m^2$. Thus, $P(q)$ is just the sum of two delta functions with weight 1/2 (central panel in Fig. 12).

Next, one can consider averages over quenched disorder and study

$$[\, P_J(q) \,] \equiv \int dJ\, P(J) \sum_{\alpha\beta} w_\alpha^J w_\beta^J\, \delta(q - q_{\alpha\beta}) \,. \tag{3.104}$$

How can one access $P_J(q)$ or $[\, P_J(q) \,]$? It is natural to reckon that

$$P_J(q) = Z^{-2} \sum_{\sigma s} e^{-\beta E_J(\sigma)} e^{-\beta E_J(s)}\, \delta\left(N^{-1} \sum_i \sigma_i s_i - q \right) \tag{3.105}$$

that is to say, $P_J(q)$ is the probability of finding an overlap q between two *real* replicas of the system with identical disordered interactions in equilibrium at temperature T. This identitiy gives a way to compute $P_J(q)$ and its average in a numerical simulation: one just has to simulate two independent systems with identical disorder in equilibrium and calculate the overlap.

But there is also, as suggested by the notation, a way to relate the pure state structure to the replica matrix q_{ab}. Let us consider the simple case

$$\begin{aligned} [\, m_i \,] &= \left[Z_J^{-1} \sum_{\{s_i\}} s_i\, e^{-\beta E_J(\{s_i\})} \right] = \left[\frac{Z_J^{n-1}}{Z_J^n} \sum_{\{s_i^1\}} s_i^1\, e^{-\beta E_J(\{s_i^1\})} \right] \\ &= \left[\frac{1}{Z_J^n} \sum_{\{s_i^a\}} s_i^1 e^{-\beta \sum_{a=1}^n E_J(\{s_i^a\})} \right] \end{aligned} \tag{3.106}$$

where we singled out the replica index of the spin to average. This relation is valid for all n, in particular for $n \to 0$. In this limit the denominator approaches one and the average over disorder can be simply evaluated

$$[\, m_i \,] = \sum_{\{s_i^a\}} s_i^1 e^{-\beta E^{eff}(\{s_i^a\})} \tag{3.107}$$

and introducing back the normalization factor $Z^n = 1 = \sum_{\{s_i^a\}} e^{-\beta \sum_{a=1}^n E_J(\{s_i^a\})}$ $= [\sum_{\{s_i^a\}} e^{-\beta \sum_{a=1}^n E_J(\{s_i^a\})}] = e^{-\beta E^{eff}(\{s_i^a\})}$ we have

$$[\, m_i \,] = \langle\, s_i^a \,\rangle_{E_{eff}} \tag{3.108}$$

with a any replica index. The average is taken over the Gibbs measure of a system with effective Hamiltonian E_{eff}. In a replica symmetric problem in which all replicas are identical this result should be independent of the label a. Instead, in a problem with replica symmetry breaking the averages on the right-hand-side need not be identical for all a. This could occur in a normal vectorial theory with dimension n in which not all components take the same expected value. It is reasonable to assume that the full thermodynamic average is achieved by the sum over all these cases,

$$[\, m_i \,] = \lim_{n \to 0} \frac{1}{n} \sum_{a=1}^{n} \langle\, s_i^a \,\rangle \; . \tag{3.109}$$

Let us now take a less trivial observable and study the spin-glass order parameter q

$$\begin{aligned} q \;\; &\equiv \;\; [\, \langle\, s_i \,\rangle^2 \,] = \left[Z_J^{-1} \sum_{\{s_i\}} s_i \; e^{-\beta E_J(\{s_i\})} \; Z_J^{-1} \sum_{\{\sigma_i\}} \sigma_i \; e^{-\beta E_J(\{\sigma_i\})} \right] \\ &= \;\; \left[\frac{Z^{n-2}}{Z^n} \sum_{\{s_i\},\{\sigma_i\}} s_i \sigma_i \; e^{-\beta E_J(\{s_i\}) - \beta E_J(\{\sigma_i\})} \right] \\ &= \;\; \left[\frac{1}{Z_J^n} \sum_{\{s_i^a\}} s_i^1 s_i^2 \; e^{-\beta \sum_{a=1}^n E_J(\{s_i^a\})} \right] \end{aligned} \tag{3.110}$$

In the $n \to 0$ limit the denominator is equal to one and one can then perform the average over disorder. Introducing back the normalization one then has

$$q = \langle\, s_i^a s_i^b \,\rangle_{E_{eff}(\{s_i^a\})} \tag{3.111}$$

for any arbitrary pair of replicas $a \neq b$ (since $\langle\, s_i^a s_i^a \,\rangle = 1$ for Ising spins). The average is done with an effective theory of n interacting replicas characterized by $E_{eff}(\{s_i^a\})$. Again, if there is replica symmetry breaking the actual thermal average is the sum over all possible pairs of replicas:

$$q = \lim_{n \to 0} \frac{1}{n(n-1)} \sum_{a \neq b} q^{ab} \; . \tag{3.112}$$

A similar argument allows one to write

$$q^{(k)} = [\, \langle\, s_{i_1} \dots s_{i_k} \,\rangle^2 \,] = \lim_{n\to 0} \frac{1}{n(n-1)} \sum_{a\neq b} q_{ab}^k \; . \tag{3.113}$$

One can also generalize this argument to obtain

$$P(q) = [\, P_J(q) \,] = \lim_{n\to 0} \frac{1}{n(n-1)} \sum_{a\neq b} \delta(q - q^{ab}) \tag{3.114}$$

Thus, the replica matrix q_{ab} can be ascribed to the overlap between pure states.

Note that a small applied field, though uncorrelated with a particular pure state, is necessary to have non-zero local magnetizations and then non-zero q values.

The function $P(q)$ then extends the concept of order parameter to a function. In zero field the symmetry with respect to simultaneous reversal of all spins translates into the fact that $P_J(q)$ must be symmetric with respect to $q = 0$. $[\, P_J(q) \,]$ can be used to distinguish between the droplet picture prediction for finite dimensional spin-glasses – two pure states – that simply corresponds to

$$[\, P_J(q) \,] = \frac{1}{2}\delta(q - q_{ea}) + \frac{1}{2}\delta(q + q_{ea}) \tag{3.115}$$

(see the central panel in Fig. 12) and a more complicated situation in which $[\, P_J(q) \,]$ has the two delta functions at $\pm q_{ea}$ plus non-zero values on a finite support (right panel in Fig. 12) as found in mean-field spin-glass models.

The linear susceptibility

Taking into account the multiplicity of pure states, the magnetic susceptibility, eq. (3.24), and using (3.99) becomes

$$T\chi = T[\, \chi_J \,] = 1 - \frac{1}{N} \sum_i [\, \langle\, s_i \,\rangle^2 \,] = 1 - \sum_{\alpha\beta} [\, w_\alpha^J w_\beta^J \,]\, q_{\alpha\beta} = \int dq\, (1-q)\, P(q) \; . \tag{3.116}$$

There are then several possible results for the susceptibiliy depending on the level of replica symmetry breaking in the system:

1. In a replica symmetric problem or, equivalently, in the droplet model,

$$\chi = \beta(1 - q_{ea}) \; . \tag{3.117}$$

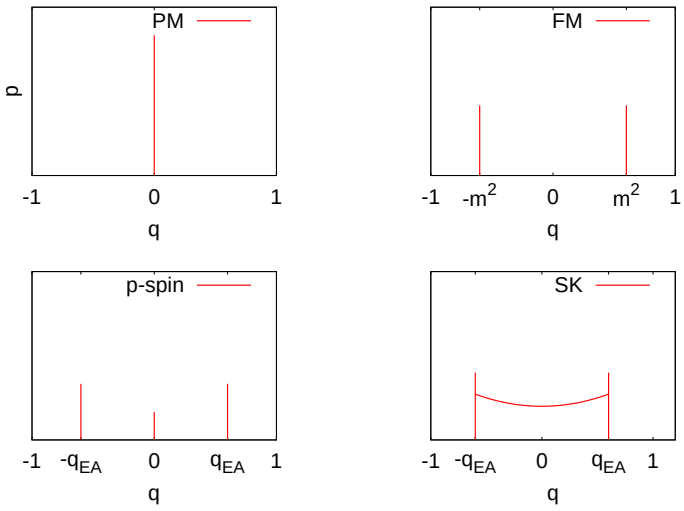

Figure 12: $[\,P_J(q)\,]$ in a paramagnet, a ferromagnet, a replica symmetric system, a system with one-step replica-symmetry breaking a system with full RSB.

This is also the susceptibility within a pure state of a system with a higher level of RSB.

2. At the one step RSB level, this becomes

$$\chi = \beta\,[1-(1-m)q_{ea}]\,. \tag{3.118}$$

3. For systems with full RSB one needs to know the complete $P(q)$ to compute χ, as in (3.116).

Note that in systems with RSB (one step or full) the susceptibility is larger than $\beta(1-q_{ea})$.

A system with $q_{ea}=1$ in the full low-temperature phase (as the REM model or $p\to\infty$ limit of the p spin model, see below) has just one configuration in each state. Systems with $q_{ea}<1$ below T_c have states formed by a number of different configurations that is exponentially large in N. (Note that $q_{ea}<1$ means that the two configurations differ in a number of spins that is proportional to N.) The logarithm of this number is usually called the intra-state entropy.

Even if the number of pure states can be very large (exponential in N)

only a fraction of them can have a non-negligible weight. This is the case if one finds, for example, $\sum_\alpha w_\alpha^2 < +\infty$

Symmetry and ergodicity breaking

In all $p \geq 2$ spin models there is a phase transition at a finite T_s at which the rather abstract *replica symmetry* is broken. This symmetry breaking is accompanied by ergodicity breaking as in the usual case. Many pure states appear at low temperatures, each one has its reversed $s_i \to -s_i$ counterpart, but not all of them are related by real-space symmetry properties.

The one-step RSB scenario

In this case the transition has first-order and second-order aspects. The order parameters q_0 and q_1 jump at the critical point as in a first-order transition but the thermodynamic quantities are continuous.

The full RSB scenario

Right below T_c an exponential in N number of equilibrium states appear. The transition is continuous, the order parameter approaches zero right below T_c. Lowering further the temperature each ergodic component breaks in many other ones. In this sense, the full spin-glass phase, $T < T_c$, is 'critical' and not only the single point T_c.

3.6.2 The pinning field

We can nevertheless choose a possible direction, given by another field $\sigma(x)$, and compute the free–energy of our system when it is weakly pinned by this external quenched field

$$F_\phi[\sigma, g, \beta] = -\frac{1}{\beta} \log \int d\phi(x)\ e^{-\beta H[\phi] - \frac{g}{2}\int dx (\sigma(x)-\phi(x))^2} \tag{3.119}$$

where $g > 0$ denotes the strength of the coupling. This free-energy (3.119) will be small when the external perturbing field $\sigma(x)$ lies in a direction corresponding to the bottom of a well of the unperturbed free-energy. Therefore, we should be able to obtain useful information about the free-energy landscape by scanning the entire space of the configurations $\sigma(x)$ to locate all the states in which the system can freeze after spontaneous ergodicity breaking ($g \to 0$). According to this intuitive idea, we now consider the field $\sigma(x)$ as a thermalized variable with the "Hamiltonian" $F_\phi[\sigma, g, \beta]$. The free-energy of

the field σ at inverse temperature βm where m is a positive free parameter therefore reads

$$F_\sigma(m,\beta) = \lim_{g\to 0^+} -\frac{1}{\beta m}\log\int d\sigma(x)\ e^{-\beta m F_\phi[\sigma,g,\beta]} \tag{3.120}$$

When the ratio m between the two temperatures is an integer, one can easily integrate $\sigma(x)$ in eq.(3.120) after having introduced m copies $\phi^\rho(x)$ ($\rho = 1...m$) of the original field to obtain the relation

$$F_\sigma(m,\beta) = \lim_{g\to 0^+} -\frac{1}{\beta m}\log\int\prod_{\rho=1}^{m} d\phi^\rho(x)\ e^{-\beta\sum_\rho H[\phi^\rho]+\frac{1}{2}\sum_{\rho,\lambda} g^{\rho\lambda}\int dx\phi^\rho(x)\phi^\lambda(x)} \tag{3.121}$$

where $g^{\rho\lambda} = g(\frac{1}{m} - \delta^{\rho\lambda})$. Let us define two more quantities related to the field σ : its internal energy $W(m,\beta) = \frac{\partial(mF_\sigma)}{\partial m}$ and its entropy $S(m,\beta) = \beta m^2\frac{\partial F_\sigma}{\partial m}$. Since the case $m = 1$ will be of particular interest, we shall use hereafter $F_{hs}(\beta) \equiv W(m=1,\beta)$ and $\mathcal{S}_{hs}(\beta) \equiv S(m=1,\beta)$ where hs stands for "hidden states". We stress that $S(m,\beta)$ and $\beta^2\frac{\partial F_\phi}{\partial\beta}$ which are respectively the entropies of the fields σ and ϕ are two distinct quantities with different physical meanings.

When the pinning field $\sigma(x)$ is thermalized at the same temperature as $\phi(x)$, that is when $m = 1$, one sees from eq.(3.121) that $F_\phi(\beta) = F_\sigma(m = 1,\beta)$. The basic idea of this letter is to decompose F_σ into its energetic and entropic contributions to obtain

$$\mathcal{S}_{hs}(\beta) = \beta\Big[F_{hs}(\beta) - F_\phi(\beta)\Big] \tag{3.122}$$

To get some insights on the significance of the above relation, we shall now turn to the particular case of disordered mean-field systems. We shall see how it rigorously gives back some analytical results derived within the mean-field TAP and dynamical approaches. We shall then discuss the physical meaning of identity (3.122) for the general case of glassy systems.

3.7 Finite dimensional systems

We start now the discussion on the statics of spin-glass models by describing briefly scaling arguments and the droplet theory. Similar arguments can be used to study other models with strong disorder, as a manifold in a random potential.

3.7.1 The Griffiths phase

The effects of quenched disorder show up already in the paramagnetic phase of finite dimensional systems. Below the critical point of the pure case (no disorder) finite regions of the system can order due to fluctuations in the couplings. Take the case of random ferromagnetic interactions. Fluctuations in bonds can be such that in a given region they take higher values than on average. In practice, at the working temperature T that is higher than the transition temperature of the full system, T_c^{dis}, a particular region can behave as if it had have an effective T_c^{loc} that is actually higher than T_c, see Fig. **??**. Similarly, fluctuations can make a region more paramagnetic than the average if the J_{ij}'s take smaller values $[\, J_{ij} \,]$. (Note that T_c is typically proportional to J, the strength of the ferromagnetic couplings. In the disordered case we normalize the J_{ij}'s in such a way that $[\, J_{ij} \,] = J_{pure}$. We can then compare the disordered and the pure problems.)

These properties manifest in non-analyticities of the free-energy that appear in a full interval of temperatures above (and below) the critical temperature of the disordered model, as shown by Griffiths. For instance, deviations from Curie-Weiss ($\chi = 1/T$) behaviour appear below the Néel temperature of dilute antiferromagnets in a uniform field. These are sometimes described with a Lorentzian distribution of local temperatures with the corresponding Curie-Weiss law at each T. It is clear that Griffiths effects will also affect the relaxation of disordered systems above freezing. We shall not discuss these features in detail here.

3.7.2 Droplets and domain-wall stiffness

Let us now just discuss one simple argument that is at the basis of what is needed to derive the results of the droplet theory without entering into the complications of the calculations.

It is clear the structure of *droplets*, meaning patches in which the spins point in the direction of the opposite state, plays an important role in the thermodynamic behaviour of systems undergoing a phase transition. At criticality one observes ordered domains of the two equilibrium states at all length scales – with *fractal* properties. Right above T_c finite patches of the system are indeed ordered but these do not include a finite fraction of the spins in the sample and the magnetization density vanishes. However, these patches are enough to generate non-trivial thermodynamic properties very close to

T_c and the richness of critical phenomena. M. Fisher and others developed a droplet phenomenological theory for critical phenomena in clean systems. Later D. S. Fisher and D. Huse extended these arguments to describe the effects of quenched disorder in spin-glasses and other random systems; this is the so-called *droplet model*.

Critical droplet in a ferromagnet

Let us study the stability properties of an equilibrium ferromagnetic phase under an applied external field that tends to destabilize it. If we set $T = 0$ the free-energy is just the energy. In the ferromagnetic case the free-energy cost of a spherical droplet of radius R of the equilibrium phase parallel to the applied field embedded in the dominant one (see Fig. 13-left) is

$$\Delta F(R) = -2\Omega_d R^d h m_{eq} + \Omega_{d-1} R^{d-1} \sigma_0 \tag{3.123}$$

where σ_0 is the interfacial free-energy density (the energy cost of the domain wall) and Ω_d is the volume of a d-dimensional unit sphere. We assume here that the droplet has a regular surface and volume such that they are proportional to R^{d-1} and R^d, respectively. The excess free-energy reaches a maximum

$$\Delta F_c = \frac{\Omega_d}{d} \frac{\Omega_{d-1}^d}{\Omega_d^d} \left(\frac{d-1}{2dhm_{eq}} \right)^{d-1} \sigma_0^d \tag{3.124}$$

at the critical radius

$$R_c = \frac{(d-1)\Omega_{d-1}\sigma_0}{2d\Omega_d h m_{eq}} , \tag{3.125}$$

see Fig. 13 ($h > 0$ and $m > 0$ here, the signs have already been taken into account). The free-energy difference vanishes at

$$\Delta F(R_0) = 0 \qquad \Rightarrow \qquad R_0 = \frac{\Omega_{d-1}\sigma_0}{2\Omega_d h m_{eq}} . \tag{3.126}$$

Several features are to be stressed:

1. The barrier vanishes in $d = 1$; indeed, the free-energy is a linear function of R in this case.
2. Both R_c and R_0 have the same dependence on hm_{eq}: they monotonically decrease with increasing hm_{eq} vanishing for $hm_{eq} \to \infty$ and diverging for $hm_{eq} \to 0$.

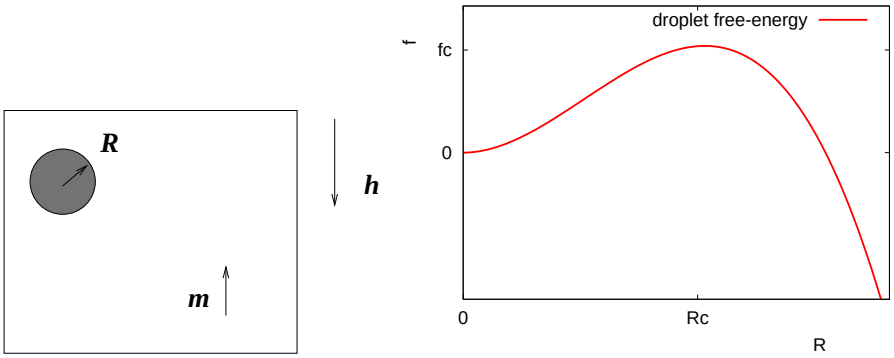

Figure 13: Left: the droplet. Right: the free-energy density $f(R)$ of a spherical droplet with radius R.

3. In dynamic terms that we shall discuss later, the passage above the barrier is done *via* thermal activation; as soon as the system has reached the height of the barrier it rolls on the right side of 'potential' ΔF and the favorable phase nucleates.
4. As long as the critical size R_c is not reached the droplet is not favorable and the system remains positively magnetized.

In this example the field drives the system from one state to the other. In studies of phase transitions at zero external field, temperature generates fluctuations of different size and the question is whether these are favourable or not. The study of droplet fluctuations is useful to establish whether an ordered phase can exist at low (but finite) temperatures. One then studies the free-energy cost for creating large droplets with thermal fluctuations that may destabilize the ordered phase, in the way we have done with the simple Ising chain. Indeed, a fundamental difference between an ordered and a disordered phase is their stiffness (or rigidity). In an ordered phase the free-energy cost for changing one part of the system with respect to the other part far away is of the order k_BT and usually diverges as a power law of the system size. In a disordered phase the information about the reversed part propagates only a finite distance (of the order of the correlation length, see below) and the stiffness vanishes.

The calculation of the stiffness is usually done as follows. Antiparallel configurations (or more generally the two ground states) are imposed at the

opposite boundaries of the sample. A domain wall is then generated somewhere in the bulk. Its free-energy cost, *i.e.* the difference between the free-energies of the modified configuration and the equilibrium one, is measured and one tests when creating a wall is favourable.

The Imry-Ma argument for the random field Ising model

Take a ferromagnetic Ising model in a random field, defined in eq. (3.19). In zero applied field and low enough temperature, if $d > 1$ there is phase transition between a paramagnetic and a ferromagnetic phase. Under the effect of a random field with very strong typical strength, the spins align with the local external fields and the system is paramagnetic. It is, however, non-trivial to determine the effect of a relatively weak random field on the ferromagnetic phase at sufficiently low temperature. The long-range ferromagnetic order could be preserved or else the field could be enough to break up the system into large but finite domains of the two ferromagnetic phases.

A qualitative argument to estimate whether the ferromagnetic phase survives or not in presence of the external random field due to Imry and Ma. Let us fix $T = 0$ and switch on a random field. If a domain $\mathcal{D}$ of the opposite order (say down) is created within the bulk of the ordered state (say up) the system pays an energy due to the unsatisfied links lying on the boundary that is

$$\Delta E_{border} \sim 2JL^{d-1} \tag{3.127}$$

where L is the linear length of the border and $d-1$ is the dimension of the border of a domain embedded in d a dimensional volume, assuming it is compact. By creating a domain boundary the system can also gain a magnetic energy in the interior of the domain due to the external field:

$$\Delta E_{rf} \sim -hL^{d/2} \tag{3.128}$$

since there are $N = L^d$ spins inside the domain of linear length L and, using the central limit theorem, $-h\sum_{j\in\mathcal{D}} s_i \sim -h\sqrt{N} = -hL^{d/2}$. The comparison between these two energy scales yields

$$JL_0^{d-1} \sim hL_0^{d/2} \qquad \left(\frac{h}{J}\right)^{\frac{2}{d-2}} \sim L_0 \tag{3.129}$$

In the large L limit ΔE diverges to $+\infty$ with increasing L in $d > 2$. The marginal case $d = 2$ is more subtle and we do not discuss it in detail here.

One can also search for an extreme in $\Delta E(L)$ finding

$$L_c \sim \left(\frac{4J(d-1)}{hd}\right)^2 . \tag{3.130}$$

Several comments are in order:

1. In $d = 1$ the energy difference is a monotonically decreasing function of L thus suggesting that the creation of droplets is very favorable and there is no barrier to cross to do it.
2. In $d > 2$ the energy difference first decreases from $\Delta E(L = 0) = 0$ to reach a nagative minimum at L_c, and then increases back to pass through zero at L_0 and diverge at infinity. This indicates that the creation of domains at zero temperature is not favorable in $d > 2$. Just domains of finite length, upto L_0 can be created. Note that L_0 increases with h/J in $d > 2$ and thus a higher field tends to generate larger droplets and thus disorder the sample.

With this argument one cannot show the existence of a phase transition at h_c nor the nature of it. The argument is such that it suggests that order can be supported by the system at zero temperature and small fields.

An elastic line in a random potential

Let us take an interface model of the type defined in eq. (3.21) with $N = 1$. If one assumes that the interfaces makes an excursion of longitudinal length L and transverse length ϕ the leastic energy cost is

$$E_{elast} = \frac{c}{2}\int d^d x\, (\nabla\phi(\vec{x}))^2 \qquad \Rightarrow \qquad \Delta E_{elast} \sim cL^d(L^{-1}\phi)^2 = cL^{d-2}\phi^2 \tag{3.131}$$

If the excursion is sufficiently large, the interface meets $\phi L^d/\Delta^{d+1}$ impurities (that is to say the volume of the displacement over the typical volume between impurities given by the correlation length of disorder to the power given by the number of dimensions). Each impurity applies a pinning force of the order of $dV/d\phi \sim \sqrt{W/\Delta^d}$ and then the energy gain due to the random potential is

$$\Delta E_{random} \sim \sqrt{W/\Delta^d} . \tag{3.132}$$

The balance between the cost of elastic energy and the gain in random energy leads to

$$\phi \sim \Delta(L/\xi)^{(4-d)/3} \tag{3.133}$$

where $\xi = (c^2\Delta^4/W)^{1/(4-d)}$ is the *Larkin length* and $\alpha = (4-d)/3$ is the *Flory exponent* for the roughness of the surface. One then concludes that for $d > 4$ disorder is irrelevant and the interface is flat ($\phi \to 0$ when $L \to \infty$). Since the linearization of the elastic energy [see the discussion leading to eq. (3.21)] holds only if $\phi/L \ll 1$, the result (3.133) may hold only for $d > 1$ where $\alpha < 1$.

The $3d$ Edwards-Anderson model in a uniform magnetic field

A very similar reasoning is used to argue that there cannot be spin-glass order in an Edwards-Anderson model in an external field. The only difference is that the domain wall energy is here assumed to be proportional to L^y with an *a priori* unknown d-dependent exponent y that is related to the geometry of the domains.

Comments These arguments are easy to implement when one knows the equilibrium states. They cannot be used in models in which the energy is not a slowly varying function of the domain wall position.

3.7.3 The droplet theory

The droplet theory is a phenomenological model that assumes that the low temperature phase of a spin-glass model has only two equilibrium states related by an overall spin flip. It is then rather similar to a ferromagnet, only that the nature of the order in the two equilibrium states is not easy to see, it is not just most spins pointing up or most spins pointing down with some thermal fluctuations within. At a glance, one sees a disordered paramagnetic like configuration and a more elaborate order parameter has to be measured to observe the order. The spin-glass phase is then called a *disguised ferromagnet* and a usual spontaneous symmetry breaking (between the two equilibrium states related spin reversal symmetry) leading to usual ergodicity breaking is supposed to take place at T_c.

Once this assumption has been done, renormalization group arguments are used to describe the scaling behavior of several thermodynamic quantities. The results found are then quantitatively different from the ones for a ferromagnet but no *novelties* appear.

We shall not develop these arguments here.

3.8 The random manifold

The problem of an **oriented manifold** embedded in a space with random impurities is relevant for a large class of physical systems. The dimension of the manifold is called d while the dimension of the embedding space is called N; there are then N transverse dimensions to the manifold. Both d and N are important to determine the behaviour of the manifold. Different choices of d and N are associated with different physical problems. If $N = 1$ the model describes the interface between two coexisting phases. For $d = 1$ the model is that of a directed polymer which also describes the interaction of a flux line in a type II superconductor. This problem shares many of the interesting features of other disordered system such as spin-glasses.

Attention has been first paid to the study of the equilibrium properties of the manifold. Mainly two approaches have been applied. On the one hand, Mézard and Parisi [24] proposed a Gaussian Variational method complemented by the replica analysis with an ensuing replica symmetry breaking solution. This study allowed to obtain very interesting results such as non-trivial - Flory-like - exponents for the displacement of the manifold, sample to sample susceptibility fluctuations, etc. On the other hand, the functional renormalization group and the relation between the two in the large N limit was discussed by Le Doussal and collaborators [11]. The extension of the large N treatment and the Gaussian Variational Approach (GVA) to the out of equilibrium relaxation has been developed and we discuss it below [14]. The dynamic functional renormalization group to treat the out of equilibrium dynamics is not ready yet.

The model of a manifold of internal dimension d embedded in a random medium is described, in terms of an N component displacement field, $\vec{\phi} = (\phi_1, \phi_2, \ldots, \phi_N)$, by the Hamiltonian

$$H = \int d^d x \left[\frac{1}{2} (\vec{\nabla}\vec{\phi}(\vec{x}))^2 + V(\vec{\phi}(\vec{x}), \vec{x}) + \frac{\mu}{2} \vec{\phi}^2(\vec{x}) \right] . \tag{3.134}$$

μ is a mass, which effectively constraints the manifold to fluctuate in a restricted volume of the embedding space. The elastic terms has to be read as

$$\vec{\nabla}\vec{\phi}(\vec{x}) = \sum_{i=1}^{d} \sum_{\alpha=1}^{N} \frac{\partial}{\partial x_i} \phi_\alpha(\vec{x}) \frac{\partial}{\partial x_i} \phi_\alpha(\vec{x}) . \tag{3.135}$$

The Hamiltonian is invariant under rotations of the vector $\vec{\phi}$. $(\vec{\phi}, \vec{x}) = \vec{\phi}(\vec{x})$ is a point in the $N + d$ dimensional space. V is a Gaussian random potential

with zero mean and correlations

$$\overline{V(\vec{\phi},\vec{x})V(\vec{\phi}',\vec{x}')} = -N\delta^d(\vec{x}-\vec{x}')\;\Delta\left(\frac{|\vec{\phi}-\vec{\phi}'|^2}{N}\right)\;. \tag{3.136}$$

The factors N are introduced to have a good $N\to\infty$ limit. The overline represents the average over the distribution of the random potential V. We label with greek indices the N-components of the field $\vec{\phi}$, $\phi_\alpha, \alpha = 1,\ldots,N$. The internal coordinate $\vec{x}$ has d components $\vec{x} = (x_1,\ldots,x_d)$ and we label them with latin indices, $x_i, i = 1,\ldots,d$. Note the similarity with the $O(N)$ coarsening problem. We study this problem in the infinite volume limit $-\infty < \phi_\alpha < \infty$ and $-\infty < x_i < \infty$.

Equilibrium properties

The equilibrium properties of the manifold are often described in terms of the displacement of the manifold $D^{st}(\vec{x},\vec{x}')$ that is characterized by the roughness exponent ζ:

$$D^{st}(\vec{x},\vec{x}') \equiv \overline{\langle\left(\vec{\phi}(\vec{x})-\vec{\phi}(\vec{x}')\right)^2\rangle} \sim |\vec{x}-\vec{x}'|^{2\zeta}\;. \tag{3.137}$$

The angular brackets denote a thermal average. The random potential and the thermal fluctuations make the manifold roughen and this impies that the fluctuations of the field $\vec{\phi}$ diverge at large distances $|\vec{x}-\vec{x}'|\gg 1$.

In the absence of disorder the manifold is flat if the internal dimension is larger than two: for $d > 2$, $\zeta = 0$. Instead, if the internal dimension is smaller that two the manifold roughens: for $d < 2$, $\zeta = (2-d)/2$. The situation changes in the presence of disorder where ζ depends on d and N non-trivially. For instance, for $d > 4$ the manifold remains flat; for $2 < d < 4$ there is only a disorder phase with a non-trivial exponent ζ, finally, for $d < 2$, and large enough N there is a high-temperature phase and a randomness dominated low-temperature phase with ζ increasing with N and approaching $1/2$ for $N\to\infty$ as suggested by numerical simulations for finite N and calculations for $N\to\infty$. Whether there is a finite upper critical N_c such that for $N > N_c$ $\zeta = 1/2$ is not clear.

There are several models which can be studied for $N\to\infty$ corresponding to different choices of the random potential correlation $\Delta(z)$. A common

choice is the 'power law model'

$$\Delta(z) = \frac{(\theta + z)^{1-\gamma}}{2(1-\gamma)} \, . \tag{3.138}$$

There are two physically distinct cases. If $\gamma(1-d/2) < 1$ the correlations grow with the distance z and the potential is called **long-range**. If $\gamma(1-d/2) > 1$ the correlations decay with the distance and the potential is called **short-range**. The statics of these models, studied with the Gaussian Variational method complemented by the replica method [24], is solved with a one step replica symmetric ansatz in the short-range case and with a full replica symmetry breaking scheme in the long-range one.

4 The Langevin equation

Examples of experimental and theoretical interest in condensed matter and biophysics in which quantum fluctuation can be totally neglected are manifold. In this context one usually concentrates on systems in contact with an environment: one selects some relevant degrees of freedom and treats the rest as a bath. It is a canonical view. Among these instances are colloidal suspensions which are particles suspended in a liquid, typically salted water, a 'soft condensed matter' example; spins in ferromagnets coupled to lattice phonons, a 'hard condensed matter' case; and proteins in the cell a 'biophysics' instance. These problems are modeled as stochastic processes with Langevin equations, the Kramers-Fokker-Planck formalism or master equations depending on the continuous or discrete character of the relevant variables and analytic convenience.

The Langevin equation is a stochastic differential equation that describes phenomenologically a large variety of problems. It models the time evolution of a set of slow variables coupled to a much larger set of fast variables that are usually (but not necessarily) assumed to be in thermal equilibrium at a given temperature. We first introduce it in the context of Brownian motion and we derive it in more generality in Sect. 2.

The Langevin equation[5] for a particle moving in one dimension in contact with a **white-noise** bath reads

$$\boxed{m\dot{v} + \gamma_0 v = F + \xi \,, \qquad v = \dot{x} \,,} \tag{4.1}$$

with x and v the particle's position and velocity. ξ is a Gaussian white noise with zero mean and correlation $\langle \xi(t)\xi(t')\rangle = 2\gamma_0 k_B T \delta(t-t')$ that mimics thermal agitation. $\gamma_0 v$ is a friction force that opposes the motion of the particle. The force F designates all external deterministic forces and depends, in most common cases, on the position of the particle x only. In cases in which the force derives from a potential, $F = -dV/dx$. The generalization to higher dimensions is straightforward. Note that γ_0 is the parameter that controls the strength of the coupling to the bath (it appears in the friction term as

[5] P. Langevin, *Sur la théorie du mouvement brownien*, Comptes-Rendus de l'Académie des Sciences **146** (1908), 530-532.

well as in the noise term). In the case $\gamma_0 = 0$ one recovers Newton equation of motion. The relation between the friction term and thermal correlation is non-trivial. Langevin fixed it by requiring $\langle v^2(t)\rangle \to \langle v^2\rangle_{eq}$. We shall give a different argument for it in the next section.

4.1 Derivation of the Langevin equation

Let us take a system in contact with an environment. The interacting system+environment ensemble is 'closed' while the system is 'open'. The nature of the environment, *e.g.* whether it can be modeled by a classical or a quantum formalism, depends on the problem under study. We focus here on the classical problem. A derivation of a generalized Langevin equation with memory is very simple starting from Newton dynamics of the full system [40, 32]. We shall then study the coupled system

$$H_{tot} = H_{syst} + H_{env} + H_{int} + H_{counter} = H_{syst} + \tilde{H}_{env} \ . \tag{4.2}$$

For simplicity we use a single particle moving in $d = 1$: H_{syst} is the Hamiltonian of the isolated particle,

$$H_{syst} = \frac{p^2}{2M} + V(x) \ , \tag{4.3}$$

with p and x its momentum and position. H_{env} is the Hamiltonian of a thermal bath that, for simplicity, we take to be an ensemble of N independent Harmonic oscillators with masses m_a and frequencies ω_a, $a = 1, \ldots, N$

$$H_{env} = \sum_{a=1}^{N} \frac{\pi_a^2}{2m_a} + \frac{m_a\omega_a^2}{2} q_a^2 \tag{4.4}$$

with π_a and q_a their momenta and positions. This is indeed a very usual choice since it may represent phonons. H_{int} is the coupling between system and environment. We shall restrict the following discussion to a linear interaction in the oscillator coordinates, q_a, and in the particle coordinate,

$$H_{int} = x \sum_{a=1}^{N} c_a q_a \ , \tag{4.5}$$

with c_a the coupling constants. The counter-term $H_{counter}$ is added to avoid the generation of a negative harmonic potential on the particle – due to the

coupling to the oscillators – that may render the dynamics unstable. We choose it to be

$$H_{counter} = \frac{1}{2}\sum_{a}^{N}\frac{c_a^2}{m_a\omega_a^2}x^2 \ . \tag{4.6}$$

The generalization to more complex systems and/or to more complicated baths and higher dimensions is straightforward. The calculations can also be easily generalized to an interaction of the oscillator coordinate with a more complicated dependence on the system's coordinate, $\mathcal{V}(x)$, that may be dictated by the symmetries of the system, see Ex. 1.

Hamilton's equations for the particle are

$$\dot{x}(t) = \frac{p(t)}{m} \ , \qquad \dot{p}(t) = -V'[x(t)] - \sum_{a=1}^{N} c_a q_a(t) - \sum_{a=1}^{N}\frac{c_a^2}{m_a\omega_a^2}x(t) \tag{4.7}$$

(the counter-term yields the last term) while the dynamic equations for each member of the environment read

$$\dot{q}_a(t) = \frac{\pi_a(t)}{m_a} \ , \qquad \dot{\pi}_a(t) = -m_a\omega_a^2 q_a(t) - c_a x(t) \ , \tag{4.8}$$

showing that they are all massive harmonic oscillators **forced by the chosen particle**. These equations are readily solved by

$$q_a(t) = q_a(0)\cos(\omega_a t) + \frac{\pi_a(0)}{m_a\omega_a}\sin(\omega_a t) - \frac{c_a}{m_a\omega_a}\int_0^t dt' \sin[\omega_a(t-t')]x(t') \tag{4.9}$$

with $q_a(0)$ and $\pi_a(0)$ the initial coordinate and position at time $t = 0$ when the particle is set in contact with the bath. It is convenient to integrate by parts the last term. The replacement of the resulting expression in the last term in the RHS of eq. (4.7) yields

$$\boxed{\dot{p}(t) = -V'[x(t)] + \xi(t) - \textstyle\int_0^t dt' \ \Gamma(t-t')\dot{x}(t') \ ,} \tag{4.10}$$

with the **symmetric and stationary kernel** Γ given by

$$\boxed{\Gamma(t-t') = \textstyle\sum_{a=1}^{N}\frac{c_a^2}{m_a\omega_a^2}\cos[\omega_a(t-t')] \ ,} \tag{4.11}$$

$\Gamma(t-t') = \Gamma(t'-t)$, and the **time-dependent force** ξ given by

$$\boxed{\xi(t) = -\textstyle\sum_{a=1}^{N} c_a\left[\frac{\pi_a(0)}{m_a\omega_a}\sin(\omega_a t) + \left(q_a(0) + \frac{c_a x(0)}{m_a\omega_a^2}\right)\cos(\omega_a t)\right] \ .} \tag{4.12}$$

This is the equation of motion of the **reduced** system.

The third term on the RHS of eq. (4.10) represents a rather complicated **friction force**. Its value at time t depends explicitly on the history of the particle at times $0 \leq t' \leq t$ and makes the equation **non-Markovian**. One can rewrite it as an integral running up to a total time $\mathcal{T} > \max(t, t')$ introducing the **retarded friction**:

$$\boxed{\gamma(t-t') = \Gamma(t-t')\theta(t-t')\ .} \tag{4.13}$$

Until this point the dynamics of the system remain deterministic and are completely determined by its initial conditions as well as those of the reservoir variables. The **statistical element** comes into play when one realizes that it is impossible to know the initial configuration of the large number of oscillators with great precision and one proposes that the initial coordinates and momenta of the oscillators have a canonical distribution at an **inverse temperature** β. Then, one chooses $\{\pi_a(0), q_a(0)\}$ to be initially distributed according to a canonical phase space distribution:

$$\boxed{P(\{\pi_a(0), q_a(0)\}, x(0)) = 1/\tilde{\mathcal{Z}}_{env}[x(0)]\ e^{-\beta \tilde{H}_{env}[\{\pi_a(0), q_a(0)\}, x(0)]}} \tag{4.14}$$

with $\tilde{H}_{env} = H_{env} + H_{int} + H_{counter}$, that can be rewritten as

$$\tilde{H}_{env} = \sum_{a=1}^{N} \left[\frac{m_a \omega_a^2}{2} \left(q_a(0) + \frac{c_a}{m_a \omega_a^2} x(0) \right)^2 + \frac{\pi_a^2(0)}{2m_a} \right] . \tag{4.15}$$

The randomness in the initial conditions gives rise to a random force acting on the reduced system. Indeed, ξ is now a **Gaussian random variable**, that is to say a noise, with

$$\langle \xi(t) \rangle = 0\,, \qquad \langle \xi(t)\xi(t') \rangle = k_B T\ \Gamma(t-t')\ . \tag{4.16}$$

One can easily check that higher-order correlations vanish for an odd number of ξ factors and factorize as products of two time correlations for an even number of ξ factors. In consequence ξ has Gaussian statistics. Defining the inverse of Γ over the interval $[0, t]$, $\int_0^t dt''\ \Gamma(t-t'')\Gamma^{-1}(t''-t') = \delta(t-t')$, one has the Gaussian pdf:

$$P[\xi] = \mathcal{Z}^{-1} e^{-\frac{1}{2k_B T} \int_0^t dt \int_0^t dt'\ \xi(t)\Gamma^{-1}(t-t')\xi(t')}\ . \tag{4.17}$$

$\mathcal{Z}$ is the normalization. A random force with non-vanishing correlations on a finite support is usually called a **coloured noise**. Equation (4.10) is now a genuine Langevin equation. A multiplicative retarded noise arises from a model in which one couples the coordinates of the oscillators to a generic function of the coordinates of the system, see Ex. 1 and eq. (4.24).

The use of an **equilibrium measure** for the oscillators implies the relation between the friction kernel and the noise-noise correlation, which are proportional, with a constant of proportionality of value $k_B T$. This is a generalized form of the **fluctuation-dissipation relation**, and it applies to the environment.

Different choices of the environment are possible by selecting different ensembles of harmonic oscillators. The simplest one, that leads to an approximate Markovian equation, is to consider that the oscillators are coupled to the particle via coupling constants $c_a = \tilde{c}_a/\sqrt{N}$ with $\tilde{c}_a$ of order one. One defines

$$\boxed{S(\omega) \equiv \frac{1}{N} \sum_{a=1}^{N} \frac{\tilde{c}_a^2}{m_a \omega_a} \, \delta(\omega - \omega_a)} \tag{4.18}$$

a function of ω, of order one with respect to N, and rewrites the kernel Γ as

$$\boxed{\Gamma(t-t') = \int_0^\infty d\omega \, \frac{S(\omega)}{\omega} \, \cos[\omega(t-t')] \, .} \tag{4.19}$$

A common choice is

$$\boxed{\frac{S(\omega)}{\omega} = 2\gamma_0 \left(\frac{|\omega|}{\tilde{\omega}}\right)^{\alpha-1} f_c\left(\frac{|\omega|}{\Lambda}\right) \, .} \tag{4.20}$$

The function $f_c(x)$ is a high-frequency cut-off of typical width Λ and is usually chosen to be an exponential. The frequency $\tilde{\omega} \ll \Lambda$ is a reference frequency that allows one to have a coupling strength γ_0 with the dimensions of viscosity. If $\alpha = 1$, the friction is said to be **Ohmic**, $S(\omega)/\omega$ is constant when $|\omega| \ll \Lambda$ as for a white noise. When $\alpha > 1$ ($\alpha < 1$) the bath is **superOhmic** (**subOhmic**). The exponent α is taken to be > 0 to avoid divergencies at low frequency. For the exponential cut-off the integral over ω yields

$$\Gamma(t) = 2\gamma_0 \tilde{\omega}^{-\alpha+1} \, \frac{\cos[\alpha \arctan(\Lambda t)]}{[1+(\Lambda t)^2]^{\alpha/2}} \, \Gamma\mathrm{a}(\alpha) \, \Lambda^\alpha \tag{4.21}$$

with $\Gamma\mathrm{a}(x)$ the Gamma-function, that in the Ohmic case $\alpha = 1$ reads

$$\Gamma(t) = 2\gamma_0 \, \frac{\Lambda}{[1+(\Lambda t)^2]} \, , \tag{4.22}$$

and in the $\Lambda \to \infty$ limit becomes a delta-function, $\Gamma(t) \to 2\gamma_0\delta(t)$. At long times, for any $\alpha > 0$ and different from 1, one has

$$\lim_{\Lambda t\to\infty} \Gamma(t) \;=\; 2\gamma_0\tilde{\omega}^{-\alpha+1}\, \cos(\alpha\pi/2)\Gamma a(\alpha)\, \Lambda^{-1}\, t^{-\alpha-1}\,, \qquad (4.23)$$

a **power law decay**.

Time-dependent, $f(t)$, and constant non-potential forces, f^{np}, as the ones applied to granular matter and in rheological measurements, respectively, are simply included in the right-hand-side (RHS) as part of the deterministic force. When the force derives from a potential, $F(x,t) = -dV/dx$.

In so far we have discussed systems with position and momentum degrees of freedom. Other variables might be of interest to describe the dynamics of different kind of systems. In particular, a continuous Langevin equation for classical spins can also be used if one replaces the hard Ising constraint, $s_i = \pm 1$, by a soft one implemented with a potential term of the form $V(s_i) = u(s_i^2 - 1)^2$ with u a coupling strength (that one eventually takes to infinity to recover a hard constraint). The soft spins are continuous unbounded variables, $s_i \in (-\infty, \infty)$, but the potential energy favors the configurations with s_i close to ± 1. Even simpler models are constructed with spherical spins, that are also continuous unbounded variables globally constrained to satisfy $\sum_{i=1}^N s_i^2 = N$. The extension to fields is straightforward and we shall discuss one when dealing with the $O(N)$ model.

Exercise Prove that or a non-linear coupling $H_{int} = \mathcal{V}[x] \sum_a c_a q_a$ there is a choice of counter-term for which the Langevin equation reads

$$\dot{p}(t) = -V'[x(t)] + \xi(t)\mathcal{V}'[x(t)] - \mathcal{V}'[x(t)] \int_0^t dt'\; \Gamma(t-t')\mathcal{V}'[x(t')]\dot{x}(t') \quad (4.24)$$

with the same Γ as in eq. (4.11) and $\xi(t)$ given by eq. (4.12) with $x(0) \to \mathcal{V}[x(0)]$. The noise appears now **multiplying** a function of the particles' coordinate.

Another derivation of the Langevin equation uses collision theory and admits a generalization to relativistic cases [41].

4.2 Properties

4.2.1 Irreversibility and dissipation.

The friction force $-\gamma_0 v$ in eq. (4.1) – or its retarded extension in the non-Markovian case – explicitly breaks time-reversal ($t \to -t$) invariance, a property that has to be respected by any set of microscopic dynamic equations. Newton equations describing the whole system, the particle and all the molecules of the fluid, are time reversal invariant. However, time-reversal can be broken in the **reduced** equation in which the fluid is treated in an effective statistical form and the fact that it is in equilibrium is assumed from the start.

Even in the case in which all forces derive from a potential, $F = -dV/dx$, the energy of the particle, $mv^2/2 + V$, is not conserved and, in general, flows to the bath leading to **dissipation**. At very long times, however, the particle may reach a stationary regime in which the particle gives and receives energy from the bath at equal rate, on average.

Exercise Prove the time-irreversibility of the Langeving equation and the fact that the symmetry is restored if $\gamma_0 = 0$. Show that $d\langle H\rangle/dt \neq 0$ when $\gamma_0 \neq 0$.

4.2.2 Discretization of stochastic differential equations

The way in which a stochastic differential equation with white noise is to be discretized is a subtle matter that we shall not discuss in these lectures, unless where it will be absolutely necessary. There are basically two schemes, called the Itô and Stratonovich calculus, that are well documented in the literature.

In short, we shall use a prescription in which the pair velocity-position of the particle at time $t + \delta$, with δ an infinitesimal time-step, depends on the pair velocity-position at time t and the value of the noise at time t.

4.2.3 Markov character

In the case of a white noise (delta correlated) the full set of equations defines a **Markov process**, that is a stochastic process that depends on its history only through its very last step.

4.2.4 Generation of memory

The Langevin equation (4.1) is actually a set of two first order differential equations. Notice, however, that the pair of first-order differential equations

could also be described by a single second-order differential equation:

$$m\ddot{x} + \gamma_0 \dot{x} = F + \xi \ . \tag{4.25}$$

Having replaced the velocity by its definition in terms of the position $x(t)$ depends now on $x(t-\delta)$ and $x(t-2\delta)$. This is a very general feature: by integrating away some degrees of freedom (the velocity in this case) one generates memory in the evolution. Generalizations of the Langevin equation, such as the one that we have just presented with colored noise, and the ones that will be generated to describe the slow evolution of super-cooled liquids and glasses in terms of correlations and linear responses, do have memory.

4.2.5 Smoluchowski (overdamped) limit

In many situations in which friction is very large, the characteristic time for the relaxation of the velocity degrees of freedom to their Maxwellian distribution, t_r^v, is very short (see the examples in Sect. 2.3). In consequence, observation times are very soon longer than this time-scale, the inertia term $m\dot{v}$ can be dropped, and the Langevin equation becomes

$$\gamma_0 \dot{x} = F + \xi \tag{4.26}$$

(for simplicity we wrote the white-noise case). Indeed, this **overdamped** limit is acceptable whenever the observation times are much longer than the characteristic time for the velocity relaxation. Inversely, the cases in which the friction coefficient γ_0 is small are called **underdamped**.

In the overdamped limit with white-noise the friction coefficient γ_0 can be absorbed in a rescaling of time. One defines the new time τ

$$t = \gamma_0 \tau \tag{4.27}$$

the new position, $\tilde{x}(\tau) = x(\gamma_0 \tau)$, and the new noise $\eta(\tau) = \xi(\gamma_0 \tau)$. In the new variables the Langevin equation reads $\dot{\tilde{x}}(\tau) = F(\tilde{x}, \tau) + \eta(\tau)$ with $\langle \eta(\tau)\eta(\tau') \rangle = 2k_B T \delta(\tau - \tau')$.

4.3 The basic processes

We shall discuss the motion of the particle in some $1d$ representative potentials: under a constant force, in a harmonic potential, in the flat limit

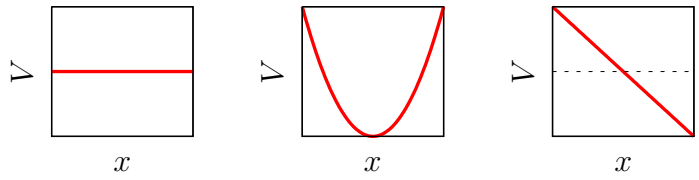

Figure 14: Three representative one-dimensional potentials.

of these two (Fig. 14) and the escape from a metastable state and the motion in a double well potential (Fig. 17).

4.3.1 A constant force

Let us first consider the case of a **constant force**, F. The first thing to notice is that the Maxwell-Boltzmann measure

$$P_{gb}(v,x) \propto e^{-\beta\left(\frac{v^2}{2m}+V(x)\right)} \tag{4.28}$$

is not normalizable if the size of the line is infinite, due to the $\exp[-\beta V(x)] = \exp(\beta F x)$ term. Let us then study the evolution of the particle's velocity and position to show how these variables behave and the fact that they do very differently.

The problem to solve is a set of two coupled stochastic first order differential equations on $(v(t)x(t))$, one needs two initial conditions v_0 and x_0.

The velocity

The time-dependent velocity follows from the integration of eq. (4.1) over time

$$v(t) = v_0\, e^{-\frac{\gamma_0}{m}t} + \frac{1}{m}\int_0^t dt'\, e^{-\frac{\gamma_0}{m}(t-t')}\,[\,F+\xi(t')\,]\,, \qquad v_0 \equiv v(t=0)\,.$$

The velocity is a **Gaussian variable** that inherits its average and correlations from the ones of ξ. Using the fact that the noise has zero average

$$\langle v(t)\rangle = v_0\, e^{-\frac{\gamma_0}{m}t} + \frac{F}{\gamma_0}\left(1-e^{-\frac{\gamma_0}{m}t}\right)\,.$$

In the short time limit, $t \ll t_r^v = m/\gamma_0$, this expression approaches the Newtonian result ($\gamma_0 = 0$) in which the velocity grows linearly in time $v(t) =$

$v_0 + F/m\ t$. In the opposite long time limit, $t \gg t_r^v = m/\gamma_0$, for all initial conditions v_0 the averaged velocity decays exponentially to the constant value F/γ_0. The saturation when the bath is active ($\gamma_0 \neq 0$) is due to the friction term. The two limiting values match at $\simeq t_r^v \gg 1$. The **relaxation time** separating the two regimes is

$$\boxed{t_r^v = \frac{m}{\gamma_0}\ .} \tag{4.29}$$

The velocity mean-square displacement is

$$\sigma_v^2(t) \equiv \langle (v(t) - \langle v(t) \rangle)^2 \rangle = \frac{k_B T}{m} \left(1 - e^{-2\frac{\gamma_0}{m}t}\right) \tag{4.30}$$

independently of F. This is an example of the **regression theorem** according to which the fluctuations decay in time following the same law as the average value. The short and long time limits yield

$$\sigma_v^2(t) \equiv \langle (v(t) - \langle v(t) \rangle)^2 \rangle \simeq \frac{k_B T}{m} \begin{cases} \frac{2\gamma_0}{m}\ t & t \ll t_r^v \\ 1 & t \gg t_r^v \end{cases} \tag{4.31}$$

and the two expressions match at $t \simeq t_r^v/2$. The asymptotic limit is the result expected from equipartition of the kinetic energy, $\langle (v(t) - \langle v(t) \rangle)^2 \rangle \to \langle (v(t) - \langle v \rangle_{stat})^2 \rangle_{stat}$ that implies for the kinetic energy $\langle K \rangle_{stat} = k_B T/2$ (only if the velocity is measured with respect to its average). In the heuristic derivation of the Langevin equation for $F = 0$ the amplitude of the noise-noise correlation, say A, is not fixed. The simplest way to determine this parameter is to require that equipartition for the kinetic energy holds $A/(\gamma_0 m) = T/m$ and hence $A = \gamma_0 T$. This relation is known under the name of **fluctuation–dissipation theorem** (FDT) **of the second kind** in Kubo's nomenclature. It is important to note that this FDT characterizes the surrounding fluid and not the particle, since it relates the noise-noise correlation to the friction coefficient. In the case of the Brownian particle this relation ensures that after a transient of the order of t_r^v, the bath maintains the mean kinetic energy of the particle constant and equal to its equilibrium value.

The velocity **two-time connected correlation** reads

$$\langle [v(t) - \langle v(t) \rangle][v(t') - \langle v(t') \rangle] \rangle = \frac{k_B T}{m} \left[e^{-\frac{\gamma_0}{m}|t-t'|} - e^{-\frac{\gamma_0}{m}(t+t')} \right]\ .$$

This is sometimes called the **Dirichlet correlator**. This and all other higher-order velocity correlation functions approach a **stationary limit** when

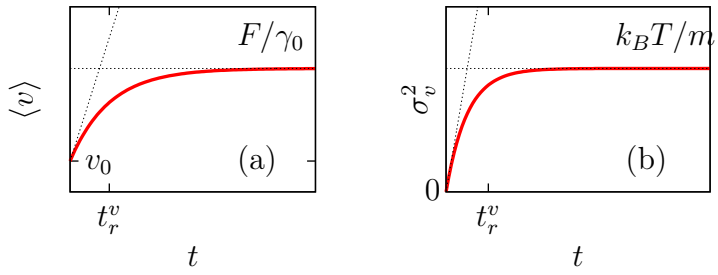

Figure 15: Results for the constant force problem. (a) Mean velocity as a function of time. (b) Velocity mean-square displacement as a function of time. In both cases the linear behavior at short times, $t \ll t_r^v$ and the saturation values are shown.

the shortest time involved is longer than t_r^v. At $t = t'$ on recovers the mean-square displacement computed in eq. (4.30). When both times are short compared to t_r^v the two-time correlator behaves as $\sim 2k_BT\gamma_0/m^2 \ \max(t, t')$. When at least one of the two times is much longer than t_r^v the second term vanishes and one is left with an exponential decay as a function of time delay:

$$C^c_{vv}(t, t') \equiv \langle [v(t) - \langle v(t) \rangle][v(t') - \langle v(t') \rangle \rangle \to \frac{k_BT}{m} e^{-\frac{\gamma_0}{m}|t-t'|} \qquad t, t' \gg t_r^v \ . \tag{4.32}$$

The two-time connected correlation falls off to, say, $1/e$ in a **decay time** $t_d^v = m/\gamma_0$. In this simple case $t_r^v = t_d^v$ but this does not happen in more complex cases.

More generally one can show that for times $t_1 \geq t_2 \geq \ldots \geq t_n \geq t_r^v$:

$$\boxed{\langle v(t_1 + \Delta) \ldots v(t_n + \Delta) \rangle = \langle v(t_1) \ldots v(t_n) \rangle \quad \text{(TTI)}} \tag{4.33}$$

for all delays Δ. **Time-translation invariance (TTI)** or **stationarity** is one generic property of **equilibrium dynamics**. Another way of stating (4.33) is

$$\langle v(t_1) \ldots v(t_n) \rangle = f(t_1 - t_2, \ldots, t_{n-1} - t_n) \ . \tag{4.34}$$

Another interesting object is the linear response of the averaged velocity to a small perturbation applied to the system in the form of $V \to V - hx$,

i.e. a change in the slope of the potential in this particular case. One finds

$$R_{vx}(t,t') \equiv \left.\frac{\delta\langle v(t)\rangle_h}{\delta h(t')}\right|_{h=0} = \frac{1}{m}\, e^{-\frac{\gamma_0}{m}(t-t')}\, \theta(t-t') \tag{4.35}$$

$$\simeq \frac{1}{k_B T}\langle [v(t) - \langle v(t)\rangle][v(t') - \langle v(t')\rangle]\rangle\, \theta(t-t') \tag{4.36}$$

the last identity being valid in the limit t or $t' \gg t_r^v$. This is an FDT relation between a linear response, $R_{vx}(t,t')$, and a connected correlation, $C^c_{vv}(t,t')$, that holds for one of the particle variables, its velocity, when this one reaches the stationary state.

$$\boxed{k_B T\; R_{vx}(t,t') = C^c_{vv}(t,t')\; \theta(t-t') \qquad \text{(FDT)}\;.} \tag{4.37}$$

In conclusion, the velocity is a Gaussian variable that after a characteristic time t_r^v verifies 'equilibrium'-like properties: its average converges to a constant (determined by F), its multi-time correlation functions become stationary and a fluctuation-dissipation theorem links its linear response to the connected correlation at two times. More general FDT's are discussed in the exercise proposed below.

The position

The particle's position, $x(t) = x_0 + \int_0^t dt' v(t')$ is still a Gaussian random variable:

$$\begin{aligned} x(t) &= x_0 + v_0\; t_r^v + \frac{F}{\gamma_0}(t - t_r^v) + t_r^v \left(\frac{F}{\gamma_0} - v_0\right) e^{-\frac{\gamma_0}{m}t} \\ &\quad + \frac{1}{m}\int_0^t dt' \int_0^{t'} dt''\; e^{-\frac{\gamma_0}{m}(t'-t'')}\; \xi(t'')\;. \end{aligned} \tag{4.38}$$

Its noise-average behaves as the Newtonian result, **ballistic motion**, $\langle x(t)\rangle = x_0 + v_0 t + F/(2m)\; t^2$ at short times $t \ll t_r^v$ and it crossover to

$$\boxed{\langle x(t)\rangle \to x_0 + v_0\; t_r^v + \tfrac{F}{\gamma_0}(t - t_r^v)} \tag{4.39}$$

for $t \gg t_r^v$. Note the reduction with respect to ballistic motion ($x \propto F t^2$) due to the friction drag and the fact that this one-time observable does not saturate to a constant.

The position mean-square displacement approaches

$$\boxed{\sigma_x^2(t) \equiv \langle (x(t) - \langle x(t) \rangle)^2 \rangle \to 2D_x t \quad \text{with} \quad D_x \equiv \frac{k_B T}{\gamma_0} \quad \text{(Diffusion)}} \tag{4.40}$$

in the usual $t \gg t_r^v$ limit, that is to say **normal diffusion** with the **diffusion constant** D_x. This expression can be computed using $x(t) - \langle x(t) \rangle$ as obtained from the $v(t) - \langle v(t) \rangle$ above (and it is quite a messy calculation) or one can simply go to the Smoluchowski limit, taking advantage of the knowledge of what we have just discussed on the behaviour of velocities, and obtain diffusion in two lines. In contrast to the velocity mean-square displacement this quantity does not saturate at any finite value. Similarly, the particle displacement between two different times t and t' is

$$\Delta_{xx}(t, t') \equiv \langle [x(t) - x(t')]^2 \rangle \to 2D_x |t - t'| \, . \tag{4.41}$$

It is interesting to note that the force dictates the mean position but it does not modify the fluctuations about it (similarly to what it did to the velocity). Δ_{xx} is stationary for time lags longer than t_r^v.

The two-time position-position connected correlation reads

$$C_{xx}^c(t, t') = \langle (x(t) - \langle x(t) \rangle)(x(t') - \langle x(t') \rangle) \rangle = \tag{4.42}$$

Exercise: compute it.

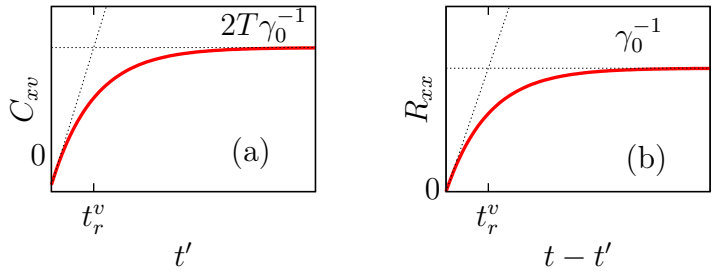

Figure 16: Results for the constant force problem. (a) The correlation between the position and the velocity of the particle measured at different times. (b) The linear response of the position to a kick applied linearly to itself at a previous time. In both cases the linear behavior at short times, $t \ll t_r^v$ and the saturation values are shown.

Another way to measure the diffusion coefficient directly from the velocity that is commonly used in the literature is

$$\boxed{D_x = \lim_{\tau\to\infty} \lim_{t'\to\infty} \int_0^\tau dt' \langle v(\tau + t')v(t')\rangle \ .} \tag{4.43}$$

One can check that it gives the same result.

The linear response of the particle's position to a kick linearly applied to itself at a previous time, in the form $V \to V - hx$ at $t' < t$, is

$$R_{xx}(t,t') \equiv \left.\frac{\delta\langle x(t)\rangle_h}{\delta h(t')}\right|_{h=0} = \frac{1}{\gamma_0}\left[1 - e^{-\frac{\gamma_0}{m}(t-t')}\right]\theta(t-t') \ , \tag{4.44}$$

with the limits

$$R_{xx}(t,t') \to \begin{cases} m^{-1}\ (t-t')\ \theta(t-t') & t-t' \ll t_r^v \ , \\ \gamma_0^{-1}\ \theta(t-t') & t-t' \gg t_r^v \ . \end{cases} \tag{4.45}$$

A simple calculation proves that in the short time-differences limit this is the results for Newton dynamics (**Exercise:** Show it.)

The correlation between the position and the velocity reads

$$\begin{aligned} \langle (x(t) - \langle x(t)\rangle)(v(t') - \langle v(t')\rangle)\rangle &= \frac{2k_BT}{m}\left[\frac{m}{\gamma_0} - \left(1 + \frac{m}{\gamma_0}\right)e^{-\frac{\gamma_0}{m}t'}\right] \\ &\to \frac{2k_BT}{\gamma_0} \end{aligned} \tag{4.46}$$

and it is only a function of t'. One notices that in the asymptotic limit in which both sides of the equation saturate

$$\boxed{2k_BT\ R_{xx}(t,t') = C_{xv}^c(t,t') \quad \text{for } \ t-t' \gg t_r^v \ \text{ and } \ t' \gg t_r^v \ ,} \tag{4.47}$$

with a factor of 2 different from the relation in eq. (4.37).

In conclusion, the position is also a Gaussian variable but it is explicitly out of equilibrium. Its average and variance grow linearly in time, the latter as in normal diffusion, and the fluctuation-dissipation relation has an additional factor of 1/2 (or 2, depending on on which side of the equality one writes it) with respect to the form expected in equilibrium.

The energy

The averaged potential energy diverges in the long-time limit since the potential is unbounded in the $x \to \infty$ limit: $\langle H(t)\rangle = k_B T/2 - F\langle x(t)\rangle \simeq k_B T/2 + F/\gamma_0 t$ for $t \gg t_r^v$.

Two kinds of variables

This example shows that even in this very simple problem the velocity and position variables have distinct behaviour: the former is in a sense trivial, after the transient t_r^v and for longer times, all one-time functions of $v - F/\gamma_0$ saturate to their equilibrium values and the correlations are stationary. Instead, the latter remains non-trivial and evolving out of equilibrium. One can loosely ascribe the different behaviour to the fact that the velocity feels a confining potential $K = mv^2/2$ while the position feels an unbounded potential $V = -Fx$ in the case in which a force is applied, or a flat potential $V = 0$ if F is switched off. In none of these cases the potential is able to take the particle to equilibrium with the bath. The particle slides on the slope and its excursions forward and backward from the mean get larger and larger as time increases.

Quite generally, the classical problems we are interested in are such that the friction coefficient γ_0 is large and the inertia term can be neglected, in other words, all times are much longer than the characteristic time t_r^v. We shall do it in the rest of the lectures.

Ergodicity

The ergodic hypothesis states that, in equilibrium, one can exchange ensemble averages by time averages and obtain the same results. Out of equilibrium this hypothesis is not expected to hold and one can already see how dangerous it is to take time-averages in these cases by focusing on the simple velocity variable. Ensemble and time averages coincide if the time-averaging is done over a time-window that lies after t_r^v but it does not if the integration time-interval goes below t_r^v.

Tests of equilibration have to be done very carefully in experiments and simulations. One can be simply mislead by, for instance, looking just at the velocities statistics.

A measure for the time dependent fluctuating position and velocity can be written down, taking advantage of the fact that both variables are Gaussian:

$$P(v,x) \propto \exp\left[-\frac{1}{2}\int dt \int dt' \; \delta y^t(t) A(t,t') \delta y(t')\right] \tag{4.48}$$

with the 2×2 matrix A being the inverse of the matrix of correlations, ${A^{-1}}_{ij}(t,t') = \langle \delta y_i(t) \delta y_j(t') \rangle$ with $i,j = 1,2$, $\delta y^t(t) = (\delta v(t)\ \delta x(t))$ and $\delta v(t) = v(t) - \langle v(t) \rangle$ (similarly for x). The correlations are given above so the dynamic pdf can be easily constructed.
Exercise. Confront

$$\langle v^m(t) x^n(t) x^k(t') \rangle \qquad \text{and} \qquad \langle v^m(t) x^n(t) k x^{k-1}(t') v(t') \rangle \ ; \tag{4.49}$$

conclude.

Effect of a colored bath: anomalous diffusion

The **anomalous diffusion** of a particle governed by the generalized Langevin equation, eq. (4.10), with colored noise characterized by power-law correlations, eq. (4.11), a problem also known as fractional Brownian motion, was studied in detail by N. Pottier [**?**]. The particle's velocity equilibrates with the environment although it does at a much slower rate than in the Ohmic case: its average and mean-square displacement decay as a power law - instead of exponentially - to their asymptotic values (still satisfying the regression theorem). The particle's mean square displacement is determined by the exponent of the noise-noise correlation, $\langle x^2(t) \rangle \simeq t^\alpha$, i.e. the dynamics is **subdiffusive** for $\alpha < 1$, **diffusive** for $\alpha = 1$ and **superdiffusive** for $\alpha > 1$. A time-dependent diffusion coefficient verifies $D_x(t) \equiv 1/2\ d\langle x^2(t) \rangle / dt \propto t^{\alpha - 1}$: it is finite and given by eq. (4.41) for normal diffusion, it diverges for superdiffusion and it vanishes for subdiffusion. The ratio between the linear response and the time-derivative of the correlation ratio reads $TR_{xx}(t,t')/\partial_{t'} C_{xx}(t,t') = D_x(t-t')/[D_x(t-t') + D_x(t')]$. It approaches $1/2$ for normal diffusion and the two-time dependent function $1/[1 + (t'/(t-t'))^{\alpha-1}]$ in other cases.

4.3.2 Relaxation in a quadratic potential

Another relevant example is the relaxation of a particle in a harmonic potential, with its minimum at $x^* \neq 0$:

$$V(x) = \frac{k}{2}(x - x^*)^2 \ , \tag{4.50}$$

in contact with a white noise. The potential confines the particle and one can then expect the coordinate to reach an equilibrium distribution.

This problem can be solved exactly keeping inertia for all values of γ_0 but the calculation is slightly tedious. The behaviour of the particle velocity has already been clarified in the constant force case. We now focus on the overdamped limit,

$$\gamma_0 \dot{x} = -k(x - x^*) + \xi \ , \tag{4.51}$$

with k the spring constant of the harmonic well, that can be readily solved,

$$x(t) = x_0 \ e^{-\frac{k}{\gamma_0}t} + \gamma_0^{-1} \int_0^t dt' \ e^{-\frac{k}{\gamma_0}(t-t')} \ [\xi(t') + kx^*] \ , \qquad x_0 = x(0) \ . \tag{4.52}$$

This problem become formally identical to the velocity dependence in the previous example.

Convergence of one-time quantities

The averaged position is

$$\boxed{\langle x(t) - x^* \rangle = (x_0 - x^*) e^{-\frac{k}{\gamma_0}t} \to 0 \qquad t_r^x \gg \gamma_0/k \quad \text{(Convergence)}} \tag{4.53}$$

Of course, one-time quantities should approach a constant asymptotically if the system equilibrates with its environment.

Two-time quantities

The two-time connected correlation (where one extracts, basically, the asymptotic position x^*) reads

$$\langle \delta x(t) \delta x(t') \rangle = k_B T \ k^{-1} \ e^{-\frac{k}{\gamma_0}(t+t')} \left[e^{2\frac{k}{\gamma_0} \min(t,t')} - 1 \right] \ . \tag{4.54}$$

Again, the **Dirichlet correlator** ($\delta x(t) = x(t) - \langle x(t) \rangle$). For at least one of the two times going well beyond the position relaxation time $t_r^x = \gamma_0/k$ the memory of the initial condition is lost and the connected correlation becomes **stationary**:

$$C_c(t,t') = \langle \delta x(t) \delta x(t') \rangle \to k_B T \ k^{-1} \ e^{-\frac{k}{\gamma_0}|t-t'|} \qquad \min(t,t') \gg t_r^x \ . \tag{4.55}$$

For time-differences that are longer than $t_d^x = \gamma_0/k$ the correlation decays to $1/e$ and one finds $t_d^x = t_r^x$. Interestingly enough, the relaxation and decay times diverge when $k \to 0$ and the potential becomes flat.

Note that when the time-difference $t - t'$ diverges the average of the product factorizes, in particular, for the correlation one gets

$$\langle x(t)x(t')\rangle \to \langle x(t)\rangle\langle x(t')\rangle \to x^*\langle x(t')\rangle \tag{4.56}$$

for any t', even finite. We shall see this factorization property at work later in more complicated cases.

Fluctuation-dissipation theorem (FDT)

One can also compute the linear response to an infinitesimal perturbation that couples linearly to the position changing the energy of the system as $H \to H - fx$ at a given time t':

$$R(t,t') = \left.\frac{\delta\langle x(t)\rangle_f}{\delta f(t')}\right|_{f=0} . \tag{4.57}$$

The explicit calculation yields

$$\begin{aligned} &R(t,t') = \gamma_0^{-1}\ e^{-k\gamma_0^{-1}(t-t')}\ \theta(t-t') \\ &\boxed{R(t,t') = \tfrac{1}{k_BT}\ \tfrac{\partial C_c(t,t')}{\partial t'}\ \theta(t-t') \quad \text{(FDT)}} \end{aligned} \tag{4.58}$$

The last equality holds for times that are longer than t_r^x. It expresses the **fluctuation-dissipation theorem (FDT)**, a model-independent relation between the two-time linear response and correlation function. Similar - though more complicated - relations for higher-order responses and correlations also exist in equilibrium. There are many ways to prove the FDT for stochastic processes. We shall discuss one of them in Sect. 4.1 that is especially interesting since it applies easily to problems with correlated noise.

It is instructive to examine the relation between the linear response and the correlation function in the limit of a flat potential ($k \to 0$). The linear response is just $\gamma_0^{-1}\theta(t-t')$. The Dirichlet correlator approaches the diffusive limit:

$$\langle \delta x(t)\delta x(t')\rangle = 2\gamma_0^{-1}k_BT\ \min(t,t') \qquad \text{for} \qquad k \to 0 \tag{4.59}$$

and its derivative reads $\partial_{t'}\langle \delta x(t)\delta x(t')\rangle = 2\gamma_0^{-1}k_BT\ \theta(t-t')$. Thus,

$$\begin{aligned} &R(t,t') = \frac{1}{2k_BT}\ \partial_{t'}\langle \delta x(t)\delta x(t')\rangle\ \theta(t-t') \\ &\boxed{R(t,t') = \tfrac{1}{2k_BT}\ \partial_{t'}C_c(t,t')\ \theta(t-t') \quad \text{(FDR for diffusion)}} \end{aligned} \tag{4.60}$$

A factor $1/2$ is now present in the relation between R and C_c. It is another signature of the fact that the coordinate is not in equilibrium with the environment in the absence of a confining potential.

Exercise Evaluate the two members of the FDT, eq. (4.58), in the case of the tilted potential $V(x) = -Fx$.

Reciprocity or Onsager relations

Let us compare the two correlations $\langle x^3(t)x(t')\rangle$ and $\langle x^3(t')x(t)\rangle$ within the harmonic example. One finds $\langle x^3(t)x(t')\rangle = 3\langle x^2(t)\rangle\langle x(t)x(t')\rangle$ and $\langle x^3(t')x(t)\rangle = 3\langle x^2(t')\rangle\langle x(t')x(t)\rangle$. Given that $\langle x^2(t)\rangle = \langle x^2(t')\rangle \to \langle x^2\rangle_{eq}$ and the fact that the two-time self-correlation is symmetric,

$$\langle x^3(t)x(t')\rangle = \langle x^3(t')x(t)\rangle \ . \tag{4.61}$$

With a similar argument one shows that for any functions A and B of x:

$$\begin{aligned} &\langle A(t)B(t')\rangle = \langle A(t')B(t)\rangle \\ &\boxed{C_{AB}(t,t') = C_{AB}(t',t) \qquad \text{(Reciprocity)}} \end{aligned} \tag{4.62}$$

This equation is known as **Onsager relation** and applies to A and B that are even under time-reversal (e.g. they depend on the coordinates but not on the velocities or they have an even number of verlocities).

All these results remain unaltered if one adds a linear potential $-Fx$ and works with connected correlation functions.

4.3.3 Thermally activated processes

The phenomenological **Arrhenius law** [6] yields the typical time needed to escape from a potential well as an exponential of the ratio between the height of the barrier and the thermal energy scale k_BT, (with prefactors that can be calculated explicitly, see below). This exponential is of crucial importance for understanding slow (glassy) phenomena, since a mere barrier of $30k_BT$ is enough to transform a microscopic time of 10^{-12}s into a macroscopic time scale. See Fig. 17-right for a numerical study of the Coulomb glass that demonstrates the existence of an Arrhenius time-scale in this problem. In the glassy literature such systems are called **strong** glass formers as opposed to **weak** ones in which the characteristic time-scale depends on temperature

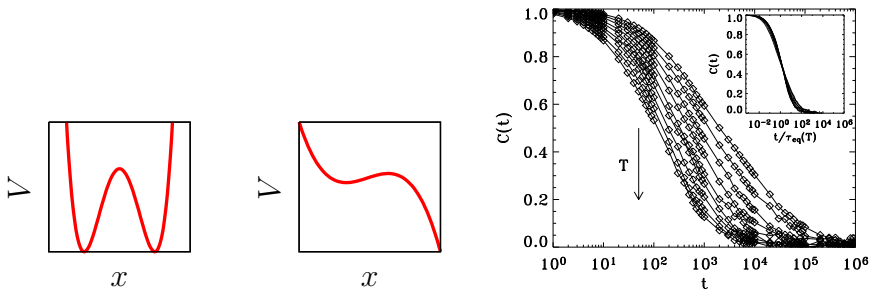

Figure 17: Left: sketch of a double-well potential. Center: sketch of a potential with a local minimum. Right: correlation function decay in a classical model of the $3d$ Coulomb glass at nine temperatures ranging from $T = 0.1$ to $T = 0.05$ in steps of 0.05 and all above T_g. In the inset the scaling plot $C(t) \sim f(t/t_A)$ with a characteristic time-scale, t_A, that follows the Arrhenius activated law, $t_A \simeq 0.45/T$. Figure taken from [25].

in a different way.

In 1940 Kramers estimated the **escape rate** from a potential well as the one shown in Fig. 17-center due to thermal fluctuations that give sufficient energy to the particle to allow it to surpass the barrier [7]. After this seminal paper this problem has been studied in great detail [41] given that it is of paramount importance in many areas of physics and chemistry. An example is the problem of the dissociation of a molecule where x represents an effective one-dimensional **reaction coordinate** and the potential energy barrier is, actually, a **free-energy barrier**.

Kramers assumed that the reaction coordinate is coupled to an equilibrated environment with no memory and used the probability formalism in which the particle motion is described in terms of the time-dependent probability density $P(x, v, t)$ (that for such a stochastic process follows the Kramers partial differential equation).

If the thermal energy is at least of the order of the barrier height, $k_B T \sim \Delta V$, the reaction coordinate, x, moves freely from the vicinity of one well to the vicinity of the other.

[6] S. A. Arrhenius, *On the reaction velocity of the inversion of cane sugar by acids*, Zeitschrift für Physikalische Chemie 4, 226 (1889).

[7] H. A. Kramers, *Brownian motion in a field of force and the diffusion model of chemical reactions* Physica **7**, 284 (1940).

The treatment we discuss applies to the opposite weak noise limit in which the thermal energy is much smaller than the barrier height, $k_BT \ll \Delta V$, the random force acts as a small perturbation, and the particle current over the top of the barrier is very small. Most of the time x relaxes towards the minimum of the potential well where it is located. Eventually, the random force drives it over the barrier and it escapes to infinity if the potential has the form in Fig. 17-center, or it remains in the neighbourhood of the second well, see Fig. 17-left.

The treatment is simplified if a constant current can be imposed by injecting particles within the metastable well and removing them somewhere to the right of it. In these conditions Kramers proposed a very crude approximation whereby P takes the stationary canonical form

$$P_{st}(x,v) = \mathcal{N} e^{-\beta\frac{v^2}{2} - \beta V(x)} \; . \tag{4.63}$$

If there is a sink to the right of the maximum, the normalization constant $\mathcal{N}$ is fixed by further assuming that $P_{st}(x,v) \sim 0$ for $x \geq \tilde{x} > x_{max}$. The resulting integral over the coordinate can be computed with a saddle-point approximation justified in the large β limit. After expanding the potential about the minimum and keeping the quadratic fluctuations one finds

$$\mathcal{N}^{-1} = \frac{2\pi}{\beta\sqrt{V''(x_{min})}}\, e^{-\beta V(x_{min})} \; .$$

The escape rate, r, over the top of the barrier can now be readily computed by calculating the outward flow across the top of the barrier:

$$r \equiv \frac{1}{t_A} \equiv \int_0^\infty dv\; v P(x_{max}, v) = \frac{\sqrt{V''(x_{min})}}{2\pi}\, e^{-\beta(V(x_{max}) - V(x_{min}))} \; . \tag{4.64}$$

Note that we here assumed that no particle comes back from the right of the barrier. This assumption is justified if the potential quickly decreases on the right side of the barrier.

The crudeness of the approximation (4.63) can be grasped by noting that the equilibrium form is justified only near the bottom of the well. Kramers estimated an improved $P_{st}(x,v)$ that leads to

$$r = \frac{\left(\frac{\gamma^2}{4} + V''(x_{max})\right)^{1/2} - \frac{\gamma}{2}}{\sqrt{V''(x_{max})}}\; \frac{\sqrt{V''(x_{min})}}{2\pi}\, e^{-\beta(V(x_{max}) - V(x_{min}))} \; . \tag{4.65}$$

This expression approaches (4.64) when $\gamma \ll V''(x_{max})$, *i.e.* close to the underdamped limit, and

$$r = \frac{\sqrt{V''(x_{max})V''(x_{min})}}{2\pi\gamma}\, e^{-\beta(V(x_{max})-V(x_{min}))} \tag{4.66}$$

when $\gamma \gg V''(x_{max})$, *i.e.* in the overdamped limit (see Sect. 4.2.5 for the definition of these limits).

The inverse of (4.65), t_A, is called the **Arrhenius time** needed for **thermal activation** over a barrier $\Delta V \equiv V(x_{max}) - V(x_{min})$. The prefactor that characterises the well and barrier in the harmonic approximation is the **attempt frequency** with which the particles tend to jump over the barrier. In short,

$$\boxed{t_A \simeq \tau\, e^{\beta|\Delta V|} \qquad \text{(Arrhenius time)}} \tag{4.67}$$

The one-dimensional reaction coordinate can be more or less easily identified in problems such as the dissociation of a molecule. In contrast, such a single variable is much harder to visualize in an interacting problem with many degrees of freedom. The Kramers problem in higher dimensions is highly non-trivial and, in the infinite-dimensional **phase-space**, is completely out of reach.

5 Dynamics through a phase transition

Take a piece of material in contact with an external reservoir. The material will be characterized by certain observables, energy density, magnetization density, *etc.* The external environment will be characterized by some parameters, like the temperature, magnetic field, pressure, *etc.* In principle, one is able to tune the latter and study the variation of the former. Note that we are using a **canonical setting** in the sense that the system under study is not isolated but open.

Sharp changes in the behavior of macroscopic systems at critical points (or lines) in parameter space have been observed experimentally. These correspond to **equilibrium phase transitions**, a non-trivial collective phenomenon appearing in the thermodynamic limit. We shall assume that the main features of, and analytic approaches used to study, phase transitions are known.

Imagine now that one changes an external parameter instantaneously or with a finite rate going from one phase to another in the (equilibrium) phase diagram. The kind of internal system interactions are not changed. In the statistical physics language the first kind of procedure is called a **quench** and the second one an **annealing** and these terms belong to the metalurgy terminology. We shall investigate how the system evolves by trying to accomodate to the new conditions and equilibrate with its environment. We shall first focus on the dynamics at the critical point or going through phase transitions between well-known phases (in the sense that one knows the order parameter, the structure, and all thermodynamic properties on both sides of the transition). Later we shall comment on cases in which one does not know all characteristics of one of the phases and sometimes one does not even know whether there is a phase transition.

The evolution of the **free-energy landscape** (as a function of an order parameter) with the control parameter driving a phase transition is a guideline to grasp the dynamics following a quench or annealing from, typically, a disordered phase to the phase transition or into the ordered phase. See Fig. 18 for a sketch. We shall discuss quenches to the phase transition and below it. In the former case, the system can get to a critical point (Fig. 18-left) in which the free-energy is metastable in the sense that its second deriva-

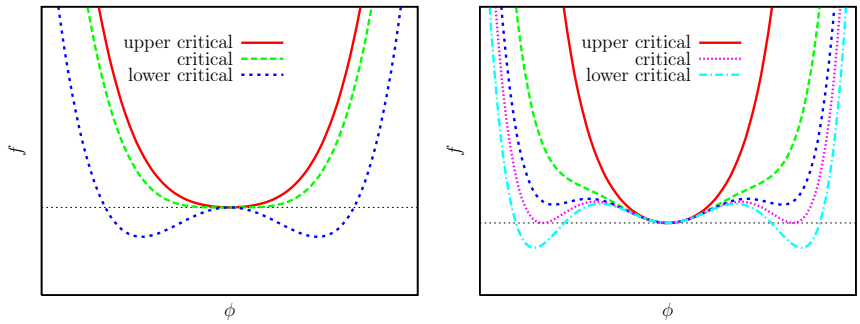

Figure 18: Left: second-order phase transition. Right: first order phase transition.

tive vanishes (second order phase transition cases) or to a first-order phase transition (Fig. 18-right) in which various minima are degenerate. In the latter case the initial state becomes **unstable**, that is to say a maximum, and the phase transition is of second-order (see Fig. 18-left) or **metastable**, that is to say a local minimum, and the phase transition is of first order (see Fig. 18-right) in the final externally imposed conditions.[8] In the former case the **ordering process** occurs **throughout the material**, and not just at **nucleation sites**. Two typical examples are spinodal decomposition, *i.e.* the method whereby a mixture of two or more materials can separate into distinct regions with different material concentrations, or magnetic domain growth in ferromagnetic materials. Instead, in the latter case, the stable phase conquers the system through the **nucleation of a critical localized bubble** via thermal activation and its further growth.

Having described the dependence of the free-energy landscape on the external parameters we now need to choose the microscopic dynamics of the order parameter. Typically, one distinguishes two classes: one in which the order parameter is locally conserved and another one in which it is not. **Conserved** order parameter dynamics are found for example in phase separation in magnetic alloys or inmiscible liquids. Ferromagnetic domain growth is an exemple of the **non-conserved** case.

[8]Strictly speaking metastable states with infinite life-time exist only in the mean-field limit.

5.1 Time-dependent Ginzburg-Landau description

The kinetics of systems undergoing critical dynamics or an ordering process is an important problem for material science but also for our generic understanding of pattern formation in non-equilibrium systems. The late stage dynamics is believed to be governed by a few properties of the systems whereas material details should be irrelevant. Among these relevant properties one may expect to find the number of degenerate ground states, the nature of the conservation laws and the hardness or softness of the domain walls that is intimately related to the dimension of the order parameter. Thus, classes akin to the universality ones of critical phenomena have been identified. These systems constitute a first example of a problem with **slow dynamics**. Whether all systems with slow dynamics, in particular structural and spin glasses, undergo some kind of simple though slow domain growth is an open question.

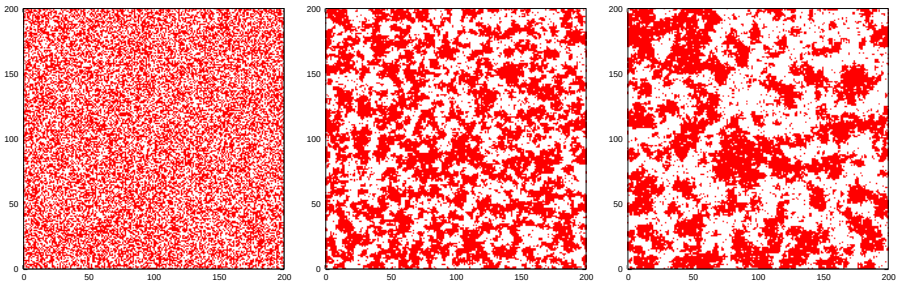

Figure 19: Monte Carlo simulations of a $2d$ Ising model. Three snapshots at $t = 1,\ 3 \times 10^5,\ 3 \times 10^6$ MCs after a quench to T_c.

Take a magnetic system, such as the ubiquitous Ising model with ferromagnetic uniform interactions, and quench it to its Curie point or into the low temperature phase starting from a random initial condition. Classically, the spins do not have an intrinsic dynamics; it is defined via a stochastic rule of Glauber, Metropolis or similar type with or without locally conserved magnetization. For the purpose of the following discussion it is sufficient to focus on non-conserved local microscopic dynamics. Three snapshots taken after times 1, 3×10^5 and 3×10^6 MCs in a critical and two sub-critical quenches are shown in Figs. 19, 20, and 21.

Time-dependent macroscopic observables are then expressed in terms of the values of the spins at each time-step. For instance, the magnetization

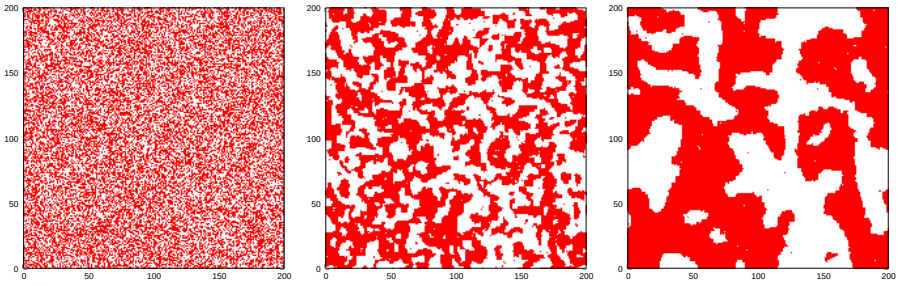

Figure 20: Monte Carlo simulations of a $2d$ Ising model. Three snapshots at $t = 1,\ 3 \times 10^5,\ 3 \times 10^6$ MCs after a quench to $0.5\ T_c$. Thermal fluctuations within the domains are visible.

density and its two-time self correlation function are defined as

$$m(t) \equiv N^{-1} \sum_{i=1}^{N} \langle\, s_i(t) \,\rangle \ , \qquad C(t,t') \equiv N^{-1} \sum_{i=1}^{N} \langle\, s_i(t) s_i(t') \,\rangle \ , \tag{5.1}$$

where the angular brackets indicate an average over many independent runs (i.e. random numbers) starting from identical initial conditions and/or averages over different initial configurations.

In **critical quenches**, patches with equilibrium critical fluctuations grow in time but their linear extent never reaches the equilibrium correlation length that diverges. Clusters of neighbouring spins pointing the same direction of many sizes are visible in the figures and the structure is quite intricate with clusters within clusters and so on and so forth. The interfaces look pretty rough too.

In **quenches into the ordered phase through a second order phase transition** the ferromagnetic interactions tend to align the neighbouring spins in parallel direction and in the course of time domains of the two ordered phases form and grow, see Fig. 22. At any finite time the configuration is such that both types of domains exist. If one examines the configurations in more detail one reckons that there are some spins reversed within the domains. These 'errors' are due to thermal fluctuations and are responsible of the fact that the magnetization of a given configuration within the domains is smaller than one and close to the equilibrium value at the working temperature (apart from fluctuations due to the finite size of the domains). The total magnetization, computed over the full system, is zero (up to fluctuating time-dependent corrections that scale with the square root of the inverse

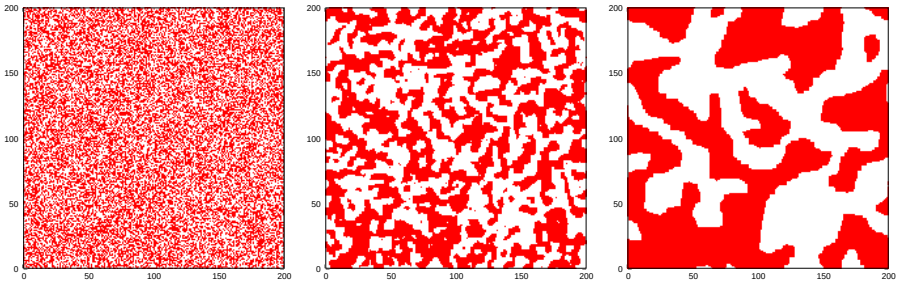

Figure 21: Monte Carlo simulations. Three snapshots at $t = 1,\ 3\times10^5, 3\times10^6$ MCs after a quench to 0.01 T_c. There is almost perfect order within the domains ($m_{eq} \simeq 1$).

system size). The thermal averaged spin, $\langle s_i(t)\rangle$ vanishes for all i and all finite t, see below for a more detailed discussion of the time-dependence. As time passes the typical size of the domains increases and the interfaces get flatter in a way that we shall also discuss below.

Quenches across first order phase transitions will be discussed separately below.

In order to treat phase-transitions and the coarsening process analytically it is preferable to introduce a coarse-grained description in terms of a continuous coarse-grained field,

$$\phi(\vec{x},t) \equiv \frac{1}{V}\sum_{i\in V_{\vec{x}}} s_i(t)\ , \tag{5.2}$$

the fluctuating magnetization density. In a first approximation a Landau-Ginzburg free-energy functional is introduced

$$F[\phi] = \int d^dx\ \left\{\frac{c}{2}\left[\nabla\phi(\vec{x},t)\right]^2 + V[\phi(\vec{x},t)]\right\}\ . \tag{5.3}$$

With the choice of the potential one distinguishes between a second order and a first order phase transition. In the former case, the typical form is the ϕ^4 form:

$$V(\phi) = a\phi^4 + b(g)\phi^2\ . \tag{5.4}$$

The first term in eq. (5.3) represents the energy cost to create a domain wall or the elasticity of an interface. The second term depends on a parameter, g, and changes sign from positive at $g > g_c$ to negative at $g < g_c$. Above the

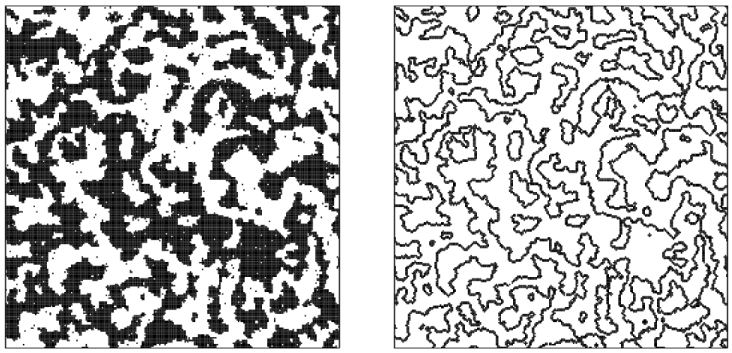

Figure 22: Snapshot of the $2d$ Ising model at a number of Monte Carlo steps after a quench from infinite to a subcritical temperature. Left: the up and down spins on the square lattice are represented with black and white sites. Right: the domain walls are shown in black.

critical point determined by $b(g_c) = 0$ it has a single minimum at $\phi = 0$, at g_c it is flat at $\phi = 0$ and below g_c it has a double well structure with two minima, $\phi = \pm[-b(g)/(2a)]^{1/2} = \langle\phi\rangle_{eq}(g)$, that correspond to the equilibrium states in the ordered phase. Equation (5.3) is exact for a fully connected Ising model where $V(\phi)$ arises from the multiplicity of spin configurations that contribute to the same $\phi(\vec{x}) = m$. The order-parameter dependent free-energy density reads $f(m) = -Jm^2 - hm + k_BT\{(1+m)/2\ln[(1+m)/2] + (1-m)/2\ln[(1-m)/2]$ that close to the critical point where $m \simeq 0$ becomes $f(m) \simeq (k_BT - 2J)/2\ m^2 - hm + k_BT/12\ m^4$ demonstrating the passage from a harmonic form at $k_BT > k_BT_c = 2J$, to a quartic well at $T = T_c$, and finally to a double-well structure at $T < T_c$.

Exercise. Prove the above.

With a six-order potential one can mimic the situation in the right panel of Fig. 18.

When discussing dynamics one should write down the stochastic evolution of the individual spins and compute time-dependent averaged quantities as the ones in (5.1). This is the procedure used in numerical simulations. Analytically it is more convenient to work with a field-theory and an evolution equation of Langevin-type. This is the motivation for the introduction

of continuous field equations that regulate the time-evolution of the coarse-grained order parameter. Ideally these equations should be derived from the spin stochastic dynamics but in practice they are introduced phenomenologically. In the magnetic case as well as in many cases of interest, the domain wall and interface dynamics can be argued to be **overdamped** (i.e. $t \gg t_r^{\dot{\phi}}$).

Two very similar approaches are used. Assuming T is only relevant to determine the equilibrium coarse-grained field one uses the phenomenological **zero-temperature time-dependent Ginzburg-Landau** equation or **model A** in the classification of Hohenberg-Halperin deterministic equation

$$\frac{\partial \phi(\vec{x},t)}{\partial t} = -\frac{\delta F[\phi]}{\delta \phi(\vec{x},t)} \tag{5.5}$$

(the friction coefficient has been absorbed in a redefinition of time). Initial conditions are usually chosen to be random with short-range correlations

$$[\, \phi(\vec{x},0)\phi(\vec{x}',0)\,]_{ic} = \Delta\delta(\vec{x}-\vec{x}') \tag{5.6}$$

thus mimicking the high-temperature configuration ($[\ldots]_{ic}$ represent the average over its probability distribution). The numeric solution to this equation with the quartic potential and $b<0$ shows that such a random initial condition evolves into a field configuration with patches of ordered region in which the field takes one of the two values $[-b/(2a)]^{1/2}$ separated by sharp walls. It ignores temperature fluctuations within the domains meaning that the field is fully saturated within the domains and, consequently, one has access to the aging part of the correlations only, see *e.g.* eq. (5.20). The phase transition is controlled by the parameter b in the potential.

Another, similar approach, is to add a thermal noise to the former

$$\frac{\partial \phi(\vec{x},t)}{\partial t} = -\frac{\delta F[\phi]}{\delta \phi(\vec{x},t)} + \xi(\vec{x},t)\ . \tag{5.7}$$

This is the field-theoretical extension of the Langevin equation in which the potential is replaced by the order-parameter-dependent funcitonal free-energy in eq. (5.3) with a potential form with fixed parameters (independent of T). ξ is a noise taken to be Gaussian distributed with zero mean and correlations

$$\langle \xi(\vec{x},t)\xi(\vec{x}',t')\rangle = 2k_B T\delta^d(\vec{x}-\vec{x}')\delta(t-t')\ . \tag{5.8}$$

The friction coefficient has been absorbed in a redefinition of time. For a quartic potential a dynamic phase transition arises at a critical T_c; above

T_c the system freely moves above the two minima and basically ignores the double well structure while below T_c this is important. Within the growing domains the field ϕ fluctuates about its mean also given by $[-b/(2a)]^{1/2}$ and the fluctuations are determined by T. One can describe the rapid relaxation at ties such that the domain walls do not move with this approach. This formulation is better suited to treat critical and sub-critical dynamics in the same field-theoretical framework.

These equations do not conserve the order parameter neither locally nor globally. Extensions for cases in which it is conserved exist (model B). Cases with vectorial or even tensorial order parameters can be treated similarly and are also of experimental relevance, notably for vectorial magnets or liquid crystals.

5.2 Relaxation and equilibration time

We wish to distinguish the **relaxation time**, t_r, defined as the time needed for a given initial condition to reach equilibrium in one of the (possibly many equivalent) phases, from the **decorrelation time**, t_d, defined as the time needed for a given configuration to decorrelate from itself. To lighten the notation we do not signal out the variable that we study to study these typical times (as we did with the velocity and position in the examples of Sect. 4.3). We further define the **reversal time**, t_R, as the time needed to go from one to another of the equivalent equilibrium phases. We focus on second-order phase transitions here.

5.2.1 Quench from $T \gg T_c$ to $T > T_c$

If one quenches the system to $T > T_c$ the relaxation time, t_r, needed to reach configurations sampled by the Boltzmann measure depends on the system's parameters but not on its size. Hence it is finite even for an infinite-size system. Once a short transient overcome, the average of a local spin approaches the limit given by the Boltzmann measure, $\langle s_i(t)\rangle \to \langle s_i\rangle_{eq} = m = 0$, for all i and all other more complex observables satisfy equilibrium laws. The relaxation time is estimated to behave as $|T - T_c|^{-\nu z_{eq}}$ close to T_c, with ν the critical exponent characterizing the divergence of the equilibrium correlation length, $\xi \sim (T - T_c)^{-\nu}$, and z_{eq} the equilibrium exponent that links times and lengths, $\xi \sim t^{1/z_{eq}}$.

The relaxation of the two-time self-correlation at $T > T_c$, when the time t' is chosen to be longer than t_r, decays exponentially

$$\lim_{t' \gg t_r} \langle s_i(t) s_i(t') \rangle \simeq e^{-(t-t')/t_d} \tag{5.9}$$

with a decorrelation time that increases with decreasing temperature and close to (but still above) T_c diverges as the power law, $t_d \sim (T - T_c)^{-\nu z_{eq}}$. The divergence of t_d is the manifestation of **critical slowing down**. The asympotic value verifies

$$\lim_{t-t' \gg t' \gg t_r} \langle s_i(t) s_i(t') \rangle = \lim_{t \gg t_r} \langle s_i(t) \rangle \lim_{t' \gg t_r} \langle s_i(t') \rangle = \langle s_i \rangle_{eq} \langle s_i \rangle_{eq} = m^2 = 0 \ , \tag{5.10}$$

cfr. eq. (4.56).

5.2.2 Quench from $T \gg T_c$ to $T \leq T_c$

At or below T_c, coarsening from an initial condition that is **not correlated with the equilibrium state** and with no bias field does not take the system to equilibrium in finite times with respect to a function of the system's linear size, L. More explicitly, if the growth law is a power law [see eq. (5.28)] one needs times of the order of $L^{z_{eq}}$ (critical) or L^{z_d} (subcrititcal) to grow a domain of the size of the system. This gives a rough idea of the time needed to take the system to one of the two equilibrium states. For any shorter time, domains of the two types exist and the system is **out of equilibrium**.

The self-correlation of such an initial state evolving at $T \leq T_c$ involves power laws or logarithms and although one cannot associate to it a decay time as one does to an exponential, one can still define a characteristic time that, quite generally, turns out to be related to the age of the system, $t_d \simeq t_w$ [see eq. (5.26)].

In contrast, the relaxation time of an **equilibrium** magnetized configuration at temperature T vanishes since the system is already equilibrated while the decorrelation time t_d is a finite function of T.

The relaxation of the two-time self-correlation at $T < T_c$, when the time t' is chosen to be longer than t_r, that is to say, once the system has thermalized in one of the two equilibrium states, decays exponentially

$$\langle s_i(t) s_i(t') \rangle \simeq e^{-(t-t')/t_d} \tag{5.11}$$

with a decorrelation time that decreases with decreasing temperature and close to T_c (but below it) also diverges as a power law, $t_d \sim (T - T_c)^{-\nu z_{eq}}$. The asympotic value verifies

$$\lim_{t-t' \gg t' \gg t_r} \langle s_i(t) s_i(t') \rangle = \lim_{t \gg t_r} \langle s_i(t) \rangle \lim_{t' \gg t_r} \langle s_i(t') \rangle = \langle s_i \rangle_{eq} \langle s_i \rangle_{eq} = m^2 \geq 0 \ , \tag{5.12}$$

cfr. eqs. (4.56) and (5.10), depending on $T = T_c$ or $T > T_c$.

5.2.3 Summary

The lesson to learn from this comparison is that the relaxation time and the decorrelation time not only depend upon the working temperature but they also depend upon the initial condition. Moreover, in all critical or low-temperature cases we shall study the relaxation time depends on (L, T) – and diverges in the infinite size limit – while the decorrelation time depends on (T, t_w). For a random initial condition and an infinite system one has

$$t_r^\phi \simeq \begin{cases} \text{finite} & T > T_c \ , \\ |T - T_c|^{-\nu z_{eq}} & T \gtrsim T_c \ , \\ \infty & T \leq T_c \end{cases}$$

while for a finite system

$$t_r^\phi \simeq \begin{cases} L^{z_{eq}} & T = T_c \ , \\ L^{z_d} & T < T_c \ . \end{cases}$$

Still another time scale is given by the time needed to reverse an equilibrium configuration in the low-T phase. This one is expected to be given by an Arrhenius law, with the height of the barrier being determined by the extensive free-energy barrier between the two minima, i.e. $\Delta F \simeq L^d f$, therefore,

$$\boxed{t_R^\phi \simeq e^{\beta L^d f} \qquad \text{Reversal time-scale .}} \tag{5.13}$$

The Ginzburg-Landau description allows for a pictorial interpretation of these results. The dynamics of the full system is visualized as the motion of its representative point in the Ginzburg-Landau potential. At high T the potential is harmonic in the deterministic Allen-Cahn equation, or the double-well structure in the time-dependent stochastic Ginzburg-Landau equation is completely ignored. The relaxation is similar to the one of a particle in a

harmonic potential studied in Sect. 4.3.2. At low T, the initial position in the double-well potential depends on the type of initial condition $\phi(\vec{x},0)=0$ or $\phi(\vec{x},0)\neq 0$. In the first case, the point sits on top of the central barrier and it does not detach from it in finite times with respect to a function of L. In the second case, the point starts from within one well and it simply rolls to the bottom of the well. This relaxation is similar to the one in the harmonic case. To reverse the configuration from, say, positive to negative magnetization the point needs to jump over the barrier in the double well potential and it does via thermal activation ruled by the Arrhenius law.

Note however that the phase-space of the system is actually N-dimensional while the description that is given here is projected onto one single coordinate, the one of the order-parameter. This reduction might lead to some misunderstandings and one should be very careful with it.

5.3 Short-time dynamics

Take an initial configuration $\phi(\vec{x},t)=\phi_0=0$ on average with small fluctuations, as in equilibrium at very high temperature, and quench the system. At very short time one can expand the non-linear potential and the GL equation (5.5), for the Fourier components, $\phi(\vec{k},t)=L^{-d/2}\int d^dx\ \phi(\vec{x},t)e^{-i\vec{k}\vec{x}}$ with $\vec{k}=2\pi/L\ (n_1,\ldots,n_d)$ and n_k integer, reads

$$\frac{\partial\phi(\vec{k},t)}{\partial t}=[-k^2-V''(0)]\phi(\vec{k},t)+\xi(\vec{k},t)\ . \tag{5.14}$$

If $V''(0)>0$ all modes decay exponentially and no order develops. If $V''(0)\leq 0$ instead modes with $-k^2-V''(0)>0$ are unstable and grow exponentially until a time $t^*\simeq -1/V''(0)$ when the small ϕ expansion ceases to be justified. The instability of the small wave-vector modes indicates that the system tends to order. To go beyond this analysis one needs to consider the full non-linear equation.

5.4 Growing length and dynamic scaling

In usual coarsening systems the averaged space-time correlation function

$$\boxed{NC(r,t)=\textstyle\sum_{ij/|\vec{r}_i-\vec{r}_j|=r}\langle s_i(t)s_j(t)\rangle}$$

allows for the identification of a growing length from, for example,

$$R_{\rm a}(T,t) \equiv \int d^d r \; r^{\rm a+1} C(r,t) / \int d^d r \; r^{\rm a} C(r,t) \tag{5.15}$$

(a is a parameter chosen to weight preferentially short or long distances; the time-dependence of $R_{\rm a}(t)$ should not depend on a.) Here and in the following $\langle \ldots \rangle$ stands for an average over different realizations of thermal histories at heat-bath temperature T and/or initial conditions. In presence of quenched disorder one adds an average over it and denotes it $[\ldots]$. The stochastic time-dependent function $N^{-1} \sum_{ij/|\vec{r}_i - \vec{r}_j| = r} s_i(t) s_j(t)$ after a quench from a random initial condition does not fluctuate in the thermodynamic limit. Therefore, the averages are not really necessary but they are usually written down. In spin-glasses and glasses this observable does not yield information on the existence of any growing length as we shall discuss below.

The spherically averaged structure factor $S(k,t)$ – the Fourier transform of $C(r,t)$ – can be measured experimentally with small-angle scattering of neutrons, x-rays or light and from it $R_{\rm a}(T,t)$ can be extracted.

The ordering process is characterized by the growth of a **typical length**, $R(T,t)$. The growth regimes are summarized in the following equation and in Fig. 23:

$$R(T,t) \;\sim\; \begin{cases} \to \xi(T) & T > T_c \quad \text{saturation,} \\ R_c(t) \to \xi(T) & T \geq T_c \quad \text{critical coarsening,} \\ R(T,t) > \xi(T) & T < T_c \quad \text{sub-critical coarsening.} \end{cases} \tag{5.16}$$

After a quench to the high temperature phase $T > T_c$ the system first grows equilibrium regions until reaching the correlation length ξ and next relaxes in equilibrium as explained in the previous section. The correlation length could be very short and the transient non-equilibrium regime be quite irrelevant ($T \gg T_c$). In the critical region, instead, the correlation length grows and it becomes important. In a critical quench the system never orders sufficiently and $R(T_c,t) < \xi$ for all finite times. Finally, a quench into the subcritical region is characterized by two growth regimes: a first one in which the critical point dominates and the growth is as in a critical quench; a second one in which the proper sub-critical ordering is at work. The time-dependence of the growth law is different in these two regimes as we shall see below. (Note that below T_c ξ does not measure the size of ordered regions but the typical distance until which a fluctuation has an effect.)

In the asymptotic time domain, when $R(T,t)$ has grown much larger than any microscopic length in the system, a **dynamic scaling symmetry** sets

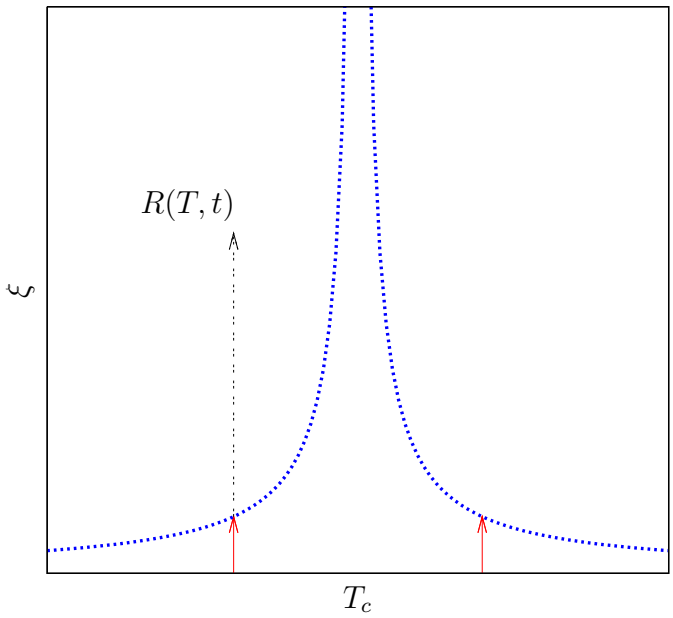

Figure 23: Sketch of the growth process in a second-order phase transition. The thick line is the equilibrium correlation length $\xi \simeq |T - T_c|^{-\nu}$. The thin arrows (solid red and dashed black) indicate the growing length R in the critical coarsening and sub-critical coarsening regimes.

in, similarly to the usual scaling symmetry observed in equilibrium critical phenomena. According to this hypothesis, the growth of $R(T,t)$ is the only relevant process and the whole time-dependence enters only through $R(T,t)$.

5.5 Critical coarsening

The scaling behavior of binary systems quenched to the critical point is quite well understood. It can be addressed with scaling arguments and renormalization group approaches [27] which give explicit expressions for many of the quantities of interest up to two loops order. Numerical simulations confirm the analytic results and probe exponents and scaling functions beyond the available perturbative orders. In this case the system builds correlated critical clusters with fractal dimension $D = (d + 2 - \eta)/2$, where η is the usual static critical exponent, in regions growing algebraically as

$R(T_c, t) \equiv R(t) \sim t^{1/z_{eq}}$; henceforth we simplify the notation and avoid writing T_c within R.

In the asymptotic time regime the space-time correlation function has the scaling form

$$\boxed{C(r,t) = R(t)^{-2(d-D)} f\left(\frac{r}{R(t)}\right) \quad \text{Multiplicative separation.}} \tag{5.17}$$

The pre-factor $R(t)^{-2(d-D)}$ takes into account that the growing domains have a **fractal nature** (hence their *density* decreases as their size grows) and the dependence on $r/R(t)$ in $f(x)$ expresses the similarity of configurations at different times once lengths are measured in units of $R(t)$. At distances and times such that $r/R(t) \ll 1$ the equilibrium power-law decay, $C_{eq}(r) \simeq r^{2-d-\eta}$, should be recovered, thus $f(x) \simeq x^{-2(d-D)}$ at $x \to 0$. $f(x)$ falls off rapidly for $x \gg 1$ to ensure that spins are uncorrelated at distances larger than $R(t)$.

For two-time quantities, when t' is sufficiently large one has

$$\boxed{C(t,t') = C_{st}(t-t')\ f_c\left(\frac{R(t)}{R(t')}\right) \quad \text{Multiplicative separation.}} \tag{5.18}$$

Here $C_{st}(t-t') \simeq R(t-t')^{-2(d-D)} = R(t-t')^{2-d-\eta}$. The scaling function $f_c(x)$ describes the non-equilibrium behavior. It satisfies $f_c(1) = 1$ and $f_c(x \to \infty) = 0$, see the sketch in Fig. 24 (a). In the scaling forms the equilibrium and non-equilibrium contributions enter in a **multiplicative** structure. Non-equilibrium effects are taken into account by taking ratios between the sizes of the correlated domains at the observation times t' and t in the scaling functions.

5.6 Sub-critical coarsening

5.6.1 Dynamic scaling hypothesis

The **dynamic scaling hypothesis** states that at late times and in the scaling limit

$$r \gg \xi(g)\ , \qquad R(g,t) \gg \xi(g)\ , \qquad r/R(g,t) \ \text{ arbitrary}\ , \tag{5.19}$$

where r is the distance between two points in the sample, $r \equiv |\vec{x} - \vec{x}'|$, and $\xi(g)$ is the equilibrium correlation length that depends on all parameters

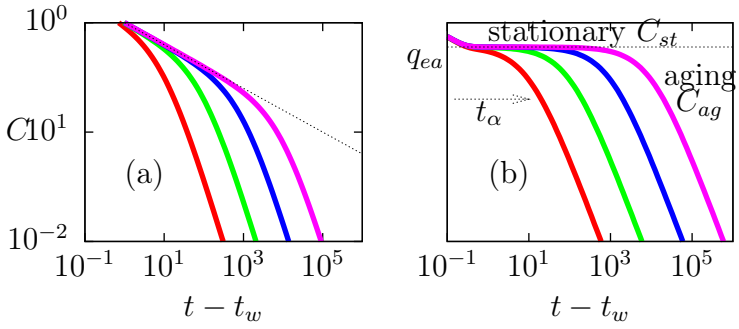

Figure 24: Sketch of the decay of the two-time correlation at T_c (a) and $T < T_c$ (b) for different values of the waiting-time, increasing from left to right.

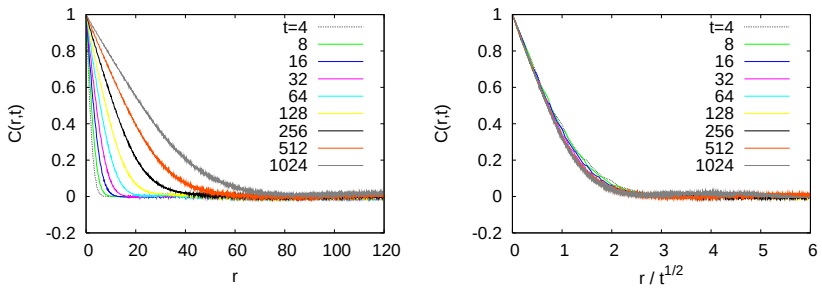

Figure 25: The equal-time correlation as a function of distance in the 2dIM quenched below T_c. Raw (left) and scaled (right) data.

(T and possibly others) collected in g, there exists a **single characteristic length**, $R(g,t)$, such that the domain structure is, in statistical sense, independent of time when lengths are scaled by $R(g,t)$. Time, denoted by t, is typically measured from the instant when the critical point is crossed. In the following we ease the notation and write only the time-dependence in R. This hypothesis has been proved analytically in very simple models only, such as the one dimensional Ising chain with Glauber dynamics or the Langevin dynamics of the d-dimensional $O(N)$ model in the large N limit (see Sect. 5.9).

The late stage of phase-ordering in binary systems is characterized by a

patchwork of large domains the interior of which is basically thermalized in one of the two equilibrium phases while their boundaries are slowly moving. This picture suggests the splitting of the degrees of freedom (spins) into two categories, providing statistically independent contributions to observables such as correlation or response functions. More precisely, a quasi-equilibrium stationary contribution arises as due to bulk spins, while boundaries account for the non-equilibrium part. Then asymptotically one has

$$\boxed{C(r,t) \simeq C_{st}(r) + C_{ag}(r,t) \qquad \text{Additive separation.}} \tag{5.20}$$

The first term describes the equilibrium fluctuations in the low temperature broken symmetry pure states

$$C_{st}(r) = (1 - \langle s_i \rangle_{eq}^2)\ g\left(\frac{r}{\xi}\right), \tag{5.21}$$

where $\langle s_i \rangle_{eq}$ is the equilibrium expectation value of the local spin, and $g(x)$ is a function with the limiting values $g(0) = 1$, $\lim_{x\to\infty} g(x) = 0$. The second term takes into account the motion of the domain walls through

$$C_{ag}(r,t) = \langle s_i \rangle_{eq}^2\ f\left(\frac{r}{R(t)}\right), \tag{5.22}$$

with $f(1) = 1$ and $\lim_{x\to\infty} f(x) = 0$. Both C_{st} and C_{ag} obey (separately) scaling forms with respect to the equilibrium and the non-equilibrium lengths ξ, $R(t)$. In particular, eq. (5.22) expresses the fact that system configurations at different times are statistically similar provided that lengths are measured in units of $R(t)$, namely the very essence of dynamical scaling.

Monte Carlo simulations of the Ising model and other systems quenched below criticality and undergoing domain growth demonstrate that in the long waiting-time limit $t' \gg t_0$, the spin self-correlation $\langle s_i(t) s_i(t') \rangle$ separates into two additive terms

$$\boxed{C(t,t') \sim C_{st}(t-t') + C_{ag}(t,t') \quad \text{Additive separation}} \tag{5.23}$$

see Fig. 26, with the first one describing equilibrium thermal fluctuations within the domains,

$$C_{st}(t-t') \;=\; \begin{cases} 1 - \langle s_i \rangle_{eq}^2 = 1 - m^2\ , & t - t' = 0\ , \\ 0\ , & t - t' \to \infty\ , \end{cases} \tag{5.24}$$

and the second one describing the motion of the domain walls

$$C_{ag}(t,t') \;=\; \langle s_i\rangle_{eq}^2 \; f_c\left(\frac{R(t)}{R(t')}\right) = \left\{ \begin{array}{ll} \langle s_i\rangle_{eq}^2 \,, & t' \to t^- \,, \\ 0 \,, & t-t' \to \infty \,. \end{array} \right. \tag{5.25}$$

To ease the notation we have not written the explicit T-dependence in R that, as we shall see below, is less relevant than t. Note that by adding the two contributions one recovers $C(t,t)=1$ as expected and $C(t,t')\to 0$ when $t \gg t'$. The first term is identical to the one of a system in equilibrium in one of the two ordered states, see eq. (5.12) for its asymptotic $t-t' \gg t'$ limit; the second one is inherent to the out of equilibrium situation and existence and motion of domain walls. They vary in completely different two-time scales. The first one changes when the second one is fixed to $\langle s_i\rangle_{eq}^2$, at times such that $R(t)/R(t') \simeq 1$. The second one varies when the first one decayed to zero. The mere existence of the second term is the essence of the aging phenomenon with older systems (longer t') having a slower relaxation than younger ones (shorter t'). The scaling of the second term as the ratio between 'two lengths' is a first manifestation of **dynamic scaling**.

A decorrelation time can also be defined in this case by expandind the argument of the scaling function around $t' \simeq t$. Indeed, calling $\Delta t \equiv t-t'$ one has $R(t)/R(t') \simeq R(t'+\Delta t)/R(t') \simeq [R(t')+R'(t')\Delta t]/R(t') \simeq 1 + \Delta t/[d\ln R(t')/dt']^{-1}$ and one identifies a **t'-dependent decorrelation time**

$$\boxed{t_d \simeq [d\ln R(t')/dt']^{-1} \quad \text{decorrelation time}} \tag{5.26}$$

which is, in general, a growing function of t'.

In order to fully characterise the correlation functions one then has to determine the typical growing length, R, and the scaling functions, g, f, f_c, *etc.* It turns out that the former can be determined with semi-analytic arguments and the predictions are well verified numerically – at least for clean system. The latter, instead, are harder to obtain. We shall give a very brief state of the art report in Sect. 5.7. For a much more detailed discussion of these methods see the review articles in [26].

The time-dependent typical domain length, $R(t)$, is determined numerically by using several indirect criteria or analytically within certain approximations. The most common ways of measuring R are with numerical simulations of lattice models or the numerical integration of the continuous partial differential equation for the evolution of the order parameter. In both cases one

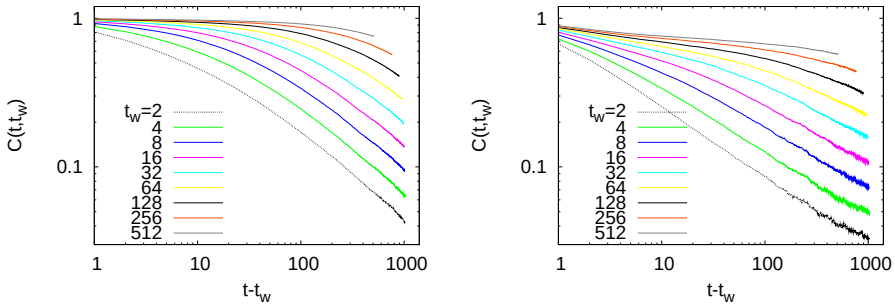

Figure 26: The two-time self-correlation in the $2d$IM with non-conserved order parameter dynamics at several waiting-times given in the key at temperature $T = 0.5$ (left) and $T = 2$ (right). Data obtained with Monte Carlo simulations. Note that the plateau is located at a lower level in the figure on the right consistently with the fact that $\langle\phi\rangle_{eq}$ decreases with increasing temperature.

– Computes the 'inverse perimeter density' $R(t) = -\langle H\rangle_{eq}/[\langle H(t)\rangle - \langle H\rangle_{eq}]$ with $\langle H(t)\rangle$ the time-dependent averaged energy and $\langle H\rangle_{eq}$ the equilibrium energy both measured at the working temperature T.

– Puts the dynamic scaling hypothesis to the test and extracts R from the analysis.

5.6.2 $R(t)$ in clean one dimensional cases with non-conserved order parameter

In one dimension, a space-time graph allows one to view coarsening as the diffusion and annhilitation upon collision of point-like particles that represent the domain walls. In the Glauber Ising chain with non-conserved dynamics one finds that the typical domain length grows as $t^{1/2}$ while in the continuous case the growth is only logarithmic, $\ln t$.

5.6.3 $R(t)$ in non-conserved curvature driven dynamics ($d > 2$)

The time-dependent Ginzburg-Landau model allows us to gain some insight on the mechanism driving the domain growth and the direct computation of the averaged domain length. In clean systems temperature does not play a very important role in the domain-growth process, it just adds some

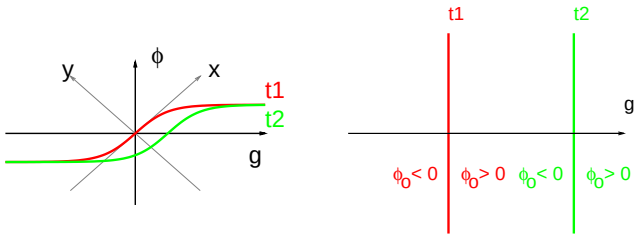

Figure 27: Left: domain wall profile. Right: view from the top. (g is n.)

thermal fluctuations within the domains, as long as it is smaller than T_c. In dirty cases instead temperature triggers thermal activation.

We focus first on the clean cases at $T = 0$ and only later we discuss thermal effects. Equation (5.5) for $\theta = 0$ is just a gradient descent in the energy landscape F. Two terms contribute to F: the bulk-energy term that is minimized by $\phi = \pm\phi_0$ and the elastic energy $(\nabla\phi)^2$ which is minimized by flat walls if present. As a consequence the minimization process implies that regions of constant field, $\phi(\vec{x}, t) = \pm\phi_0$, grow and they separated by flatter and flatter walls.

Take a **flat domain wall** separating regions where the configuration is the one of the two equilibrium states, $\phi(\vec{x}, t) = \pm\phi_0 + \delta\phi(\vec{x}, t)$. Linearizing eq. (5.5) around $\pm\phi_0$ and looking for static configurations, *i.e.* $\delta\phi(\vec{x}, t) = \delta\phi(\vec{x}) = \delta\phi(n)$ where n is the distance from the wall along the normal direction one finds $d^2\delta\phi(n)/dn^2 = -V''(\phi_0)\delta\phi(n)$. This equation has the solution $\delta\phi(n) \sim e^{-\sqrt{V''(\phi_0)}n}$ where n is the perpendicular distance to the wall . The order parameter approaches $\pm\phi_0$ on both sides of the wall very rapidly. This means that the free-energy of a configuration with an interface (sum of the elastic and potential terms) is concentrated in a very narrow region close to it. In consequence, the domain-wall curvature is the driving force for domain growth.

Allen and Cahn showed that the local wall velocity is proportional to the local curvature working with the GL equation at $\theta = 0$. The proof goes as follows. Take the GL equation and trasform the derivatives to apply in the

direction normal to the wall:

$$\frac{\partial\phi(\vec{x},t)}{\partial t} = -\left.\frac{\partial\phi(\vec{x},t)}{\partial n}\right|_t \left.\frac{\partial n}{\partial t}\right|_\phi , \qquad \vec{\nabla}\phi(\vec{x},t) = \left.\frac{\partial\phi(\vec{x},t)}{\partial n}\right|_t \hat{n} ,$$
$$\nabla^2\phi(\vec{x},t) = \left.\frac{\partial^2\phi(\vec{x},t)}{\partial n^2}\right|_t + \left.\frac{\partial\phi(\vec{x},t)}{\partial n}\right|_t \vec{\nabla}\cdot\hat{n}$$

where the subscripts mean that the derivatives are taken at t or ϕ fixed. Using now $\frac{\partial^2\phi(\vec{x},t)}{\partial n^2}|_t = V'(\phi)$ (note that the derivative is taken at fixed t) in the GL equation one finds the Allen-Cahn result

$$v \equiv \partial_t n|_\phi = -\vec{\nabla}\cdot\hat{n} \equiv -\kappa \tag{5.27}$$

valid in all d with κ the geodesic curvature.

Equation (5.27) allows one to get an intuition about the typical growth law in such processes. Take a spherical wall in any dimension. The local curvature is constant and $\kappa = (d-1)/R$ where R is the radius of the pshere within the hull. Equation (5.27) is recast as $dR/dt = -(d-1)/R$ that implies $R^2(t) = R^2(0) - 2(d-1)t$.

A closer look at the $2d$ equation allows one to go beyond and prove, in this case, that all areas enclosed by domain walls irrespective of their being other structures within (the so-called hull-enclosed areas) tend to diminish at constant rate $dA/dt = -\lambda$. This, of course, does not mean that all domains reduce their area since a domain can gain area from the disappearance of an internal domain of the opposite sign, for instance. The proof is simple and just uses the Gauss-Bonnet theorem: $\frac{dA}{dt} = \oint \vec{v}\wedge d\vec{\ell} = \oint v d\ell$. The local wall-velocity, $\vec{v}$, is proportional to the local geodesic curvature, κ, and the Gauss-Bonnet theorem implies $\oint \kappa d\ell = 2\pi$ for a planar $2d$ manifold with no holes. Therefore, the hull-enclosed area decreases with constant velocity for any geometry.

There are a number of ways to find the growth law

$$\boxed{R(t) = \lambda\, t^{1/z_d}} \tag{5.28}$$

with z_d the **dynamic exponent**, in **pure and isotropic** systems (see [26]). The effects of temperature enter only in the parameter λ and, for clean systems, growth is slowed down by an increasing temperature since thermal fluctuation tend to roughen the interfaces thus opposing the curvature driven mechanism. We estimate the T dependence of λ in Sect. 5.6.5.

In curvature driven Ising or Potts cases with non-conserved order parameter the domains are sharp and $z_d = 2$ with λ a weakly T-dependent coefficient. For systems with continuous variables such as rotors or XY models and the same type of dynamics, a number of computer simulations have shown that domain walls are thicker and $z_d = 4$.

5.6.4 $R(t)$ in conserved order parameter and the role of bulk diffusion

A different type of dynamics occurs in the case of phase separation (the water and oil mixture ignoring hydrodynamic interactions or a binary allow). In this case, the material is locally conserved, *i.e.* water does not transform into oil but they just separate. The main mechanism for the evolution is diffusion of material through the bulk of the opposite phase. After some discussion, it was established, as late as in the early 90s, that for scalar systems with **conserved order parameter** $z_d = 3$.

5.6.5 Crossover between critical and sub-critical coarsening: $\lambda(T)$

In the case of non-conserved scalar order-parameter dynamics behaves as

$$\boxed{R(t) \sim t^{1/z_{eq}}} \tag{5.29}$$

with z_{eq} the equilibrium dynamics exponent (note that z_{eq} is different from z_d). We shall not discuss critical dynamics in detail; this problem is treated analytically with dynamic renormalization group techniques and it is very well discussed in the literature [27]. In short, the exponent z_{eq} is given by [9]

$$z_{eq} = 2 + \frac{N+2}{(N+8)^2}\left[3\ln\frac{4}{3} - \frac{1}{2}\right]\epsilon^2 + O(\epsilon^3) \tag{5.30}$$

where N is the dimension of the possibly vector field, $N = 1$ for a scalar one, and $\epsilon = 4 - d$ with d the dimension of space. Note that z_{eq} is larger than 2 for all finite N and it approaches 2 in the large N limit (at least up to this order in perturbation theory). In particular, one finds

$$z_{eq} \simeq \begin{cases} 2.0538 & d = 2 \\ 2.0134 & d = 3 \\ 2 & d = 4 \end{cases} \tag{5.31}$$

for $N = 1$. Numerical simulations indicate $z_{eq} \simeq 2.13$ in $d = 2$.

Matching critical coarsening with sub-critical one allows one to find the T-dependent prefactor λ [12]. The argument goes as follows. The out of equilibrium growth at criticality and in the ordered phase are given by

$$R(t) \sim \begin{cases} t^{1/z_{eq}} & \text{at} \quad T = T_c \,, \\ (\lambda(T)t)^{1/z_d} & \text{at} \quad T < T_c \,. \end{cases} \tag{5.32}$$

z_{eq} is the equilibrium dynamic critical exponent and z_d the out of equilibrium growth exponent. Close but below criticality one should have an interpolating expression of the kind

$$R(t) \sim \xi^{-a}\, t^{1/z_d}\, f\left(\frac{t}{\xi^{z_{eq}}}\right) \qquad \text{at} \qquad T = T_c - \epsilon \tag{5.33}$$

with ξ the T-dependent equilibrium correlation length, $\xi(T) \sim (T_c - T)^{-\nu}$. The last factor tends to one, $f(x \to \infty) \to 1$, when $R(t) \gg \xi$, that is to say when the argument diverges and the system enters the sub-critical coarsening regime. It is however non-trivial when $R(t) \sim \xi$, the argument is finite and critical coarsening must be described. In particular, we determine its behaviour for $x = O(1)$ by requiring that eq. (5.33) matches the subcritical growing length which is achieved by (i) recovering the correct t dependence, (ii) cancelling the ξ factor. (i) implies

$$f(x) \sim x^{-1/z_d + 1/z_{eq}} \qquad \text{for} \qquad x = O(1) \,. \tag{5.34}$$

Then eq. (5.33) becomes

$$R(t) \sim \xi^{-a + z_{eq}/z_d - 1}\, t^{1/z_{eq}} \tag{5.35}$$

and to eliminate ξ we need

$$a = z_{eq}/z_d - 1 \,. \tag{5.36}$$

Comparing now the subcritical growing length and (5.33) in the very long times limit such that $R(t) \gg \xi$ and $f(x \to \infty) \to 1$:

$$[\lambda(T)]^{1/z_d} \sim \xi^{-a} \sim (T_c - T)^{\nu(z_{eq} - z_d)/z_d} \,. \tag{5.37}$$

5.6.6 The $2d$ XY model

The critical dynamics of an infinite system prepared in a non-equilibrium initial condition occurs, necessarily, out of equilibrium. Indeed, since the equilibrium correlation length, $\xi(T_c)$, diverges, the longest relaxation time, $t_r(T_c)$, and hence the equilibration time also diverges. At criticality one observes *critical slowing down* or, in other words, a slow dynamics associated to the decay of correlations as power laws of time. An infinite critical system evolves towards equilibrium – without ever reaching it – through a non-equilibrium scaling regime characterized by a single length scale $\xi(t)$ ($< \xi(T_c) \to \infty$). This dynamic correlation length can be extracted from the decay of the equal-time two-point correlation function that, according to the conventional scaling theory of non-equilibrium critical dynamics [**?**], is given by eq. (xxx) above.

The XY model in $d = 2$ is quite special since it is critical at all temperatures below T_{kt}. It is then worth analyzing this special case in detail. Moreover, it has topological defects and the rate of approach to the equilibrium state is affected by them.

The model is fully solvable in the spin-wave approximation in which the field is supposed to vary smoothly in space and, hence, vortices are neglected. The functional Langevin equation acting on the angle between the local spins and a chosen axis is linear in Fourier space and it can be readily solved. The angle correlation functions in equilibrium are

$$\langle (\theta(r) - \theta(0))^2 \rangle = \frac{k_B T}{\pi J} \ln r/a \tag{5.38}$$

leading to

$$C(r) = \langle \mathbf{s}(r)\mathbf{s}(0) \langle = \left(\frac{a}{r}\right)^{k_B T/\pi J} = \left(\frac{a}{r}\right)^{\eta(T)} \tag{5.39}$$

The equilibrium correlation length is $\xi(T) = a/\ln(k_B T/\pi J)$ that tends to zero only at $T \to \infty$ and diverges at $T \to 0$.

Spin-waves are non-local and extensive while vortices are local and intensive. The latter cannot be eliminated by simple perturbations but they annihilate.

The global correlation and linear response, $C(t,t') = V^{-1} \int d^2x \, \langle \, \mathbf{s}(\vec{x},t) \cdot \mathbf{s}(\vec{x},t') \, \rangle$ and $R(t,t') = V^{-1} \int d^2x \, \left. \frac{\delta \langle \, \mathbf{s}(\vec{x},t) \, \rangle}{\delta \mathbf{h}(\vec{x},t')} \right|_{\mathbf{h}=0}$ take the following scaling forms

in the limit $t - t' \gg \Lambda^{-2}$:

$$C(t,t') \sim \frac{1}{(t-t')^{\eta(T)/2}} \Phi\left(\frac{R(t)}{R(t')}\right) \tag{5.40}$$

$$R(t,t') \sim \frac{1}{4\pi\rho(T)(t-t')^{1+\eta(T)/2}} \Phi\left(\frac{R(t)}{R(t')}\right) \tag{5.41}$$

with Φ a scaling function and $R(t)$ the growing correlation length (that should not be confused with the linear response). The first remarkable property of these functions is that they are both decomposed in the product of a function of the time-difference $t - t'$ and a function of the ratio $\lambda \equiv R(t')/R(t)$, like in the general critical coarsening case. When $t - t' \ll R(t')$ and $\lambda \sim 1$, the decay is stationary

$$C(t,t') \sim (t-t')^{-\eta(T)/2} , \quad R(t,t') \sim (t-t')^{-1-\eta(T)/2}$$

and the FDR equals one. This limit defines a quasi-equilibrium regime. When the time difference increases and λ becomes smaller than one the relaxation enters an aging regime in which the decay of the correlation and response depends on the waiting-time t'. The behaviour in the aging regime depends on the initial conditions as discussed below.

Uniform initial conditions.

The uniform initial condition contains no free vortices and none are generated by thermal fluctuations at any $T < T_{kt}$. The evolution is well captured by the simple spin-wave approximation and after a simple calculation one finds

$$\Phi\left(\frac{\xi(t)}{\xi(t')}\right) = \left[\frac{(1+\lambda)}{4\lambda}\right]^{\eta(T)/4} , \qquad R(t) = t \, . \tag{5.42}$$

Beyond the crossover time $t - t' \sim t'$, when $C(2t', t') \sim t'^{-\eta(T)/2}$ and λ becomes smaller than one, the correlation and response decay to zero as power laws of the waiting-time t'. There is no clear-cut separation of time-scales characterised by the correlation reaching a constant value independently of the waiting-times but only a t' dependent pseudo-plateau where the behaviour of the two-time correlation changes. This is to be confronted to the behaviour of ferromagnetic coarsening systems quenched to the low-temperature phase for which the crossover occurs at $C(2t', t') = m_{eq}^2$. Above this plateau, the

relaxation corresponds to the equilibrium fluctuations of short wave-length while below the plateau the decorrelation is due to the domain-wall motion that manifests into a scaling in terms of $\lambda = t'/t$ only. In the 2d XY case the order parameter vanishes and there is no plateau at any finite value of C.

In the aging regime the fluctuation – dissipation ratio is larger than one. This *a priori* surprising result can be understood when interpreted in terms of the effective – temperature. The completely order configuration is the equilibrium state at zero temperature. The evolution of this initial state at finite temperature can be thought of as representing a sudden inverse quench of the system from $T = 0$ to $T > 0$. If the FDR is related to a remembrance of the temperature of the initial condition, in this case this is lower than the working temperature T and thus, the effective temperature also turns out to be lower than T.

Random initial conditions.

When random initial conditions with only short-ranged spatial correlations are considered, free vortices and antivortices are present initially. The relaxation occurs vis the annihilation of vortex-antivortex pairs and this coarsening process is much slower than the relaxation of spin-waves. The simple Gaussian theory is no more suited to describe this dynamics and a full analytic treatment is too hard to implement. With scaling and numeric analysis the dynamic correlation length has been estimated to be [26]

$$\boxed{R(t) \sim (t/\ln t)^{1/2} \ .}$$

The numerical simulations of Berthier, Holdsworth and Sellitto have proven that the two-time correlation and response are correctly described by the scaling form (5.40) and (5.41) with this length scale and the full decay looks like the one shown in the sketch above. The FDR is rather different from the one following the evolution of a uniform initial condition. The non-equilibrium susceptibility is now smaller than the equilibrium value, and in terms of the effective temperature [10] this means that the fluctuations of the wave-lengths longer than $R(t)$ occur at a $T_{eff} > T$ and hence keep a memory of the initial temperature $T = \infty$.

5.6.7 Role of disorder: thermal activation

The situation becomes much less clear when there is quenched disorder in the form of non-magnetic impurities in a magnetic sample, lattice dislo-

cations, residual stress, *etc.* Qualitatively, the dynamics are expected to be slower than in the pure cases since disorder pins the interfaces. In general, based on an argument due to Larkin (and in different form to Imry-Ma) one expects that in $d < 4$ the late epochs and large scale evolution is no longer curvature driven but controlled by disorder. Indeed, within a phase space view disorder generates metastable states that trap the system and thus slow down the relaxation.

A hand-waving argument to estimate the growth law in dirty systems is the following. Take a system in one equilibrium state with a domain of linear size R of the opposite equilibrium state within it. This configuration could be the one of an excited state with respect to the fully ordered one with absolute minimum free-energy. Call $\Delta F(R)$ the free-energy barrier between the excited and equilibrium states. The thermal activation argument (see Sect. 3.7.3) yields the activation time scale for the decay of the excited state (*i.e.* erasing the domain wall)

$$t_A \sim \tau \; e^{\Delta F(R)/(k_B T)} \; . \tag{5.43}$$

For a barrier growing as a power of R, $\Delta F(R) \sim \Upsilon(T, J) R^{\psi}$ (where J represents the disorder) one inverts (5.43) to find the linear size of the domains still existing at time t, that is to say, the growth law

$$\boxed{R(t) \sim \left(\frac{k_B T}{\Upsilon(T)} \; \ln \frac{t}{\tau} \right)^{1/\psi} \; .} \tag{5.44}$$

All smaller fluctuation would have disappeared at t while typically one would find objects of this size. The exponent ψ is expected to depend on the dimensionality of space but not on temperature. In 'normal' systems it is expected to be just $d - 1$ – the surface of the domain – but in spin-glass problems, it might be smaller than $d-1$ due to the presumed fractal nature of the walls. The prefactor Υ is expected to be weakly temperature dependent.

One assumes that the same argument applies out of equilibrium to the reconformations of a portion of any domain wall or interface where R is the observation scale.

However, already for the (relatively easy) random ferromagnet there is no consensus about the actual growth law. In these problems there is a competition between the 'pure' part of the Hamiltonian, that tries to minimize the total $(d - 1)$ dimensional area of the domain wall, and the 'impurity' part that makes the wall deviate from flatness and pass through the locations of

lowest local energy (think of $J_{ij} = J + \delta J_{ij}$ with J and δJ_{ij} contributing to the pure and impurity parts of the Hamiltonian, respectively). The activation argument in eq. (5.43) together with the power-law growth of barriers in $\Delta F(R) \sim \Upsilon(T, J) R^{\psi}$ imply a logarithmic growth of $R(t)$. Simulations, instead, suggest a power law with a temperature dependent exponent. Whether the latter is a pre-asymptotic result and the trully asymptotic one is hidden by the premature pinning of domain walls or it is a genuine behaviour invalidating $\Delta F(R) \sim \Upsilon(T, J) R^{\psi}$ or even eq. (5.43) is still an open problem. See the discussion below for a plausible explanation of the numerical data that does not invalidate the theoretical expectations.

In the $3d$ RFIM the curvature-driven growth mechanism that leads to (5.28) is impeded by the random field roughening of the domain walls. The dependence on the parameters T and h has been estimated. In the early stages of growth, one expects the zero-field result to hold with a reduction in the amplitude $R(t) \sim (A - Bh^2)\, t^{1/2}$. The time-window over which this law is observed numerically decreases with increasing field strength. In the late time regime, where pinning is effective Villain deduced a logarithmic growth $R(t) \sim (T/h^2) \ln t/t_0$ by estimating the maximum barrier height encountered by the domain wall and using the Arrhenius law to derive the associated time-scale.

In the case of spin-glasses, if the mean-field picture with a large number of equilibrium states is realized in finite dimensional models, the dynamics would be one in which all these states grow in competition. If, instead, the phenomenological droplet model applies, there would be two types of domains growing and $R(t) \sim (\ln t)^{1/\psi}$ with the exponent ψ satisfying $0 \leq \psi \leq d - 1$. Some refined arguments that we shall not discuss here indicate that the dimension of the bulk of these domains should be compact but their surface should be rough with fractal dimension $d_s > d - 1$.

5.6.8 Temperature-dependent effective exponents

The fact that numerical simulations of dirty systems tend to indicate that the growing length is a power law with a T-dependent exponent can be explained as due to the effect of a T-dependent cross-over length L_T. Indeed, if below $L_T \sim T^{\phi}$ the growth process is as in the clean limit while above L_T quenched disorder is felt and the dynamics is thermally activated:

$$R(t) \sim \begin{cases} t^{1/z_d} & \text{for} \quad R(t) \ll L_T \,, \\ (\ln t)^{1/\psi} & \text{for} \quad R(t) \gg L_T \,. \end{cases} \tag{5.45}$$

These growth-laws can be first inverted to get the time needed to grow a given length and then combined into a single expression that interpolates between the two regimes:

$$t(R) \sim e^{(R/L_T)^\psi} R^{z_d} \tag{5.46}$$

where the relevant T-dependent length-scale L_T has been introduced.

Now, by simply setting $t(R) \sim R^{\overline{z}(T)}$ one finds $\overline{z}(T) \sim z_d + \frac{1}{\ln R(t)} \left(\frac{R^\psi(t)}{L_T^\psi} \right)$ that replacing $R \sim t^{1/\overline{z}(T)}$ becomes $\overline{z}(T) \sim z_d + \frac{\overline{z}(T)}{\ln t} \left(\frac{t^{\psi/\overline{z}(T)}}{L_T^\psi} \right)$. Using now $\overline{z}(T) \simeq z_d$ in the correction term and focusing on times such that $t^{\psi/z_d}/\ln t$ is almost constant and equal to c one finds $\overline{z}(T) - z_d \simeq \mathrm{c}\ z_d/L_T^\psi$. Similarly, by equating $t(R) \sim \exp(R^{\overline{\psi}(T)}/T)$ one finds that $\overline{\psi}(T)$ is a decreasing function of T approaching ψ at high T.

5.7 Scaling functions for subcritical coarsening

Even though the qualitative behaviour of the solution to eq. (5.5) is easy to grasp, it is still too difficult to solve analytically and not much is known exactly on the scaling functions. A number of approximations have been developed but none of them is fully satisfactorily (see [26] for a critical review of this problem).

The **super-universality hypothesis** states that in cases in which temperature and quenched disorder are 'irrelevant' in the sense that they do not modify the nature of the low-temperature phase (*i.e.* it remains ferromagnetic in the case of ferromagnetic Ising models) the scaling functions are not modified. Only the growing length changes from the, say, curvature driven $t^{1/2}$ law to a logarithmic one. This hypothesis has been verified in a number of two and three dimensional models including the RBIM and the RFIM.

5.7.1 Breakdown of dynamic scaling

Some special cases in which dynamic scaling does not apply have also been exhibited. Their common feature is the existence of two (or more) growing lengths associated to different ordering mechanisms. An example is given by the Heisenberg model at $T \to 0$ in which the two mechanisms are related to the vectorial ordering within domains separated by couples of parallel spins that annhilate in a way that is similar to domain-wall annihilation in the Ising chain.

5.8 Annealing

There has been recent interest in understanding how a finite rate cooling affects the defect density found right after the quench. A scaling form involving equilibrium critical exponents was proposed by Zurek following work by Kibble. The interest is triggered by the similarity with the problem of quantum quenches in atomic gases, for instance. An interplay between critical coarsening (the dynamics that occurs close in the critical region) that is usually ignored (!) and sub-critical coarsening (once the critical region is left) is the mechanism determining the density of defects right after the end of the cooling procedure.

The growing length satisfies a scaling law

$$\begin{array}{rcll} R(t,\epsilon(t)) & \sim & \epsilon^{-\nu}(t)\ f[t\epsilon^{z_{eq}\nu}(t)] & \epsilon(t)=|T(t)-T_c| \\ f(x) & \to & \begin{cases} \text{ct} & x \ll -1 \\ \sqrt{x} & x \gg 1 \end{cases} & \begin{array}{r} \text{Equilibrium at high } T \\ \text{Coarsening at low } T \end{array} \end{array}$$

with t measured from the instant when the critical point is crossed and $x \in (-1,1)$ is the critical region. A careful analysis of this problem can be found in [15].

5.9 An instructive case: the large N approximation

A very useful approximation is to upgrade the scalar field to a vectorial one with N components

$$\phi(\vec{x},t) \to \vec{\phi}(\vec{x},t) = (\phi_1(\vec{x},t),\ldots,\phi_N(\vec{x},t))\ , \tag{5.47}$$

and modify the free-energy

$$F = \int d^dx \left[\frac{1}{2}(\nabla\vec{\phi})^2 + \frac{N}{4}(\phi_0^2 - N^{-1}\phi^2)^2\right]\ , \tag{5.48}$$

with $\phi^2 = \sum_{\alpha=1}^N \phi_\alpha^2$ and ϕ_0 finite. The $T=0$ dynamic equation then becomes

$$\partial_t\phi_\alpha(\vec{x},t) = \nabla^2\phi_\alpha(\vec{x},t) - 4\phi_\alpha(\vec{x},t)\,[\phi_0^2 - N^{-1}\phi^2(\vec{x},t)] \tag{5.49}$$

and it is clearly **isotropic** in the N dimensional space implying

$$C_{\alpha\beta}(\vec{x},t;\vec{x}',t') = \delta_{\alpha\beta}C(\vec{x},t;\vec{x}',t') \tag{5.50}$$

In the limit $N \to \infty$ while keeping the dimension of real space fixed to d, the cubic term in the right-hand-side can be replaced by

$$-\phi_\alpha(\vec{x},t)N^{-1}\phi^2(\vec{x},t) \to -\phi_\alpha(\vec{x},t)N^{-1}[\,\phi^2(\vec{x},t)\,]_{ic} \equiv -\phi_\alpha(\vec{x},t)\,a(t) \quad (5.51)$$

since $N^{-1}\phi^2(\vec{x},t)$ does not fluctuate, it is equal to its average over the initial conditions and it is therefore not expected to depend on the spatial position if the initial conditions are chosen from a distribution that is statistically translational invariant. For the scalar field theory the replacement (5.51) is just the **Hartree approximation**. The dynamic equation is now **linear** in the field $\phi_\alpha(\vec{x},t)$ that we rename $\phi(\vec{x},t)$ (and it is now order 1):

$$\partial_t\phi(\vec{x},t) = [\nabla^2 + a(t)]\phi(\vec{x},t)\ , \quad (5.52)$$

where the time-dependent harmonic constant $a(t) = \phi_0^2 - [\phi^2(\vec{x},t)]_{ic} = \phi_0^2 - [\phi^2(\vec{0},t)]_{ic}$ has to be determined self-consistently. Equation (5.52) can be Fourier transformed

$$\partial_t\phi(\vec{k},t) = [-k^2 + a(t)]\phi(\vec{k},t)\ , \quad (5.53)$$

and it takes now the form of almost independent oscillators under different time-dependent harmonic potentials coupled only through the self-consistent condition on $a(t)$. The stability properties of the oscillators depend on the sign of the prefactor in the RHS. The solution is

$$\phi(\vec{k},t) = \phi(\vec{k},0)\ e^{-k^2t+\int_0^t dt'\ a(t')} \quad (5.54)$$

and the equation on $a(t)$ reads:

$$a(t) \ = \ \phi_0^2 - \Delta\ e^{2\int_0^t dt' a(t')}\left(\frac{2\pi}{4t}\right)^{d/2}\ , \quad (5.55)$$

where one used $[\phi^2(\vec{x},t)]_{ic} = [\phi^2(\vec{0},t)]_{ic}$ and a delta-correlated Gaussian distribution of initial conditions with strength Δ. The self-consistency equation is not singular at $t = 0$ since there is an underlying cut-off in the integration over k corresponding to the inverse of the lattice spacing, this implies that times should be translated as $t \to t + 1/\Lambda^2$ with $\Lambda = 1/a$ the lattice spacing.

Without giving all the details of the calculation, eq. (5.55), generalized to the finite T case, can be solved at all temperatures [16]. One finds that there exists a finite $T_c(d)$ and

Upper-critical quench

$$a(t) \to -\xi^{-2} \tag{5.56}$$

with ξ the equilibrium correlation length, and the 'mass' (in field theoretical terms) or the harmonic constant saturates to a finite value: $-k^2 + a(t) \to -k^2 - \xi^{-2}$.

Critical quench

$$a(t) \to -w/(2t) \quad \text{with} \quad w = 0 \ \text{ for } \ d > 4 \ \text{ and } \ w = (d-4)/2 \ \text{ for } \ d < 4 \ . \tag{5.57}$$

The dynamics is trivial for $d > 4$ but there is critical coarsening in $d < 4$. z_{eq} equals 2 in agreement with the result from the ϵ expansion once evaluated at $N \to \infty$.

Sub-critical coarsening

In the long times limit in which the system tends to decrease its elastic and potential energies $[\,\phi^2(\vec{x},t)\,]_{ic}$ must converge to $\phi_0^2 \neq 0$ **below criticality** and this imposes $2\int_0^t dt'\, a(t') \simeq \frac{d}{2}\ \ln(t/t_0)$ with $t_0 = \pi/2\ (\Delta/\phi_0^2)^{2/d}$ at large times, *i.e.*

$$a(t) \simeq \frac{d}{4t} \qquad \text{for} \qquad t \gg t_0 \tag{5.58}$$

and the time-dependent contribution to the spring constant vanishes asymptotically. Knowing the long-time behaviour of $a(t)$ implies that each mode $[\phi(\vec{k},t)]_{ic}$ with $\vec{k} \neq 0$ vanishes asymptotically but the $\vec{k} = 0$ mode grows as $t^{d/4}$. The growth of the $\vec{k} = 0$ reflects the domain growth process whereby all modulations tend to disappear and the configuration gets more and more uniform as time passes.

We focus now on two interesting cases: quenches to T_c and $T < T_c$. The asymptotic behaviour of the space-time correlation function in the aging regime is

$$[\,\phi(\vec{x},t)\phi(\vec{x}',t')\,]_{ic} = \phi_0^2 \left[\frac{4tt'}{(t+t')^2}\right]^{d/4} \exp\left[-\frac{(\vec{x}-\vec{x}')^2}{4(t+t')}\right] \ , \tag{5.59}$$

for $t \geq t'$ for a quench to $T < T_c$ and

$$[\,\phi(\vec{x},t)\phi(\vec{x}',t')\,]_{ic} = \phi_0^2\, t'^{1-d/2} f(t/t') \ \exp\left[-\frac{(\vec{x}-\vec{x}')^2}{4(t+t')}\right] \ , \tag{5.60}$$

for a quench to T_c. We focus on $d < 4$. These expressions capture the main features of the domain growth process:

1. In Fourier space all $k \neq 0$ modes have an exponential decay while the $k = 0$ one is fully massless asympotically and diffuses.
2. In sub-critical quenches, for any finite and fixed $(\vec{x} - \vec{x}')$, in the long times limit the exponential factor approaches one and one obtaines a function of t'/t only.
3. In critical quenches the two-time dependent prefactor is of the form expected from dynamic scaling.
4. Due to the exponential factor, for fixed but very large time t and t' the correlation falls off to zero over a distance $|\vec{x} - \vec{x}'| \propto \sqrt{t + t'}$. This means that, at time t, the typical size of the regions in the states $\pm\phi_0$ is $R(t) \propto t^{1/2}$. This holds for critical and sub-critical quenches as well and it is a peculiar property of the large N $O(N)$ model that has $z_{eq} = z_d$.
5. For fixed $|\vec{x} - \vec{x}'|$, the correlation always falls to zero over a time separation $t - t'$ *which is larger than* t'. This means that the time it takes to the system to decorrelate from its configuration at time t' is of the order of t' itself, $t_d \simeq t'$. The age of the system is the characteristic time-scale for the dynamical evolution: the older is the system, the slower is its dynamics. After a time of the order of the age of the system any point $\vec{x}$ will be swept by different domain walls and the correlation will be lost.
6. In a critical quench the correlation always decays to zero due to the prefactor that goes as $t^{(2-d)/2}$ and vanishes in all $d > 2$. The aging curves have an envelope that approaches zero as a power law.
7. In a sub-critical quench, for any finite and fixed $(\vec{x} - \vec{x}')$, in the long t' and t limit such that $t'/t \to 1$ the time dependence disappears and the correlation between two points converges to ϕ_0^2. This means that, typically, if one looks at a finite spatial region on a finite time-scale this region will be in one of the two states $\pm\phi_0$, i.e. within a domain.

Note that we have obtained the field and then computed correlations from the time-dependent configuration. We have not needed to compute the linear response. We shall see later that in other more complex glassy systems one cannot follow this simple route and one needs to know how the linear response behave. We refer to the reviews in [29] for detailed accounts on the behaviour of the linear response in critical dynamics.

5.10 Nucleation and growth

In a **first-order** phase transition the equilibrium state of the system changes abruptly. Right at the transition the free-energies of the two states involved are identical and the transition is driven by lowering the free-energy as the new phase forms, see Fig. 18. The original phase remains meta-stable close to the transition. The nucleation of a sufficiently large bubble of the trully stable phase into the metastable one needs to be thermally activated to trigger the growth process [28]. The rate of the process can be very low or very fast depending on the height of the free-energy barrier between the two states and the ambient temperature.

Two types of nucleation are usually distinguished: homogeneous (occuring at the bulk of the meta-stable phase) and heterogeneous (driven by impurities or at the surface). The more intuitive examples of the former, on which we focus here, are the condensation of liquid droplets from vapour and the crystallization of a solid from the melt.

The **classical theory of nucleation** applies to cases in which the identification of the nucleous is easy. It is based on a number of assumptions that we now list. First, one associates a number of particles to the nucleous (although in some interesting cases this is not possible and a different approach is needed). Second, one assumes that there is no memory for the evolution of the number densities of clusters of a given size in time (concretely, a Markov master equation is used). Third, one assumes that clusters grow or shrink by attachment or loss of a single particle, that is to say, coallescence and fission of clusters are neglected. Thus, the length-scale over which the slow part of the dynamics takes place is the one of the critical droplet size, the first one to nucleate. Fourth, the transition rates satisfy detail balance and are independent of the droplet form. They just depend on the free-energy of the droplet with two terms: a contribution proportional to the droplet volume and the chemical potential difference between the stable and the metastable states, Δf, and a contribution proportional to the bubble surface that is equal to the surface area times the surface tension, σ, that is assumed to be the one of coexisting states in equilibrium - that is to say the energy of a flat domain wall induced by twisted boundary conditions. Fift, the bubble is taken to be

spherical and thus dependent of a single parameter, the radius. Thus

$$\Delta F[R] = \sigma\ \Omega_{d-1}\ R^{d-1} - |\Delta f|\ \Omega_d\ R^d \tag{5.61}$$

for $d > 1$. Ω_d is the volume of the unit sphere in d dimensions. For small radii the surface term dominates and it is preferable to make the droplet disappear. In contrast, for large radii the bulk term dominates and the growth of the bubble is favoured by a decreasing free-energy. Thus the free-energy difference has a maximum at

$$\boxed{R^* = \frac{(d-1)\ \Omega_{d-1}\ \sigma}{d\ \Omega_d\ |\Delta f|} \propto \sigma |\Delta f|^{-1}} \tag{5.62}$$

and the system has to thermally surmount the barrier $\Delta F^* \equiv \Delta F[R^*]$. The Kramers escape theory, see Sect. 3.7.3, implies that the nucleation rate or the average number of nucleations per unit of volume and time is suppressed by the Arrhenius factor

$$\boxed{r_A = t_A^{-1} \sim e^{-\beta \Delta F^*} \qquad \text{with} \qquad \Delta F^* = \frac{(d-1)^{d-1}}{d^d}\ \frac{\Omega_{d-1}^d}{\Omega_d^{d-1}}\ \frac{\sigma^d}{|\Delta f|^{d-1}}} \tag{5.63}$$

As expected, ΔF^* increases with increasing σ and/or $|\Delta f|^{-1}$ and r^{-1} vanishes for $T \to 0$ when thermal agitation is switched off. The implicit assumption is that the time to create randomly the critical droplet is much longer than the time involved in the subsequent growth. The relaxation of the entire system is thus expected to be given by the inverse probability of escape from the metastable well. The determination of the prefactor [that is ignored in eq. (5.63)] is a hard task.

6 Classical dynamic generating functional and symmetries

In this Section we discuss some static and dynamic aspects of classical statistical systems in the canonical ensemble. In this chapter we introduce the classical path integral formalism. The symmetry arguments follow closely the discussion in [**?**].

6.1 Classical statics: the reduced partition function

In order to analyze the statistical static properties of the classical coupled system, we study the partition function or Gibbs functional, Z_{tot} that reads

$$Z_{tot}[\eta] = \sum_{\substack{conf\ osc \\ conf\ syst}} \exp(-\beta H_{tot} - \beta\eta x) \tag{6.1}$$

where the sum represents an integration over the phase space of the full system, the particle's and the oscillators', and η is a source. Having chosen a quadratic bath and a linear coupling, the integration over the oscillators' coordinates and momenta can be easily performed. This yields the reduced Gibbs functional

$$Z_{red}[\eta] \propto \sum_{conf\ syst} \exp\left[-\beta\left(H_{syst} + H_{counter} + \eta x - \frac{1}{2}\sum_{a=1}^{N_b}\frac{c_a^2}{m_a\omega_a^2}\,x^2\right)\right] . \tag{6.2}$$

The 'counterterm' $H_{counter}$ is chosen to cancel the last term in the exponential and it avoids the renormalization of the particle's mass (the coefficient of the quadratic term in the potential) due to the coupling to the environment that could have even destabilize the potential taking negative values. An alternative way of curing this problem would be to take a vanishingly small coupling to the bath in such a way that the last term must vanish by itself (say, all $c_a \to 0$). However, this might be problematic when dealing with the stochastic dynamics since a very weak coupling to the bath implies also a very slow relaxation. It is then conventional to include the counterterm to cancel the mass renormalization. One then finds

$$Z_{red}[\eta] \propto \sum_{conf\ syst} \exp\left[-\beta\left(H_{syst} + \eta x\right)\right] = Z_{syst}[\eta] . \tag{6.3}$$

The interaction with the reservoir does not modify the statistical properties of the particle since $Z_{red} \propto Z_{syst}$. We shall see in Sect. 3.7.3 that this does not happen quantum mechanically. (For a non-linear coupling $H_{int} = \sum_\alpha c_\alpha q_\alpha \mathcal{V}(x)$ the counterterm is $H_{counter} = \frac{1}{2}\sum_\alpha \frac{c_\alpha^2}{m_\alpha \omega_\alpha^2}[\mathcal{V}(x)]^2$.)

6.2 Classical dynamics: generating functional

In Sect. 3.7.3 we showed a proof of the (generally non-Markov) Langevin equation based on the integration over a large ensemble of harmonic oscillators that act as a bath with which the system is set in contact.

Observables which are functions of the solution to the Langevin equation can also be computed using a dynamic generating functional that reads [42]

$$Z_d[\eta] \equiv \int \mathcal{D}\xi \; dP(t_0) \; e^{-\frac{1}{2k_B T}\int_{t_0}^{\mathcal{T}} dt' \int_{t_0}^{\mathcal{T}} dt'' \, \xi(t')\Gamma^{-1}(t'-t'')\xi(t'') + \int_{t_0}^{\mathcal{T}} dt' \, \eta(t') x_\xi(t')}$$

$x_\xi(t)$ is the solution to the Langevin equation with initial condition $x_0 = x(t_0), \dot{x}_0 = \dot{x}(t_0)$ at the initial time t_0. The factor $dP(t_0)$ is the measure of the initial condition, $dP(t_0) \equiv dx_0 d\dot{x}_0 P_{\rm i}[x_0, \dot{x}_0]$. The Gaussian factor is proportional to $P[\xi]$ the functional probability measure of the noise. The measure is $\mathcal{D}\xi \equiv \prod_{k=0}^{\mathcal{N}} d\xi(t_k)$ with $k = 0, \ldots, \mathcal{N}$, $t_k = t_0 + k(\mathcal{T}t - t_0)/\mathcal{N}$ and $\mathcal{N} \to \infty$ while $(\mathcal{T} - t_0)$ remains finite. The inverse kernel Γ^{-1} is defined within the interval $[t_0, \mathcal{T}]$: $\int_{t_0}^{\mathcal{T}} dt'' \Gamma(t - t'')\Gamma^{-1}(t'' - t') = \delta(t - t')$.

A very useful expression for $Z_d[\eta]$, usually called the Martin-Siggia-Rose generating functional (actually derived by Janssen [**?**]), is obtained by introducing the identity

$$\mathrm{Eq}[x(t)] \equiv m\ddot{x}(t) + \int_{t_0}^{\mathcal{T}} dt' \; \gamma(t - t')\dot{x}(t') + V'[x(t)] = \xi(t) \tag{6.4}$$

valid at each time t, with the delta function

$$1 = \int \mathcal{D}x \;\; \delta\left[\mathrm{Eq}[x(t)] - \xi(t)\right] \left| \det \frac{\delta \mathrm{Eq}[x(t)]}{\delta x(t')} \right| , \tag{6.5}$$

with $\mathcal{D}x \equiv \prod_{k=1}^{\mathcal{N}} dx(t_k)$. The factor $|\det \ldots|$ is the determinant of the operator $\delta(t - t')\{m\partial_t^2 + V''[x(t)]\} + \gamma(t - t')\partial_{t'}$ and ensures that the integral equals one.[9] The delta function can be exponentiated with an auxiliary field

[9] Its origin is in the change of variables. In the same way as in the one dimensional integral, $\int dx \; \delta[g(x)] = \int dz \; 1/|g'[g^{-1}(z)]| \; \delta(z) = 1/|g'[g^{-1}(0)]|$, to get 1 as a result one includes the inverse of the Jacobian within the integral: $\int dx \; \delta[g(x)] \; |g'(x)| = 1$.

$i\hat{x}$ (using the Fourier representation of the δ-function). $\mathcal{D}i\hat{x} = \prod_{k=1}^{\mathcal{N}-1} di\hat{x}(t_k)$. The determinant can be exponentiated with time-dependent anticommunting variables – opening the way to the use of super-symmetry [23], a subject that we shall not touch in these notes. However, since it does not yield a relevant contribution to the kind of dynamics we are interested in, we forget it (one can show that the determinant is a constant for Langevin processes with coloured noise and/or inertia and that the discretization of an over-damped Langevin equation with white-noise can also be chosen to set it to one – Itô convention, see App. **??**). Z_d reads

$$
\begin{aligned}
Z_d[\eta,\hat{\eta}] \equiv \int \mathcal{D}\xi\mathcal{D}x\mathcal{D}i\hat{x}\; dP(t_0) \\
\times e^{-\int_{t_0}^{\mathcal{T}} dt'\, i\hat{x}(t')\left[m\ddot{x}(t')+\int_{t_0}^{\mathcal{T}} dt''\;\gamma(t'-t'')\dot{x}(t'')+V'[x(t')]-\xi(t')\right]} \\
\times e^{-\frac{1}{2k_BT}\int_{t_0}^{\mathcal{T}} dt'\int_{t_0}^{\mathcal{T}} dt''\,\xi(t')\Gamma^{-1}(t'-t'')\xi(t'')+\int_{t_0}^{\mathcal{T}} dt'\,[\eta(t')x(t')+\hat{\eta}(t')i\hat{x}(t')]}
\end{aligned}
$$

where we have introduced a new source $\hat{\eta}(t)$, coupled to the auxiliary field $i\hat{x}(t)$. The integration over the noise $\xi(t)$ is Gaussian and it can be readily done; it yields

$$
+\frac{k_BT}{2}\int_{t_0}^{\mathcal{T}} dt' \int_{t_0}^{\mathcal{T}} dt''\; i\hat{x}(t')\,\Gamma(t'-t'')\,i\hat{x}(t'') \tag{6.6}
$$

and, for a **coloured bath**, the environment generates a **retarded interaction** in the effective action. In the usual white noise case, this term reduces to, $k_BT\gamma_0\int_{t_0}^{\mathcal{T}} dt'\;[i\hat{x}(t')]^2$, a local expression. In the end, the generating function and resulting **Martin-Siggia-Rose-Jaenssen-deDominicis** (MSRJD) action reads

$$
\begin{aligned}
\mathcal{Z}_d[\eta,\hat{\eta}] &\equiv \int \mathcal{D}x\mathcal{D}i\hat{x}\; dP(t_0)\; e^{S[x,i\hat{x},\eta,\hat{\eta}]} \\
S[x,i\hat{x},\eta,\hat{\eta}] &= -\int dt'\, i\hat{x}(t')\left\{m\ddot{x}(t')+\int dt''\;\gamma(t'-t'')\dot{x}(t'')+V'[x(t')]\right\} \\
&\quad +\frac{k_BT}{2}\int dt'\int dt''\, i\hat{x}(t')\Gamma(t'-t'')i\hat{x}(t'')+\text{sources}\;.
\end{aligned} \tag{6.7}
$$

All integrals runs over $[t_0,\mathcal{T}]$. Causality in the integral over t' is ensured by the fact that γ is proportional to θ.

The MSRJD action has two kinds of contributions: the ones that depend on the characteristics of the bath (through Γ) and the ones that do not. The

latter also exist in a functional representation of Newton dynamics and we call them S^{det} (for deterministic) while the former contain all information abour thermal fluctuations and dissipation and we call it S^{diss} (for dissipation):

$$S[x, i\hat{x}, \eta, i\hat{\eta}] = S^{diss}[x, i\hat{x}; \Gamma] + S^{det}[x, i\hat{x}, \eta, i\hat{\eta}] \ . \tag{6.8}$$

If the distribution of the initial condition were to be included in the action as an additional term, $\ln P_{\rm i}[x_0, i\hat{x}_0]$, 6t would be part of S^{det}.

Interestingly enough, the **dynamic generating functional at zero sources is identical to one** for any model:

$$\mathcal{Z}_d[\eta = 0, \hat{\eta} = 0] = 1 \tag{6.9}$$

as can be concluded from its very first definition. In particular, it does not depend on the coupling constants of the chosen model. This property will be utilized in disordered systems to render the dynamic calculations relatively easier than the static ones.

6.3 Generic correlation and response.

The mean value at time t of a generic observable A is

$$\langle A(t) \rangle = \int \mathcal{D}x\mathcal{D}i\hat{x} \ dP(t_0) \ A[x(t)] \ e^{S[x, i\hat{x}]} \ , \tag{6.10}$$

where $S[x, i\hat{x}]$ is ashort-hand notation for $S[x, i\hat{x}, \eta = 0, \hat{\eta} = 0]$. The self-correlation and linear response of x are given by

$$C(t, t') = \langle x(t)x(t') \rangle = \frac{1}{Z_d[\eta, \hat{\eta}]} \left. \frac{\delta^2 Z_d[\eta, \hat{\eta}]}{\delta\eta(t)\delta\eta(t')} \right|_{\eta=\hat{\eta}=0} = \left. \frac{\delta^2 Z_d[\eta, \hat{\eta}]}{\delta\eta(t)\delta\eta(t')} \right|_{\eta=\hat{\eta}=0} \tag{6.11}$$

$$\begin{aligned} R(t, t') &= \left. \frac{\delta\langle x(t) \rangle}{\delta h(t')} \right|_{h=0} = \langle x(t) \frac{\delta S[x, i\hat{x}; h]}{\delta h(t')} \rangle|_{h=0} = \langle x(t) i\hat{x}(t') \rangle \\ &= \frac{1}{Z_d[\eta, \hat{\eta}]} \left. \frac{\delta^2 Z_d[\eta, \hat{\eta}]}{\delta\eta(t)\delta\hat{\eta}(t')} \right|_{\eta=\hat{\eta}=0} = \left. \frac{\delta^2 Z_d[\eta, \hat{\eta}]}{\delta\eta(t)\delta\hat{\eta}(t')} \right|_{\eta=\hat{\eta}=0} \end{aligned} \tag{6.12}$$

with $h(t')$ a small field applied at time t' that modifies the potential energy according to $V \to V - h(t')x(t')$. The $i\hat{x}$ auxiliary function is sometimes called the **response field** since it allows one to compute the linear response

by taking its correlations with x. Similarly, we define the two-time correlation between two generic observables A and B,

$$C_{AB}(t,t') \equiv \int \mathcal{D}x\mathcal{D}i\hat{x}dP(t_0)\, A[x(t)]B[x(t')]\, e^{S[x,i\hat{x}]} = \langle A[x(t)]B[x(t')]\rangle \quad (6.13)$$

and the linear response of A at time t to an infinitesimal perturbation linearly applied to B at time $t' < t$,

$$R_{AB}(t,t') \equiv \left.\frac{\delta\langle A[x(t)]\rangle_{f_B}}{\delta f_B(t')}\right|_{f_B=0}, \quad (6.14)$$

with $V(x) \mapsto V(x) - f_B B(x)$. The function $B(x)$ depends only on x (or on an even number of time derivatives, that is to say, it is even with respect to $t \to -t$). By plugging eq. (6.10) in this definition we get the **classical Kubo formula** for generic observables:

$$R_{AB}(t,t') = \left.\langle A[x(t)]\,\frac{\delta S[x,i\hat{x};f_B]}{\delta f_B(t')}\rangle\right|_{f_B=0} = \langle A[x(t)]i\hat{x}(t')B'[x(t')]\rangle \quad (6.15)$$

with $B'[x(t')] = \partial_x B[x(t')]$. This relation is also causal and hence proportional to $\theta(t-t')$; it is valid in and out of equilibrium. For $B[x] = x$ it reduces to the correlation between x and $i\hat{x}$.

If the system has **quenched random exchanges** or any kind of **disorder**, one may be interested in calculating the averaged correlations and responses over different realizations of disorder. Surprisingly, this average is very easy to perform in a dynamic calculation [43]. The normalization factors $1/Z_d[\eta,\hat{\eta}]$ in (6.11) and (6.12) have to be evaluated at zero external sources in which they are trivially independent of the random interactions. Hence, it is sufficient to average $Z_d[\eta,\hat{\eta}]$ over disorder and then take variations with respect to the sources to derive the thermal and disorder averaged two-point functions. This property contrasts with an equilibrium calculation where the expectation values are given by $[\langle A\rangle] = [1/Z\sum_{conf} A\exp(-\beta H)]$, with $[\cdot]$ denoting the disorder average. In this case, the partition function Z depends explicitly on the random exchanges and one has to introduce **replicas** [24] to deal with the normalization factor and do the averaging.

Having assumed the initial equilibration of the environment ensures that a normal system will eventually equilibrate with it. The interaction with the bath allows the system to dissipate its energy and to relax until thermalization is reached. However, in some interesting cases, as the dyamics

across phase transitions and glassy models, the time needed to equilibrate is a fast growing function of N, the number of dynamic degrees of freedom. Thus, the evolution of the system in the thermodynamic limit occurs out of equilibrium. In real systems, a similar situation occurs when the equilibration time crosses over the observation time and falls out of the experimental time-window.

A final interesting remark on the relevance of quenched disorder is the following. When a system with quenched disorder evolves out of equilibrium at finite temperature, the correlation function and the response function do not depend on the realization of disorder if the size of the system is large enough (the realization of disorder has to be a typical one). These quantities are **self-averaging**. This statement is easily checked in a simulation. When times get sufficiently long as to start seeing the approach to equilibrium, dependencies on the realizations of disorder appear.

6.4 Time-reversal

Since it will be used in the rest of this chapter, we introduce the time-reversed variable $\bar{x}$ by $\bar{x}(t) \equiv x(-t)$ for all t. The time-reversed observable is defined as

$$A_{\rm r}([x],t) \equiv A([\bar{x}],-t). \tag{6.16}$$

It has the effect of changing the sign of all odd time-derivatives in the expression of local observables, *e.g.* if $A[x(t)] = \partial_t x(t)$ then $A_{\rm r}[x(t)] = -\partial_t x(-t)$. As an example for non-local observables, the time-reversed Langevin equation reads

$$\mathrm{EQ}_{\rm r}([x],t) \;=\; m\ddot{x}(t) - F_{\rm r}([x],t) - \int_{-\mathcal{T}}^{\mathcal{T}} du\; \gamma(u-t)\dot{x}(u)\;. \tag{6.17}$$

Notice the change of sign in front of the friction term that is no longer dissipative in this new equation.

6.5 An equilibrium symmetry

If the initial time t_0 is set to $t_0 = -\mathcal{T}$ and the system is in equilibrium at this instant, $P_{-\mathcal{T}}$ is given by the Maxwell-Boltzmann measure. One can then check that the zero-source action, $S[x, i\hat{x}]$, is fully invariant under the

field transformation $\mathcal{T}_c$ defined as

$$\mathcal{T}_c \equiv \left\{ \begin{array}{rcl} x_u & \mapsto & x_{-u} \ , \\ i\hat{x}_u & \mapsto & i\hat{x}_{-u} + \beta d_u x_{-u} \ . \end{array} \right.$$

We introduced the notation $x_t = x(t)$ so as to make the notation more compact. Note that $d_u x_{-u} = -d_{-u} x_{-u}$. This transformation does not involve the kernel Γ and it includes a time-reversal. The invariance is achieved independently by the deterministic (S^{det}) and dissipative (S^{diss}) terms in the action. The former includes the contribution from the initial condition, $\ln P_{-\mathcal{T}}$. Moreover, the path-integral measure is invariant since the Jacobian associated to this transformation is also block triangular with ones on the diagonal. The proof goes as follows.

6.5.1 Invariance of the measure

The Jacobian $\mathcal{J}_c$ of the transformation $\mathcal{T}_c$ is the determinant of a triangular matrix:

$$\mathcal{J}_c \equiv \det \frac{\delta(x,\hat{x})}{\delta(\mathcal{T}_c x, \mathcal{T}_c \hat{x})} = \det{}^{-1}_{uv} \begin{bmatrix} \frac{\delta x_{-u}}{\delta x_v} & 0 \\ \frac{\delta \hat{x}_{-u}}{\delta x_v} & \frac{\delta \hat{x}_{-u}}{\delta \hat{x}_v} \end{bmatrix} = \left(\det{}^{-1}_{uv} \left[\delta_{u+v} \right] \right)^2 = 1$$

and it is thus identical to one.

6.5.2 Invariance of the integration domain

Before and after the transformation, the functional integration on the field x is performed for values of x_t on the real axis. However, the new domain of integration for the field $\hat{x}$ is complex. For all times, $\hat{x}_t$ is now integrated over the complex line with a constant imaginary part $-i\beta\partial_t x_t$. One can return to an integration over the real axis by closing the contour at both infinities. Indeed the integrand, e^S, goes to zero sufficiently fast at $x_t \to \pm\infty$ for neglecting the vertical ends of the contour thanks to the term $\beta^{-1}\gamma_0(i\hat{x}_t)^2$ (in the white noise limit or the correspondong ones in colored noise cases) in the action. Furthermore the new field is also integrated with the boundary conditions $\hat{x}(-\mathcal{T}) = \hat{x}(\mathcal{T}) = 0$.

6.5.3 Invariance of the action functional

The deterministic contribution satisfies

$$\begin{aligned} S^{\rm det}[\mathcal{T}_{\rm c}x, \mathcal{T}_{\rm c}\hat{x}] &= \ln P_{\rm i}(x_{\mathcal{T}}, \dot{x}_{\mathcal{T}}) - \int_u \left[i\hat{x}_{-u} + \beta\partial_u x_{-u}\right]\left[m\partial_u^2 x_{-u} + V'(x_{-u})\right] \\ &= \ln P_{\rm i}(x_{\mathcal{T}}, \dot{x}_{\mathcal{T}}) - \int_u i\hat{x}_u \left[m\ddot{x}_u + V'(x_u)\right] + \beta\int_u \dot{x}_u \left[m\ddot{x}_u + V'(x_u)\right] \\ &= \ln P_{\rm i}(x_{\mathcal{T}}, \dot{x}_{\mathcal{T}}) - \int_u i\hat{x}_u \left[m\ddot{x}_u + V'(x_u)\right] + \beta\int_u \partial_u \ln P_{\rm i}(x_u, \dot{x}_u) \\ &= S^{\rm det}[x, \hat{x}] \ , \end{aligned}$$

where we used the initial equilibrium measure $\ln P_{\rm i}(x, \dot{x}) = -\beta\left(\frac{1}{2}m\dot{x}^2 + V(x)\right) - \ln \mathcal{Z}$. In the first line we just applied the transformation, in the second line we made the substitution $u \mapsto -u$, in the third line we wrote the last integrand as a total derivative the integral of which cancels the first term and recreates the initial measure at $-\mathcal{T}$.

Secondly, we show that the dissipative contribution is also invariant under $\mathcal{T}_{\rm c}$. We have

$$\begin{aligned} S^{\rm diss}[\mathcal{T}_{\rm c}x, \mathcal{T}_{\rm c}\hat{x}] &= \int_u \left[i\hat{x}_{-u} + \beta\partial_u x_{-u}\right]\int_v \beta^{-1}\,\gamma_{u-v}\, i\hat{x}_{-v} \\ &= \int_u \left[i\hat{x}_u - \beta\dot{x}_u\right]\int_v \gamma_{v-u}\beta^{-1} i\hat{x}_v \\ &= S^{\rm diss}[x, \hat{x}] \ . \end{aligned}$$

In the first line we just applied the transformation, in the second line we made the substitution $u \mapsto -u$ and $v \mapsto -v$ and in the last step we exchanged u and v.

6.5.4 Invariance of the Jacobian (Grassmann variables)

Finally we show that the Jacobian term in the action is invariant once it is expressed in terms of a Gaussian integral over conjugate Grassmann fields (c and c^*) and provided that the transformation $\mathcal{T}_{\rm c}$ is extended to act on these as follows[10]

$$\mathcal{T}_{\rm c} \equiv \left\{ \begin{array}{rcl} x_u & \mapsto & x_{-u} \ , \\ i\hat{x}_u & \mapsto & i\hat{x}_{-u} + \beta\partial_u x_{-u} \ , \end{array} \right. \qquad \left\{ \begin{array}{rcl} c_u & \mapsto & c^*_{-u} \ , \\ c^*_u & \mapsto & -c_{-u} \ . \end{array} \right. \tag{6.18}$$

[10] More generally, the transformation on c and c^* is $c_u \mapsto \alpha\, c^*_{-u}$ and $c^*_u \mapsto -\alpha^{-1}\, c_{-u}$ with $\alpha \in C^*$.

We start from

$$S^{\mathcal{J}}[c,c^*,x] = \int_u \int_v c_u^* \left[m\partial_u^2 \delta_{u-v} + \partial_u \gamma_{u-v} \right] c_v + \int_u c_u^* V''(x_u) c_u \qquad (6.19)$$

and we have

$$\begin{aligned} & S^{\mathcal{J}}(\mathcal{T}_c c, \mathcal{T}_c c^*, \mathcal{T}_c x) \\ & \quad = -\int_u \int_v c_{-u} \left[m\partial_u^2 \delta_{u-v} + \partial_u \gamma_{u-v} \right] c_{-v}^* + \int_u c_{-u} \left[-V''(x_{-u}) \right] c_{-u}^* \\ & \quad = \int_u \int_v c_v^* \left[m\partial_u^2 \delta_{v-u} - \partial_u \gamma_{v-u} \right] c_u + \int_u c_u^* V''(x_u) c_u \\ & \quad = S^{\mathcal{J}}(c,c^*,x) \; . \end{aligned}$$

In the first line we just applied the transformation, in the second line we exchanged the anti-commuting Grassmann variables and made the substitutions $u \mapsto -u$ and $v \mapsto -v$, finally in the last step we used $\partial_v \gamma_{v-u} = -\partial_v \gamma_{u-v}$ and we exchanged u and v. Finally the set of boundary conditions [$c(-\mathcal{T}) = \dot{c}(-\mathcal{T}) = c^*(\mathcal{T}) = \dot{c}^*(\mathcal{T})$] is left invariant.

6.6 Consequences of the transformation

We now use the transformation $\mathcal{T}_c$ to derive a number of exact results.

6.6.1 The fluctuation-dissipation theorem

This symmetry implies

$$\begin{aligned} \langle x_t i\hat{x}_{t'} \rangle_{S[x,i\hat{x}]} &= \langle \mathcal{T}_c x_t \mathcal{T}_c i\hat{x}_{t'} \rangle_{S[\mathcal{T}_c x, \mathcal{T}_c i\hat{x}]} \\ &= \langle x_{-t} i\hat{x}_{-t'} \rangle_{S[x,i\hat{x}]} + \beta \langle x_{-t} d_{t'} x_{-t'} \rangle_{S[x,i\hat{x}]} \end{aligned} \qquad (6.20)$$

that, using time-translational invariance and $\tau \equiv t - t'$, becomes

$$R(\tau) - R(-\tau) = -\beta d_\tau C(-\tau) = -\beta d_\tau C(\tau) \; . \qquad (6.21)$$

For generic observables one can similarly apply the $\mathcal{T}_c$ transformation to expression (6.15) of the linear response

$$R_{AB}(\tau) - R_{A_r B_r}(-\tau) = -\beta d_\tau C_{AB}(-\tau) = -\beta d_\tau C_{AB}(\tau) \; . \qquad (6.22)$$

where we defined A_r and B_r as

$$A_r([x],t) \equiv A([\bar{x}],-t)\ . \tag{6.23}$$

Take for instance a function $A[x(t),t] = \int du f(x(u))\delta(u-t)+\int du f(\dot{x}(u))\delta(u-t)+\int du f(\ddot{x}(u))\delta(u-t)+\ldots$ then $A_r[x(t),t] = A[x(-t),-t] = \int du f(x(-u))\delta(u+t) + \int du f(\dot{x}(-u))\delta(u+t) + \int du f(\ddot{x}(-u))\delta(u+t) + \ldots$.

Relations between higher order correlation functions evaluated at different times $t_1, t_2, \ldots t_n$ are easy to obtain within this formalism.

6.6.2 Fluctuation theorems

Let us assume that the system is initially prepared in thermal equilibrium with respect to the potential $V(x,\lambda_{-\mathcal{T}})$[11]. The expression for the deterministic part of the MSRJD action functional is

$$\begin{aligned} S^{\rm det}[x,\hat{x};\lambda,\mathrm{f}] &= -\beta\mathcal{H}([x_{-\mathcal{T}}],\lambda_{-\mathcal{T}}) - \ln\mathcal{Z}(\lambda_{-\mathcal{T}}) \\ &\quad - \int_u i\hat{x}_u\left[m\ddot{x}_u + V'(x_u,\lambda_u) - \mathrm{f}_u[x]\right]\ , \end{aligned}$$

where $\mathcal{H}([x_t],\lambda_t) \equiv \frac{1}{2}m\dot{x}_t^2 + V(x_t,\lambda_t)$ and f is a non-conservative force applied on the system. The external work done on the system along a given trajectory between times $-\mathcal{T}$ and $\mathcal{T}$ is given by

$$\begin{aligned} W[x;\lambda,\mathrm{f}] &\equiv \int_{u_{\lambda_{\mathcal{T}}}}^{u_{\lambda_{\mathcal{T}}}} dE = \int_{u_{\lambda_{\mathcal{T}}}}^{u_{\lambda_{\mathcal{T}}}} d_u V = \int_{u_{\lambda_{\mathcal{T}}}}^{u_{\lambda_{\mathcal{T}}}} \partial_u\lambda_u\ \partial_\lambda V + \int_u \dot{x}_u\ \partial_x V \\ &= \int_{u_{\lambda_{\mathcal{T}}}}^{u_{\lambda_{\mathcal{T}}}} \partial_{u_{\lambda_{\mathcal{T}}}}^{u_{\lambda_{\mathcal{T}}}}\lambda_u\ \partial_\lambda V(x_u,\lambda_u) + \int_{u_{\lambda_{\mathcal{T}}}}^{u_{\lambda_{\mathcal{T}}}} \dot{x}_u\ \mathrm{f}_u[x] \end{aligned} \tag{6.24}$$

where we take into account the time variation of the parameter λ.

Fluctuation Theorem 1.

The transformation $\mathcal{T}_{\rm c}$ does not leave $S^{\rm det}$ invariant but yields

$$S^{\rm det}[x,\hat{x};\lambda,\mathrm{f}] \xmapsto{\mathcal{T}_{\rm c}} S^{\rm det}[x,\hat{x};\bar{\lambda},\mathrm{f}_{\rm r}] - \beta\Delta\mathcal{F} - \beta W[x;\bar{\lambda},\mathrm{f}_{\rm r}] \tag{6.25}$$

[11] This is in fact a restriction on the initial velocities, $\dot{x}_{-\mathcal{T}}$, that are to be taken from the Maxwell distribution with temperature β^{-1}, independently of the positions $x_{-\mathcal{T}}$. These latter can be chosen from a generic distribution since the initial potential can be tailored at will through the λ dependence of V.

where $S^{\rm det}[x,\hat{x};\bar{\lambda},{\rm f_r}]$ is the MSRJD action of the system that is prepared (in equilibrium) and evolves under the time-reversed protocol ($\bar{\lambda}(u)\equiv\lambda(-u)$) and external forces (${\rm f_r}([x],u)\equiv{\rm f}([\bar{x}],-u)$). $\Delta\mathcal{F}$ is the change in free energy: $\beta\Delta\mathcal{F}=\ln\mathcal{Z}(\lambda(-\mathcal{T}))-\ln\mathcal{Z}(\lambda(\mathcal{T}))$ between the initial and the final 'virtual' equilibrium states. W is defined above. The dissipative part of the action, $S^{\rm diss}$ does not involve λ and it is still invariant under $\mathcal{T}_c$. This means that, contrary to the external forces, the interaction with the bath is not time-reversed: the friction is still dissipative after the transformation. This immediately yields

$$\langle A[x,\hat{x}]\rangle_{S_{\rm c}[x,\hat{x};\lambda,{\rm f}]}=e^{-\beta\Delta\mathcal{F}}\langle A[\mathcal{T}_{\rm c}x,\mathcal{T}_{\rm c}\hat{x}]e^{-\beta W[x;\bar{\lambda},{\rm f_r}]}\rangle_{S_{\rm c}[x,\hat{x};\bar{\lambda},{\rm f_r}]} \tag{6.26}$$

for any functional A of x and $\hat{x}$. In particular for a local functional of the field, $A[x(t)]$, it leads to the Crooks relation

$$\langle A[x(t)]\rangle_{S_{\rm c}[x,\hat{x};\lambda,{\rm f}]}=e^{-\beta\Delta\mathcal{F}}\langle A_{\rm r}[x(-t)]e^{-\beta W[x;\bar{\lambda},{\rm f_r}]}\rangle_{S_{\rm c}[x,\hat{x};\bar{\lambda},{\rm f_r}]}\ , \tag{6.27}$$

or also

$$\begin{aligned}&\langle A[x(t)]B[x(t')]\rangle_{S_{\rm c}[x,\hat{x};\lambda,{\rm f}]}\\ &=e^{-\beta\Delta\mathcal{F}}\langle A_{\rm r}[x(-t)]B_{\rm r}[x(-t')]e^{-\beta W[x;\bar{\lambda},{\rm f_r}]}\rangle_{S_{\rm c}[x,\hat{x};\bar{\lambda},{\rm f_r}]}.\end{aligned} \tag{6.28}$$

Setting $A[x,\hat{x}]=1$, we obtain the Jarzynski equality

$$1=e^{\beta\Delta\mathcal{F}}\langle e^{-\beta W[x;\lambda,{\rm f}]}\rangle_{S_{\rm c}[x,\hat{x};\lambda,{\rm f}]}\ . \tag{6.29}$$

Setting $A[x,\hat{x}]=\delta(W-W[x;\lambda,{\rm f}])$ we obtain the transient fluctuation theorem

$$P(W)=P_{\rm r}(-W)\ e^{\beta(W-\Delta\mathcal{F})}\ , \tag{6.30}$$

where $P(W)$ is the probability for the external work done between $-\mathcal{T}$ and $\mathcal{T}$ to be W given the protocol $\lambda(t)$ and the non-conservative force ${\rm f}([x],t)$. $P_{\rm r}(W)$ is the same probability, given the time-reversed protocol $\bar{\lambda}$ and time-reversed force ${\rm f_r}$.

Fluctuation Theorem 2.

The result we prove in the following lines is not restricted to Langevin processes with an equilibrium dissipative bath. It applies to generic classical equations of motion, with or without stochastic noise. In short, the

proof consists in applying time-reversal on the system and yields an equality between observables and their time-reversed counterparts in a so-called backward (B) process in which the system is prepared in equilibrium with respect to the final conditions of the forward process and is evolved according to the time-reversed equations of motions and protocol. Let us rewrite the action as

$$\begin{aligned} S_{\rm c}[x,\hat{x},\lambda] &= -\beta\mathcal{H}(x_{-\mathcal{T}},\dot{x}_{-\mathcal{T}},\lambda_{-\mathcal{T}}) - \int_u i\hat{x}_u \ {\rm EQ}([x_u],\lambda_u) \\ &\quad + \frac{1}{2}\int_u\int_v i\hat{x}_u \ \beta^{-1}\Gamma_{uv} \ i\hat{x}_v - \ln\mathcal{Z}(\lambda_{-\mathcal{T}}) \ , \end{aligned}$$

and apply the following time-reversal of the fields

$$\mathcal{T}_{\rm tr} \equiv \left\{ \begin{array}{rcl} x_u & \mapsto & x_{-u} \ , \\ i\hat{x}_u & \mapsto & i\hat{x}_{-u} \ . \end{array} \right. \tag{6.31}$$

This yields

$$\begin{aligned} S_{\rm c}[x,\hat{x},\lambda] \ \mapsto \ & -\beta\mathcal{H}([x_{\mathcal{T}}],\bar{\lambda}_{\mathcal{T}}) - \int_u i\hat{x}_u {\rm EQ}_{\rm r}([x_u],\bar{\lambda}_u) \\ & + \frac{1}{2}\int_u\int_v i\hat{x}_u \ \beta^{-1}\Gamma_{uv} \ i\hat{x}_v - \ln\mathcal{Z}(\lambda_{-\mathcal{T}}) \end{aligned}$$

or, by introducing zeroes:

$$\begin{aligned} & -\beta W_{\rm r} - \beta\mathcal{H}([x_{-\mathcal{T}}],\bar{\lambda}_{-\mathcal{T}}) - \int_u i\hat{x}_u {\rm EQ}_{\rm r}([x_u],\bar{\lambda}_u) \\ & \quad + \frac{1}{2}\int_u\int_v i\hat{x}_u \ \beta^{-1}\Gamma_{uv} \ i\hat{x}_v - \beta\Delta\mathcal{F} - \ln\mathcal{Z}(\bar{\lambda}_{-\mathcal{T}}) \ , \end{aligned} \tag{6.32}$$

where $\Delta\mathcal{F} \equiv \mathcal{F}(\lambda_{\mathcal{T}}) - \mathcal{F}(\lambda_{-\mathcal{T}})$ is the free-energy difference between the two 'virtual' equilibrium states corresponding to $\lambda_{\mathcal{T}}$ and $\lambda_{-\mathcal{T}}$. $W_{\rm r} \equiv \mathcal{H}([x_{\mathcal{T}}],\bar{\lambda}_{\mathcal{T}}) - \mathcal{H}([x_{-\mathcal{T}}],\bar{\lambda}_{-\mathcal{T}})$ is the work applied on the system that evolves with the time-reversed equation of motion ${\rm EQ}_{\rm r}$ and under the time-reversed protocol $\bar{\lambda}$. In particular and contrary to the previous paragraph, the friction is no longer dissipative after the transformation. This defines the backward (B) process. Finally, for any observable $A[x,\hat{x}]$ we get the relation

$$\langle A[x,\hat{x}]\rangle_F = e^{-\beta\Delta\mathcal{F}}\langle A[\bar{x},\overline{\hat{x}}]e^{-\beta W_{\rm r}}\rangle_B \ . \tag{6.33}$$

In particular, for two-time correlations, it reads

$$\langle A[x(t)]B[x(t')]\rangle_F = e^{-\beta\Delta\mathcal{F}}\langle A_{\rm r}[x(-t)]B_{\rm r}[x(-t')]e^{-\beta W_{\rm r}}\rangle_B \ . \tag{6.34}$$

Setting $A[x,\hat{x}] = \delta(W - W[x;\lambda,f])$ we obtain the transient fluctuation theorem

$$P_F(W) = P_B(-W)\ e^{\beta(W-\Delta\mathcal{F})}\ , \tag{6.35}$$

where $P_F(W)$ is the probability for the external work done between $-\mathcal{T}$ and $\mathcal{T}$ to be W in the forward process. $P_B(W)$ is the same probability in the backward process.

6.7 Equations on correlations and linear responses

Take any Langevin process in the MSRJD path-integral formalism. From the following four identities

$$\left\langle \frac{\delta i\hat{x}(t)}{\delta i\hat{x}(t')} \right\rangle = \left\langle \frac{\delta x(t)}{\delta x(t')} \right\rangle = \delta(t-t')\ , \qquad \left\langle \frac{\delta x(t)}{\delta i\hat{x}(t')} \right\rangle = \left\langle \frac{\delta i\hat{x}(t)}{\delta x(t')} \right\rangle = 0\ , \tag{6.36}$$

where the angular brackets indicate an average with the MSRJD weight, after an integration by parts, one derives four equations

$$\left\langle x(t)\frac{\delta S}{\delta x(t')} \right\rangle = -\delta(t-t')\ , \qquad \left\langle i\hat{x}(t)\frac{\delta S}{\delta i\hat{x}(t')} \right\rangle = -\delta(t-t')\ , \tag{6.37}$$

$$\left\langle x(t)\frac{\delta S}{\delta i\hat{x}(t')} \right\rangle = 0\ , \qquad \left\langle i\hat{x}(t)\frac{\delta S}{\delta x(t')} \right\rangle = 0\ . \tag{6.38}$$

The second and third one read

$$\begin{aligned} &\left\langle i\hat{x}(t)\left\{m\ddot{x}(t') + \int dt''\ \gamma(t'-t'')\ \dot{x}(t'') + V'[x(t')]\right\}\right\rangle \\ &\qquad\qquad +k_BT\int dt''\ \Gamma(t'-t'')\ \langle i\hat{x}(t)i\hat{x}(t'')\rangle = \delta(t-t')\ , \\ &\left\langle x(t)\left\{m\ddot{x}(t') + \int dt''\ \gamma(t'-t'')\ \dot{x}(t'') + V'[x(t')]\right\}\right\rangle \\ &\qquad\qquad +k_BT\int dt''\ \Gamma(t'-t'')\ \langle x(t)i\hat{x}(t'')\rangle = 0\ , \end{aligned} \tag{6.39}$$

while the other ones, once causality is used (basically $\langle x(t')i\hat{x}(t)\rangle = 0$ for $t > t'$ and $\langle i\hat{x}(t)i\hat{x}(t')\rangle = 0$) do not yield further information. All terms are easily identified with the four types of two-time correlations apart from the ones that involve the potential and are not necessarily quadratic in the fields.

The linear terms in two-time functions can be put together after identifying the **free-operator**

$$G_0^{-1}(t',t'') = \delta(t'-t'')m\frac{d^2}{dt''^2} + \gamma(t'-t'')\frac{\partial}{\partial t''} \tag{6.40}$$

The non-linear terms can be approximated in a number of ways: perturbation theory in a small parameter, Gaussian approximation of the MSRJD action, self-consistent approximations, etc. The choice should be dictated by some knowledge on the system's behaviour one wishes to reproduce. In short then

$$\begin{aligned} 0 &= \int dt'' G_0^{-1}(t',t'')C(t'',t) + \langle x(t)V'[x(t')]\rangle + k_B T\int dt''\Gamma(t'-t'')R(t,t'') \ , \\ \delta(t-t') &= \int dt'' G_0^{-1}(t',t'')R(t'',t) + \langle i\hat{x}(t)V'[x(t')]\rangle \ . \end{aligned} \tag{6.41}$$

6.8 Classical statics: the reduced partition function

In order to analyze the statistical static properties of the classical coupled system, we study the partition function or Gibbs functional, Z_{tot} that reads

$$Z_{tot}[\eta] = \sum_{\substack{conf\ osc \\ conf\ syst}} \exp(-\beta H_{tot} - \beta\eta x) \tag{6.42}$$

where the sum represents an integration over the phase space of the full system, the particle's and the oscillators', and η is a source. Having chosen a quadratic bath and a linear coupling, the integration over the oscillators' coordinates and momenta can be easily performed. This yields the reduced Gibbs functional

$$Z_{red}[\eta] \propto \sum_{conf\ syst} \exp\left[-\beta\left(H_{syst} + H_{counter} + \eta x - \frac{1}{2}\sum_{a=1}^{N_b}\frac{c_a^2}{m_a\omega_a^2}\,x^2\right)\right] \tag{6.43}$$

The 'counterterm' $H_{counter}$ is chosen to cancel the last term in the exponential and it avoids the renormalization of the particle's mass (the coefficient of the quadratic term in the potential) due to the coupling to the environment that could have even destabilize the potential taking negative values. An alternative way of curing this problem would be to take a vanishingly small coupling to the bath in such a way that the last term must vanish by itself (say, all $c_a \to 0$). However, this might be problematic when dealing with the stochastic dynamics since a very weak coupling to the bath implies also a very slow relaxation. It is then conventional to include the counterterm to cancel the mass renormalization. One then finds

$$Z_{red}[\eta] \propto \sum_{conf\ syst} \exp\left[-\beta\left(H_{syst} + \eta x\right)\right] = Z_{syst}[\eta]\ . \tag{6.44}$$

The interaction with the reservoir does not modify the statistical properties of the particle since $Z_{red} \propto Z_{syst}$. We shall see in Sect. 3.7.3 that this does not happen quantum mechanically. (For a non-linear coupling $H_{int} = \sum_\alpha c_\alpha q_\alpha \mathcal{V}(x)$ the counterterm is $H_{counter} = \frac{1}{2}\sum_\alpha \frac{c_\alpha^2}{m_\alpha\omega_\alpha^2}[\mathcal{V}(x)]^2$.)

7 Quantum formalism

We now consider a quantum system

$$[\hat{p}, \hat{x}] = -i\hbar \ . \tag{7.45}$$

The density operator evolves according to the equation

$$\frac{\partial \hat{\rho}(t)}{\partial t} = -\frac{i}{\hbar}[\hat{H}(t), \hat{\rho}(t)] \tag{7.46}$$

that is solved by

$$\hat{\rho}(t) = \hat{U}(t, t_0)\hat{\rho}(t_0)[\hat{U}(t, t_0)]^\dagger = \hat{U}(t, t_0)\hat{\rho}(t_0)\hat{U}(t_0, t) \tag{7.47}$$

with

$$\hat{U}(t, t_0) = T\ e^{-\frac{i}{\hbar}\int_{t_0}^{t} dt' \hat{H}(t')} \qquad\qquad t > t_0 \ . \tag{7.48}$$

Averaged observables read

$$\begin{aligned} \langle \hat{A}(t) \rangle = \frac{\mathrm{Tr}\left\{\hat{A}\ \hat{\rho}(t)\right\}}{\mathrm{Tr}\hat{\rho}(t)} &= \frac{\mathrm{Tr}\left\{\hat{A}\ T\ e^{-\frac{i}{\hbar}\hat{H}t}\ \hat{\rho}_0\ [T\ e^{-\frac{i}{\hbar}\hat{H}t}]^\dagger\right\}}{\mathrm{Tr}\left\{T\ e^{-\frac{i}{\hbar}\hat{H}t}\ \hat{\rho}_0\ [T\ e^{-\frac{i}{\hbar}\hat{H}t}]^\dagger\right\}} \\ &= \frac{\mathrm{Tr}\left\{T\ [e^{-\frac{i}{\hbar}\hat{H}t}]^\dagger\ \hat{A}\ T\ e^{-\frac{i}{\hbar}\hat{H}t}\hat{\rho}_0\right\}}{\mathrm{Tr}\hat{\rho}_0} \ . \end{aligned} \tag{7.49}$$

(To ease the notation we do not write the possible time-dependence in the Hamiltonian and the integral over t in the exponential.) We then use the Heisenberg operators

$$\hat{A}_H(t) \equiv [T\ e^{-\frac{i}{\hbar}\hat{H}t}]^\dagger\ \hat{A}\ T\ e^{-\frac{i}{\hbar}\hat{H}t} \tag{7.50}$$

The under-script H recalls that these are operators in the Heisenberg representation but we shall drop it in the following.

7.1 Equilibrium

7.1.1 Feynman path integral

Feynman's path-integral represents the (forward) propagator $\mathcal{K}(x,t;x',t') = \langle x|e^{-iH(t-t')/\hbar}|x'\rangle$ as a sum over all paths leading from, in the Lagrangain representation, $x' = x(t')$ to $x = x(t)$ with $t > t'$ weighted with the exponential of the action (times $i/\hbar$):

$$\mathcal{K}(x,t;x',t') = \int_{x(t')=x'}^{x(t)=x} \mathcal{D}x\ e^{\frac{i}{\hbar}S[x,\dot{x}]} \tag{7.51}$$

$$S[x,\dot{x}] = \int_{t'}^{t} dt''\ \left\{\frac{m}{2}\dot{x}^2(t'') - V[x(t'')]\right\}\ . \tag{7.52}$$

The formalism is well-suited to compute any type of time-ordered correlation since the evolution is done towards the future. A concise review article on the construction of path-integrals with some applications is [20]; several books on the subject are [21].

7.1.2 The Matsubara imaginary-time formalism

The statistical properties of a canonical quantum system and, in particular, its equilibrium partition function, can also be obtained with the path-integral method,

$$Z = \mathrm{Tr}e^{-\beta H} = \mathrm{Tr}e^{-iH(t=-i\beta\hbar)/\hbar} = \int dx\ \mathcal{K}(x,-i\beta\hbar;x,0)\ . \tag{7.53}$$

Having used an imaginary-time $t = -i\beta\hbar$ corresponds to a Wick-rotation. The propagator $\mathcal{K}$ is now represented as a path-integral with periodic boundary conditions to ensure the fact that one sums over the same initial and finite state. Introducing $\tau = it$, $\tau:\ 0 \to \beta\hbar$ (since $t:\ 0 \to -i\beta\hbar$), defining functions of τ, $\tilde{x}(\tau) = x(t = -i\tau)$ and dropping the tilde one has

$$\mathcal{K}(x,-i\beta\hbar;x,0) = \int_{x(0)=x(\beta\hbar)} \mathcal{D}x\ e^{-\frac{1}{\hbar}S^E[x,\dot{x}]} \tag{7.54}$$

with the Euclidean action

$$S^E[x,\dot{x}] = \int_0^{\beta\hbar} d\tau \left[\frac{m}{2}\dot{x}^2(\tau) + V[x(\tau)]\right]\ . \tag{7.55}$$

7.1.3 The equilibrium reduced density matrix

We now follow the same route as in the derivation of the classical Langevin equation by coupling the system to an ensemble of quantum harmonic oscillators,

$$[\hat{\pi}_a, \hat{q}_b] = -i\hbar\delta_{ab} \ . \tag{7.56}$$

The equilibrium density matrix reads

$$\rho_{tot}(x'', q_a''; x', q'_a) = \frac{1}{Z_{tot}} \langle x'', q_a''| \ e^{-\beta \hat{H}_{tot}} \ |x', q_a'\rangle \ , \tag{7.57}$$

with the partition function given by $Z_{tot} = \mathrm{Tr} e^{-\beta \hat{H}_{tot}}$ and the trace taken over all the states of the full system. As usual the density matrix can be represented by a functional integral in imaginary time,

$$\rho_{tot}(x'', q_a''; x', q'_a; \eta) = \frac{1}{Z_{tot}} \int_{x(0)=x'}^{x(\hbar\beta)=x''} \mathcal{D}x \int_{q_a(0)=q_a'}^{q_a(\hbar\beta)=q_a''} \mathcal{D}q_a \ e^{-\frac{1}{\hbar} S^e_{tot}[\eta]} \ . \tag{7.58}$$

The Euclidean action S^E has contributions from the system, the reservoir, the interaction and the counterterm: $S^E_{tot}[\eta] = S^E_{syst} + S^E_{env} + S^E_{int} + S^E_{counter} + \int_0^{\beta\hbar} d\tau \ \eta(\tau) x(\tau)$ and we have included a source η coupled to the particle's coordinate in order to use it to compute expectation values of the kind defined in (7.49). The environment action is

$$S^E_{env} = \sum_{\alpha=1}^{N} \int_0^{\beta\hbar} d\tau \ \left\{ \frac{m_\alpha}{2} [\dot{q}_\alpha(\tau)]^2 + \frac{m_\alpha \omega_\alpha^2}{2} [q_\alpha(\tau)]^2 \right\} \ , \tag{7.59}$$

that is to say, we choose an ensemble of independent oscillators. For simplicity we take a linear coupling

$$S^E_{int} = \int_0^{\hbar\beta} d\tau \, x(\tau) \sum_{a=1}^{N} c_a q_a(\tau) \tag{7.60}$$

but others, as used in the derivation of the Langevin equation, are also possible. As in the classical case, the path integral over the oscillators' coordinates and positions is quadratic. The calculation of expectation values involves a trace over states of the full system. For operators that depend only on the particle, as $A(\hat{x})$ above, the trace over the oscillators can be done explicitly. Hence, if one constructs the reduced equilibrium density operator $\hat{\rho}_{red} = \mathrm{Tr}_{env} \ \hat{\rho}_{tot}$ that acts on the system's Hilbert space, the expectation value of the observables of the system is given by

$$\langle A(x) \rangle = \frac{\mathrm{Tr}_{syst} \ A(\hat{x}) \hat{\rho}_{red}}{\mathrm{Tr} \hat{\rho}_{tot}} \ . \tag{7.61}$$

In the path-integral formalism this amounts to performing the functional integral over periodic functions $q_\alpha(\tau)$. From the point of view of the oscillators the system's coordinate is an external τ-dependent force. Using a Fourier representation, $q_\alpha(\tau) = \sum_{n=-\infty}^{\infty} q_\alpha^n \; e^{i\nu_n \tau}$ with $\nu_n = \frac{2\pi n}{\beta\hbar}$ the Matsubara frequencies, the integration over the $q_\alpha(\tau)$ can be readily done [22]. A long series of steps, very carefully explained in [19] allow one to obtain the reduced density matrix:

$$\begin{aligned}\rho_{red}(x'', x'; \eta) &= \mathrm{Tr}_{env}\rho_{tot}(x'', q_a''; x', q'_a; \eta) \\ &= \frac{1}{Z_{red}} \int_{x(0)=x'}^{x(\hbar\beta)=x''} \mathcal{D}x \;\; e^{-\frac{1}{\hbar}S^E_{syst} - \frac{1}{\hbar}\int_0^{\hbar\beta} d\tau \int_0^\tau d\tau' \; x(\tau)K(\tau-\tau')x(\tau')}\end{aligned} \tag{7.62}$$

where Z_{red} is the partitition function of the reduced system, $Z_{red} = Z_{tot}/Z_{env}$ and Z_{env} the partition function of the isolated ensemble of oscillators. The interaction with the reservoir generated a renormalization of the mass – cancelled by the counterterm – but also a retarded interaction in the effective action controled by the kernel

$$K(\tau) = \frac{2}{\pi\hbar\beta} \sum_{n=-\infty}^{\infty} \int_0^\infty d\omega \; \frac{S(\omega)}{\omega} \; \frac{\nu_n^2}{\nu_n^2 + \omega^2} \, e^{i\nu_n\tau} \; , \tag{7.63}$$

with $S(\omega)$ the spectral density of the bath, see eq. (4.20) for its definition. The last retarded interaction in (7.62) remains. The imaginary time dependence of K varies according to $S(\omega)$. Power laws in S lead to power-law decays in K and thus to a long-range interaction in the imaginary-time direction.

The effect of the quantum bath is more cumbersome than in the classical case and it can lead to rather spectacular effects. A well-known example is the localization transition, as function of the coupling strength to an Ohmic bath in the behaviour of a quantum particle in a double well potential [39]. This means that quantum tunneling from the well in which the particle is initially located to the other one is completely suppressed by sufficiently strong couplings to the bath. In the context of interacting macroscopic systems, *e.g.* ferromagnets or spin-glasses, the locus of the transition between the ordered and the disordered phase depends strongly on the coupling to the bath and on the type of bath considered [**?**], as discussed in Section **??**.

7.2 Quantum dynamics

We shall see that the distinction between the effect of a reservoir on the statistical properties of a classical and quantum system is absent from a fully dynamic treatment. In both classical and quantum problems, the coupling to an environment leads to a *retarded* interaction. In classical problems one generally argues that the retarded interaction can be simply replaced by a local one due to the very short correlation times involved in cases of interest, *i.e* one uses white baths, but in the quantum problems one cannot do the same.

7.2.1 Schwinger-Keldysh path integral

The Schwinger-Keldysh formalism [44, 45] allows one to analyse the real-time dynamics of a quantum system. The starting point is the time dependent density operator

$$\hat{\rho}(t) = T\ e^{-\frac{i}{\hbar}\hat{H}t}\ \hat{\rho}(0)\ \overline{T}\ e^{\frac{i}{\hbar}\hat{H}t}\ . \tag{7.64}$$

We have set the initial time to be $t_o = 0$. Introducing identities, an element of the time-dependent density matrix reads

$$\begin{aligned}\rho(x'', x'; t) = & \\ \int_{-\infty}^{\infty} dX dX'\ \langle x''|\ T\ e^{-\frac{i}{\hbar}\hat{H}t}\ |X\rangle\ \langle X|\ \hat{\rho}(0)\ |X'\rangle & \\ \times \langle X'|\ \overline{T}\ e^{\frac{i}{\hbar}\hat{H}t}\ |x'\rangle\ . & \end{aligned} \tag{7.65}$$

The first and third factors are the coordinate representation of the evolution operators $e^{-i\hat{H}t/\hbar}$ and $e^{i\hat{H}t/\hbar}$, respectively, and they can be represented as functional integrals:

$$\langle x''|\ T\ e^{-\frac{i}{\hbar}\hat{H}t}\ |X\rangle = \int_X^{x''} \mathcal{D}x^+\ e^{\frac{i}{\hbar}S^+} \tag{7.66}$$

$$\langle X'|\ \overline{T} e^{\frac{i}{\hbar}\hat{H}t}\ |x'\rangle = \int_{x'}^{X'} \mathcal{D}x^-\ e^{-\frac{i}{\hbar}S^-}\ . \tag{7.67}$$

Interestingly enough, the evolution operator in eq. (7.128) gives rise to a path integral going backwards in time, from $x^-(t) = x'$ to $x^-(0) = X'$. The full time-integration can then be interpreted as being closed, going forwards from $t_0 = 0$ to t and then backwards from t to $t_0 = 0$. This motivates the name closed time-path formalism. A doubling of degrees of freedom (x^+, x^-) appeared and it is intimately linked to the introduction of Lagrange

multipliers in the functional representation of the Langevin dynamics in the classical limit, see Sect. 6.2. The action of the system has two terms as in (7.52) one evaluated in x^+ and the other in x^-.

$$S^{\pm}_{syst}[\eta^+] = \pm \int_0^t dt' \left[\frac{m}{2} \left(\dot{x}^{\pm}(t') \right)^2 - V(x^{\pm}(t')) + \eta^{\pm}(t') x^{\pm}(t') \right] \tag{7.68}$$

where we have introduced two time-dependent sources $\eta^{\pm}(t)$, that appear in the exponential with the sign indeicated.

7.2.2 Green functions

We define the position and fermionic Green functions

$$G^B_{ab}(t,t') \equiv -i\langle T_C \; x_a(t) x_b(t') \rangle \tag{7.69}$$
$$G^F_{ab}(t,t') \equiv -i\langle T_C \; \psi_a(t) \psi^\dagger_b(t') \rangle \tag{7.70}$$

where $a, b = \pm$ and T_C is time ordering on the close contour (see App. 8).

The definitions (7.69) and (7.70) and the fact that the insertion evaluated at the later time can be put on the upper $(+)$ or lower $(-)$ branch indistinctively *** GIVE EXAMPLE WITH DRAWING *** yield the following relations between different Green functions

$$G_{++}(t,t') = G_{-+}(t,t')\theta(t-t') + G_{+-}(t,t')\theta(t'-t) \; , \tag{7.71}$$
$$G_{--}(t,t') = G_{+-}(t,t')\theta(t-t') + G_{-+}(t,t')\theta(t'-t) \; , \tag{7.72}$$

that hold for the bosonic and fermionic cases as well. We thus erase the superscripts B, F that become superflous. Adding the last two identities one finds

$$G_{++} + G_{--} - G_{+-} - G_{-+} = 0 \qquad \text{for all } t \text{ and } t' \; . \tag{7.73}$$

In both cases one defines MSRDJ-like fields. For bosons these are

$$\sqrt{2}\, x(t) = x_+(t) + x_-(t) \; , \qquad \sqrt{2\hbar}\, \hat{x}(t) = x_+(t) - x_-(t) \; , \tag{7.74}$$

while for fermions they are

$$\sqrt{2}\, \psi(t) \equiv \psi^+(t) + \psi^-(t) \qquad \sqrt{2\hbar}\, \hat{\psi}(t) \equiv \psi^+(t) - \psi^-(t)$$
$$\sqrt{2}\, \psi^\dagger(t) \equiv \psi^{+\dagger}(t) + \psi^{-\dagger}(t) \qquad \sqrt{2\hbar}\, \hat{\psi}^\dagger(t) \equiv \psi^{+\dagger}(t) - \psi^{-\dagger}(t) \; .$$

One then constructs the Green functions

$$\begin{aligned}
G^B_{xx}(t,t') &\equiv -i\langle T_C\ x(t)x(t')\rangle = \frac{1}{2}\left(G^B_{++}+G^B_{--}+G^B_{-+}+G^B_{+-}\right)\\
&\equiv -2i\ G^B_K(t,t')\\
G^B_{x\hat{x}}(t,t') &\equiv -i\langle T_C\ x(t)\hat{x}(t')\rangle = \frac{1}{2\hbar}\left(G^B_{++}-G^B_{--}+G^B_{-+}-G^B_{+-}\right)\\
&\equiv -G^B_R(t,t')\\
G^B_{\hat{x}x}(t,t') &\equiv -i\langle T_C\ \hat{x}(t)x(t')\rangle = \frac{1}{2\hbar}\left(G^B_{++}-G^B_{--}-G^B_{-+}+G^B_{+-}\right)\\
&\equiv -\ G^B_A(t,t')\\
G^B_{\hat{x}\hat{x}}(t,t') &\equiv -i\langle T_C\ \hat{x}(t)\hat{x}(t')\rangle = \frac{1}{2\hbar^2}\left(G^B_{++}+G^B_{--}-G^B_{-+}-G^B_{+-}\right)\\
&\equiv -\ G^B_4(t,t')=0\ , \qquad (7.75)
\end{aligned}$$

and the fermionic ones

$$\begin{aligned}
G^F_{\psi\psi}(t,t') &\equiv -i\langle T_C\ \psi(t)\psi^\dagger(t')\rangle = \frac{1}{2}\left(G^F_{++}+G^F_{--}+G^F_{-+}+G^F_{+-}\right)\\
&\equiv -2iG^F_K(t,t')\ ,\\
G^F_{\psi\hat{\psi}}(t,t') &\equiv -i\langle T_C\ \psi(t)\hat{\psi}^\dagger(t')\rangle = \frac{1}{2\hbar}\left(G^F_{++}-G^F_{--}+G^F_{-+}-G^F_{+-}\right)\\
&\equiv -G^F_R(t,t')\ ,\\
G_{\hat{\psi}\psi}(t,t') &\equiv -i\langle T_C\ \hat{\psi}(t)\psi^\dagger(t')\rangle = \frac{1}{2\hbar}\left(G^F_{++}-G^F_{--}-G^F_{-+}+G^F_{+-}\right)\\
&\equiv -G^F_A(t,t')\ ,\\
G^F_{\hat{\psi}\hat{\psi}}(t,t') &\equiv -i\langle T_C\ \hat{\psi}(t)\hat{\psi}^\dagger(t')\rangle = \frac{1}{2\hbar^2}\left(G^F_{++}+G^F_{--}-G^F_{-+}-G^F_{+-}\right)\\
&\equiv -G^F_4(t,t')=0\ , \qquad (7.76)
\end{aligned}$$

From the definition of G^B_K it is obvious that

$$G^B_K(t,t') = G^B_K(t',t) \quad \in \text{ Re}\ . \qquad (7.77)$$

Using eq. (7.73) the 'rotated' Green functions are rewritten as

$$G_K = \frac{i}{2}(G_{++}+G_{--}) = \frac{i}{2}(G_{+-}+G_{-+})\ , \qquad (7.78)$$

$$G_R = -\frac{1}{\hbar}(G_{++}-G_{+-}) = \frac{1}{\hbar}(G_{--}-G_{-+})\ , \qquad (7.79)$$

$$G_A = -\frac{1}{\hbar}(G_{++}-G_{-+}) = \frac{1}{\hbar}(G_{--}-G_{+-})\ . \qquad (7.80)$$

Using eqs. (7.71)-(7.72) one also finds

$$G_R(t,t') = -\frac{1}{\hbar}[G_{+-}(t,t') - G_{-+}(t,t')]\ \theta(t-t')\ , \tag{7.81}$$

$$G_A(t,t') = \frac{1}{\hbar}[G_{+-}(t,t') - G_{-+}(t,t')]\ \theta(t'-t)\ . \tag{7.82}$$

which show explicitly the retarded and advanced character of G_R and G_A, respectively. Moreover,

$$G^B_R(t,t') = G^B_A(t't) \ \in \ \mathrm{Re}\ , \tag{7.83}$$

$$G^F_R(t,t') = [G^F_A(t',t)]^*\ , \tag{7.84}$$

$$G^F_K(t,t') = [G^F_K(t',t)]^*\ .\ . \tag{7.85}$$

Inverting the above relations one has

$$\begin{array}{ll} iG_{++} = G_K - i\hbar(G_R+G_A)/2\ , & iG_{+-} = G_K + i\hbar(G_R-G_A)/2\ , \\ iG_{-+} = G_K - i\hbar(G_R-G_A)/2\ , & iG_{--} = G_K + i\hbar(G_R+G_A)/2\ . \end{array} \tag{7.86}$$

Going back to an operational formalism

$$G^B_R(t,t') \ \equiv \ \frac{2i}{\hbar}\theta(t-t')\ \langle[\hat{x}(t),\hat{x}(t')]\rangle\ , \tag{7.87}$$

$$G^B_K(t,t') \ \equiv \ \langle\{\hat{x}(t),\hat{x}(t')\}\rangle\ , \tag{7.88}$$

for bosons (see App. 8), where one recognizes the Kubo formulæ in the first two lines, and

$$G^F_R(t,t') \ \equiv \ \frac{2i}{\hbar}\theta(t-t')\ \langle\{\hat{\psi}(t),\hat{\psi}^\dagger(t')\}\rangle\ , \tag{7.89}$$

$$G^F_K(t,t') \ \equiv \ \langle[\hat{\psi}(t),\hat{\psi}^\dagger(t')]\rangle\ , \tag{7.90}$$

for fermions.

7.2.3 Generic correlations

A generic two time correlation that depends only on the system is given by

$$\langle\hat{A}(t)\hat{B}(t')\rangle = Z^{-1}_{red}(0)\ \mathrm{Tr}\hat{A}(t)\hat{B}(t')\hat{\rho}_{red}(0)\ . \tag{7.91}$$

Clearly $\langle \hat{A}(t)\hat{B}(t')\rangle \neq \langle \hat{B}(t')\hat{A}(t)\rangle$ and one can define symmetrized and anti-symmetrized correlations:

$$C_{\{A,B\}}(t,t') = \langle \hat{A}(t)\hat{B}(t') + \hat{B}(t')\hat{A}(t)\rangle/2 \,, \tag{7.92}$$
$$C_{[A,B]}(t,t') = \langle \hat{A}(t)\hat{B}(t') - \hat{B}(t')\hat{A}(t)\rangle/2 \,, \tag{7.93}$$

respectively.

Within the Keldysh path-integral representation these correlations can be written as

$$\begin{aligned} C_{\{A,B\}}(t,t') &= \langle A[x^+](t)\{B[x^+](t') + B[x^-](t')\}\rangle/2 \,, \\ C_{[A,B]}(t,t') &= \langle A[x^+](t)\{B[x^+](t') - B[x^-](t')\}\rangle/2 \,, \end{aligned} \tag{7.94}$$

7.2.4 Linear response and Kubo relation

The linear response is defined as the variation of the averaged observable A at time t due to a change in the Hamiltonian operated at time t' in such a way that $\hat{H} \to \hat{H} - f_B\hat{B}$. In linear-response theory, it can be expressed in terms of the averaged commutator:

$$R_{AB}(t,t') \equiv \left.\frac{\delta\langle \hat{A}(t)\rangle}{\delta f_B(t')}\right|_{f_B=0} = \frac{2i}{\hbar}\theta(t-t')\langle[\hat{A}(t),\hat{B}(t')]\rangle \,. \tag{7.95}$$

In the case $\hat{A} = \hat{x}$ and $\hat{B} = \hat{x}$ this implies $R_{xx}(t,t') = G^B_R(t,t')$. The path-integral representation is in terms of the Keldysh fields x^+, x^-:

$$R_{AB}(t,t') = i\langle A[x^+](t)\,\Big\{B[x^+](t') - B[x^-](t')\Big\}\rangle/\hbar \,. \tag{7.96}$$

7.2.5 Quantum FDT

Proofs and descriptions of the quantum FDT can be found in several textbooks [32, 46]. We first present a standard derivation that applies to bosonic and fermionic Green functions in the canonical and grand-canonical ensembles. We next show it for generic correlations and linear responses in the bosonic case. In so doing we recall its expression in the time-domain and in a mixed time-Fourier notation that gave us insight as to how to extend it to the case of glassy non-equilibrium dynamics [33].

Canonical ensemble

Let us consider the canonical ensemble and let us write

$$iG_{+-}(t,t') = \langle T_C\ \phi^+(t)\phi^-(t')\rangle \tag{7.97}$$

where $\phi^+ = x^+$ and $\phi^- = x^-$ (bosons) or $\phi^+ = \psi^+$ and $\phi^- = \psi^{-\dagger}$ (fermions). This is equal to

$$iG_{+-}(t,t') = (-1)^\zeta\ \langle \phi^-(t')\phi^+(t)\rangle \tag{7.98}$$

with $\zeta = 1$ for fermions and $\zeta = 0$ for bosons. Using the analytic properties of Green functions, we have

$$iG_{+-}(t+i\beta\hbar,t') = (-1)^\zeta\ \langle \phi^-(t')\phi^+(t+i\beta\hbar)\rangle\ . \tag{7.99}$$

In the canonical ensemble, $\langle\cdots\rangle \propto \mathrm{Tr}\cdots\rho_0 \propto \mathrm{Tr}\cdots e^{-\beta H}$ and after expanding $\phi^+(t+i\beta\hbar) = \rho_0\phi^+(t)\rho_0^{-1}$ (in the Heisenberg representation) we get

$$iG_{+-}(t+i\beta\hbar,t') = (-1)^\zeta\ \frac{\mathrm{Tr}\left[\phi^-(t')\rho_0\phi^+(t)\right]}{\mathrm{Tr}\rho_0}\ . \tag{7.100}$$

Using the cyclic property of the trace

$$iG_{+-}(t+i\beta\hbar,t') = (-1)^\zeta\langle\phi^+(t)\phi^-(t')\rangle \tag{7.101}$$

and we recognize

$$G_{+-}(t+i\beta\hbar,t') = (-1)^\zeta\ G_{-+}(t,t') \tag{7.102}$$

If the systen has reached equilibrium, time translational invariance implies

$$G_{+-}(t-t'+i\beta\hbar) = (-1)^\zeta\ G_{-+}(t-t')\ . \tag{7.103}$$

After Fourier transforming with respect to $t-t'$ we get the KMS relation

$$G_{+-}(\omega)e^{\beta\hbar\omega} = (-1)^\zeta\ G_{-+}(\omega)\ . \tag{7.104}$$

Using eqs. (7.86), we have on the one hand

$$\hbar[G_R(\omega) - G_A(\omega)] = G_{+-}(\omega) - G_{-+}(\omega)\ . \tag{7.105}$$

Inserting the KMS relation (7.104) we get

$$\hbar[G_R(\omega) - G_A(\omega)] = G_{+-}(\omega)[1-(-1)^\zeta e^{\beta\hbar\omega}] \tag{7.106}$$

On the other hand,

$$G_K(\omega) \;=\; \frac{i}{2}[G_{+-}(\omega)+G_{-+}(\omega)] = \frac{i}{2}G_{+-}(\omega)[1+(-1)^{\zeta}e^{\beta\hbar\omega}] \;. \quad (7.107)$$

Combining this relation with eq. (7.104) we obtain the quantum FDTs

$$\boxed{G_K(\omega) = \frac{i\hbar}{2}\,[G_R(\omega)-G_A(\omega)]\left[\frac{1+(-1)^{\zeta}e^{\beta\hbar\omega}}{1-(-1)^{\zeta}e^{\beta\hbar\omega}}\right]} \quad (7.108)$$

Using $G_R(\omega)-G_A(\omega) = R(\omega)-R^*(\omega) = 2i\mathrm{Im}G_R(\omega)$ for bosons and fermions:

$$G_K^F(\omega) = -\frac{i\hbar}{2}\,[G_R^F(\omega)-G_A^F(\omega)]\;\tanh\frac{\beta\hbar\omega}{2} \quad (7.109)$$

$$\boxed{G_K^F(\omega) = \hbar\;\mathrm{Im}G_R^F(\omega)\;\tanh\tfrac{\beta\hbar\omega}{2}\;,} \quad (7.110)$$

$$G_K^B(\omega) \;=\; -\frac{i\hbar}{2}\,[G_R^B(\omega)-G_A^B(\omega)]\;\mathrm{cotanh}\frac{\beta\hbar\omega}{2} \quad (7.111)$$

$$\boxed{G_K^B(\omega) = \hbar\;\mathrm{Im}G_R^B(\omega)\;\mathrm{cotanh}\tfrac{\beta\hbar\omega}{2}\;.} \quad (7.112)$$

In the case of bosons the FDT can be easily extended to

$$C_{\{A,B\}}(\omega) = \hbar\;\mathrm{Im}R_{AB}^B(\omega)\;\mathrm{cotanh}\frac{\beta\hbar\omega}{2}\;. \quad (7.113)$$

Grand canonical ensemble

In the grand-canonical ensemble, the proof remains essentially the same. The initial density operator reads $\hat{\rho}_0 \propto e^{-\beta\hat{H}+\beta\mu\hat{N}}$, where $\hat{N}$ is the number operator which commutes with $\hat{H}$ (the number of particules is conserved in non-relativistic quantum mechanics). For concreteness, let us focus on fermions The three first steps in the proof presented above imply

$$G_{+-}^F(t+i\beta\hbar,t') = -\mathrm{Tr}\left[\hat{\psi}^{-\dagger}(t')e^{-\beta\hat{H}}\hat{\psi}^{+}(t)e^{\beta\mu\hat{N}}\right]/\mathrm{tr}\hat{\rho}_0 \quad (7.114)$$

Since $\hat{H}$ and $\hat{N}$ commute and since for any operator $f(\hat{N})$, one has the property that $\hat{\psi} f(\hat{N}) = f(\hat{N}+1)\hat{\psi}$, we have

$$\hat{\psi}^+(t) e^{\beta\mu\hat{N}} = e^{\beta\mu(\hat{N}+1)} \hat{\psi}^+(t) \tag{7.115}$$

and so

$$G^F_{+-}(t + i\beta\hbar, t') = -e^{\beta\mu} \, \mathrm{Tr}\left[\psi^{-\dagger}(t')\rho_0\psi^+(t)\right] / \mathrm{Tr}\rho_0 \, . \tag{7.116}$$

At this point, we can follow the same steps as in the proof for the canonical ensemble, namely use the cyclic property of the trace, time-translational invariance and a Fourier transform, to obtain the fermionic KMS relation in the grand-canonical ensemble

$$G^F_{+-}(\omega) e^{\beta\hbar\omega} = -e^{\beta\mu} G^F_{-+}(\omega) \, . \tag{7.117}$$

and the grand-canonical fermionic quantum FDT relation

$$G^F_K(\omega) = -\frac{i\hbar}{2}[G^F_R(\omega) - G^F_A(\omega)] \tanh\left(\beta\frac{\hbar\omega - \mu}{2}\right) \tag{7.118}$$

or, equivalently

$$\boxed{G^F_K(\omega) = \hbar \, \mathrm{Im}R(\omega) \, \tanh\left(\beta\tfrac{\hbar\omega-\mu}{2}\right)} \tag{7.119}$$

FDT for Generic observables in time-domain

If at time t' the system is characterized by a density functional $\rho(t')$, the two-time correlation functions are given by eq. (7.91), (7.92) and (7.93). In linear response theory $R_{AB}(t,t')$ and the correlation $C_{[A,B]}(t,t')$ are related by the Kubo formula (7.95). If the system has reached equilibrium with a heat-bath at temperature T at time t', the density functional $\rho_{syst}(t')$ is just the Boltzmann factor $\exp(-\beta H_{syst})/Z_{syst}$. It is then immediate to show that, in equilibrium, time-translation invariance, $C_{AB}(t,t') = C_{AB}(t-t')$, and the KMS properties

$$C_{AB}(t,t') \;\; = \;\; C_{BA}(t', t + i\beta\hbar) = C_{BA}(-t - i\beta\hbar, -t') \tag{7.120}$$

hold. Using now these identities and assuming, for definiteness, that $t > 0$ it is easy to verify the following equation

$$C_{\{A,B\}}(\mathcal{T}) + \frac{i\hbar}{2} R_{AB}(\mathcal{T}) = C_{\{A,B\}}(\mathcal{T}^*) - \frac{i\hbar}{2} R_{AB}(\mathcal{T}^*) \, , \tag{7.121}$$

where $\mathcal{T} = t + i\beta\hbar/2$. This is a way to express FDT through an analytic continuation to complex times.

In terms of the Fourier transform defined in App. **??** the KMS relations read $C_{AB}(\omega) = \exp(-\beta\hbar\omega) C_{BA}(-\omega)$ and lead to $2C_{[A,B]}(\omega) = \left(1 - e^{\beta\hbar\omega}\right) C_{AB}(\omega)$, $2C_{\{A,B\}}(\omega) = \left(1 + e^{\beta\hbar\omega}\right) C_{AB}(\omega)$ and $C_{[A,B]}(\omega) = -\tanh(\beta\hbar\omega/2)\, C_{\{A,B\}}(\omega)$. Back in the Kubo relation this implies

$$\boxed{R_{AB}(t-t') = -\tfrac{i}{\hbar}\,\theta(t-t') \int_{-\infty}^{\infty} \tfrac{d\omega}{\pi}\, e^{i\omega(t-t')}\, \tanh(\beta\hbar\omega/2)\, C_{\{A,B\}}(\omega)} \quad (7.122)$$

(recall $C_{\{A,B\}}(\omega) = C_{\{A,B\}}(-\omega)$.) Using $\int_0^\infty dt\, \exp(-i\omega t) = \lim_{\epsilon\to 0^+} \frac{i}{-\omega + i\epsilon} = \pi\delta(\omega) - i\frac{P}{\omega}$ one has

$$R_{AB}(\omega) = -\frac{1}{\hbar} \lim_{\epsilon\to 0^+} \int_{-\infty}^{\infty} \frac{d\omega'}{\pi}\, \frac{1}{\omega - \omega' + i\epsilon}\, \tanh\frac{\beta\hbar\omega'}{2}\, C_{\{A,B\}}(\omega') \quad (7.123)$$

from which we obtain the real and imaginary relations

$$\begin{aligned} \mathrm{Im}R_{AB}(\omega) &= \frac{1}{\hbar}\, \tanh\frac{\beta\hbar\omega}{2}\, C_{\{A,B\}}(\omega')\,, \\ \mathrm{Re}R_{AB}(\omega) &= -\frac{1}{\hbar}\, P \int_{-\infty}^{\infty} \frac{d\omega'}{\pi}\, \frac{1}{\omega - \omega'}\, \tanh\left(\frac{\beta\hbar\omega'}{2}\right) C_{\{A,B\}}(\omega') \end{aligned} \quad (7.124)$$

If $\beta\hbar\omega/2 \ll 1$, $\tanh(\beta\hbar\omega/2) \sim \beta\hbar\omega/2$ and eq. (7.122) becomes the classical FDT:

$$R_{AB}(t-t') = -\frac{1}{k_B T} \frac{dC_{AB}(t-t')}{dt}\, \theta(t-t')\,. \quad (7.125)$$

7.2.6 The influence functional

As in the derivation of the Langevin equation we model the environment as an ensemble of many non-interaction variables that couple to the relevant system's degrees of freedom in some convenient linear way. The choice of the environment variables depends on the type of bath one intends to consider. Phonons are typically modeled by independent quantum harmonic oscillators that can be dealt with exactly. We then consider a system $(\hat{x}, \hat{p})$ coupled to an environment made of independent harmonic oscillators $(\hat{q}_a, \hat{\pi}_a)$. An element of the total density function reads

$$\begin{aligned} &\rho(x'', q''_a; x', q'_a; t) = \\ &\int_{-\infty}^{\infty} dX dX' dQ_a dQ'_a\, \langle x'', q''_a|\, T\, e^{-\frac{i}{\hbar}\hat{H}_{tot}t}\, |X, Q_a\rangle\, \langle X, Q_a|\, \hat{\rho}_{tot}(0)\, |X', Q'_a\rangle \\ &\qquad \times \langle X', Q'_a|\, \overline{T}\, e^{\frac{i}{\hbar}\hat{H}_{tot}t}\, |x', q'_a\rangle\,. \end{aligned} \quad (7.126)$$

The first and third factors are the coordinate representation of the evolution operators $e^{-i\hat{H}_{tot}t/\hbar}$ and $e^{i\hat{H}_{tot}t/\hbar}$, respectively, and they can be represented as functional integrals:

$$\langle x'', q_a''|\, T\; e^{-\frac{i}{\hbar}\hat{H}_{tot}t}\,|X, Q_a\rangle \;=\; \int_X^{x''} \mathcal{D}x^+ \int_{Q_a}^{q_a''} \mathcal{D}q_a^+\; e^{\frac{i}{\hbar}S_{tot}^+} \tag{7.127}$$

$$\langle X', Q_a'|\, \overline{T} e^{\frac{i}{\hbar}\hat{H}_{tot}t}\,|x', q_a'\rangle \;=\; \int_{x'}^{X'} \mathcal{D}x^- \int_{q_a'}^{Q_a'} \mathcal{D}q_a^-\; e^{-\frac{i}{\hbar}S_{tot}^-}\,. \tag{7.128}$$

The action S_{tot} has the usual four contributions, from the system, the reservoir, the interaction and the counterterm.

As usual we are interested in the dynamics of the system under the effect of the reservoir. Hence, we compute the reduced density matrix

$$\rho_{red}(x'', x'; t) = \int_{-\infty}^{\infty} dq_a\; \langle x'', q_a|\, \hat{\rho}_{tot}(t)\,|x', q_a\rangle\;. \tag{7.129}$$

7.2.7 Initial conditions

Factorization

The initial density operator $\hat{\rho}_{tot}(0)$ has the information about the initial state of the whole system. If one assumes that the system and the bath are set in contact at the initial time, the operator factorizes

$$\hat{\rho}(0) = \hat{\rho}_{syst}(0)\hat{\rho}_{env}(0)\;. \tag{7.130}$$

(Other initial preparations, where the factorization does not hold, can also be considered and may be more realistic in certain cases [19] and see below.) If the environment is initially in equilibrium at an inverse temperature β,

$$\hat{\rho}_{env}(0) = Z_{env}^{-1}\; e^{-\beta\hat{H}_{env}}\;, \tag{7.131}$$

the dependence on the bath variables is quadratic; they can be traced away to yield the reduced density matrix:

$$\begin{aligned}\rho_{red}(x'', x'; t) \;=\; & \int_{-\infty}^{\infty} dX \int_{-\infty}^{\infty} dX' \int_{x^+(0)=X}^{x^+(t)=x''} \mathcal{D}x^+ \int_{x^-(0)=X'}^{x^-(t)=x'} \mathcal{D}x^- \\ & \times e^{\frac{i}{\hbar}S_{eff}}\; \langle X|\, \hat{\rho}_{syst}(0)\,|X'\rangle\end{aligned} \tag{7.132}$$

with the effective action $S_{eff} = S^+_{syst} - S^-_{syst} + S_{env\,eff}$. The last term has been generated by the interaction with the environment and it reads [19]

$$\frac{i}{\hbar}S_{env} = -i\int_0^{\mathcal{T}} dt' \int_0^{\mathcal{T}} dt''\ \frac{[x^+(t') - x^-(t')]}{\hbar}\ 4\eta(t'-t'')\ \frac{[x^+(t'') + x^-(t'')]}{2}$$
$$-\int_0^{\mathcal{T}} dt' \int_0^{\mathcal{T}} dt''\ \frac{[x^+(t') - x^-(t')]}{\hbar}\ \hbar\nu(t'-t'')\ \frac{[x^+(t'') - x^-(t'')]}{\hbar}\ . \quad (7.133)$$

The noise and dissipative kernels ν and η are given by

$$\nu(t) = \int_0^\infty d\omega\ S(\omega)\ \coth\left(\frac{1}{2}\beta\hbar\omega\right)\ \cos(\omega t)\ , \quad (7.134)$$

$$\eta(t) = \theta(t)\frac{d\Gamma(t)}{dt} = -\theta(t)\int_0^\infty d\omega\ S(\omega)\ \sin(\omega t)\ . \quad (7.135)$$

One can easily check that $\nu(t) = \nu(-t)$ and $\eta(t)$ is causal; moreover they verify the bosonic FDT, as they should since the bath was assumed to be in equilibrium. η is like a response and ν is a correlation One can also write the bath-generated action in the form

$$S_{\rm K,eff} \equiv -\sum_{a,b=\pm}\frac{1}{2}\int\int dtdt'\ x^a(t)\Sigma_{ab}(t,t')x^b(t')\,, \quad (7.136)$$

with

$$\Sigma_{++} = 2\eta - i\nu \quad \Sigma_{+-} = 2\eta + i\nu\ , \quad (7.137)$$

$$\Sigma_{-+} = -2\eta + i\nu \quad \Sigma_{--} = -2\eta - i\nu \quad (7.138)$$

and $\Sigma_{++} + \Sigma_{--} + \Sigma_{+-} + \Sigma_{-+} = 0$. Although these relation resemble the ones satisfied by the G_{ab}s a more careful analysis shows that the matricial Σ is more like G^{-1} than G (see the discussion on the classical dynamics of the random manifold and the dependence on k; the relation between G and Σ is the same here).

In these equations, as in the classical case, $S(\omega)$ is the spectral density of the bath:

$$S(\omega) = \frac{\pi}{2}\sum_{a=1}^{N_b}\frac{c_a^2}{m_a\omega_a}\delta(\omega-\omega_a)\ , \quad (7.139)$$

that can also be taken of the form in (4.20),

$$S(\omega) = 2\gamma_0\tilde{\omega}\ \left(\frac{\omega}{\tilde{\omega}}\right)^\alpha\ e^{-\omega/\Lambda}\ . \quad (7.140)$$

Figure 28: The kernel ν in the Ohmic $\alpha = 1$ case for different values of T ($\Lambda = 5$).

Figure 29: The kernel ν at $T = 0$ for different values of α ($\hbar = 1 = \gamma_0 = \tilde{\omega} = 1$ and $\Lambda = 5$) in linear (left) and logarithmic (right) scales.

As usual, a counterterm cancels the mass renormalization. The η and Γ kernels are independent of T and $\hbar$ and are thus identical to the classical ones, see eq. (4.21).The kernel ν does depend on T and $\hbar$. After a change of variables in the integral, in the cases in which $S(\omega) \propto \omega^{\alpha}$,

$$\nu(t) = t^{-(1+\alpha)} g\left(\frac{\beta\hbar}{t}, \Lambda t\right) \tag{7.141}$$

and

$$\lim_{\beta\hbar/t \to 0} \beta\hbar\nu(t) = 2\Gamma(t) \; . \tag{7.142}$$

The classical limit is realized at high temperature and/or long times.

Figure 29-left shows the time-dependence of the kernels ν in the quantum Ohmic case for different values of T. In the right panel of the same figure we show the dependence on α of the kernel ν.

Upper critical initial conditions for the system

Next, we have to choose an initial density matrix for the system. One natural choice, having in mind the quenching experiments usually performed in classical system, is the diagonal density matrix

$$\langle X| \, \hat{\rho}_{syst}(0) \, |X'\rangle = \delta(X - X') \tag{7.143}$$

that corresponds to a random 'high-temperature' situation and that simplifies considerably the expression in (7.132). As in the classical stochastic problem, $\mathrm{Tr}\hat{\rho}_{red}(0) = 1$ and it is trivially independent of disorder. Hence, there is no need to introduce replicas in such a quantum dynamic calculation.

Equilibrium initial conditions for the system

One might also be interested in using equilibrium initial conditions for the isolated system

$$\langle X| \, \hat{\rho}_{syst}(0) \, |X'\rangle = Z_{sys}^{-1} \langle X| \, e^{-\beta H_{syst}} \, |X'\rangle \; . \tag{7.144}$$

This factor introduces interesting real-time – imaginary-time correlations.

7.2.8 Transformation to 'MSR-like fields'

Newton dynamics

We use $x_\pm = x \pm (\hbar/2)\,\hat{x}$. We first study the kinetic terms:

$$\frac{i}{\hbar}\int dt\,\frac{m}{2}\left(\dot{x}_+^2 - \dot{x}_-^2\right) \;=\; \frac{i}{\hbar}\int dt\,\frac{m}{2}\left[\left(\dot{x}+\frac{\hbar}{2}\dot{\hat{x}}\right)^2 - \left(\dot{x}-\frac{\hbar}{2}\dot{\hat{x}}\right)^2\right] \tag{7.145}$$

expanding the squares the integrand equals $-2\hbar\,\dot{\hat{x}}\dot{x}$ and integrating by parts

$$-\int dt\; i\hat{x}\; m\ddot{x}\;. \tag{7.146}$$

The potential term

The potential term is treated similarly

$$-\frac{i}{\hbar}\left[V(x_+) - V(x_-)\right] \;=\; -\frac{i}{\hbar}\left[V\left(x+\frac{\hbar}{2}\hat{x}\right) - V\left(x-\frac{\hbar}{2}\hat{x}\right)\right] \tag{7.147}$$

Note that this expression is specially simple for quadratic and quartic potentials:

$$= \begin{cases} -xi\hat{x} & \text{quadratic} \qquad V(y) = y^2 \\ -4xi\hat{x}\left[x^2 - \phi_0^2 + \left(\frac{\hbar}{2}\right)^2 (i\hat{x})^2\right] & \text{quartic} \qquad V(y) = (y^2 - y_0^2)^2 \end{cases}$$

The noise terms

We introduce the variables x and $i\hat{x}$ in the action terms generated by the coupling to the environment and the classical limit of the kernel ν:

$$\begin{aligned} \frac{i}{\hbar}\,S_{env} \;&=\; -\int_0^{\mathcal{T}} dt' \int_0^{\mathcal{T}} dt''\; i\hat{x}(t')\; 2\theta(t'-t'')\frac{d\Gamma(t'-t'')}{dt'}\; 2x(t'') \\ &\quad + \int_0^{\mathcal{T}} dt' \int_0^{\mathcal{T}} dt''\; i\hat{x}(t')\hbar\nu(t'-t'')i\hat{x}(t'') \\ &=\; 4\int_0^{\mathcal{T}} dt' \int_0^{\mathcal{T}} dt''\; i\hat{x}(t')\;\gamma(t'-t'')\;\dot{x}(t'') \\ &\quad + \int_0^{\mathcal{T}} dt' \int_0^{\mathcal{T}} dt''\; i\hat{x}(t')\hbar\nu(t'-t'')i\hat{x}(t'')\;. \end{aligned} \tag{7.148}$$

(Apart from a border term that can be treated more carefully and check that it disappears.)

7.2.9 Classical limit

In the classical limit, $\hbar \to 0$, the Schwinger-Keldysh effective action reduces to the one in the functional representation of a Newton classical mechanics (no bath) or a Langevin process with coloured noise (bath). The kinetic term eq. (7.146) is already in the expected form with no nead to take $\hbar \to 0$. The potential term

$$-\frac{i}{\hbar}\left[V(x_+) - V(x_-)\right] = -V'(x) i\hat{x} + O(\hbar^2) \;\simeq\; -V'(x) i\hat{x} \tag{7.149}$$

upto first order in $\hbar$. In the noise terms we just have to take the classical limit of the kernel ν:

$$\begin{aligned} \frac{i}{\hbar}\, S_{env} \;\simeq\; & 4\int_0^{\mathcal{T}} dt' \int_0^{\mathcal{T}} dt''\; i\hat{x}(t')\, \gamma(t'-t'')\, \dot{x}(t'') \\ & +2k_B T \int_0^{\mathcal{T}} dt' \int_0^{\mathcal{T}} dt''\; i\hat{x}(t')\, \Gamma(t'-t'')\, i\hat{x}(t'') \end{aligned} \tag{7.150}$$

with $O(\hbar)$ corrections (apart from a border term that can be treated more carefully and check that it disappears.)

7.2.10 A particle or manifold coupled to a fermionic reservoir

The coupling to leads are modeled by interactions to electron creation and destruction operators in the form:

$$H_{int} = \frac{1}{N}\sum_{k,k'=1}^{N} V_{kk'}\hat{x}\left(\hat{\psi}^\dagger_{Lk}\hat{\psi}_{Rk'} + \hat{\psi}^\dagger_{Rk}\hat{\psi}_{Lk'}\right) \tag{7.151}$$

L and R are left and right labels associated to two leads. $\hat{\psi}^\dagger_{L(R)k}$ and $\hat{\psi}_{L(R)k}$ are creation and destruction operators, respectively, acting on the left (L) and right (R) leads. k is the wave-vector of the electron. N is the number of fermionic degrees of freedom that we take $N \to \infty$. $V_{kk'}$ is the coupling constant for the kk' reservoir degrees of freedom. For simplicy we take $V_{kk'} = \hbar\omega_c$.

The influence functional is

$$F[x_+,x_-] = \int^{\Psi^-(\infty)=\Psi^+(\infty)} \mathcal{D}\psi\mathcal{D}\psi^\dagger\; e^{\frac{i}{\hbar}\left(S_{\rm int}[x^+,\Psi^+]-S_{\rm int}[x^-,\Psi^-]\right)} \times e^{\frac{i}{\hbar}\left(S_{\rm env}[\Psi^+]-S_{\rm env}[\Psi^-]\right)}\;\langle\Psi^+(0)|\rho_{\rm env}|\Psi^-(0)\rangle$$

The coordinates Ψ represent the fermionic variables of the reservoirs: $\Psi \equiv (\psi_L,\psi_L^\dagger,\psi_R,\psi_R^\dagger)$. We expand the reservoir-system coupling at second order (first order gives no contribution) to exhibit an effective action $S_{\rm K,eff}$ by the following procedure

$$\begin{aligned}\langle e^{\frac{i}{\hbar}S_{\rm K,int}}\rangle_{\rm env} &\simeq 1+\langle\frac{i}{\hbar}S_{\rm K,int}\rangle_{\rm env}+\frac{1}{2}\langle\Big(\frac{i}{\hbar}S_{\rm K,int}\Big)^2\rangle_{\rm env}\simeq e^{\frac{1}{2}\langle\left(\frac{i}{\hbar}S_{\rm K,int}\right)^2\rangle_{\rm env}}\\ &\equiv e^{\frac{i}{\hbar}S_{\rm K,eff}}\;. \end{aligned}\tag{7.152}$$

We used the notation $\langle ...\rangle_{\rm env}$ to represent the functional integral over the fermions evolution. The electron reservoirs' contribution to the action is

$$S_{\rm K,int}\equiv-\sum_{a=\pm}a\int dt\;\hbar\omega_c\sum_{i=1}^{N}x^a(t)\frac{1}{M}\sum_{k=1}^{M}\left(\psi_{Lk}^{a\dagger}\psi_{Rk}^a+\psi_{Rk}^{a\dagger}\psi_{Lk}^a\right)\;.\tag{7.153}$$

We have

$$-\frac{1}{\hbar^2}\langle S_{\rm K,int}^2\rangle_{\rm env}=-\frac{1}{\hbar^2}\sum_{a,b=\pm}ab\int dtdt'\;(\hbar\omega_c)^2x^a(t)x^b(t')\tag{7.154}$$

$$\times\frac{1}{M^2}\sum_{kk'qq'=1}^{M}\langle\Big(\psi_{Lk}^{a\dagger}(t)\psi_{Rk'}^a(t)+L\leftrightarrow R\Big)\Big(\psi_{Lq'}^{b\dagger}(t')\psi_{Rq'}^b(t')+L\leftrightarrow R\Big)\rangle_{\rm env}\,.$$

Since left and right reservoirs are independant, operators of left reservoir commute with the right ones and the averaging factorizes : $\langle T\psi_R\psi_L^\dagger\psi_L\psi_R^\dagger\rangle = \langle T\psi_R\psi_R^\dagger\rangle\langle T\psi_L^\dagger\psi_L\rangle$. Sites i and $j\neq i$ live in different spaces so we have $\langle T\psi_i\psi_j^\dagger\rangle=\delta_{ij}\langle T\psi_i\psi_i^\dagger\rangle$. Conservation of mometum implies $\langle T\psi_k\psi_{q'}^\dagger\rangle=\delta_{kq'}\langle T\psi_k\psi_k^\dagger\rangle$ and similarly $\langle T\psi_{k'}\psi_q^\dagger\rangle=\delta_{k'q}\langle T\psi_{k'}\psi_{k'}^\dagger\rangle$. Moreover, we use the fermionic property $\langle T\psi_i\psi_i\rangle=\langle T\psi_i^\dagger\psi_i^\dagger\rangle=0$ to finally simplify the expression (7.154) into

$$-\frac{1}{\hbar^2}\langle S_{\rm K,int}^2\rangle_{\rm env}=-\frac{1}{\hbar^2}\sum_{a,b=\pm}ab\int\int dtdt'\;(\hbar\omega_c)^2x^a(t)x^b(t')\tag{7.155}$$

$$\times\left(\frac{1}{M}\sum_{k=1}^{M}\langle\psi_{Lk}^{a\dagger}(t)\psi_{Lk}^b(t')\rangle_{\rm env}\frac{1}{M}\sum_{k=1}^{M}\langle\psi_{Rk}^a(t)\psi_{Rk}^{b\dagger}(t')\rangle_{\rm env}+L\leftrightarrow R\right)$$

Recalling the definition of the fermionic green functions $G_{a,b}(t,t') \equiv -i\frac{1}{M}\sum_{k=1}^{M}\langle T_C\ \psi_k^a(t)\psi_k^{b\dagger}(t')\rangle$, and reconstructing an exponential into an effective action $S_{\rm K,eff}$ of the general form

$$S_{\rm K,eff} \equiv -\sum_{a,b=\pm}\frac{1}{2}\int\int dtdt'\ x^a(t)\Sigma_{ab}(t,t')x^b(t')\,, \tag{7.156}$$

we identify the self-energy components

$$\boxed{\Sigma_{ab}(t,t') \equiv -iab\hbar\omega_c^2\ \Big[G_{ab}^R(t,t')G_{ba}^L(t',t) + L\leftrightarrow R\Big]}\,. \tag{7.157}$$

For a single free fermion, $H=\hbar\omega_0\psi^\dagger\psi$, in equilibirum in the grand-canonical ensemble, $\rho_0 \propto e^{-\beta(H-\mu N)}$, the Green function is

$$G_{+-}(\tau) = in_F e^{-i\omega_0\tau} \qquad\qquad G_{-+}(\tau) = -i(1-n_F)e^{-i\omega_0\tau} \tag{7.158}$$

where n_F is the Fermi factor $n_F \equiv [1+e^{\beta(\hbar\omega_0-\mu)}]^{-1}$. After the Keldysh rotation we have

$$G_K(\tau) = -2\tanh[\beta/2\ (\hbar\omega_0-\mu)]\ e^{-i\omega_0\tau}\ , \qquad G_R(\tau) = \frac{i}{\hbar}e^{-i\omega_0\tau}\theta(\tau) = G_A^*(-\tau) \tag{7.159}$$

The reservoir has a collection of free fermions ($N\to\infty$) with a distribution of energy levels, or density of states, $\varrho_F(\omega_0)$. Thus,

$$\begin{aligned}
G_K(\tau) &= -2\int d\omega_0\ \varrho(\omega_0)\ \tanh[\beta(\hbar\omega_0-\mu)/2]\, e^{-i\omega_0\tau} \\
&= -2\ \langle\tanh[\beta(\hbar\omega_0-\mu)/2]\, e^{-i\omega_0\tau}\,\rangle_{\omega_0} \\
G_R(\tau) &= \int d\omega_0\ \varrho(\omega_0)\,\frac{i}{\hbar}e^{-i\omega_0\tau}\,\theta(\tau) = \frac{i}{\hbar}\,\langle\, e^{-i\omega_0\tau}\,\rangle_{\omega_0}\,\theta(\tau) \\
G_A(\tau) &= \int d\omega_0\ \varrho(\omega_0)\,\frac{-i}{\hbar}e^{-i\omega_0\tau}\,\theta(-\tau) = -\frac{i}{\hbar}\,\langle\, e^{-i\omega_0\tau}\,\rangle_{\omega_0}\,\theta(-\tau)
\end{aligned} \tag{7.160}$$

where we introduced a short-hand notation, the angular brackets, for the integration over energy levels. In the end, the explicit calculation of the kernels Σ originating from the coupling to the bath yields

$$\begin{aligned}
\Sigma_K(\tau) &= -\frac{(\hbar\omega_c)^2}{2}\langle\langle\Big\{\tanh[\frac{\beta_L}{2}(\hbar\omega_L-\mu_L)]\ \tanh[\frac{\beta_R}{2}(\hbar\omega_R-\mu_R)]-1\Big\} \\
&\quad\times\cos[(\omega_L-\omega_R)\tau]\rangle_{\omega_L}\rangle_{\omega_R} \\
\Sigma_R(\tau) &= (\hbar\omega_c)^2\frac{1}{\hbar}\langle\langle\Big\{\tanh[\frac{\beta_L}{2}(\hbar\omega_L-\mu_L)]-\tanh[\beta\beta_R 2(\hbar\omega_R-\mu_R)]\Big\} \\
&\quad\times\sin[(\omega_L-\omega_R)\tau]\rangle_{\omega_L}\,\rangle_{\omega_R}\theta(\tau)
\end{aligned} \tag{7.161}$$

Two important energy scales characterize the density of states, $\varrho(\omega)$: their 'mean-square-displacement' or bandwidth, $\hbar\omega_F$, and whether they have a finite cut-off, $\hbar\omega_{cut}$ or not. Some typical examples one can use are

$$\varrho(\omega) = \begin{cases} \omega_F^{-1}\sqrt{1-(\omega-\omega_F)^2/\omega_F^2} & \text{semi-circle} \quad \hbar\omega_F,\ \hbar\omega_{cut} < \infty\ , \\ \omega_F^{-1}\sqrt{\frac{\omega}{\omega_F}}e^{-\frac{1}{2}\left(\frac{\omega}{\omega_F}\right)^2} & \sim \text{Oscil.} \quad \hbar\omega_F < \infty\ \hbar\omega_{cut} \to \infty \\ \omega_F^{-1}\left(\frac{\omega}{\omega_F}\right)^{(d-2)/2} & \text{Elect. gas} \quad \hbar\omega_F \to \infty\ \hbar\omega_{cut} \to \infty\ . \end{cases} \tag{7.162}$$

Clearly, the maximal current one can apply to the system is $eV_{max} = \hbar\omega_{cut} - \mu_0$.

Some interesting limiting cases of the kernels Σ are worth mentioning:

- For $\hbar\omega_F \gg \hbar\omega$ and k_BT. We obtain the Ohmic ($\propto \omega$) behaviour

$$\mathrm{Im}\Sigma_R(\omega) \simeq 2\pi(\hbar\omega_c)^2\frac{1}{\hbar}\rho^2(\mu_0/\hbar + eV/\hbar)\ \omega \tag{7.163}$$

  Interesting enough, this expression is independent of T. Simultaneously,

$$\Sigma_K(\omega) \simeq 2\pi(\hbar\omega_c)^2\frac{1}{\hbar}\rho^2(\mu_0/\hbar + eV/\hbar)\frac{eV\sinh(\beta eV) - \hbar\omega\sinh(\beta\hbar\omega)}{\cosh(\beta eV) - \cosh(\beta\hbar\omega)} \tag{7.164}$$

- In equilibrium $V = 0$ one recovers the FDT relation

$$\mathrm{Im}\Sigma_R(\omega) \simeq 2\pi(\hbar\omega_c)^2\frac{1}{\hbar}\rho^2(\mu_0/\hbar)\omega \tag{7.165}$$

$$\Sigma_K(\omega) \simeq 2\pi(\hbar\omega_c)^2\rho^2(\mu_0/\hbar)\omega\coth\beta\frac{\hbar\omega}{2} \tag{7.166}$$

  eqs. (7.163) and (7.164). For $\hbar\omega \ll k_BT \ll \hbar\omega_F$

$$\Sigma_K(\omega) \simeq 4\pi(\hbar\omega_c)^2\frac{1}{\hbar}\rho^2(\mu_0/\hbar)\ k_BT\ . \tag{7.167}$$

- At $T = 0$ and $eV \ll \hbar\omega_F$, one derives from eq. (7.164)

$$\Sigma_K(\omega = 0, T = 0, V) \simeq 2\pi(\hbar\omega_c)^2\frac{1}{\hbar}\rho^2(\mu_0/\hbar)|eV| \tag{7.168}$$

This last expression is of the same form as eq. (7.167) suggesting the definition of an equivalent temperature

$$\boxed{k_B T^* \equiv |eV|/2} \tag{7.169}$$

A 'FDT like' relation is verified up to the second order in $\frac{eV}{\hbar\omega_F}$

$$\Sigma_K[T=0,\omega=0,\mathcal{O}(\frac{eV}{\hbar})^2] = \hbar\coth(\beta^*\frac{\hbar\omega}{2})\text{Im }\Sigma_R[\mathcal{O}(\omega)^1,\mathcal{O}(\frac{eV}{\hbar})^1] \tag{7.170}$$

7.2.11 Other baths

The electron-phonon interactions, in which the phonons are considered the bath, was dealt with in [17]. Spin baths are reviewed in [18].

8 Quantum glassiness

In this section we discuss the dynamics of a number of quantum systems. See the slides and a review article by L. F. Cugliandolo in the arXiv.

8.1 Quantum driven coarsening

Take the quantum O(N) model and couple it to two electronic reservoirs. As we have seen this environment encompasses as a limit the oscillator case, and allows for the application of a current through the system.

In MSR fields the action reads

$$\begin{aligned}\frac{i}{\hbar}S &= \int dtd^dx \left\{ i\vec{\hat{\phi}}(\vec{x},t)[m\ddot{\vec{\phi}}(\vec{x},t) + \nabla^2\vec{\phi}(\vec{x},t)] \right\} \\ &\quad + \frac{4}{N} i\vec{\hat{\phi}}(\vec{x},t)\cdot\vec{\phi}(\vec{x},t)\left[\phi^2 - \phi_0^2 - \left(\frac{\hbar}{2} i\vec{\hat{\phi}}(\vec{x},t)\right)^2\right] \\ &= + \int dtd^dx \left[i\vec{\hat{\phi}}(\vec{x},t) 4\gamma(t-t')\dot{\vec{\phi}}(\vec{x},t) + i\vec{\hat{\phi}}(\vec{x},t)\hbar\nu(t-t')\vec{\phi}(\vec{x},t)\right]\end{aligned}$$

Apart from the last term in the potential part this action is like the MSR one for a vector field theory in a strange bath. In the large N limit we assume that the term between sqaure brackets can be replaced by its average (as in the classical case) the value of which will be fixed self-consistently. The contribution $\langle (i\hat{\phi})^2 \rangle$ vanishes due to causality. We are then in presence of an effective classical field theory in contact with an environment with quantum character.

The main results are [13]

- There is a coarsening phase in the (T, Γ, eV) phase diagram. It survives the finite current imposed by the leads. Whether there is a finite critical eV_{max} (at $T = \Gamma = 0$) or the ordering phase extends to infinity in this direction depends upon the type of electron bath used.

- The coupling strength, say g, between the baths and the system plays a very important role in the determination of the phase diagram. The extent of the 'sub-critical' region in which the system will undergo coarsening after a quench (or annealing) increases for increasing coupling strength although the classical critical temperature is not modified by g. The effect is highly non-trivial in this very simple model: the action

is 'almost' classical, apart from the last term that arises from the coupling to the bath and involves the kernel ν. Although at long-times this kernel becomes classical one cannot simply argue that it will not have an effect on the dynamics of the system; on the contrary, its short-time effects alter the dynamics and make the phase transition occur elsewhere.

This effect is similar to the Caldeira-Leggett localisation phenomenon.

A static calculation in which the partition function of the system and the environment (in the case $V = 0$) gives the same critical line as the dynamic one for this model. This is not necessarily the case, as we shall see below with the random manifold.

- In the ordering phase the correlations and linear responses present a separation of two-time scales, similar to the one encountered in the classical limit with a well-defined plateau in the correlation achieved at a value that depends on the parameters (T, Γ, eV).

- The relaxation in the stationary regime depends strongly on the parameters (T, Γ, eV). The correlations may ne non-monotonic and present oscillations depending on the values of these parameters. The correlations and linear-responses are related by the quantum FDT.

- The study of the correlation functions in the aging regime yields a growing correlation length $R(t; T, \Gamma, eV)$ with a weak dependence upon the parameters T, Γ, eV and $t^{1/2}$ growth in time as in the classical limit.

- The scaling functions are the same as in the classical limit and do not depend on the parameters (T, Γ, eV). This is an extension of the super-universality hypothesis to the quantum case.

- The relation between the linear-response and the correlation is not the equilibrium FDT but a modified one with an effective temperature that for diverges in the coarsening regime.

We conclude that the environment plays a dual rôle: its quantum character basically determines the phase diagram but the coarsening process at long times and large length-scales only 'feels' a classical white bath at temperature T^*. The two-time dependent decoherence phenomenon (absence of oscillations, validity of a classical FDT when $t/t_w = O(1)$, etc.) is intimately

related to the development of a non-zero (actually infinite) effective temperature, T_{eff}, of the system as defined from the deviation from the (quantum) FDT. T_{eff} should be distinguished from T^* as the former is generated not only by the environment but by the system interactions as well ($T_{eff} > 0$ even at $T^* = 0$). Moreover, we found an extension of the irrelevance of T in classical ferromagnetic coarsening ($T = 0$ 'fixed-point' scenario): after a suitable normalization of the observables that takes into account all microscopic fluctuations (e.g. q_{EA}) the scaling functions are independent of all parameters including V and Γ. Although we proved this result through a map- ping to a Langevin equation that applies to quadratic models only, we expect it to hold in all instances with the same type of ordered phase, say ferromagnetic, and a long-time aging dynamics dominated by the slow motion of large domains. Thus, a large class of coarsening systems (classical, quantum, pure and disordered) should be characterized by the same scaling functions.

A Conventions

A.1 Fourier transform

The convention for the Fourier transform is

$$f(\tau) = \int_{-\infty}^{\infty} \frac{d\omega}{2\pi}\, e^{-i\omega\tau}\, f(\omega)\ , \tag{A.171}$$

$$f(\omega) = \int_{-\infty}^{\infty} d\tau\ e^{+i\omega\tau}\, f(\tau)\ . \tag{A.172}$$

The Fourier transform of the theta function reads

$$\theta(\omega) = i\mathrm{vp}\frac{1}{\omega} + \pi\delta(\omega)\ . \tag{A.173}$$

The convolution is

$$[f\cdot g](\omega) = f\otimes g(\omega) \equiv \int \frac{d\omega'}{2\pi} f(\omega')g(\omega-\omega')\ . \tag{A.174}$$

A.2 Commutation relations

We defined the commutator and anticommutator: $\{A,B\} = (AB+BA)/2$ and $[A,B] = (AB-BA)/2$.

A.3 Time ordering

We define the time odering operator acting on bosons as

$$T\hat{q}(t)\hat{q}(t') \equiv \theta(t,t')\hat{q}(t)\hat{q}(t') + \theta(t',t)\hat{q}(t')\hat{q}(t)\ . \tag{A.175}$$

For fermions, we define the time ordering operator as

$$T\hat{\psi}(t)\hat{\psi}(t') \equiv \theta(t,t')\hat{\psi}(t)\hat{\psi}(t') - \theta(t',t)\hat{\psi}(t')\hat{\psi}(t)\ , \tag{A.176}$$

$$T\hat{\psi}(t)\hat{\psi}^\dagger(t') \equiv \theta(t,t')\hat{\psi}(t)\hat{\psi}^\dagger(t') - \theta(t',t)\hat{\psi}^\dagger(t')\hat{\psi}(t)\ , \tag{A.177}$$

In both cases $\theta(t,t')$ is the Heaviside-function.

We define the time-ordering operator T_C on the Keldysh contour in such a way that times are ordered along it:

$$\begin{aligned} T_C\ x_+(t)x_-(t') &= x_-(t')x_+(t) \qquad & T_C\ x_-(t)x_+(t') &= x_-(t)x_+(t') \\ T_C\psi_+(t)\psi_-(t') &= -\psi_-(t')\psi_+(t) \qquad & T_C\psi_-(t)\psi_+(t') &= \psi_-(t)\psi_+(t') \end{aligned} \quad \text{(A.178)}$$

for all t and t'.

B The instanton calculation

The path-integral formalism yields an alternative calculation of the Kramers escape time, the Arrhenius exponential law and its prefactor that, in principle, is easier to generalize to multidimensional cases. For the sake of simplicity let us focus on the overdamped limit in which we neglect inertia. We first rederive the Arrhenius exponential using a simplified saddle-point argument, and then show how Kramers calculation can be recovered by correctly computing the fluctuations around this saddle point. Starting from the following representation of the probability to reach the top of the barrier from the potential well:

$$P(x_{max},t|x_{min}) = \left\langle \int_{x(0)=x_{min}}^{x(t)=x_{max}} \mathcal{D}x\ \delta(\xi - eq[x]) \left| \det\left(\frac{\delta eq[x](t)}{\delta x(t')}\right)\right| \right\rangle_\xi ,$$

and neglecting the determinant (which is justified if one follows the Itô convention), then, for a Gaussian white noise ξ:

$$P(x_{max},t|x_{min}) = \int_{x(0)=x_{min}}^{x(t)=x_{max}} \mathcal{D}x\ e^{-\frac{1}{4k_BT}\int_0^t dt'\left(\dot{x}+\frac{dV}{dx}\right)^2}$$

Expanding the square, we find a total derivative contribution to the integral equal to $2[V(x_{max}) - V(x_{min})]$, plus the sum of two squares: $\int_0^t dt'[\dot{x}^2 + (V'(x))^2]$. For small T, the path, x^*, contributing most to the transition probability is such that this integral is minimized. Using standard rules of functional derivation one finds

$$\frac{d^2x^*}{dt'^2} = V'(x^*)V''(x^*) \quad \Rightarrow \quad \dot{x}^* = \pm V'(x^*).$$

In order to be compatible with the boundary conditions $x^*(0) = x_{min}$ and $x(t) = x_{max}$, the + solution must be chosen, corresponding to an overdamped

motion in the inverted potential $-V(x)$. The 'action' of this trajectory is

$$\int_0^t dt' \left[\dot{x}^{*2} + (V'(x^*))^2\right] = 2\int_0^t dt' \dot{x}^* V'(x^*) = 2[V(x_{max}) - V(x_{min})],$$

that doubles the contribution of the total derivative above. Hence,

$$P(x_{max}, t|x_{min}) \approx e^{-\beta(V(x_{max})-V(x_{min}))},$$

independently of t, as in eq. (4.64). This type of calculation can be readily extended to cases in which the noise ξ has temporal correlations, or non Gaussian tails, and to see how these effects change the Arrhenius result. The calculation of the attempt frequency is done using the standard dilute gas instanton approximation dveeloped by several authors [35] but we shall not discuss it here.

The path-integral that we have just computed is a sum over the subset of noise trajectories that lead from the initial condition to a particular final condition that we imposed. Imposing a boundary condition in the future destroys the causal character of the theory.

In a one dimensional problem as the one treated in this Section there is only one possible 'reaction path'. In a multidimensional problem, instead, a system can transit from one state to another following different paths that go through different saddle-points. The lowest saddle-point might not be the most convenient way to go and which is the most favorable path is, in general, difficult to established.

References

[1] P. G. Debenedetti, *Metastable liquids* (Princeton Univ. Press, 1997). E. J. Donth, *The glass transition: relaxation dynamics in liquids and disordered materials* (Springer, 2001). K. Binder and W. Kob, *Glassy Materials and Disordered Solids: An Introduction to their Statistical Mechanics* (World Scientific, 2005).

[2] K. H. Fischer and J. A. Hertz, *Spin glasses* (Cambridge Univ. Press, 1991). M. Mézard, G. Parisi, and M. A. Virasoro, *Spin glass theory and beyond* (World Scientific, 1986).

[3] L. F. Cugliandolo, *Dynamics of glassy systems*, in Les Houuches 2002 (Springer, 2003).

[4] O.C. Martin, R. Monasson, R. Zecchina, *Statistical mechanics methods and phase transitions in optimization problems* Theoretical Computer Science **265** (2001) 3-67. M. Mézard and A. Montanari, *Information, Physics, and Computation*, (Oxford Graduate Texts, 2009).

[5] D. J. Amit, *Modeling Brain Function: The World Of Attractor Neural Networks*, (Cambridge Univ. Press, 1992). N. Brunel, *Network models of memory*, in Les Houches 2003 (Elsevier, 2004).

[6] R. Zwanzig, J. Stat. Phys. **9**, 215 (1973). S. Nordholm and R. Zwanzig, J. Stat. Phys. **13**, 347-371 (1975). K. Kawasaki, J. Phys. A **6**, 1289-1295 (1973).

[7] U. Weiss, *Quantum dissipative systems*, Series in modern condensed matter physics vol. 10, World Scientific (1999).

[8] J. Dunkel and P. Hänggi, Phys. Rep. **471**, 1-73 (2009).

[9] R. Bausch, H. K. Janssen, and H. Wagner, Z. Phys. B **24**, 113 (1976).

[10] L. F. Cugliandolo, J. Kurchan, and L. Peliti, Phys. Rev. E **55**, 3898 (1997).

[11] P. Le Doussal, Exact results and open questions in first principle functional RG arXiv:0809.1192

[12] A. Sicilia, J. J. Arenzon, A. J. Bray, and L. F. Cugliandolo, Phys. Rev. E

[13] C. Aron, G. Biroli, and L. F. Cugliandolo, Phys. Rev. Lett. **102**, 050404 (2009).

[14] L. F. Cugliandolo and P. Le Doussal, Phys. Rev. E L. F. Cugliandolo, J. Kurchan, and P. Le Doussal, Phys. Rev. Lett.

[15] A. Sicilia, G. Biroli and L. F. Cugliandolo, Phys. Rev. E

[16] Phys. Rev. E **65**, 046136 (2002).

[17] C. Caroli, R. Combescot, P. Nozieres and D. Saint-James, J. Phys. C **5**, 21 (1972).

[18] *Theory of the spin bath* N. Prokof'ev and P. Stamp Rep. Prog. Phys. **63**, 669 (2000).

[19] H. Grabert, P. Schramm and G.-L. Ingold, Phys. Rep. **168**, 115 (1988).

[20] R. MacKenzie, *Path integral methods and applications*, VIth Vietnam School of Physics, Vung Tau, Vietnam, 27 Dec. 1999 - 8 Jan. 2000; arXiv:quantum-ph/0004090.

[21] R. P. Feynman and A. R. Hibbs, *Quantum Mechanics and Path Integrals* (New York: McGraw-Hill, 1965). H. Kleinert, *Path Integrals in Quantum Mechanics, Statistics, Polymer Physics, and Financial Markets*, 4th edition (World Scientific, Singapore, 2004) J. Zinn-Justin, *Path Integrals in Quantum Mechanics* (Oxford University Press, 2004), R. J. Rivers, *Path Integrals Methods in Quantum Field Theory* (Cambridge University Press, 1987).

[22] R. P. Feynman, *Statistical mechanics*,

[23] J. Kurchan, *Supersymmetry, replica and dynamic treatments of disordered systems: a parallel presentation* arXiv:cond-mat/0209399.

[24] M. Mézard, G. Parisi, and M. A. Virasoro, *Spin glasses and beyond*, Fischer and J. Hertz,

[25] A. B. Kolton, D. R. Grempel and D. Domínguez, Phys. Rev. B 71, 024206 (2005)

[26] A. J. Bray, Adv. Phys. **43**, 357 (1994). P. Sollich, http://www.mth.kcl.ac.uk/ psollich/

[27] P. C. Hohenberg and B. I. Halperin, Rev. Mod. Phys. **49**, 435 (1977). P. Calabrese and A. Gambassi, J.Phys. A **38**, R133 (2005).

[28] D. W. Oxtoby, *Homogeneous nucleation: theory and experiment*, J. Phys.: Condens. Matter **4**, 7626-7650 (1992). K. Binder, *Theory of first-order phase transitions*, Rep. Prog. Phys. **50**, 783-859 (1987).

[29] F. Corberi, E. Lippiello and M. Zannetti J. Stat. Mech. (2007) P07002.

[30] Viasnoff and Lequeux

[31] A. Cavagna, Supercooled Liquids for Pedestrians Physics Reports **476**, 51 (2009).

[32] U. Weiss, *Quantum dissipative systems*, Series in modern condensed matter physics vol. 10, World Scientific (1999).

[33] L. F. Cugliandolo and G. Lozano, Phys. Rev. Lett. 80, 4979 (1998) . Phys. Rev. B59, 915 (1999).

[34] L. F. Cugliandolo, D. R. Grempel, G. Lozano and H. Lozza Phys. Rev. B **70**, 024422 (2004). L. F. Cugliandolo, D. R. Grempel, G. S. Lozano, H. Lozza, C. A. da Silva Santos Phys. Rev. B **66**, 014444 (2002).

[35] J. S. Langer, *Statistical theory of decay of metastable states* Ann. of Phys. **54**, 258 (1969). C. G. Callan and S. Coleman, Phys. Rev. D **16**, 1762 (1977). B. Caroli, C. Caroli, and B. Roulet, *Diffusion in a bistable potential - systematic WKB treatment* J. Stat. Phys. **21**, 415 (1979). A. M. Polyakov, *Gauge fields and stings* (Harwood Academic Publishers, 1994).

[36] R. P. Feynmann and F. L. Vernon, Jr, Ann. Phys. **24**, 114 (1963).

[37] R. P. Feynmann and A. R. Hibbs, *Quantum mechanics and path integrals* (Mc Graw-HIll, New York, 1965).

[38] A. J. Leggett, S. Chakravarty, A. T. Dorsey, M. P. A. Fisher, A. Garg, W. Zwerner, Rev. Mod. Phys. **59**, 1 (1987).

[39] A. J. Bray and M. A. Moore, Phys, Rev. Lett. **49**, 1546 (1982).

[40] R. Zwanzig, J. Stat. Phys. **9**, 215 (1973). Kawasaki,

[41] Hanggi on Langevin's proof.

[42] C. P. Martin, E. Siggia and H. A. Rose, Phys. Rev. **A8**, 423 (1973), H. K. Janssen, Z. Phys. **B23**, 377 (1976) and *Dynamics of critical phenomena and related topics*, Lecture notes in physics **104**, C. P. Enz ed. (Springer Verlag, Berlin, 1979).

[43] C. de Dominicis, Phys. Rev. **B18**, 4913 (1978).

[44] J. Schwinger, J. Math. Phys. **2**, 407 (1961). L. V. Keldysh, Zh. Eksp. Teor. Fiz. **47**, 1515 (1964), Sov. Phys. JETP **20** 235 (1965).

[45] A. Kamenev,

[46] G. Parisi, *Statistical Field Theory*, Frontiers in Physics, Lecture Notes Series, Addison-Wesley (1988).